Faculty of Science and Engineering School
Earth and Planetary Sciences

Understanding Australia's groundwater spatio-temporal variability in relation to its hydroclimate-hydrogeology

Kexiang Hu

0000-0002-5361-9857

This thesis is presented for the Degree of
Doctor of Philosophy of
Curtin University

March 2022

Declaration

To the best of my knowledge and belief this thesis contains no material previously published by any other person except where acknowledgement has been made. This thesis contains no material, which has been accepted for the award of any other degree or diploma in any university.

Kexiang Hu

List of publications

This Ph.D thesis is a combination of 5 peer-reviewed publications (1 corresponding author, 4 first-author) and 1 submitted article in high impact journals (Table 1). Other 4 indirectly related articles (Table 1) are also listed below. Copyright permissions/authorisation of the journals are presented in Appendix A while Appendix B contains the signed declarations for author and co-author contributions regarding the published manuscripts.

Contributions directly related to this thesis:

1. Awange, J.L. **Hu, K.X.** and Khaki, M., (2019). The newly merged satellite remotely sensed, gauge and reanalysis-based Multi-Source Weighted-Ensemble Precipitation: Evaluation over Australia and Africa (1981–2016). Science of The Total Environment, 670, pp.448-465, doi: 10.1016/j.scitotenv.2019.03.148. 10.1016/j.apgeog.2018.10.007.

2. **Hu, K.X.**, Awange, J.L., Kuhn, M. and Saleem, A., (2019). Spatio-temporal groundwater variations associated with climatic and anthropogenic impacts in South-West Western Australia. Science of The Total Environment, 696, 133599, doi: 10.1016/j.scitotenv.2019.133599.

3. **Hu, K.X.**, Awange, J.L., Kuhn, M. and Nanteza, J., (2021). Inference of the spatio-temporal variability and storage potential of groundwater in data-deficient regions through groundwater models and inversion of impact factors on groundwater, as exemplified by the Lake Victoria Basin. Science of The Total Environment, 800, 149355, doi: 10.1016/j.scitotenv.2021.149355.

4. **Hu, K.X.**, Awange, J.L., Kuhn, M. and Zerihun, A., (2022). Irrigated agriculture potential of Australia's northern territory inferred from spatial assessment of groundwater availability and crop evapotranspiration. Agricultural Water Management, 264, 107466, doi: 10.1016/j.agwat.2022.107466.

5. **Hu, K.X.**, Awange, J.L. and Kuhn, M., (2022). Testing a knowledge-based approach for inferring spatio-temporal characteristics of groundwater in the Australian State of Victoria. Science of The Total Environment, 821, 153113, doi: 10.1016/j.scitotenv.2022.153113.

6. **Hu, K.X.**, Awange, J.L. and Kuhn, M., (2022). Large-scale quantification of groundwater recharge threshold conditions using machine learning classifications: Exemplified over the Australian continent. Science of The Total Environment, submitted.

Other cross-sectoral collaboration contributions indirectly related to this thesis:

7. Awange, J.L., Saleem, A., Konneh, S.S., Goncalves, R.M., Kiema, J.B.K. and **Hu, K.X.**, (2018). Liberia's coastal erosion vulnerability and LULC change analysis: Post-civil war and Ebola epidemic. Applied Geography, 101, pp.56-67, doi:10.1016/j.apgeog.2018.10.007

8. Awange, J.L., Saleem, A., Sukhadiya, R.M., Ouma, Y.O. and **Hu, K.X.**, (2019). Physical dynamics of Lake Victoria over the past 34 years (1984–2018): Is the lake dying? Science of The Total Environment, 658, pp.199-218, doi: 10.1016/j.scitotenv.2018.12.051.

9. Morgan, B., Awange, J.L., Saleem, A. and **Hu, K.X.**, (2020). Understanding vegetation variability and their "hotspots" within Lake Victoria Basin (LVB: 2003–2018). Applied Geography, 122, 102238, doi: 10.1016/j.apgeog.2020.102238.

10. Saleem, A., Awange, J.L., Kuhn, M., John, B. and **Hu, K.X.**, (2021). Impacts of extreme climate on Australia's green cover (2003–2018): A MODIS and mascon probe. Science of The Total Environment, 766, 142567, doi: 10.1016/j.scitotenv.2020.142567.

Table 1: List of peer-reviewed publications (1-5) and submitted paper (6) that correspond to the objectives and chapters of thesis, as well as indirectly related articles (7-10). Note that paper 1 is a preliminary study providing data exploration and supports for the papers 2-5, and thus, is not included in this thesis.

Paper No.	Paper	Journal	Chapter	Objective
Contributions directly related to this thesis				
1.	*Awange et al.* (2019a)	STOTEN	2-5	1-4
2.	*Hu et al.* (2019)	STOTEN	2	1
4.	*Hu et al.* (2022c)	Agric. Water Manag.	3	2
3.	*Hu et al.* (2021)	STOTEN	4	3
5.	*Hu et al.* (2022a)	STOTEN	4	3
6.	*Hu et al.* (2022b)	STOTEN	5	4
Contributions indirectly related to this thesis				
7.	*Awange et al.* (2018)	Appl. Geogr.		
8.	*Awange et al.* (2019b)	STOTEN		
9.	*Morgan et al.* (2020)	Appl. Geogr.		
10.	*Saleem et al.* (2021)	STOTEN		

Abstract

As the world's largest renewable freshwater resource, groundwater plays an important role in supporting all types of human water use. For Australia, the driest inhabited continent in the world, its groundwater accounts for almost 1/5 to 1/3 of its annual water use depending on climate conditions. In regions such as Western Australia and the Northern Territory, for example, this rate is as high as 70% to 90%. Despite this importance, Australia's groundwater remains the least understood resource. The main reason is that spatio-temporal variability groundwater information, which is fundamental for its management, is insufficient or even unavailable in many parts of Australia due to non-homogeneous hydrogeological data. Where such data are available, as in the case of boreholes, they are faced either by data inconsistencies and/or non-continuous dataset. This is further compounded by the fact that groundwater comes with its complexity triggered by multiple hydroclimatic and hydrogeological factors from one Australian region to another, which hampers its understanding.

Currently, Australia is faced with different kinds of groundwater related issues from one region to another. For instance, there is the issue of decline of groundwater level in Western Australia. This is one of the major issues requiring special attention as it leads to unsustainable groundwater use on the one hand, and environmental degradation on the other hand. Although previous studies have singled out climate change and anthropogenic impacts as the main contributors to the decline, detailed spatio-temporal information on groundwater and its corresponding hydroclimate/anthropogenic impacts are still lacking. In Australia's Northern Territory, the government's planned agricultural expansion has been put on hold due to the concern that the available water for irrigation may not be able to meet the crop water demand. Given that groundwater is almost the only reliable water source for agriculture in the Northern Territory, understanding its spatio-temporal availability under different climatic conditions, as well as balancing the available water with crop water demands, is thought to be the key to accelerating this planned agricultural expansion. Unfortunately, such information is currently unavailable. Furthermore, lack of groundwater spatio-temporal information is not easily resolved due to the high cost and time-consumption of traditional methods such as drilling and isotopes. Consequently, this hinders groundwater development and its related applications in Australia's data deficient regions. To circumvent this, there exists a possibility of obtaining Australia's spatio-temporal groundwater information without actually relying on monitoring data such as boreholes since groundwater behaviours can be inferred from the behavior of its associated hydroclimatic and hydrogeological factors. However, such preposition requires a clear understanding of the relationship between groundwater and hydroclimate-hydrogeology. Finally, groundwater recharge threshold conditions represent the balance point between recharge and discharge, and are crucial for understanding groundwater recharge mechanism, predicting ground-

water recharge timing, and helping maintain aquifer balance. Although previous studies have made several attempts to quantify the groundwater recharge threshold conditions in Australia, their results are normally limited to localised scales and with only a few conditions considered and discussed. This leaves the issue of large-scale quantification of groundwater recharge threshold conditions in Australia unsolved, possibly due to difficulties in dealing with the combined effects of various hydroclimatic and hydrogeological conditions on groundwater across the vast Australian continent.

Addressing the issues outlined above, the major objective of this thesis, therefore, is to understand Australia's spatio-temporal groundwater variation from a hydroclimate and hydrogeology perspective to better inform its management. Specifically, the study (i) investigates the spatio-temporal groundwater variation associated with climatic and anthropogenic impacts as exemplified over South-West Western Australia, (ii) evaluates Northern Territory's irrigated agricultural potential based on the balance between groundwater availability and three crop water demands of three crops, (iii) proposes a knowledge-based approach utilizing climatic, topographical and hydrogeological information to infer groundwater spatio-temporal characteristics exemplified by Lake Victoria Basin (Africa) and the Australian State of Victoria, and (iv), applies machine learning techniques to quantify the groundwater recharge threshold conditions across the Australian continent.

Acknowledgements

Pursuing a Ph.D. was a long and arduous journey, and many times I felt like giving up. Fortunately, I had two excellent supervisors by my side, Prof. Joseph L. Awange and A/Prof. Michael Kuhn, who constantly provided me with all kinds of support and gave me the motivation to persevere. Prof. Joseph L. Awange is the most responsible mentor I have ever met in my life. Although many students are afraid to pass by his office because of his hard pushing, he will read the students' articles word by word, spend hours carefully giving advice, and reply to emails during holidays. It is fair to say that my PhD journey would never have started without meeting him. A/Prof. Michael Kuhn is a friendly mentor, always smiling, patiently giving advice, and making students feel encouraged. I am very grateful to him for guiding me when I lost track several times in my academic path. Without his company, it would have been very difficult for me to complete my Ph.D career. In this regards, I would like to express my most sincere thanks to Joseph and Michael, you are the initiators of my academic career and the people who changed my destiny. Besides, I deeply appreciate the support of Dr. Ayalsew Zerihun whose valuable knowledge in the field of agriculture was instrumental. I am grateful for every moment spent with my colleagues in the laboratory, Dr. Khandu Nakhap, Dr. Ndehedehe Christopher Edet, Dr. Mehdi Khaki, Dr. Saleem Ashty Nalband, Dr. Luyen, K. Bui. and M.D. Aura Zepeda.

Special thanks to Curtin University for the funding received through the Curtin International Postgraduate Research Scholarship (CIPRS) and Research Stipend Scholarship, as well as Australian Government Research Training Program (RTP) Fee Offset Scholarship, which supported my PhD work during the entire period.

Finally, my deepest appreciation to my beloved families. Thanks to my father Ping Hu, who made a huge financial sacrifice for me to study in Australia. Thanks also to my mother Jun Chen for giving birth to me and giving me the opportunity to experience the beauty of this world. Thanks to my fiancee Xin Xu for her patience and company during the COVID-19 pandemic. To all my other families, I would like to thank you for your love and encouragement you gave. It is my luck to have you behind me.

Contents

Chapter 1
Introduction

1.1 Global perspective

Groundwater is a natural water resource buried under the surface of the earth (see global distribution in Fig 1.1), and accounts for approximately 30% of the world's freshwater (*Taylor et al.*, 2013a). Considering that, of the remaining 70%, almost 69% is a combination of ice, snow and glaciers, with rivers and lakes accounting for less than 1%, groundwater thus is the largest freshwater resource in the world (*Howard*, 2014; *Jasechko et al.*, 2014). According to recent global records (*Lall et al.*, 2020; *Jasechko et al.*, 2014), groundwater has already been an indispensable part of human water use, supporting around 50% of drinking water, approximately 40% of irrigation water and 33% of industrial water use. Apart from supporting humanity, groundwater also plays an important role in maintaining ecological stability. Many previous studies, e.g. *Xi et al.* (2009); *Nevill et al.* (2010); *Gleeson et al.* (2010); *Wang et al.* (2018) have shown that the functions of groundwater include recharging the flow of rivers and supporting the survival of surface vegetation and wildlife during dry seasons.

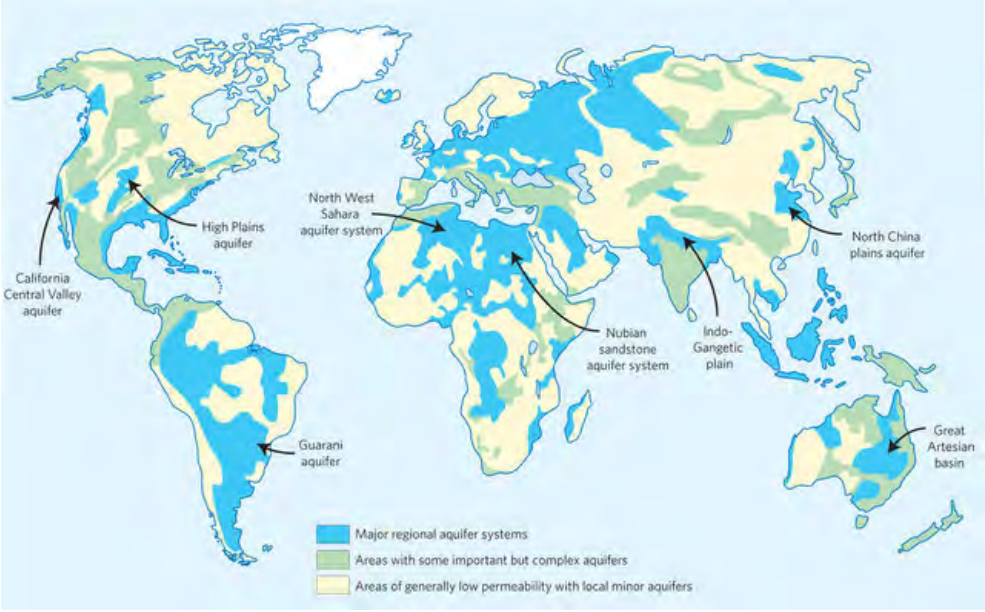

Figure 1.1: A Simplified version of a global groundwater resources map presented in *Taylor et al.* (2013a).

In recent decades, however, groundwater decline has become a common phenomenon worldwide (*Schwartz and Ibaraki*, 2011; *Hughes et al.*, 2012; *Patle et al.*, 2015; *Sun et al.*, 2015). In the United States, for instance, the

groundwater depletion rate has increased dramatically since 1950, reaching an average maximum value during the 2000-2008 period (*Konikow*, 2013). Similarly, in India, the groundwater depletion rate increased from 58% in 2004 to 62% in 2011 (*Chindarkar and Grafton*, 2019). Under the current scenario of global climate change (e.g. global warming; *Kumar* 2012) and increasing food demands due to increasing population (*Turner et al.*, 2019), the rising trend of groundwater depletion is going to persist. Particularly, increasing food demands will lead to the expansion of irrigated agriculture in those semi-arid areas, where groundwater is the only reliable freshwater source, thereby greatly increasing groundwater abstraction (*Bierkens and Wada*, 2019). According to *Gleeson et al.* (2012), the global overall rate of using groundwater was already 3.5 times higher than the sustainable rate 10 years ago. Although no reliable statistics have been found on the current state of groundwater use globally, many recent studies related to unsustainable groundwater use are still reminding us that groundwater management issues remain unresolved (*Dalin et al.*, 2019; *Perrone and Jasechko*, 2019; *Rosa et al.*, 2019; *Garg et al.*, 2022).

Failure to address groundwater management issues will have serious consequences. Considering that approximately 31% of the world's population depends solely on groundwater for survival (*Grönwall and Danert*, 2020), a major consequence is a direct threat to human life from water shortages. Another consequence is the irreversible environmental degradation, e.g. reduction of the flow of rivers, vegetation cover, and of species (*Mukherjee et al.*, 2018; *Hartfield et al.*, 2020). Also, land subsidence, seawater intrusion and water contamination are also consequences caused by the decline of groundwater (*Ajami*, 2021). Groundwater sustainability management, therefore, is a necessary task that all human beings must deal with for now and in the future.

1.2 Australian perspective

Australia is the driest populated continent on earth, with about 70% of its area classified as arid or semi-arid (see Fig 1.2; *Newsome and Corbett* 1975). Groundwater in these arid or semi-arid regions is essentially the only reliable water resource that can be accessed. The remaining 30% of the regions, e.g. south-west coast and the northern parts of Australia, have distinctive seasonality (see Fig 1.2), with most of the rainfall occurring between May and September (*Ali et al.*, 2012) and November and April (*Rogers and Beringer*, 2017), respectively. As for the dry season, these regions remain highly dependent on groundwater, which is needed to maintain surface ecosystem, as well as to support human water use. Less reliance on groundwater only exists in south-eastern Australia, which has relatively uniform rainfall (*Zhao et al.*, 2013). Nevertheless, groundwater remains important for maintaining ecosystem stability, considering that the Murray–Darling Basin in southeastern Australia is of significant environmental value to Australia.

Despite its importance to the entire Australian continent, groundwater is

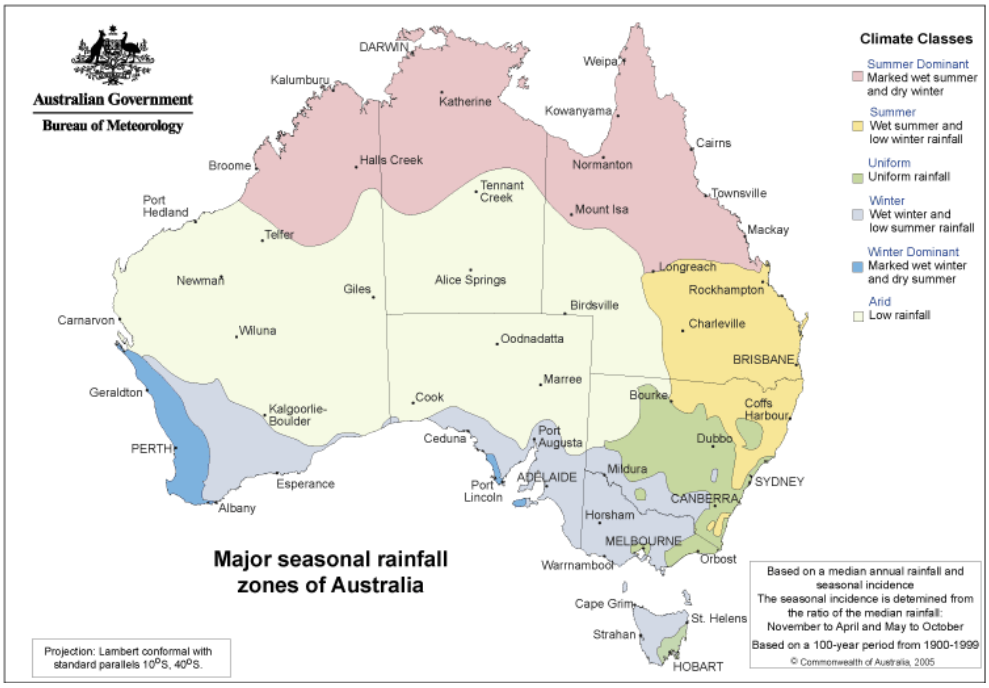

Figure 1.2: Major seasonal rainfall zones of Australia, downloaded from Bureau of Meteorology; (http://www.bom.gov.au/jsp/ncc/climate_averages/climate-classifications/).

the least understood compared to other water resources, leading to its poor management. One typical example is that groundwater decline has been a major problem in Australia over the past two decades. Ever since the millennium drought (1997-2009), many regions across the Australian continent have experienced various degrees of groundwater decline (*Barnett et al.*, 2020). Yet such a decline issue remains unresolved and is mentioned almost every year in the official water report (see, e.g. *Bureau of Meteorology* 2021, 2020a, 2018). Although the failure of groundwater management can be blamed on the one hand on complex population, policy and economic needs, it also reflects the lack of information and knowledge about groundwater in Australia on the other hand. Specifically, the lack of information may be attributed to the lack of suitable data representing the spatio-temporal variability of groundwater. For instance, previous Australian studies investigated the groundwater spatio-temporal variability using satellite and model products (see, e.g. *Chen et al.* 2016a), but the coarse spatial resolution makes the results less useful for local groundwater management. For Australian groundwater studies based on in-situ or isotope data (see, e.g. *Vanderzalm et al.* 2011; *Martinez et al.* 2015; *Keshavarzi et al.* 2016), such studies are very local and rarely provide useful spatio-temporal information due to the heterogeneity and discontinuity of hydrogeological data. As for the lack of knowledge, this may be attributed to the complex interactions of groundwater behaviours in relation to multiple hydroclimatic and hydrogeological factors. Most previous Australian studies only focused on the impacts of one or two factors (mostly climatic factors;

see, *Crosbie et al.* 2010; *Ali et al.* 2012) on groundwater instead of giving a comprehensive estimation. This thesis, therefore, seeks to address Australia's different groundwater issues through a deeper perspective, i.e. by providing groundwater spatio-temporal information at a suitable scale, and by improving the understanding of groundwater spatio-temporal variability in relation to hydroclimate and hydrogeology.

1.3 Australia's groundwater: Main concerns

Given that Australia's vast continent has different characteristics of population, industry, hydroclimate and hydrogeology, groundwater issues also appear differently in different regions. Currently, some of the main concerns about Australia's groundwater issues are: (i) climatic and anthropogenic impacts on groundwater, (ii) the necessity of groundwater for agricultural expansion, (iii) groundwater data deficiency and uncertainty, and (iv), unclear groundwater recharge threshold conditions. These are treated in detail in the following subsections.

1.3.1 Climatic and anthropogenic impacts on groundwater

Australia's groundwater decline is caused by a combination of climate change and anthropogenic impacts. Climate change associated with groundwater decline is mainly attributed to a decrease in rainfall and a rise in temperature. According to an Australian official report (*Bureau of Meteorology*, 2020b), the national average temperature of 2020 increased by 1.44 ± 0.24 °C compared to that of 1910. The winter rainfall in southwestern Australia decreased around 16% since 1970, while in southeastern Australia the decrease is 12%. Decreasing rainfall leads to fewer sources of groundwater recharge, while rising temperature contributes to increased evaporation from shallow aquifers, which ultimately results in lower groundwater levels. This is one of the major reasons that, during the millennium drought, southwestern and southeastern Australia's groundwater declines were the most pronounced (*Ali et al.*, 2012; *Chen et al.*, 2016b; *Schumacher et al.*, 2018). As for the anthropogenic impact on groundwater, e.g. groundwater abstraction, it is difficult to detect due to difficulties in data collection, e.g. many irregular groundwater abstractions are not recorded. Even if there are records, e.g. groundwater use statistics for each Australian State in *Bureau of Meteorology* (2020a), they are just summarised numbers without any detailed spatial and temporal information. The only information obtained is that southwestern and southeastern Australia are the areas with the most groundwater use in the country (*Bureau of Meteorology*, 2020a). Thus, the anthropogenic impact is certainly another major reason for groundwater decline, but detailed knowledge such as where anthropogenic impact occurs, and how the weight of influence compares to climate change, remains unclear in these regions.

1.3.2 Necessity of groundwater for agricultural expansion

Depending upon different climatic conditions, groundwater normally accounts for 1/5 to 1/3 of annual total water usage in Australia (*Bureau of Meteorology*, 2021). Among the various uses of groundwater, agriculture accounts for the largest proportion, i.e. about 70% of groundwater is used for irrigation and livestock (*Harrington and Cook*, 2014). Specific to the Australian states, New South Wales and Western Australia are, respectively, the largest and the second-largest groundwater users in agricultural fields (*Bureau of Meteorology*, 2021). However, agricultural development is limited due to climate change and groundwater decline in both states. The new spotlight of agricultural expansion, therefore, is on the Northern Territory (NT), a vast land (17.5% of Australia's area) but with only around 1% of the Australian population, with an increasing trend of rainfall (*Bureau of Meteorology*, 2020b) and the least groundwater usage among all states (*Bureau of Meteorology*, 2021), considered a place with great potential for the expansion of irrigated agriculture (*Ash et al.*, 2017). Although the Australian government also has intentions to expand the scale of irrigated agriculture in the NT, the process of agricultural expansion has been delayed due to concerns about the unsustainable development of agriculture (*Thomas et al.*, 2018). Considering that almost all agricultural water in the NT comes from groundwater (*Kinsela et al.*, 2012; *Bureau of Meteorology*, 2018, 2021), the lack of groundwater spatio-temporal information and the missing linkages between groundwater availability and crop water demands are some of the main reasons hindering agricultural expansion.

1.3.3 Groundwater data deficiency and uncertainty

In Australia, borehole observation is the most commonly used data with which to provide spatio-temporal information in official reports, see, e.g. 'Water in Australia 2019-20' (*Bureau of Meteorology*, 2021). Unlike other continents where borehole information is scattered or poorly organised, Australia's borehole information is well organised and freely available from an online application, called 'The Australian Groundwater Explorer' (see web address: `http://www.bom.gov.au/water/groundwater/explorer/map.shtml`). This application provides information on more than 850,000 borehole logs (see Figure 1.3a), but it is worth noting that only about 30,000 (around 3.5%) of these boreholes contain groundwater-level records (see Figure 1.2b; *Hu et al.* 2022a). After further filtering, such as excluding data that is discontinuous or too old (e.g. collected before 1980), the final estimated number of available boreholes that can be used for academic research is only 17,569 (2%). Given that spatio-temporal information on groundwater is fundamental to groundwater management, this number of boreholes is far from enough for the management of Australia's groundwater resources.

The Gravity Recovery and Climate Experiment (GRACE; *Tapley et al.*

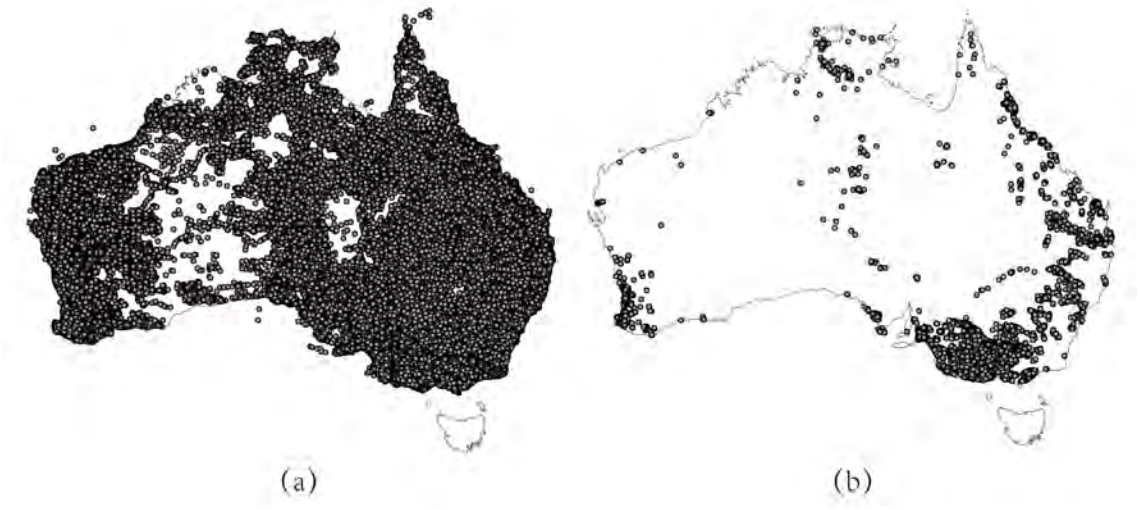

Figure 1.3: Borehole spatial distribution over the Australian continent: (a) all boreholes, and (b), boreholes with groundwater monitoring records.

2004) satellites launched in 2002 are commonly used for collecting alternative data that provides groundwater spatio-temporal information on a large scale, see, e.g. *Awange et al.* (2009); *Feng et al.* (2013); *Döll et al.* (2014); *Hu et al.* (2017); *Agutu et al.* (2019). Compared to borehole observations, GRACE has the advantage that it provides water-equivalent height changes in groundwater with complete global spatial coverage and is freely available. The disadvantage of GRACE, however, is that its coarse spatial resolution, i.e. approximately 400 km × 400 km, makes its observations difficult to apply in local areas, e.g. areas less than 200,000 km^2 (*Frappart and Ramillien*, 2018). Furthermore, GRACE itself only measures tiny variations in terms of the Earth's gravity field, which are interpreted as terrestrial water storage changes (TWSC; *Tapley et al.* 2004). GRACE should be used in combination with external datasets, such as a hydrological model (such as GLDAS; *Hu et al.* 2017) for removing other components of water, e.g. soil moisture, surface water, the canopy and snow, in order to obtain groundwater storage changes (*Cao et al.*, 2015; *Castellazzi et al.*, 2016; *Hu et al.*, 2017). During this process, uncertainties will be introduced since most of these parameters in the hydrological models are simulated (*Qiao et al.*, 2013; *Chen et al.*, 2016a). The GRACE-derived groundwater spatio-temporal information, therefore, usually requires validation by comparison with other models or with in-situ data.

Hydrological models are able to flexibly provide groundwater spatio-temporal information from local (see, e.g. *Yin et al.* 2020) to global (see, e.g. *de Graaf et al.* 2015; *Li et al.* 2019a; *Schmied et al.* 2021) scales. Typically, these groundwater models use equations to describe or simulate physical processes of the water cycle, such as the infiltration process from rainfall to groundwater, or the balance between incoming and outgoing hydrological water fluxes. Therefore, as long as some parameters (forcing/input data) in these equations are known, e.g. rainfall and evaporation, the unknown parameters can be de-

rived, e.g. groundwater. Based on this principle, some hydrological models can have vast and fine spatio-temporal coverage and resolution, for instance, the Global Land Data Assimilation System (GLDAS) products have 0.25° × 0.25° spatial and daily temporal resolution (*Li et al.*, 2019b). Nevertheless, uncertainties still arise in all kinds of models, due to the fact that (i) the forcing/input data also have uncertainties (*Rojas et al.*, 2010), (ii) many physical processes are difficult to formulate perfectly due to lack of knowledge or data, e.g. groundwater flow within the aquifer and the influence of geological conditions at different depths on groundwater are usually unclear, and (iii), different groundwater models may perform differently even for the same study region, depending on the forcing data used, the way and the complexity of modelling (*Von Freyberg et al.*, 2015). Eventually, the groundwater spatio-temporal results derived from the model still need to be verified using in-situ observations, which unfortunately are not yet available in many areas.

1.3.4 Unclear groundwater recharge threshold conditions

The main task of groundwater management is to maintain groundwater at a reasonable level and prevent it from rising or falling excessively. However, this task is not easy, because we have little control over climatic and hydrogeological conditions that determine the behaviour of groundwater recharge/discharge. A common way on how to address this is to adapt the groundwater management plan according to the climatic and hydrogeological conditions.

For adaption of the management plans, information on groundwater recharge conditions and their thresholds is important. The former represents the influencing factors that control groundwater recharge and can be used to understand the recharge mechanism, while the latter implies the necessary values for these conditions that trigger groundwater recharge, i.e., groundwater level can only rise if the condition value exceeds its threshold, and thus, it is commonly used to predict groundwater recharge timing and help managers improve plans (*Moeck et al.*, 2020). Despite the fact that wetness of unsaturated zone is theoretically the best indicator of groundwater recharge/discharge, such data are not available. Instead, previous studies, e.g., *Kumar* (2012); *Tang et al.* (2013); *Fu et al.* (2019); *Moeck et al.* (2020), have indicated that rainfall, evaporation, soil, runoff and vegetation could also be used as main potential groundwater recharge threshold conditions. For instance, groundwater recharge can be regarded as a process by which rainfall infiltrates from the surface to the ground, and thus the spatio-temporal changes of rainfall usually determine the variations of groundwater (*Taylor et al.*, 2013b; *Jasechko et al.*, 2014; *Jasechko and Taylor*, 2015). *Fu et al.* (2019) have stated that rainfall is the most important factor for groundwater recharge in Australia. Evaporation is the major output of the land-water cycle, which usually determines the amount of rainfall involved in the infiltration process (*Nanteza et al.*, 2016; *Hu et al.*, 2017; *Zhong et al.*, 2020). When rainfall reaches the ground, soil usually is the first layer to infiltrate. The rate of infiltration depends mainly on the texture and

hydraulic properties of the soils, e.g. grain size, porosity, water saturation amongst others (*Arye et al.*, 2011; *Preeja et al.*, 2011; *Das*, 2017). Some soil types are even impermeable, which prevents groundwater from recharging vertically (*Sandoval and Tiburan Jr.*, 2019). Surface runoff occurs when rainfall intensity is greater than the infiltration rate or when soil water is already saturated and rainfall continues. The significance of surface runoff for groundwater recharge is that it transfers excess rainwater from one region to another, such as streams, rivers, and floods, allowing groundwater to be recharged even without rainfall, though it also brings the risk of contamination (*Voisin et al.*, 2018). According to *Koirala et al.* (2017), vegetation can both help and prevent groundwater recharge. On the one hand, the roots of vegetation create cracks or channels in the soil that increase infiltration rates (*Ilstedt et al.*, 2016). On the other hand, vegetation needs to absorb water from the soil to survive, and thus, studies such as by *Oliverira et al.* (2016) have found a negative relationship between groundwater recharge and increasing vegetation. Unfortunately, even with clear knowledge about every step of the infiltration process, the combined effects of these factors in the unsaturated zone, e.g., each factor's influence varying in space and time, remains unclear.

1.4 Knowledge gaps and challenges

1.4.1 Understanding groundwater decline in relation to climate change and anthropogenic impacts in South-West Western Australia

Section 1.3.1 has indicated that southeastern and southwestern Australia's groundwater declines are caused by a combination of climate change and anthropogenic impacts. Given that much of Australia's population, agricultural production, and valuable ecosystems are located in southeastern Australia, its issues of groundwater decline have received a lot of attention after the millennium drought (see, e.g. *Crosbie et al.* 2010; *van Dijk et al.* 2013; *Wheeler et al.* 2014; *Chen et al.* 2016b; *Schumacher et al.* 2018; *Fu et al.* 2019; *Gonzalez et al.* 2020). Even now, these discussions are still being updated annually (see, e.g. *Colloff and Pittock* (2022)). Compared to southeastern Australia, the issue of groundwater decline in southwestern Australia requires more attention, given the high reliance on groundwater (accounting for 60-70% of total water usage; *Harrington and Cook* 2014).

From a population, agricultural and industrial concentration perspective, most previous groundwater studies in southwestern Australia are located in south-west Western Australia (the Perth Basin), see, e.g. *Ali et al.* (2012); *McFarlane et al.* (2020). Although studies such as *Ali et al.* (2012); *Skurray et al.* (2012) have investigated the impact of climate change on groundwater, the discussions are either about modelling groundwater trends under future climate change or policy issues. Useful spatio-temporal groundwater information

is not provided across south-west Western Australia (SWWA) but is scattered across a small number of local studies represented by limited boreholes (*McFarlane et al.*, 2012; *Hughes et al.*, 2012). Spatial indications of anthropogenic impacts on groundwater are also missing, except that the Gnangara groundwater system (in the northern Perth Basin) is known to be most affected by groundwater extraction (*Bekesi et al.*, 2009). In addition, from the perspective of groundwater decline outcomes, climate change and anthropogenic impacts are mixed, and no previous studies have attempted to clarify which one is the main cause of groundwater decline in SWWA. Without this information, groundwater management plans can easily be incorrect by misunderstanding the main drivers of groundwater decline.

1.4.2 Understanding the balance between groundwater use and agricultural expansion in the Northern Territory

As described in section 1.3.2, given that groundwater is the only reliable water resource for irrigated agriculture in the NT, estimates of the balance between groundwater availability and crop water demand provide key information with which to drive agricultural development. However, such estimates are challenging, due to the insufficient groundwater spatio-temporal information on the one hand, and the complex estimations of crop water demand on the other hand. For instance, the NT government has made its efforts on delineating water control districts and producing detailed reports of water resources over the past ten years, see, e.g. *Ti Tree Water Report* (2009); *Oolloo Water Allocation Plan* (2010); *Northern Territory Government* (2018). Nevertheless, these results are still insufficient compared to the vast area of NT, resulting in little agricultural land being released for expansion. As for the evaluation of irrigated agricultural water demands, it is difficult particularly on a large scale since different crops require different amounts of irrigated water in different spaces and time (*McMahon et al.*, 2013). In the NT, such evaluation has only been done in some water control districts through long-term experiments (see, e.g. *Bithell and Smith* 2011; *MacFarlane and Fairfield* 2017). Additionally, the groundwater availability and crop water demand are usually separate studies, and the linkage between them is not established in the NT.

1.4.3 Development and testing of a new approach by which to infer groundwater spatio-temporal distribution in data deficient areas

Previously, Section 1.3.3 introduced three products for providing groundwater spatio-temporal information: in-situ data, GRACE satellites, and hydrological models. However, these products have some shortcomings, such as limited coverage, coarse spatial resolution and unreliability, which cannot provide accurate Australia's groundwater spatio-temporal information while

maintaining sufficient spatial resolution.

In recent years, data assimilation techniques have been frequently used, and some studies have attempted to incorporate in-situ observations and GRACE data into models (see, e.g. *Panzeri et al.* 2016; *Rasmussen et al.* 2016; *Li et al.* 2019a) to make groundwater spatio-temporal information more accurate and reliable. For instance, the Global Land Data Assimilation System (GLDAS) Catchment Land Surface Model (CLSM; version 2.2) with data assimilated from GRACE (hereafter called GLDAS-DA) provides groundwater storage estimates in shallow aquifers (*Li et al.*, 2019a). Its $0.25° \times 0.25°$ spatial resolution is finer than that of GRACE, and the evaluation using in-situ data shows a 36% error reduction and 16% correlation improvement compared to the original model without data assimilation (*Li et al.*, 2019a). To some extent, this addresses the groundwater data deficiency and uncertainty issues. However, for those regions without in-situ data as validation, the reliability of the model is still unknown. Inspired by the geographic information system (GIS), many studies have used knowledge-based inversion analysis for very high spatial resolution of groundwater potential mapping (*Adiat et al.*, 2012; *Mananp et al.*, 2013; *Nouayti et al.*, 2019); for example, sandstone is empirically a sign of groundwater storage potential because of its high porosity and permeability in general, and according to this knowledge and inversion analysis, the sandstone distribution from geological data may provide the spatial location of groundwater to some extent. Similarly, topography and climate could also offer such information to allow inferring groundwater spatio-temporal behaviours without using actual groundwater monitoring data. Therefore, by comparing the inferred results with hydrological models (independent evaluation), and examining their linkages both spatially and temporally, the uncertainty of groundwater spatio-temporal information can be reduced or found. Nevertheless, this approach has not been proposed and tested before. Furthermore, given that knowledge-based inversion analysis procedures usually vary according to different hydroclimatic and hydrogeological conditions, it is challenging to design a universal approach by which to infer groundwater spatio-temporal information at various scales or conditions.

1.4.4 Understanding of groundwater recharge threshold conditions across the Australian continent

Groundwater recharge threshold conditions provide key information for aquifer management, as mentioned in Section 1.3.4, yet such information is rarely investigated in Australia. Previous studies, e.g. *Fu et al.* (2019), discussed the impact of climatic and non-climatic conditions on groundwater recharge in southeastern Australia, but did not provide the threshold values or rank the weights of influence for each condition on groundwater. Some studies, e.g. *Baker et al.* (2020), did provide the threshold value of rainfall for local regions, but ignored the possibility that other conditions may also have a certain impact on groundwater recharge. To the best of the authors'

knowledge, the quantification of groundwater recharge threshold conditions for both large-scale and multiple conditions in Australia has never been done before. This is due to the difficulty of handling big data and relationships among multiple variables, thus requiring some more advanced computational techniques. Machine learning is well known for its powerful capability to process big data and multiple relationships, which could be a suitable tool for solving the issue of quantifying groundwater recharge threshold conditions. Although, authors have not found any previous studies using machine learning classification techniques to quantify groundwater recharge threshold conditions, there have been many similar studies on threshold condition topics in other fields (see, e.g. *Miao et al.* 2011; *Belgiu and Drăgut* 2016; *Wu et al.* 2018; *Yang et al.* 2019). The challenge for machine learning techniques is the uncertainty in results from different data and method choices, requiring extensive testing and discussion.

1.5 Thesis objectives

The primary objective of this thesis, therefore, is to understand the spatio-temporal variability of groundwater and knowledge of its associated hydroclimate and hydrogeology, by filling the knowledge gaps identified in Section 1.4. The following list presents a short description of each objective, while for a more detailed introduction, we refer to the introductory pages of each Chapter.

(i) The climatic and anthropogenic impacts on groundwater spatio-temporal variability are investigated in south-west Western Australia (SWWA). The study put special efforts on organising the spatio-temporal information of groundwater from scattered boreholes, creating a long-term time series for 1980-2015, and spatial patterns of groundwater change in different seasons. Also, the linkages between climate variability/change and groundwater are investigated. The anthropogenic impacts on groundwater are further identified by finding the groundwater extraction hot spots.

(ii) The irrigated agricultural potential in the NT is evaluated through the balance between groundwater availability and crop water demands. On the one hand, the groundwater availability is calculated as the 20% of groundwater recharge/discharge due to the water policy of the '80-20 rules' claimed by the NT government (*MacFarlane and Fairfield*, 2017). On the other hand, the Food and Agriculture Organisation (FAO) Pennman-Monteith equation (*Allen et al.*, 1998) is used to estimate crop water demands. After that, the balance between groundwater availability and crop water demand is compared under scenarios of the average conditions between 2010 and 2019 and the 2019 dry period in order to obtain risk management information for climate extremes.

(iii) A knowledge-based approach for inferring groundwater spatio-temporal variability in data-deficient regions is proposed. The hydrological model

is used as 'background' data to provide spatio-temporal information of groundwater. The inversion analysis for rainfall, evaporation, topography and geology datasets play the role of reducing model uncertainty. To prove the reliability and generality of this approach globally, it is proposed in a data-deficient region, i.e. Lake Victoria Basin (Africa), and then tested in a data-rich region, i.e. Australian state of Victoria.

(iv) The groundwater recharge threshold conditions are quantified over the Australian continent. This is done through applying machine learning techniques such as classification tree (*Breiman et al.*, 1984), random forest (*Breiman*, 2001), and logistical regression (*Pregibon*, 1981). By using these techniques, the specific threshold values (monthly based) of each condition are provided in the format of a spatial map. Also, the possible groundwater recharge mechanism inferred by the different hydroclimatic and hydrogeological conditions is discussed.

1.6 Research outline

The structure of this thesis firstly begins with an introduction (Chapter 1) covering the background, knowledge gaps and objectives. The following Chapters 2-5 are the papers (4 peer-reviewed publications and 1 submitted manuscript; see Table 1) that correspond to each of the objectives in Chapter 1, with a brief description of their key findings. Finally, Chapter 6, concludes the overall contribution of this thesis and points out the future outlook.

Chapter 2
Understanding groundwater decline in relation to climate change and anthropogenic impacts in South-West Western Australia

This chapter is covered by the following publication (*Hu et al.* 2019):

1. **Hu, K.X.**, Awange, J.L., Kuhn, M. and Saleem, A., (2019). Spatio-temporal groundwater variations associated with climatic and anthropogenic impacts in South-West Western Australia. Science of The Total Environment, 696, 133599, doi: 10.1016/j.scitotenv.2019.133599.

This contribution addresses the groundwater decline issue in south-west Western Australia outlined in Section 1.4.1 and objective (i) in Section 1.5, by investigating the climatic and anthropogenic impacts on groundwater. Specifically, the groundwater level records from 2,997 boreholes and climate data are collected and organised. Subsequently, average long-term annual and monthly time series are generated for the 1980-2015 period, and the average monthly spatial patterns of groundwater change and rainfall are also presented through interpolation. The results suggest that climate variability/change appears to have less impact on groundwater than do anthropogenic influences, since the groundwater level continued dropping ever since the year of 2000 while annual and seasonal rainfall basically remained stable. This finding refreshes the understanding of groundwater in south-west Western Australia, as previous studies (e.g., *Ali et al.* 2012; *Skurray et al.* 2012) stressed too much on the impact of reduced rainfall after 1975 on the decline of groundwater levels. The serious level dropping only occurs around Perth regions where abnormal groundwater variations are frequently captured (hot spots) as the results of groundwater extraction. The monthly groundwater spatial patterns indicate that the recharge timing of groundwater is between May and August/September (correlating highly to rainfall), while the level reaches its maximum heights in September. Although the temporal correlation shows an average lag of 2-3 months between rainfall and groundwater variation, the spatial patterns show a different story, indicating the exitance of the threshold value for rainfall recharge groundwater in some regions. For instance, the groundwater recharge is found to immediately occur when rainfall value is above 60 mm/month in the southern part of Perth, but this phenomenon is identified as a lag in the correlation analysis and could easily lead to misunderstanding.

To avoid potential misunderstandings, two clarifications have been made for the publication presented in this Chapter:

(i) The BoM rainfall is a product based on in-situ interpolation, and thus, could have higher uncertainties over data sparse areas. The Multi-Source Weighted-Ensemble Precipitation (MSWEP) and Tropical Rainfall Measuring Mission (TRMM) products mentioned in Section 3.1.2, subsequently, were used to examine such uncertainty and to ensure the correctness of the spatial rainfall pattern in South-West Western Australia (SWWA).

(ii) The rainfall threshold for groundwater recharge found in SWWA is obtained through the visual inspection of spatial patterns of rainfall and groundwater. Considering other factors such as evaporation, soil moisture, runoff and vegetation that could also determine recharge/discharge, the rainfall threshold here may not be the most representative threshold to distinguish groundwater recharge/discharge. For the discussion about multiple threshold conditions, we refer to Chapter 5.

Science of the Total Environment 696 (2019) 133599

Contents lists available at ScienceDirect

Science of the Total Environment

journal homepage: www.elsevier.com/locate/scitotenv

Spatio-temporal groundwater variations associated with climatic and anthropogenic impacts in South-West Western Australia

K.X. Hu[a,*], J.L. Awange[a,b], M. Kuhn[a], A. Saleem[a]

[a] School of Earth and Planetary, Spatial Science Discipline, Curtin University, Perth, Australia
[b] Geodetic Institute, Karlsruhe Institute of Technology, Engler-Strasse 7, D-76131 Karlsruhe, Germany

HIGHLIGHTS

- Hotspots, i.e., regions of extreme SWWA's groundwater change are identified.
- Recharge threshold for coastal areas of SWWA is about 60–70 mm/month of rainfall.
- Coastal groundwater recharge are affected by low ENSO/IOD rainfall.
- Terrain, scarps and dams majorly impact SWWA's groundwater behaviour.
- Abstraction primarily caused noticeable central coastal SWWA groundwater decline.

GRAPHICAL ABSTRACT

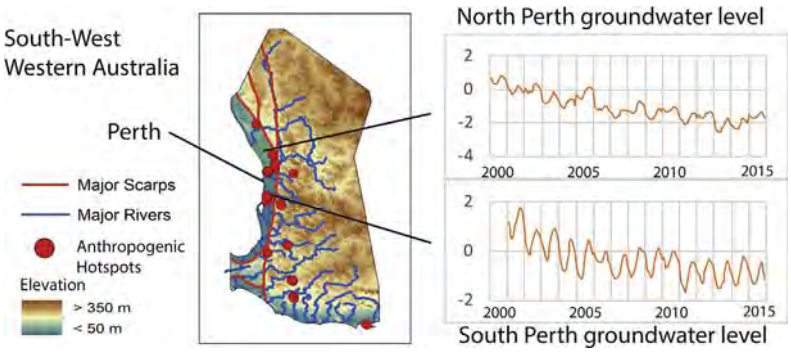

ARTICLE INFO

Article history:
Received 28 May 2019
Received in revised form 24 July 2019
Accepted 24 July 2019
Available online 2 August 2019

Editor: Ouyang Wei

Keywords:
Australia
Groundwater
Climate variability/change
Anthropogenic impacts

ABSTRACT

South-West Western Australia (SWWA) is a critical agricultural region that heavily relies on groundwater for domestic, agricultural and industrial use. However, the behaviours of groundwater associated with climate variability/change and anthropogenic impacts within this region are not well understood. This study investigates the spatio-temporal variability of groundwater in SWWA based on 2997 boreholes over the past 36 years (1980–2015). Results identify the decline in groundwater level (13 mm/month) located in the central coastal region of SWWA (i.e., north and south of Perth) to be caused by anthropogenic impacts (primary factor) and climate variability/change (secondary). In detail, anthropogenic impacts are mainly attributed to substantial groundwater abstraction, e.g., hotspots (identified by above 7 m/month groundwater level change) mostly occur in the central coastal region, as well as close to dams and mines. Impacts of climate variability/change indicate that coupled ENSO and positive IOD cause low-level rainfall in the coastal regions, subsequently, affecting groundwater recharge. In addition, correlation between groundwater and rainfall is significant at 0.748 over entire SWWA (at 95% confidence level). However, groundwater in northeastern mountainous regions hardly changes with rainfall because of very small amounts of rainfall (average 20–30 mm/month) in this region, potentially coupled with terrain and geological impacts. A marked division for groundwater bounded by the Darling and Gingin Scarps is found. This is likely due to the effects of the Darling fault, dams, central mountainous terrain and geology. For the region south of Perth and southern coastal regions, a hypothesis through multi-year analysis is postulated that rainfall of at least 60 and 65–70 mm/month, respectively, are required during the March–October rainfall period to recharge groundwater.

* Corresponding author.
E-mail address: kexiang.hu@postgrad.curtin.edu.au (K. Hu).

https://doi.org/10.1016/j.scitotenv.2019.133599
0048-9697/

1. Introduction

South-West Western Australia (SWWA; 28.5°–35.5° S; 114.5°–118° E, Fig. 1), is an essential agricultural region of Western Australia that supports the livelihood of about 65% of its total population (1.7 million; ABARES, 2018; Population Australia, 2018). It relies heavily on rain-fed and irrigated agriculture, e.g., producing cereal crops such as wheat and canola besides sheep grazing for wool production (ABARES, 2018; Hill et al., 2004). In the period 2016–2017, the gross value of agricultural production of Western Australia was $8.5 billion, of which 80% was exported to overseas markets (Agriculture and Food, 2018). Although this region is vital for its agricultural productivity, frequent droughts have caused heavy reliance on groundwater, which now accounts for about 75% of the total water usage in Western Australia (see, e.g., CSIRO, 2009; Ali et al., 2012).

Groundwater is not only a valuable resource that supports agriculture, domestic water supplies and industries in Western Australia (Taylor et al., 2013; Tregoning et al., 2012). It also plays a crucial role in aquatic ecosystems that have interconnections with surface water (Argent, 2016). This feature allows ecosystems to maintain their functions by replenishing river and stream flows through groundwater during dry periods (Kinal and Stoneman, 2012). Many studies, e.g., Barron et al. (2011), Dawes et al. (2012), Hughes et al. (2012), Kinal and Stoneman (2012), Ali et al. (2012), and Eamus (2015), indicate that groundwater levels are decreasing in SWWA due to decline in rainfall since 1975 on the one hand, and increased demands for water use on the other hand. For example, water levels in the Gnangara groundwater system have declined over the past 40 years due to over-abstraction (see, e.g., Featherstone et al., 2012; Awange, 2012; Awange and Kiema, 2013; Department of Water, 2015; Awange, 2018; Awange and Kiema, 2019). The current decline and abstractions are not sustainable, i.e., natural recharge is not keeping pace with human abstraction (Department of Water, 2015). Anthropogenic impacts such as human abstraction, land use and land cover change (LULC) together with drier climate are exerting pressure on SWWA's groundwater (CSIRO, 2009). Accurate knowledge of spatio-temporal variability of SWWA's groundwater as well as impacts of climate variability/change and anthropogenic activities, therefore, is important for water management, conservation, and to inform plans and policies governing its use.

However, understanding the spatio-temporal variability of groundwater can be challenging due to the limitations in groundwater data and their coarse spatio-temporal resolution. Currently, studies of groundwater variability are based on two main data sources; (i) local in-situ data (i.e., borehole data), e.g., Hughes et al. (2012), Tweed et al. (2007), and (ii), satellite-based Gravity Recovery and Climate Experiment (GRACE) data combined with hydrological or reanalysis models, e.g., Strassberg et al. (2009), Leblance et al. (2009), Chen et al. (2016), Hu et al. (2017). Generally, borehole data are more useful for temporal groundwater change analysis rather than study of its spatial variability (see, e.g., Hughes et al., 2012; Tweed et al., 2007) due to the complexity of spatial interpolation between boreholes, e.g., Sun et al. (2009). Tregoning et al. (2012) note that spatial interpolation of groundwater levels requires a large amount of data with sufficient density. Otherwise, the high spatial variability in the groundwater system and its complex storage dynamics make local measurements unsuitable for interpretation over a large area, and as such, introduces considerable uncertainties. GRACE-based groundwater spatio-temporal studies, on the one hand, are unable to capture the small-scale localized hydrological signals due to its coarse spatial resolution (Awange et al., 2011, 2010). On the other hand, the uncertainties of meteorological forcing inputs in the associated hydrological models degrade their derived groundwater outputs (Tregoning et al., 2012; Bhanja et al., 2016).

In addition, climate variability/change produces significant impacts on groundwater recharge. Rainfall as the main source of groundwater strongly influences its spatio-temporal variations (Hu et al., 2017), while rainfall itself is affected by climate variability/change, such as El Niño Southern Oscillation (ENSO) and Indian Ocean Dipole (IOD) (Forootan et al., 2016). A relation between groundwater and ENSO/IOD may exist, e.g., Holbrook et al. (2009) indicate that ENSO cycles have impacts on the recharge of groundwater near the coastline (see, e.g., Anyah et al., 2018). Although anthropogenic impacts on groundwater are apparent over SWWA (Department of Water, 2015), previous studies mainly focused on hydro-chemical properties, such as the age of groundwater and pollution levels (e.g., Suh et al., 2003; Han et al., 2017), rather than providing spatio-temporal details. Despite the requirement of spatio-temporal variability information on groundwater over SWWA to inform its sustainable use, studies that comprehensively undertake its analysis are currently lacking.

The aim of this study, therefore, is to undertake a spatio-temporal variability analysis of groundwater over SWWA over the past 36 years (1980–2015), through the exploitation of statistical methods of Man-Kendall test, cross-correlation, cross-validation, Kolmogorov-Smirnov test, and regression analysis to analyse 2997 borehole and precipitation data in order to (i) assess the long-term and seasonal variability trends on the one hand, and the timing of low and high groundwater availability on the other hand, (ii) analyse spatial patterns of variations and recharge/discharge, and (iii), understand impacts of climate variability/change, and identify long-term anthropogenic impacts and "hotspots" (i.e., areas of substantial abstractions).

2. Study area: South-West region of Western Australia

The study area (South-West Western Australia; SWWA; Fig. 1a) is selected based on the distribution of available boreholes (Fig. 1b), with the northern part extending up to the town of Cervantes and the Yalgoo mountainous region (Fig. 1c), and the southern part extending to the Albany coastline. Rainfall commences intermittently in March, but most of the annual rainfall falls between May and September (Ali et al., 2012; CSIRO, 2009). There is a south-west to north-east decreasing gradient in annual rainfall from around 1200 mm along the south-west coast to 350 mm in the north-east mountainous areas (CSIRO, 2009). There is also a low inter-annual variability compared to other regions in Australia (Nicholls et al., 1997; CSIRO, 2009). Previous studies, e.g., Barron et al. (2011), Dawes et al. (2012), indicate that the rainfall totals in SWWA decreased by around 20% between the late 1960s and early 1970s due to climate change and land cover changes. More details on rainfall in SWWA, such as the spatial patterns and trends can be found, e.g., in Ali et al. (2012), CSIRO (2009).

As for topographical features of SWWA, the Perth basin and Darling Plateau are divided by the Darling and Gingin Scarps (see Fig. 1c). These two scarps affect groundwater behaviour since there is on average a 200 m difference in elevation across them. Also, different geological features (sandstones in the coastal plain and granite in the hills) to the west and east of these two major scarps affect groundwater recharge/discharge (see e.g., geology and hydrogeology in CSIRO, 2009). However, since our study focuses only on groundwater behaviours (i.e., changes) and their relation to climatic and anthropogenic impacts, links to detailed geology and different aquifer formations are not discussed further here. In regions around Blackwood Plateau (Fig. 1c), Whicher Scarp to the north and Barlee Scarp to the south exist. Generally, elevation changes are highest in the northeast and lowest in the southwest for SWWA, and the groundwater naturally flows from the eastern sides of the Darling and Gingin Scarps into the coastal plains due to the effects of the hydraulic gradient (see Fig. 1c).

The Gnangara groundwater system provides the most substantial groundwater, supporting almost 50–60 % of the water use in SWWA

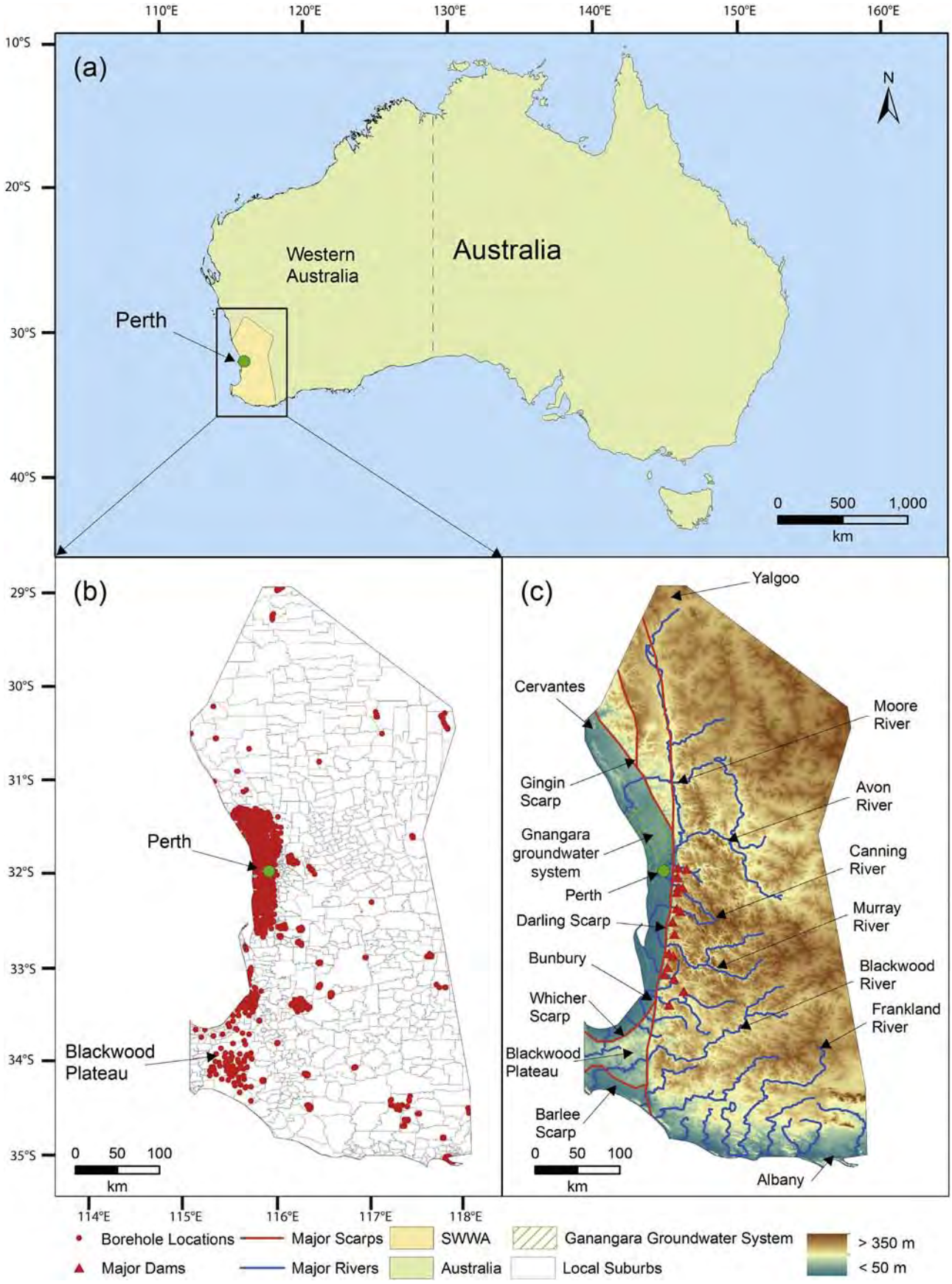

Fig. 1. Spatial features of SWWA; (a) location, (b) borehole distribution, and (c) major dams, rivers, scarps, and elevation, as well as the location of the Gnangara groundwater system. A high density of borehole data exists to the north and south of Perth, as well as Bunbury and the Blackwood Plateau. Darling and Gingin Scarps and many dams in the central SWWA affect groundwater behaviour between the coast and mountainous regions. Panel (c) is reproduced and modified according to CSIRO (2009) and Ali et al. (2012).

(see location in Fig. 1c, Skurray et al., 2012; Department of Water, 2015). However, Awange (2012), Awange and Kiema (2013), Department of Water (2015), Awange (2018), Awange and Kiema (2019) indicate that many parts of the Gnangara system are currently over-allocated and the groundwater level has declined continuously over the past 40 years. On the one hand, this situation creates significant pressure on and risk to local ecosystems. On the other hand, there are many dams located along the eastern side of the central Darling Scarp (see Fig. 1c), which provide resources for domestic water use, acting as artificial buffers. They play an important role in storing water during low demand during the rainy seasons and then discharging them during dry periods. These dams may have an influence on groundwater in the nearby regions due to the fact that there exist interconnection between groundwater and surface water. This interconnection is considered to be an anthropogenic impact, given that nearby groundwater levels tend to follow variations in the dam levels.

3. Data and methods

3.1. Data

3.1.1. Borehole data

Borehole data are acquired from "The Australian Groundwater Explorer", which is a web-based mapping application (see online: http://www.bom.gov.au/water/groundwater/explorer/) that provides groundwater level monitoring information. All downloaded available records date back to approximately 1900, while most data are after preprocessing concentrated within the 1980–2015 period. For further processing data from only this period have been considered. The groundwater level for each borehole is in daily format, instantaneous and discontinuous records, and therefore requires pre-processing into monthly, continuous records (see Section 3.2.1). The standing (or static) water level (SWL; representing measurements from the reference point on the bore, e.g., the top of casing, to the groundwater table; see detailed explanation at http://www.bom.gov.au/water/groundwater/explorer/faq.shtml) is selected to investigate spatio-temporal variations of groundwater. In addition, this study is only concerned with the variation of the SWL irrespective of the borehole's depth and the surrounding geology. This is due to the fact that our study mixes data for different aquifers and different depths, and as such could lead to erroneous interpretations between groundwater changes and geology.

3.1.2. Rainfall products

Bureau of Meteorology (BoM) rainfall data with spatial 0.25° (1980–2006), 0.05° (2007–2015) and monthly temporal resolutions are available from the Australian Government. The BoM data are generated by interpolating rain-gauge stations Australia-wide and is considered the most reliable rainfall product in Australia (Fleming et al., 2011; Fleming and Awange, 2013). Besides, use is made of the Multi-Source Weighted-Ensemble Precipitation (MSWEP), available from 1980 to 2015. MSWEP is a global rainfall dataset with 0.1° and monthly spatial and temporal resolutions, respectively. Version 2.1 of the MSWEP product validated for Australia by Awange et al. (2019) merges the highest quality rainfall data sources (BoM is not included in MSWEP, Beck et al., 2017a,b), and as such are used to check the consistency of BoM products used in this study. Here, the BoM data for the period 2007–2015 with 0.05° spatial resolution are re-scaled to a resolution of 0.25° in order to match the spatial resolution with the previous period of 1980–2006. MSWEP data are also re-scaled to a resolution of 0.25° to match those of BoM. The results show that there is almost no difference (average 2.5 mm monthly difference and 0.997 correlation at 95% confidence level) between the BoM and MSWEP datasets over SWWA. Similar results between BoM and Tropical Rainfall Measuring Mission (TRMM) 3B43 are also found in Fleming et al. (2011), Fleming and Awange (2013), thus indicating the consistency of the BoM rainfall product, which is subsequently used in this study. The monthly BoM data are downloaded from http://www.bom.gov.au/jsp/awap/rain/archive.jsp?colour=colour&map=totals&period=month&area=nat, while the MSWEP data are downloaded from http://www.gloh2o.org/.

3.1.3. Climate indices

Multivariate El Niño-Southern Oscillation Index - (MEI) is derived from tropical Pacific COADS (Comprehensive Ocean-Atmosphere Data Set) records, which is a combination of six observed variables over the tropical Pacific and includes sea-level pressure, surface zonal, and meridional wind components, sea surface temperature, and cloudiness (Wolter and Timlin, 1998). The Dipole Mode Index (DMI) measures the difference between the area mean sea surface temperature anomalies in the IODW (western equatorial Indian Ocean; 50°E–70° E and 10°S–10° N) and IODE (southeastern equatorial Indian Ocean; 90°E–110° E and 10°S–0° N, Saji and Yamagata, 2003; Cai et al., 2011), which is used to monitor the Indian Ocean Dipole (IOD). In this study, MEI and DMI are compared to BoM rainfall, and borehole derived groundwater variations in order to assess climate variability/change impacts on groundwater for the 1980–2015 period.

3.2. Methods

This section presents the pre-processing steps for the borehole data and the subsequent analysis methods employed.

3.2.1. Borehole data pre-processing

The downloaded borehole groundwater level data are pre-processed in 3 steps to obtain continuous records between 1980 and 2015 as described below:

1. **Data cleaning and selection**: Duplicate data are removed, and only the standing water level (SWL) measurements of groundwater are selected for further analysis.
2. **Generate monthly data**: Convert daily instantaneous records into monthly by averaging all available daily data for a particular month. The monthly data may still be discontinuous because of missing records leading to unequal weight and bias when analysing average monthly groundwater variations.
3. **Select data with continuous 12 months' records in a year scale**: Retain monthly data only if the 12 months' records are complete in a year.

After pre-processing, records from a total of 2997 out of 3540 borehole stations (i.e., around 85% of the data) are used. Note, however, that most of the borehole records only cover 1 to 3 years within the study period 1980–2015, with only a few boreholes covering more than 10 years. When using various merging or interpolation methods (see details of interpolation methods in Section 3.2.3) to capture the spatio-temporal variations and trends over the 36 years in SWWA, uncertainties and biases cannot be avoided and are, therefore, discussed in the results Section 4.4.

3.2.2. Monthly anomalies

Fig. 2 presents the analysis and processing flow chart of borehole data. Here, borehole data are processed in two slightly different ways: (1) inter-annual variation of annual cycles (referred here as "annual cycle variation" as a short hand) to analyse changes of the annual cycle over time (e.g. from year-to-year), and (2), monthly anomalies with respect to the long-term mean (i.e., 1980–2015) to analyse long-term trends. Both quantities are standardized (see details below) for ease of comparison between ground water and

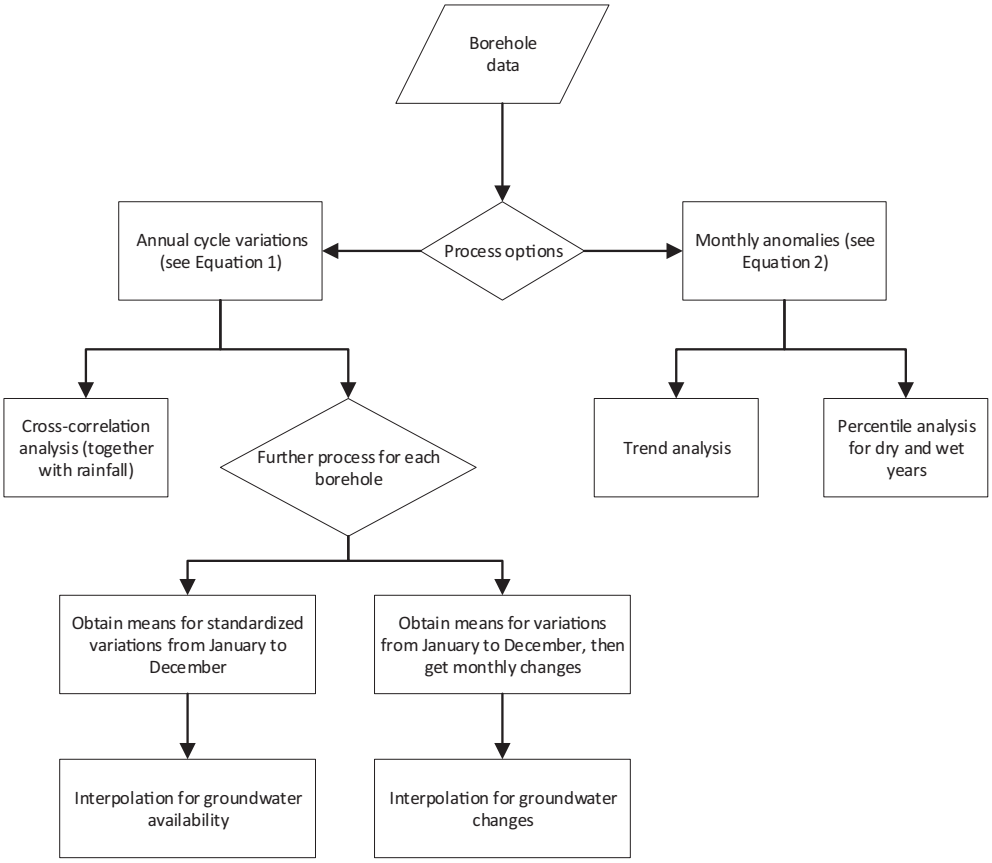

Fig. 2. Analysis and processing steps of borehole data.

rainfall data. Furthermore, results from (1) are used to spatially interpolate average monthly patterns of ground water availability and change.

Annual cycle variations for groundwater data are derived from monthly averages for a particular year by subtracting the average of that year, e.g.

$$y_m^{(i)} = -(y_i - \bar{y}_a); i = 1, \ldots, 12. \quad (1)$$

In Eq. (1), y_i are monthly averages where the index i indicates the month starting with $i = 1$ for January and $\bar{y}_a$ is the average of all monthly values in a particular year. The differences $y_m^{(i)}$ taken between y_i and $\bar{y}_a$ for each month, are used to characterise the annual cycle for a particular year. The negative sign on the right-hand side of Eq. (1) has been introduced to convert borehole observations (positive downwards) to SWL values (positive upwards). Applying this principle to individual borehole records results in annual cycle variations for each borehole. It is worth mentioning that the quantities $y_m^{(i)}$ do not contain long-term trends and variations (e.g. beyond one year), thus they are considered here to be better suited to study inter-annual variations. Furthermore, the same principle is applied to rainfall data, though without the negative sign as described above.

Monthly anomalies for groundwater data are derived from monthly averages by subtracting the long-term average (i.e., 1980–2015), e.g.,

$$y_{ma}^{(i)} = -(y_i - \bar{y}_p); i = 1, \ldots, N \times 12. \quad (2)$$

In Eq. (2), $\bar{y}_p$ is the long-term average for the complete data period considered. The monthly anomalies $y_{ma}^{(i)}$, taken between y_i and $\bar{y}_p$ for each month, are used to characterise long-term changes (e.g. trends or variations). Note that the index i is now running until $N \times 12$, with N being the number of years covered by a borehole record. Again, the negative sign on the right-hand side of Eq. (2) follows the same reasoning as given above and all monthly anomalies are averaged to obtain average monthly anomalies (for SWWA or a sub-region). It is worth mentioning that the quantities $y_{ma}^{(i)}$ preserve long-term trends and variations, thus are used here to derive linear trends.

The quantities $y_m^{(i)}$ and $y_{ma}^{(i)}$ are further used to derive spatial averages over a given region (either SWWA or a sub-region) and standardized to obtain average annual cycle variations or average monthly anomalies (see Fig. 3). The standardization has been done by, e.g.,

$$Z = \frac{X - \mu}{\sigma} \quad (3)$$

where X is the value that is being standardized, μ the mean of the distribution and σ the standard deviation of the distribution.

In addition, cross-correlation (Knapp and Carter, 1976) measures the similarity between one vector and shifted (lagged) copies of another vector as a function of the lag. In this study, cross-correlation is used to examine the relationships between groundwater and rainfall from the results of $y_m^{(i)}$. The lags are obtained between rainfall and groundwater when two variables reaches the maximum correlation. Linear trends are tested and calculated from the results of $y_{ma}^{(i)}$ using Mann-Kendall (MK) test (Mann, 1945) and ordinary least-squares method. At last, percentiles are calculated for both groundwater and rainfall from the results of $y_{ma}^{(i)}$ to identify drought years for the SWWA. Years with below the 25th percentile are identifer as dry years, while those above 75th are identified as wet years, see detailed method in Awange et al. (2008).

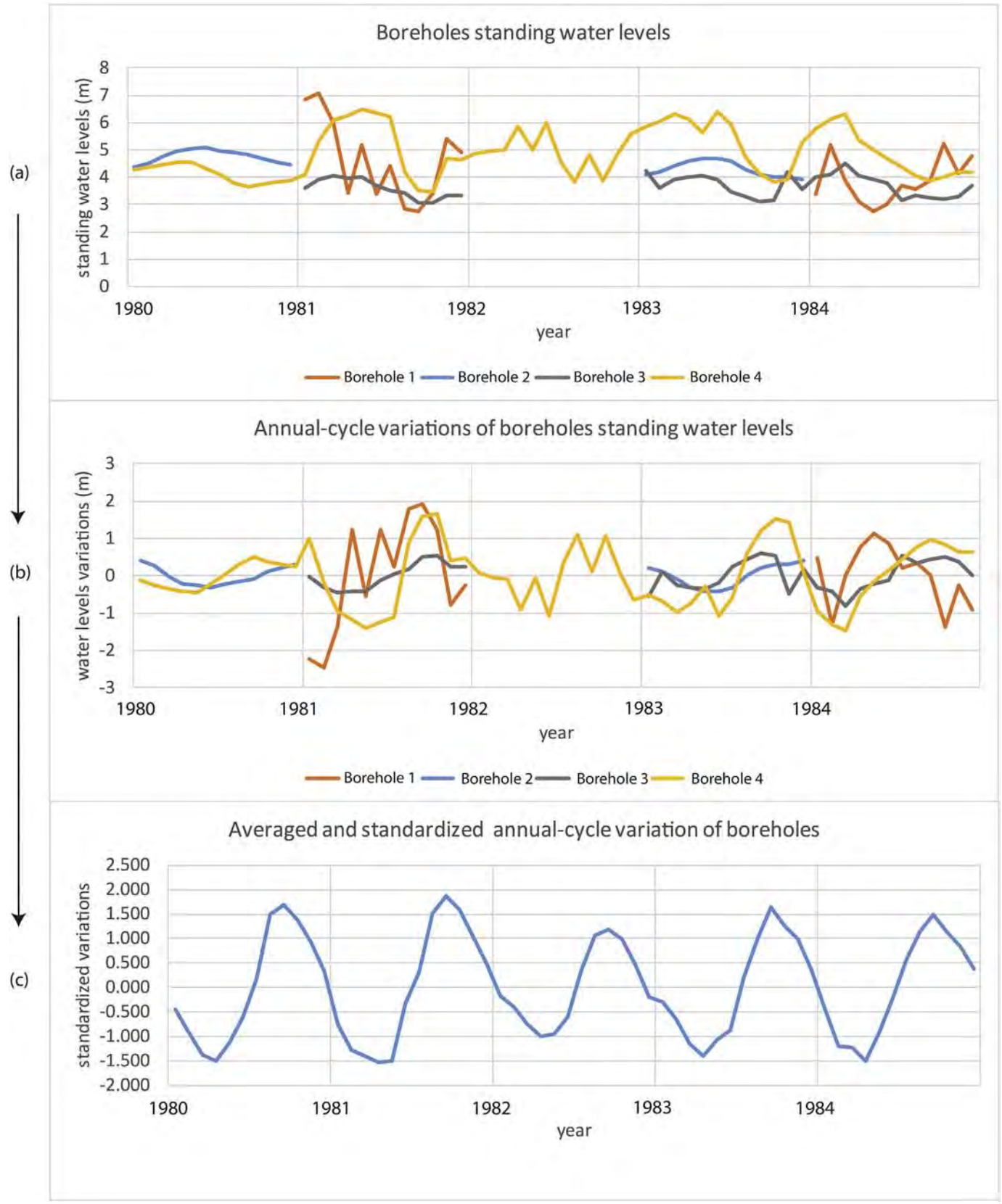

Fig. 3. Illustration of the derivation of annual cycle variation from 1980–1984. (a) The original boreholes standing water levels, (b) borehole with the annual mean for each year removed using Eq. (1), and (c), average of all boreholes variations and the derived standardized time series. Note that only 4 boreholes are shown as examples in (a) and (b) to represent all boreholes in SWWA, while the time series in (c) represents the final results averaged from 2997 boreholes.

In order to illustrate the procedure to derive annual cycle variations, Fig. 3a provides 4 randomly selected boreholes as an example for all boreholes in SWWA. One can see that these borehole data cannot even fully cover a 5-year period, thus, the data coverage for different boreholes for the 1980–2015 period is expected to be fragmented. From Fig. 3a to b, the annual mean for each borehole is removed according to Eq. (1). Since the standing water level (SWL) represents the distance from reference points (surface in most cases) to the groundwater table, the time series in Fig. 3b are inverted by considering the negative sign of the values in Fig. 3a in order to correctly show increasing and decreasing trends. Finally, as shown in Fig. 3c, all annual cycle variations are spatially averaged and subsequently standardized for ease of comparison to other products such as rainfall.

3.2.3. Spatial interpolation

To see spatial patterns of groundwater availability and groundwater changes, borehole data (see previous Section 3.2.2) are interpolated using two different interpolation methods; the Inverse Distance Weighted (IDW; Philip and Watson., 1982) and Kriging (Oliver, 1990). Both methods have been used to spatially interpolate groundwater in previous studies, e.g., Sun et al. (2009), Nikroo et al. (2008). To assess the performance of the two interpolation methods, their results are compared using cross-validation (e.g., Robinson and Metternicht, 2006), the two-sample Kolmogorov-Smirnov (K-S) test (Massey, 1951; Awange et al., 2016; Saleem and Awange, 2019), and regression analysis. Note that these validation methods are applied only to the boreholes in the regions north and south of Perth (having high data density, see Fig. 1b) due to the fact that the other regions have insufficient data coverage, thus are not suited to test the performance of the interpolation techniques.

In detail, 594 random points (around 1/3 of the total boreholes in the selected regions are extracted and used for the Kolmogorov-Smirnov test as well as for cross-validation. As shown in Fig. 4a, both the IDW and Kriging interpolation results follow the same cumulative distribution at the 95% confidence level with a k-value of 0.05, which indicates that the two interpolation methods deliver acceptably similar results. However, the K-S test shows the IDW interpolated data to be closer to the original dataset. The cross-validation results (Fig. 4b) also show IDW to have similar performance to Kriging, but with better-interpolated values that have lower root-mean-square-errors (RMSEs, i.e., IDW/Kriging interpolated values compared to the nearest points of original values) of 0.48, compared to 0.53 for Kriging. Both the RMSEs for IDW and Kriging gradually become stable (decreasing rate smaller than 0.005 per 10 points) around 580 points, which indicates that the used 594 points are sufficient for validation. Out of the total 594 locations tested, there are around 70% points showing that IDW has smaller errors compared to the Kriging method. Following these assessment results, in Section 4.2, only interpolation results using the IDW method are presented and discussed further.

Since the eastern side of the Darling Scarp has a sparse distribution of boreholes, the interpolation results are less reliable compared to those of high density areas. To roughly estimate the uncertainty in areas with sparse borehole distributions, the western side's high-density boreholes are randomly reduced to roughly match the density of the eastern side of the Darling Scarp (30–40 boreholes per degree cell). The IDW interpolation results using the original boreholes (Fig. 4c) and those using the reduced sparse boreholes (Fig. 4d) are then compared.

The comparison results indicate that major differences are present over the Blackwood Plateau and Gnangara groundwater system, where the number of boreholes used significantly affected the outputs of interpolation. It is most likely that these two regions' groundwater have features that are highly variable, i.e., caused by complex geological, topographic and anthropogenic conditions. For example, Department of Water (2009) indicate that many types of aquifers located in Blackwood Plateau and their depths varies from several meters to hundreds of meters. Taking reference from the western side of Darling Scarp, the uncertainties in the eastern side of the mountainous areas (i.e., those interpolation areas with no borehole control) are expected to be large, due to the fact that mountainous areas' hydrogeological conditions are usually more complex than that of the coastal plain.

3.2.4. Identification of anthropogenic hotspots

The month to month (current month compared to the previous month, see Section 3.2.2) changes in groundwater levels are calculated for all available borehole records to identify potential anthropogenic hotspots. This interpretation is based on the expectation that groundwater level variation (recharge/discharge) should generally exhibit gradual change. A certain area's groundwater change falling outside an expected change may, therefore, likely have resulted from anthropogenic impacts though other impacts cannot be fully excluded. Specifically, the chance of month to month changes in groundwater level over n meters (e.g., $n = 1\,\text{m}, 2\,\text{m}, 3\,\text{m}\ldots$) is separately calculated as:

$$F_n = MMC_n/MMC_t \times 100\%; \quad n = 1, 2, 3, \ldots, \tag{4}$$

where F_n are the chances of month to month changes of groundwater level above n meters for all boreholes, while MMC_n and MMC_t represent the number of records over n meters and total number of records for all boreholes, respectively.

In order to apply Eq. (4), a threshold value x ($x \in n$ meters) needs to be defined upon which a "hotspot" is identified. To do this, an example is used as an illustration. Assuming there are 100 month to month changes of groundwater level records for all boreholes in the studied region, and only 1 record shows a change above x meters; where $x \in n$. Then the chance of groundwater level change over x m is 1% according to Eq. (4), meaning that this change rarely occurs within the study regions. This x meters, thus, can be regarded as the threshold that identifies "hotspots".

Following the example illustrated above, all borehole data in the study region are analysed to determine the threshold x for which the change is equal or less than 1% in order to obtain a 99% confidence level. This confidence level incorporates the possibility that abnormal groundwater level changes could also occur due to irregular rainfall, special geological and topographic conditions, as well as anthropogenic impacts. In addition, it should be noted that minor human abstractions are difficult to detect using monthly data, since the recovery time could be short based on the amount of abstraction and the change of groundwater may be too small to be distinguished from other natural changes. Thus, the 1% is selected to detect more substantial anthropogenic impacts (e.g., abstractions). In this study, month to month groundwater changes of less than 1 m account for 73.6% of all records in SWWA, whereas those of 6 m account for around 1%, and those for 7 m and above, less than 1%. From this, therefore, boreholes with groundwater changes over 7 m resulting from month to month change analysis are identified as anthropogenic "hotspots" within SWWA, i.e., $x = 7\,\text{m}$.

Next, for those single boreholes with groundwater level changes above 7 m, the chance of 7 m is also calculated for each of them using Eq. (4), in order to see how frequently such anthropogenic impacts occur, e.g., if a borehole has 36 monthly change records, and only 1 shows above 7 m change from month to month, this means that anthropogenic impacts rarely occur in this borehole since the chance is 1/36.

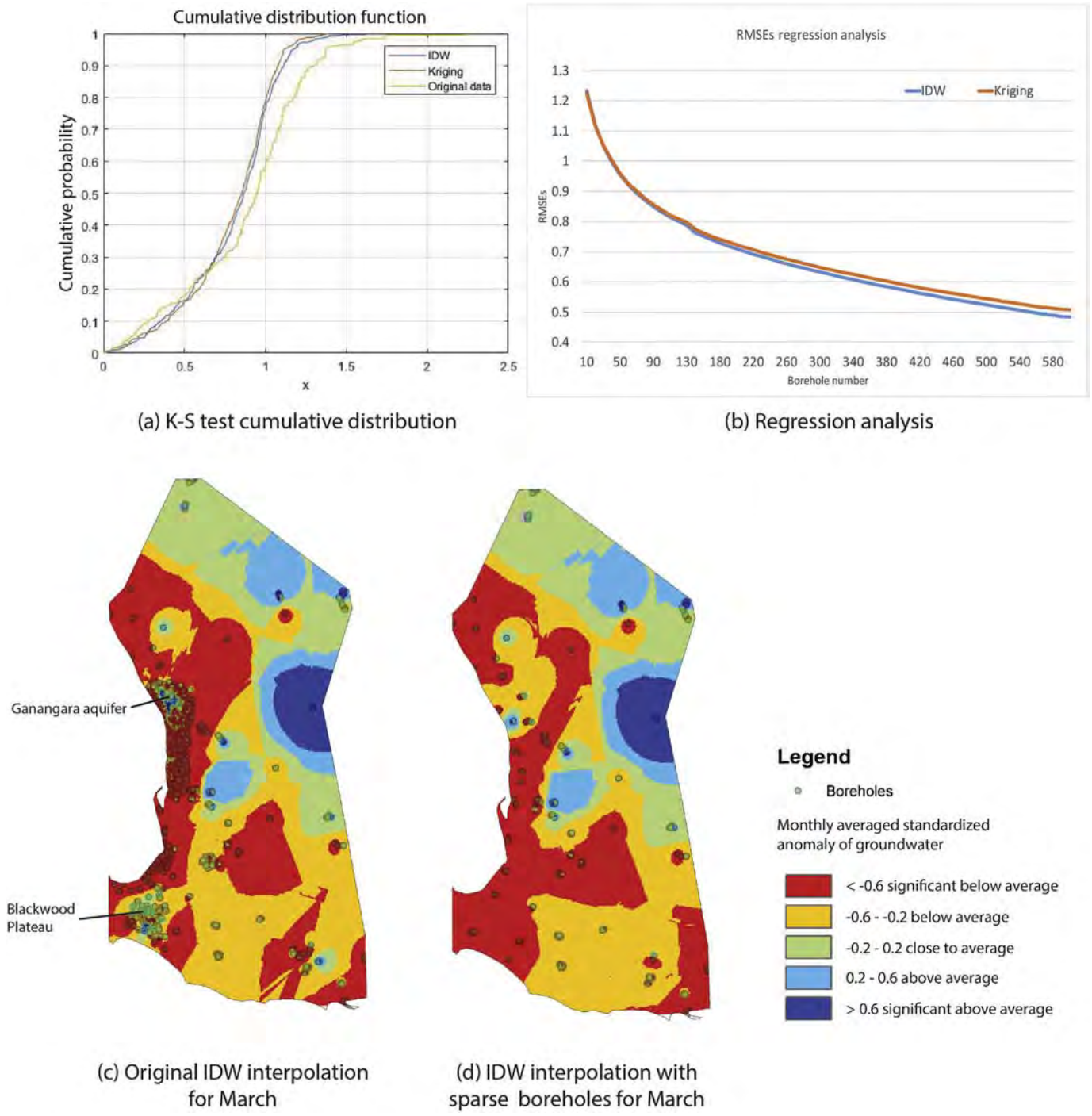

Fig. 4. Validation results for IDW and Kriging interpolation methods for the regions north and south of Perth and uncertainty simulation for sparse borehole interpolations: (a) Cumulative distribution comparison of 594 randomly generated points (IDW and Kriging) and the nearest original data; (b) regression analysis of both IDW and Kriging, RMSEs gradually decrease with increasing number of points used; (c) IDW interpolation for groundwater availability (March is randomly selected), and (d), the same IDW interpolation as (c) but using sparse boreholes. From (a) and (b), the results show that both IDW and Kriging have similar interpolated values, where IDW provides results that are relatively closer to the original dataset and hence used for further analysis. From (c) and (d), the interpolation results in Blackwood Plateau and Gnangara groundwater system are significantly affected by using different borehole densities.

4. Results and discussion

4.1. Temporal analysis

An overview of the temporal analysis is presented in Fig. 5 showing monthly averages of groundwater and rainfall in relation to the climate indices MEI and DMI. In particular Fig. 5a shows standardized monthly anomalies of groundwater and rainfall time series with long-term mean removed, as well as those of two climate indices (MEI and DMI) for examining impacts of ENSO and IOD, respectively. Fig. 5b shows annual cycle variation of groundwater and rainfall. The available numbers of used boreholes are also presented, and helps infer confidence levels for the derived groundwater time series. Fig. 5c identifies dry (below 25th percentile) and wet (above 75th

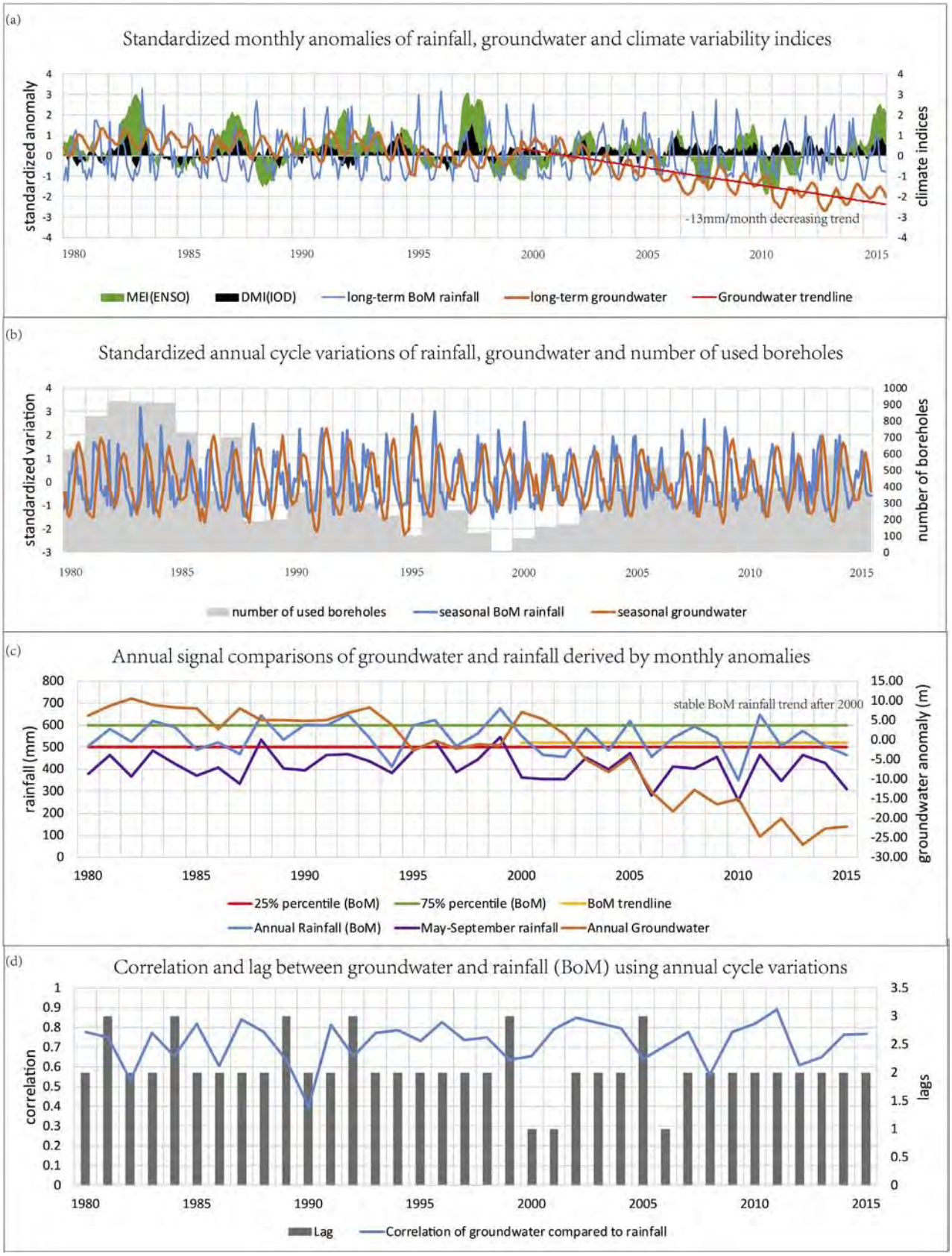

Fig. 5. Groundwater temporal analysis in comparison to rainfall and climate indices; (a) standardized monthly anomalies of rainfall, groundwater and climate variability indices, (b) standardized annual cycle variations of groundwater, rainfall and number of used boreholes, (c) annual signals' comparison of groundwater and rainfall derived by monthly anomalies, and (d) correlations and lags between groundwater and rainfall (BoM) using annual cycle variations. Note that the results are biased towards the north and south of Perth areas with a higher density of borehole data (see boreholes' distribution in Fig. 1b). The linear trend in (a) is significant (95% confidence level) when tested using Mann-Kendall, while the trend in (c) is not. The results show that the decline in groundwater level is partly due to low level rainfall since 2000.

percentile) periods in comparison to annual rainfall. Finally, correlations and time delays (lags) between rainfall and groundwater are shown for each year in Fig. 5d.

SWWA's groundwater variability follows a relative uniform intra-annual pattern based on the data in Fig. 5b, with periods of mostly increasing levels from May or June to August or September, and periods of decreasing levels in the remaining months of each year. Even though, variations in 1999 are derived from only 10 borehole stations, it appears to show no significant difference from the other years. Furthermore, groundwater variations follow rainfall variations to a large extent, with correlations consistently around 0.6–0.8(with an average of 0.74 over the entire study period) and 1–3 month(s) lag (with an average of 2 months' lag) for each year as seen in Fig. 5d, corroborating the results of Rieser et al. (2010) who also obtained similar correlations and lags between rainfall and total water storage (comprising also of groundwater) over the whole of Australia.

4.1.1. Climate impacts on groundwater level

A significant continuously decreasing trend in groundwater levels from 2000 is detected and is apparent from Fig. 5a and c, with an average reduction of 13 mm/month (or 156 mm/year). This may be partly attributed to the continued low level of rainfall (see Fig. 5c). Since 2000, most years have been identified as moderately dry or dry years (2001, 2002, 2004, 2006, 2007, 2009, 2010, 2012, 2014 and 2015; i.e., 10 out of 16 years) with annual rainfall close to or below the 25th percentile. Many studies have reported most of these years as the "Australian Millennium Drought" (see, e.g., Cai et al., 2014; Heberger, 2011). The rainfall trend between 2000–2015 is stable, however, with a 40 mm decrease in annual total values compared to previous periods (i.e., 560 mm compared to 520 mm). Based on the comparison between annual and seasonal rainfall (May–September) in Fig. 5c, there is an almost consistent difference (100–150 mm) between them, indicating the decline of annual rainfall to be due to the decline in seasonal rainfall.

On the one hand, rainfall is also affected by atmospheric and ocean interactions such as ENSO and IOD. Fig. 5a indicates that SWWA's rainfall has a similar rainfall cycle to ENSO over a period of approximately 7 years (Tudhope et al., 2001; Li et al., 2013; Niedzielski, 2014), e.g., 1982–1987, 1988–1994, 1995–2001, 2002–2010. In addition, most of the moderately dry or dry years since 2000 listed above have been labelled by BoM as El Niño years (see online records at http://www.bom.gov.au/climate/enso/enlist/), which are known to bring low levels of rainfall throughout most of Australia.

On the other hand, according to Ashok et al. (2003), IOD has been found to have significant impacts on the winter rainfall (June, July, August) of western and southern Australia. A positive IOD produces a drier climate than average during winter-spring (Fig. 5a shows IOD as continuously positive since 2000), and a wetter climate in summer. A negative IOD impact on rainfall is not apparent in SWWA according to BoM statistics (http://www.bom.gov.au/climate/iod/#tabs=Negative-IOD-impacts). Therefore, under both effects of ENSO and a positive IOD, continuous low levels of rainfall may be one of the contributing factors to the decline in groundwater levels experienced since 2000. La Niña events brought above average rainfall in 2008 and 2011 (see Fig. 5a, b and c; also see La Niña records on BoM website: http://www.bom.gov.au/climate/enso/lnlist/), years during which the groundwater balance returned to positive (inflow was greater than abstraction and outflow). However, there was no significant effect on the long-term decline because of a lack of consistent high rainfall years (e.g., one "good year" is not good enough to replenish groundwater).

4.1.2. Anthropogenic impacts on groundwater level

The continuous low levels of rainfall after 2000 is one of the causes for the decline of groundwater levels in SWWA. However, anthropogenic impacts, such as human abstraction is also a contributing factor. For example, the stable annual rainfall trend for the 2000–2010 period does not fully correlate with the increasingly declining trend of groundwater in Fig. 5c. Groundwater levels instead, drop on average around 20 m from 2000 to 2015 (but this may be mostly attributed to data from north and south of Perth, which are biased towards those areas in the spatial distribution). Similar results are mentioned e.g., in Featherstone et al. (2012), who conclude that Perth's basin groundwater levels dropped due to anthropogenic impacts. Further evidence for a major anthropogenic influence is the fact that rainfall variations between the period 1983–1988 and 1999–2004 (see, Fig. 5c) are largely similar in terms of trends and magnitudes, but groundwater behaviour within these two periods are entirely different (i.e., stable over period 1983–1988 but decreasing over the period 1999–2004).

Annual cycle variations (see Fig. 5b) show that groundwater varies according to rainfall, with the correlation from 2000–2015 between them being 0.748, with an average 2 months' lag. The annual groundwater level (Fig. 5c), however, shows a variety of responses to annual rainfall, including a stable level before 1993. After that, groundwater reaches a new low level due to a 2-year drought (from late 1993 to early 1995), and then it appears to recover after 2 years' wet conditions (late 1998 to early 2000). After 2000, groundwater declines slowly as the 'Millenium' drought starts. During the same time, groundwater abstraction increased significantly due to increased groundwater usage and population growth. For example, groundwater usage in 1985 was around 500 GLs/year according to Department of Water (2007), this usage tripled in 2005. Moreover, around 500,000 population moved to Western Australia between 2000 and 2010 about double the rate than in the period 1980–2000 (Alexander, 2018). Although the Department of Water (2007) indicates that the sustainable groundwater usage for Perth basin is 1937 GLs/year and allocation limit is 1472 GLs/year, the groundwater balance (see, Fig. 5a or c) had already significantly decreased after 2002 with groundwater usage of around 1300–1400 GLs/year. This overestimation of sustainable groundwater usage in annual water report is possibly due to a relative high rainfall value of 2007 in rainy season (see, Fig. 5b). Overall, climatic factors seem to have weaker impacts compared to anthropogenic activities that have significant effects on the decline of groundwater after 2000.

4.2. Monthly average spatio-temporal pattern analysis

For a more detailed analysis of the impacts of rainfall on groundwater, monthly averaged rainfall (Fig. 6a) are compared with spatially interpolated monthly averaged groundwater anomalies (Fig. 6b and c) for each month. Fig. 6a uses colour gradients to display details in the spatial distribution of rainfall over the study region. Fig. 6b shows the averaged groundwater level changes for each month compared to those of the previous month (e.g. difference previous month minus present month). A threshold of ± 0.2 m is set through multiple tests in order to clearly show the spatial gradients of the recharge/discharge distribution. Fig. 6c presents the monthly averaged standardized groundwater anomalies. Based on the natural breaks classification method (Jenks, 1967), five classes are established to show groundwater levels in comparison to the annual average level, namely (i) significantly below average, (ii) significantly above average, (iii) below average, (iv) above average, and (v), close to average (Fig. 6c).

4.2.1. Rainfall patterns

Fig. 6a indicates an increasing gradient for rainfall from north-east to the south-west for most months, except January, February,

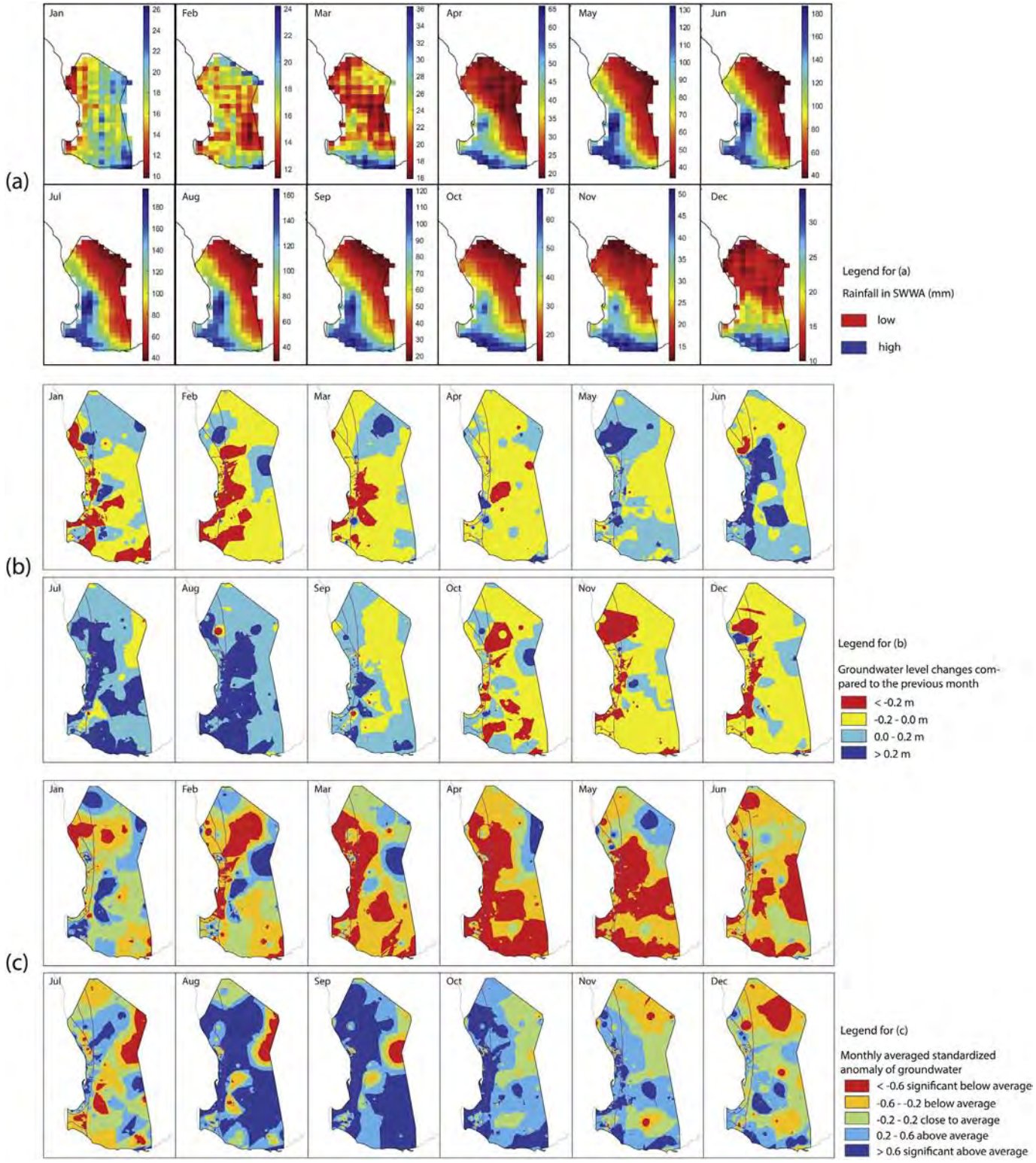

Fig. 6. Monthly averaged spatial patterns of rainfall and standardized groundwater anomalies; (a) monthly averaged rainfall patterns (mm), (b) monthly averaged groundwater level changes compared to those of the previous month, and (c), monthly averaged standardized anomalies of groundwater. The Darling and Gingin Scarps appear to be barriers that divide rainfall between coastal and inland areas during the rainy season. The recharge/discharge show consistency along the western coastline in panel (b). Groundwater behaviours also appear different on either sides of the Darling and Gingin Scarps. North of Perth and Blackwood Plateau have similar groundwater patterns in panel (c). South coastal region and south of Perth requires at least 65–70 mm/month and 60 mm/month rainfall, respectively, to influence groundwater recharge according to postulations made based on the figures above. (For interpretation of the references to colour in this figure, the reader is referred to the web version of this article.)

and March. January is the only month that clearly shows higher rainfall in the eastern mountainous areas of SWWA than in the coastal areas, though, with rather low levels. From March, rainfall gradually increases along the southern coastline of the study region. From April to November, the spatial patterns of rainfall are approximately the same, in which the Darling and Gingin Scarps roughly

act as boundaries with most of the rainfall occurring in the coastal plain. During the rainy season (May to September), major rainfall are received in regions south of Perth, Bunbury and the Blackwood Plateau (see locations in Fig. 1c). Finally, the rainfall in December displays a north-south dipole pattern with relatively low levels.

4.2.2. Groundwater recharge/discharge patterns

In order to understand the relationships between rainfall and groundwater recharge/discharge, the concept of lag between rainfall and groundwater needs to be well understood. In Section 4.1, we stated that an average 2 months' lag exists between the time it starts to rain and groundwater starts to recharge (in agreement with Rieser et al., 2010). This is usually misunderstood to mean rainfall needs to take two months' time to penetrate soils, rocks and finally become groundwater. In actual sense, a detailed water balance has to be considered, which takes into account the fact that rainfall needs to reach a threshold value in order to recharge groundwater. For example, when rainfall reaches the ground, it has to satisfy the soil and plant transpiration first (Alley, 2009) before the recharge process can begin, where the excess part takes some time (the lag) to infiltrate through soils and rocks and finally reaches the groundwater table. At this moment, only if the amount of excess rainfall (i.e., groundwater input) is greater than the amount of groundwater outflow (i.e., groundwater output, e.g., from human abstraction or natural discharge such as into the ocean), does the groundwater recharges (i.e., groundwater level raises). In other word, if the rainfall does not reach a certain threshold value, i.e., continuous low rainfall level, there will be no lag (i.e., infinite lags) since the groundwater will never recharge.

Comparing the spatial patterns of groundwater recharge/discharge to spatial rainfall in Fig. 6a and b, both lag and threshold conditions exist, i.e.,

(i) For most of the coastal regions of SWWA, there appears to be less than one month's lag between rainfall and groundwater. For example, one can see that rainfall gradually increases along the southern coastline of the study region in March (Fig. 6a), while groundwater is still discharging (Fig. 6b). Similar to April, more rainfall arrives at southern coastline and south of Perth region, while groundwater level still shows decline. During these two months, groundwater levels continue to drop because the total recharge from rainfall (50 mm for south of Perth and 65 mm for southern coastline in April, see Fig. 6a) is less than the total of all discharges (i.e., not sufficient to satisfy soil and plant transpiration, as well as groundwater outflow). In May, however, the rainfall value reaches around 120–130 mm and the groundwater balance instantly becomes positive (i.e., groundwater level raises, see Fig. 6b). Similarly from October to November, when rainfall amount falls from 70 to 50 mm in southern coastline (from 60 to 45 mm in south of Perth), the groundwater balance instantly becomes negative (i.e., groundwater level drops). Thus, a minimum of 65–70 mm/month of rainfall is postulated here as the threshold needed to maintain groundwater balance in the southern coastal region of SWWA, and around 60 mm/month for south of Perth.

(ii) One to two month(s)' lag between rainfall and groundwater exists in regions north of Perth (Gnangara groundwater system) and Blackwood Plateau. For example, rainfall during May reaches 120–130 mm already for both regions (see Fig. 6a), whereas the groundwater in these two regions are still mainly discharging (see Fig. 6b). This groundwater pattern is different compared to other coastal regions (i.e., south of Perth), where most areas are starting to recharge from May. In June–July, over half of north of Perth and Blackwood Plateau's groundwater start to recharge, then discharge in November (October for other regions, rainfall in November is 35–40 mm for both regions, north of Perth and Blackwood Plateau). Due to this obvious lag, we cannot identify the threshold value of rainfall recharging groundwater and as such, in (i), there is a small portion of north of Perth's groundwater that in discharging in May with rainfall around 180 mm, while in October, most of north of Perth's groundwater is recharging with rainfall at only 50–60 mm. Finally, this lag is most likely caused by geological conditions, e.g., large but low infiltration aquifers receive groundwater flow from other regions during the dry period, while other regions mostly rely on recharge of rainfall.

Although, the results in Fig. 6a and b show some consistencies across the western coastal regions of SWWA, in the mountainous regions, however, rainfall does not appear to be correlated to groundwater for most months, making it hard to identify lags and thresholds between rainfall and groundwater. For example, even with only the rainfall amount in January being around 20–25 mm over the northeastern mountainous regions, the groundwater level is increasing (see, Fig. 6b). Higher rainfall (40–80 mm) arrives in this region during June, however, but in contrast to January, groundwater levels are decreasing. This is possibly due to (i) the mountainous region's groundwater variations mainly depend on the groundwater flow itself, (ii) terrain effects make surface water gather in valleys and quickly flows away (e.g., Crissa and Davissonb, 1996), as well as (iii), high evaporation rate (annually 1600–1800 mm in the northeastern part of the study regions compared to rainfall values of 350 mm, see online evaporation statistics http://www.bom.gov.au/watl/evaporation/) makes it hard for surface water to become groundwater. Only when there is sufficiently long-lasting rainfall in mountainous regions (e.g., May to August 40–80 mm, see, Fig. 6a), does the surface water recharge groundwater. According to Fig. 6b, groundwater in the mountainous regions only shows recharge to some extent during July and August (possibly, May and June are replenishing surface water first, e.g., producing a lag). In central mountainous regions of SWWA, Kinal and Stoneman (2012) report a phenomenon that surface water and groundwater are disconnected in dry seasons due to low rainfall level. Besides the three reasons above, groundwater depth, e.g., 10–30 m in central mountainous region could also be a contributing factor as to why the surface water does not reach groundwater, considering generally the low infiltration about mountainous granite or basalt rocks.

A further implication of this scenario is that when El Niño cause low levels of rainfall, the coastal regions and their recharge are affected due to the high correlation between rainfall and groundwater across the western coastline of SWWA (also see, e.g., Holbrook et al., 2009). During global teleconnection episodes, recharge in the mountainous regions may be completely unrelated to rainfall for the whole year due to insufficient rainfall caused by ENSO.

In terms of recharge/discharge speed, the coastal regions are generally faster than the mountainous regions because of different geological conditions, e.g., sandy soil in coastal regions are more easily penetrable by rainfall compared to granite rocks in the mountainous areas. Furthermore, a significant proportion of rainfall in mountainous regions becomes surface water that drains to coastal regions, producing an even faster recharge time in coastal areas near mountain regions (monthly recharge over 0.2 m). In the western coastal regions, the Gnangara groundwater system and Blackwood Plateau have a similar behaviour, where the recharge/discharge speed is slower than other regions such as region south of Perth (mostly less than 0.2 m per month) possibly due to different geological and topographic conditions.

4.2.3. Groundwater availability patterns

Based on the elevation profile of SWWA, the general groundwater flow direction should be from the east (higher elevation mountainous regions) to the west (lower elevation coastal regions of Perth basin), and finally into the Indian Ocean. However, there is a clear geographical boundary along the Darling Scarp that appears to lead to different groundwater behaviours on both sides (Fig. 6c). This difference may in part be associated with rainfall since the difference in rainfall on either side of the scarp can reach 60–80 mm/month during rainy seasons. An average of 200 m difference in elevation exists across the scarp, as mentioned in Section 2, and geologically, the Darling Scarp and Darling fault's positions overlap with each other, which could be a natural barrier that blocks groundwater flow from the eastern mountainous regions to the coastal plain. This potential effect may need a detailed hydrogeological study that is beyond the scope of the current study. In addition, this boundary to the north appears to curve into mountain regions, departing from obvious landscape features, which may be biased due to sparse distribution of boreholes, and thus, is likely an artifact of the spatial interpolation (see, data density and coverage in Fig. 8a).

The coastal regions from south of Perth to Busselton experience the lowest groundwater levels from April to June, and the highest groundwater levels from October to December (Fig. 6c) in a year. The Gnangara groundwater system region, Blackwood Plateau, and central eastern side of the Darling Scarp appear to have similar groundwater behaviour, with groundwater levels from January to March being above average and from May to July, they are below average (Fig. 6c). There are approximately 7–8 months in these three regions that groundwater level discharges from the level of highest peak to the lowest level. For these three regions, the Gnangara groundwater system is profoundly affected by human abstraction (Awange, 2012; Skurray et al., 2012; Awange and Kiema, 2013; Department of Water, 2015; Awange, 2018; Awange and Kiema, 2019). Groundwater levels of the central eastern side of the Darling Scarp mostly correlate to the dams' water levels, e.g., the levels in Perth from 2012–2015 are mostly below average during April to August (see online: https://www.watercorporation.com.au/water-supply/rainfall-and-dams/dam-levels) and this mirrors the results in Fig. 6b. On the Blackwood Plateau, it is most likely that the groundwater is affected by geologic and topographic features, considering that it is surrounded by the Busselton and Darling faults (CSIRO, 2009), as well as three scarps (see Fig. 7c, Whicher, Darling and Barlee Scarps).

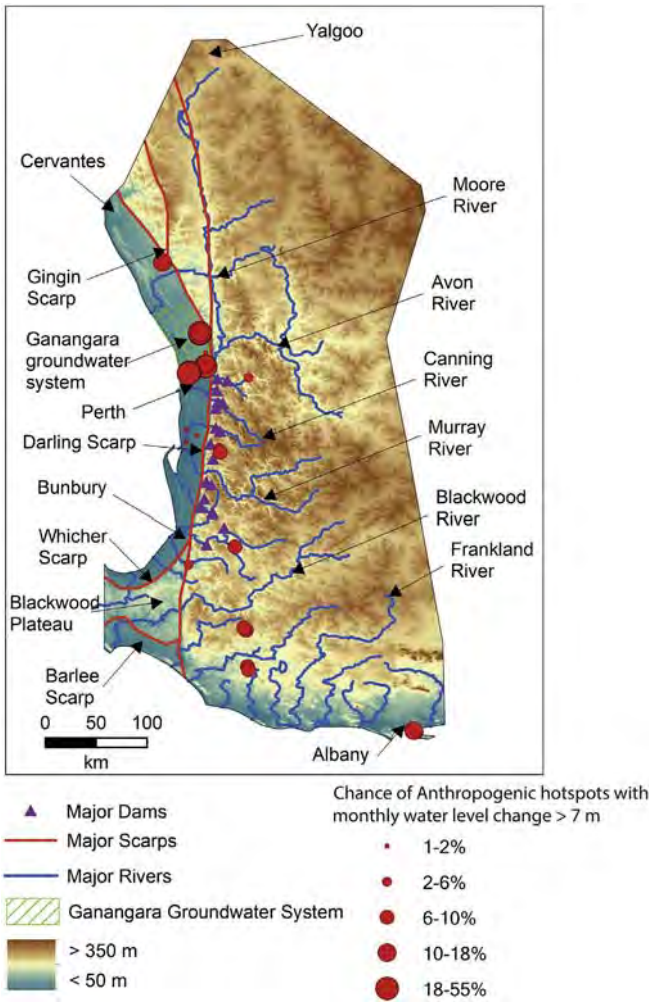

Fig. 7. Anthropogenic hotspot locations in SWWA. Most of high chance hotspots (the chance of groundwater level change above 7 m is around 18 to 55% for every month) occur in Gnangara groundwater system, others are closed to dams or mines.

4.3. Anthropogenic hotspots

Anthropogenic hotspots are identified as the boreholes with monthly groundwater level changes above 7 m (as determined in Section 3.2.4), due to the likelihood of such a large change being below 1% in the overall study region. The frequency of these level changes is calculated according to each borehole's records, and the results presented in Fig. 7. The identified anthropogenic hotspots occur mainly in the region north of Perth (the chance of groundwater level change above 7 m is around 18 to 55% for every month; see Fig. 7), where the Gnangara groundwater system is located. This is to be expected since the Gnangara groundwater system contributes 50–60 % of groundwater use in SWWA (Skurray et al., 2012; Department of Water, 2015). Other remaining hotspots (chance below 18% per month) are the region south of Perth, close to dams (e.g., North Dandalup, Wellington, Shannon Dams), or close to mines (e.g., Collie mine), all of which are impacted by human activities.

4.4. Spatial-temporal biases

Results presented in Sections 4.1 and 4.2 are likely to contain both spatial and temporal biases. According to Figs. 1b and 8a, most data in terms of high spatial density and long temporal coverage are located in the regions of north and south of Perth. Therefore, the long-term temporal analysis in Section 4.1 is more likely to represent groundwater behaviour in those regions. For the spatial-temporal interpolation results in Section 4.2, both IDW and Kriging methods show a significant difference in low density and short-term coverage areas of data (see the grey colour regions in Fig. 8a), although results between them in others areas are statistically similar. Seven study regions (Fig. 8b) are established according to their borehole density, rainfall, terrain characteristics, and groundwater systems, in order to discuss their spatial biases. Future studies will rigorously treat the problem of temporal biases.

Fig. 9 shows the monthly anomalies of groundwater and rainfall for each study region indicated in Fig. 8b, whose major findings are summarized in Table 1. In the previous Sections 4.1 and 4.2, groundwater was found to possess a good correlation with rainfall except in the mountainous regions (e.g., A and G in Fig. 8b) of the study area. Therefore, no further consideration of the relationships between annual cycle variations of rainfall and groundwater is undertaken. The North mountainous region (A in Figs. 8b and 9a) firstly appears to have more inter-seasonal rainfall variations (e.g. annual cycles change considerable from year to year) than other regions. On close examination, however, it is relatively low in magnitude, ranging from 10–45 mm (Fig. 6a). In addition, the onset of

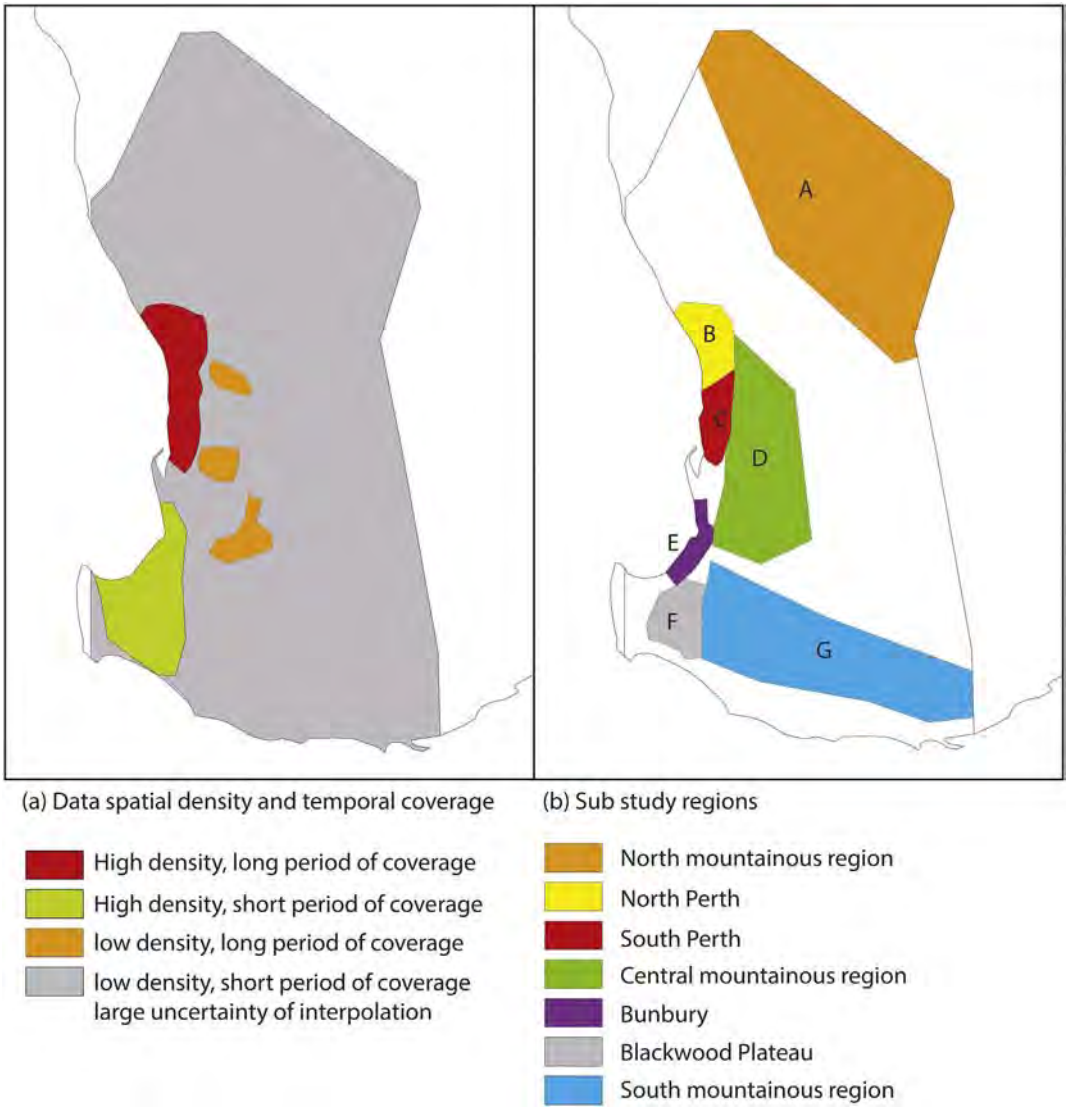

Fig. 8. (a) Spatial distribution of data density and temporal coverage where the grey regions indicate low reliability of interpolation results, and (b), sub study regions selected for bias discussions.

the rainfall peak in the region as well as in North Perth region (B in Figs. 8b and 9b) is earlier (May–July) than other regions (July–August). Groundwater in region A only weakly responds to rainfall variations except in the major rainy seasons. This weak response may be due to small rainfall amounts, terrain effects, high evaporation and/or groundwater depths (e.g., Crissa and Davissonb, 1996; Kinal and Stoneman, 2012). As already mentioned in Section 4.2.2, rather than becoming groundwater, the small amount of rainfall during dry periods in mountainous regions tend to evaporate or flow away because of terrain and geological effects (e.g., Crissa and Davissonb, 1996). Additionally, groundwater levels do not appear to decline, although, there is considerable uncertainty due to the short-term data coverage and sparse borehole distribution.

Regions B and C (Figs. 9b and c) are found where groundwater has major decline after 2000, mostly attributed to human abstraction, see previous discussions in Sections 4.1.2 and 4.3. In the Central mountainous region (D in Figs. 8b and 9d), which is adjacent to regions B and C, containing many dams located along the eastern side of the Darling Scarp, groundwater level variations mainly associate with dam levels, e.g., during the "Millennium drought", groundwater levels dropped significantly during the dry period 2002–2007, which agrees with dam level variations (see also the previous discussion in Section 4.2.3). For the Bunbury region (E in Figs. 8b and 9e), the data are temporally discontinued but all show the same regular groundwater variation patterns. The Blackwood Plateau (F in Figs. 8b and 9f) only has few years of consecutive data, with the results appearing to be affected by spatial bias (e.g., amplitudes are large for only a small number of boreholes, but small for a large number of boreholes). This possibly indicates high spatial variability of groundwater in this region. South mountainous region (G in Figs. 8b and 9g) shows some similarities to the North mountainous region, in that groundwater levels do not appear to be strongly affected by rainfall except after long-lasting heavy rainfall. However, this region has lower evaporation rates and higher rainfall values compared to Region A, thus, rainfall and groundwater have stronger links. In addition, 4 boreholes showing an apparent anomalous level of −5 m in 1995 are located in close proximity to a playground in Donnybrook (a small town in South mountainous region G), most likely are affected by anthropogenic impacts.

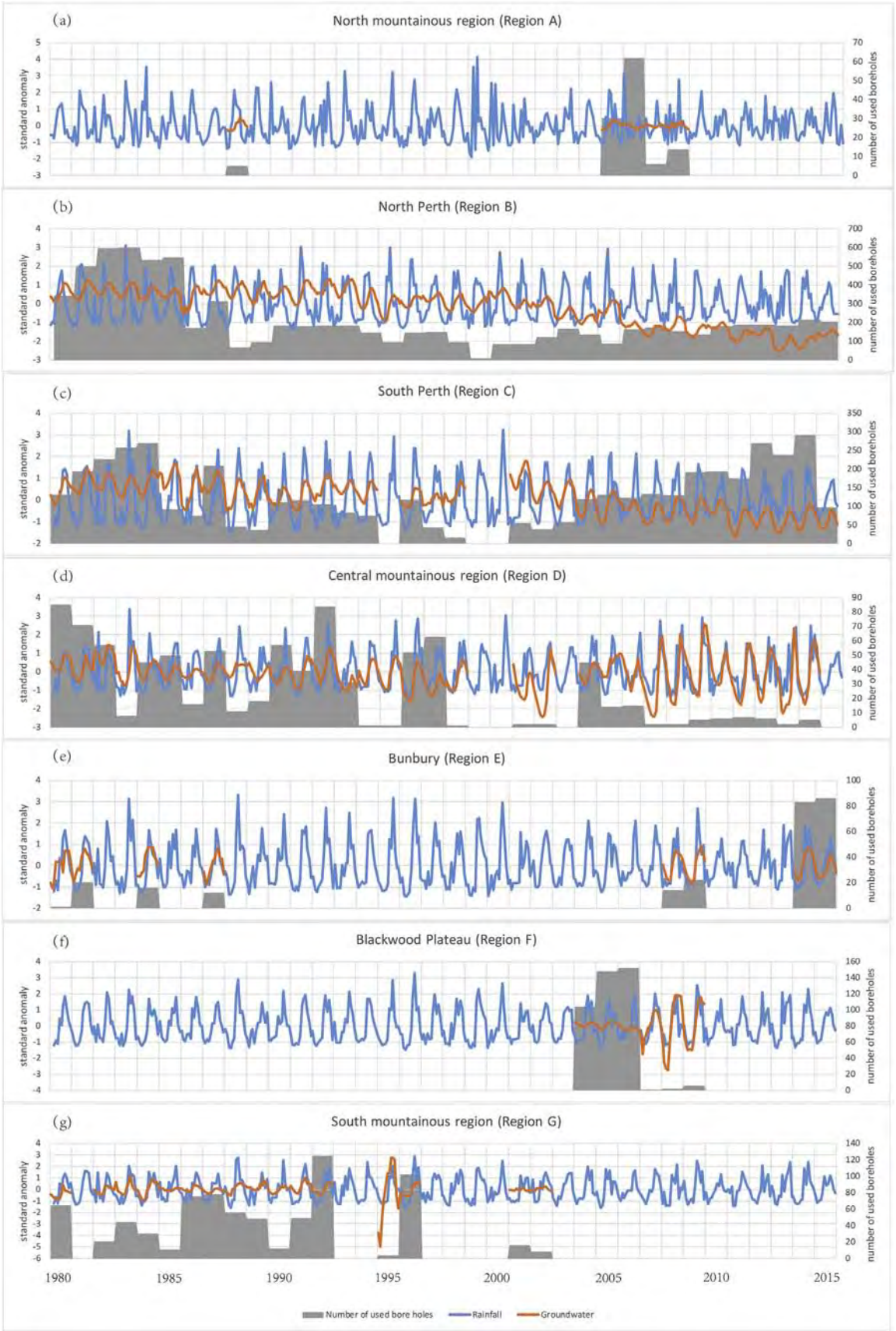

Fig. 9. Comparison of monthly anomalies between groundwater and rainfall for each sub study region presented in Fig. 8b. Rainfall patterns in most of the regions are similar, while the onset of the rainfall peaks in regions A and B are earlier (May–July) compared to other regions (July–August). The mountainous regions A and G only correlates to rainfall in rainy season. Major groundwater decline occurs in north and south of Perth (regions B and C). Blackwood Plateau (region F)'s groundwater varies spatially. Although Bunbury (region E) has insufficient data, it shows similar groundwater variations over the evaluated years.

Table 1
Summary of the major findings for each sub study region of Fig. 8b in relation to Fig. 9.

Region	Major findings
A (North mountainous region)	- Variable seasonal rainfall of small amounts, groundwater does not follow rainfall except during rainy season. - Rainfall peak occurs earlier compared to other regions (May–July vs. July–August). - Results could be biased due to only 5 years' data with very sparse borehole distribution
B (North Perth)	- This is an urban and major groundwater contribution area (Gnangara groundwater system). - Groundwater decline occurring after 2000 is caused by human abstraction (major) and continuous low rainfall (minor). - Groundwater in this region has 1–2 month(s)' lag with rainfall. Rainfall peaks are earlier compared to other regions (May–July vs. July–August). - Recharge speed is slower than other western coastal regions in SWWA.
C (South Perth)	- This is an urban area and groundwater decline occurring after 2000 is caused by human abstraction (major) and continuous low rainfall (minor). - 60 mm monthly rainfall is postulated as the threshold needed to recharge groundwater.
D (Central mountainous region)	- Groundwater follows rainfall and matches dam level variations, could be affected by terrain (Darling Scarp), geological (Darling fault and rock types), and anthropogenic effects (dam).
E (Bunbury)	- Temporally discontinuous groundwater data coverage, however shows uniform temporal groundwater variation patterns. Groundwater is stable.
F (Blackwood)	- High spatial variability of groundwater in this region, could be affected by Whicher, Barlee and Darling Scarps. - Similar to region B, the groundwater in this region has 1–2 month(s)' lag with rainfall.
G (South mountainous regions)	- Similar to Region A, but groundwater appears to have slightly better response to rainfall, particular during rainy seasons.

5. Conclusion

South-West Western Australia (SWWA) is a region that heavily relies on groundwater for agricultural and domestic water use, especially during dry periods. However, the decline of groundwater since 2000 and the lack of spatio-temporal variability studies undertaken in this region impose challenges on groundwater management. This contribution employed a suit of statistical tools such as Man-Kendall test, cross-correlation, cross-validation, Kolmogorov-Smirnov test, and regression analysis, to investigate and provide a more in-depth understanding spatio-temporal variations of groundwater in SWWA for the period 1980–2015, and identified its potential interconnections to climate variability/change and anthropogenic impacts. The major findings corresponding to objectives can be summarized as:

1. For variability of groundwater in SWWA, the north and south of Perth regions were the main regions that experienced groundwater decline since 2000, with a decreasing rate of 13 mm/month (or 156 mm/year). Other regions' groundwater levels appeared to be stable.
2. For groundwater availability, the high and low level of groundwater in SWWA are from July to January (high) and February to June (low). As for recharge/discharge, the western coastal regions exhibit a faster recharge speed than eastern mountainous regions. Among western coastal regions, north of Perth (Gnangara groundwater system) and Blackwood Plateau have slower groundwater recharge/discharge speed than other areas.
3. For spatial pattern of variations and recharge/discharge, groundwater levels over the northeastern mountainous regions were generally not affected by rainfall during dry periods, due to the fact that small amount of rainfall in the mountain regions tends to evaporate and flow away rather than become groundwater. The western coastline region's groundwater follows rainfall variations. In addition, most of SWWA region's groundwater have no lags between rainfall and groundwater. A postulated minimum threshold of rainfall to recharge groundwater for the region south of Perth and southern coastline of SWWA is around 60 mm/month and 65–70 mm/month, respectively. North of Perth (Gnangara groundwater system) and Blackwood Plateau have 1–2 month(s)'s lag between rainfall and groundwater.
4. For climate variability/change impacts to groundwater, the overall patterns of spatio-temporal variability of rainfall were relative uniform over SWWA, with the major rainy season from May to September. No significant declining trend in rainfall was detected after 2000. However, average annual total rainfall for the period 2000–2015 decreased by 40 mm compared to the period of 1980–1999. The continuous low level of rainfall after 2000, however, may partly contribute to the decline of groundwater. In addition, when ENSO caused low level of rainfall, groundwater recharge in coastal regions was significantly affected.
5. In regards to anthropogenic hotspots identification and impacts on groundwater, most are identified in the regions north of Perth (Gnangara groundwater system), and south of Perth, as well as, close to dams and mines. Anthropogenic impacts such as human abstraction were the primary reasons for groundwater decline in these regions. Finally, different behaviours of groundwater on either side of the Darling Scarp were caused by other factors such as rainfall, terrain, geological faults, aquifers and dams. A detailed analysis and discussion of these factors, however, is outside the scope of this study and will be considered in future contributions.

Declaration of Competing Interest

The authors declare that they have no known competing financial interests or personal relationships that could have appeared to influence the work reported in this paper.

Acknowledgments

Kexiang Hu is grateful for the CIPRS and Research Stipend Scholarship provided by Curtin University that is supporting his PhD studies. J.L. Awange would like to thank the financial support of the Alexander von Humboldt Foundation that supported his stay at Karlsruhe Institute of Technology. He is grateful to the good working atmosphere provided by his hosts Prof Hansjörg Kutterer and Prof Bernhard Heck. The authors would like to thank the following organizations for providing the data used in this study; the Australian Bureau of Meteorology (BoM), Princeton Climate Analytics (PCA) and Earth System Research Laboratory. In addition, special thanks to Prof. Paul Tregoning who provided valuable suggestions for this paper.

Reference

ABARES, 2018. About my region - Western Australia. Report. Australia Government, Department of Agriculture and Water Resources., retrieved from http://www.agriculture.gov.au/abares/research-topics/aboutmyregion/wa. Data accessed: 3 March, 2019.

Agriculture and Food, 2018. Western Australia's agriculture and food sector. Report. Australia Government, Department of Primary Industries and Regional Development., retrieved from https://www.agric.wa.gov.au/western-australias-agriculture-and-food-sector. Data accessed: 6 March, 2019.

Alexander, S., 2018. Population growth and the mining industry in Western Australia. Blog. ABS., retrieved from https://demogblog.blogspot.com/2018/06/population-growth-and-mining-industry.html. Data accessed: 1 July, 2019.

Ali, R., McFarlane, D., Varma, S., Dawes, W., Emelyanova, I., Hodgson, G., 2012. Potential climate change impacts on groundwater resources of south-western Australia. J. Hydrol. 475, 456–472. https://doi.org/10.1016/j.jhydrol.2012.04.043.

Alley, W., 2009. Encyclopedia of inland waters. Reference Module in Earth System and Environmental Sciences. pp. 684–690. https://doi.org/10.1016/B978-012370626-3.00015-6.

Anyah, R., Forootan, E., Awange, J., Khaki, M., 2018. Understanding linkages between global climate indices and terrestrial water storage changes over Africa using GRACE products. Sci. Total Environ. 635, 1405–1416. https://doi.org/10.1016/j.scitotenv.2018.04.159.

Argent, R., 2016. Inland water: groundwater resources, Australia State of the Environment 2016. Tech. rep.. Australian Government Department of the Environment and Energy, Canberra. https://doi.org/10.4226/94/58b656cfc28d1.

Ashok, K., Guan, Z., Yamagata, T., 2003. Influence of the Indian Ocean Dipole on the Australian winter rainfall. Geophys. Res. Lett. 30 (15), 1–4. https://doi.org/10.1029/2003GL017926. CLM6.

Awange, J., 2012. Environmental Monitoring Using GNSS: Global Navigation Satellite Systems. Springer-Verlag Berlin Heidelberg. https://doi.org/10.1007/978-3-540-88256-5.

Awange, J., 2018. GNSS Environmental Sensing: Revolutionizing Environmental Monitoring. Springer International Publishing. https://doi.org/10.1007/978-3-319-58418-8.

Awange, J., Fleming, K., Kuhn, M., Featherstone, W., Heck, B., Anjasmara, I., 2011. On the suitability of the 4 degrees × 4 degrees GRACE mascon solutions for remote sensing Australian hydrology. Remote Sens. Environ. 115 (3), 684–690. https://doi.org/10.1016/j.rse.2010.11.014.

Awange, J., Hu, K., Khaki, M., 2019. The newly merged satellite remotely sensed, gauge and reanalysis-based Multi-Source Weighted-Ensemble Precipitation: evaluation over Australia and Africa (1981–2016). Sci. Total Environ. 670, 448–465. https://doi.org/10.1016/j.scitotenv.2019.03.148.

Awange, J., Kiema, J., 2013. Environmental Geoinformatics: Monitoring and Management (Environmental Science and Engineering). Springer-Verlag Berlin Heidelberg. https://doi.org/10.1007/978-3-642-34085-7.

Awange, J., Kiema, J., 2019. Environmental Geoinformatics: Extreme Hydro-Climatic and Food Security Challenges: Exploiting the Big Data. Springer-Verlag Berlin Heidelberg. https://doi.org/10.1007/978-3-030-03017-9.

Awange, J., Mpelasoka, F., Goncalves, R., 2016. When every drop counts: analysis of droughts in Brazil for the 1901–2013 period. Sci. Total Environ. 566-567, 1472–1488. https://doi.org/10.1016/j.scitotenv.2016.06.031.

Awange, J., Ogalo, L., Bae, K., Were, P., Omondi, P., Omute, P., Omullo, M., 2008. Falling Lake Victoria water levels: is climate a contributing facotr? Climate Change 89, 281–297. https://doi.org/10.1007/s10584-008-9409-x.

Awange, J., Sharifi, M., Baur, O., Keller, W., Featherstone, W., Kuhn, M., 2010. GRACE hydrological monitoring of Australia: current limitations and future prospects. J. Spat. Sci. 54 (1), 23–26. https://doi.org/10.1080/14498596.2009.9635164.

Barron, O., Crosbie, R., Charles, S., Dawes, W., Ali, R., Evans, W., Cresswell, R., Pollock, D., Hodgson, G., Currie, D., Mpelasoka, F., Pickett, T., Aryal, S., Donn, M., Wurcker, B., 2011. Climate change impact on groundwater resources in Australia. Summary report. CSIRO Water for a Healthy Country Flagship, Australia., retrieved from: https://publications.csiro.au/rpr/download?pid=csiro:EP121194&dsid=DS1. Data accessed: 10 March, 2019.

Beck, H., van Dijk, A., Levizzani, V., Schellekens, J., Miralles, D., Martens, B., dee Roo, A., 2017a. MSWEP: 3-hourly 0.25° global gridded precipitation (1979–2015) by merging gauge, satellite, and reanalysis data. Hydrol. Earth Syst. Sci. 21,„ 589–615. https://doi.org/10.5194/hess-21-589-2017.

Beck, H., Vergopolan, N., Pan, M., Levizzani, V., van Dijk, A., Weedon, G., Brocca, L., Pappenberger, F., Huffman, G., Wood, E., 2017b. Global-scale evaluation of 22 precipitation datasets using gauge observations and hydrological modeling. Hydrol. Earth Syst. Sci. 21, 6201–6217. https://doi.org/10.5194/hess-21-6201-2017.

Bhanja, S., Rodell, M., Li, B., Saha, D., Mukherjee, A., 2016. Spatio-temporal variability of groundwater storage in India. J. Hydrol. 544, 428–437. https://doi.org/10.1016/j.jhydrol.2016.11.052.

Cai, W., Purich, A., Cowan, T., van Rensch, P., Weller, E., 2014. Did climate change-induced rainfall trends contribute to the Australian Millennium Drought? J. Climate 27 (9), 3145–3168. https://doi.org/10.1175/JCLI-D-13-00322.1.

Cai, W., van Rensch, P., Cowan, T., 2011. Teleconnection pathways of ENSO and the IOD and the mechanisms for impacts on Australian rainfall. J. Climate 24, 3910–3923. https://doi.org/10.1175/2011JCLI4129.1.

Chen, J., Wilson, C., Tapley, B., Scanlon, B., Güntner, A., 2016. Long-term groundwater storage change in Victoria, Australia from satellite gravity and in situ observations. Glob. Planet. Chang. 139, 56–65. https://doi.org/10.1016/j.gloplacha.2016.01.002.

Crissa, R., Davissonb, M., 1996. Isotopic imaging of surface water/groundwater interactions, Sacramento Valley, California. J. Hydrol. 178 (1-4), 205–222. https://doi.org/10.1016/0022-1694(96)83733-4.

CSIRO, 2009. Groundwater yields in south-west Western Australia. A report to the Australian Government from the CSIRO South-West Western Australia Sustainable Yields Project. Tech. rep.. CSIRO Water for a Healthy Country Flagship, Australia.retrieved from: https://publications.csiro.au/rpr/download?pid=legacy:726&dsid=DS1. Data accessed: 6 March, 2019.

Dawes, W., Ali, R., Varma, S., Emelyanova, I., Hodgson, G., McFarlane, D., 2012. Modelling the effects of climate and land cover change on groundwater recharge in south-west Western Australia. Hydrol. Earth Syst. Sci. 16, 2709–2722. https://doi.org/10.5194/hess-16-2709-2012.

Department of Water, 2009. SouthWest - groundwater areas allocation plan. Water report 21. Government of Western Australia, Department of Water., retrieved from https://www.water.wa.gov.au/__data/assets/pdf_file/0013/1822/86107.pdf. Data accessed: 6 March, 2019.

Department of Water, 2007. State Water Plan 2007. Report. Department of Water, Government of Western Australia.

Department of Water, 2015. Environmental management of groundwater from the Gnangara Mound. Triennial compliance report to the office of the environmental protection authority. Government of Western Australia, Department of Water.

Eamus, D., 2015. Decling groundwater is a big problem for Australia. ABC NEWS. Environmental Sciences at the University of Technology., retrieved from: https://www.abc.net.au/news/2015-06-18/eamus-declining-groundwater-is-a-big-problem-for-australia/6556586. Data accessed: 10 March, 2019.

Featherstone, W., Filmer, M., Pena, N., Morgan, L., Schenk, A., 2012. Anthropogenic land subsidence in the Perth Basin: challenges for its retrospective geodetic detection. J. R. Soc. West. Aust. 95 (1), 53–62. http://hdl.handle.net/20.500.11937/14837.

Fleming, K., Awange, J., 2013. Comparing the version 7 TRMM 3B43 monthly precipitation product with the TRMM 3B43 version 6/6A and Bureau of Meteorology datasets for Australia. Aust. Meteorol. Oceanogr. J. 63, 421–426. https://doi.org/10.22499/2.6303.007.

Fleming, K., Awange, J., Kuhn, M., Featherstone, W., 2011. Evaluating the TRMM 3B43 monthly precipitation product using gridded raingauge data over Australia. Aust. Meteorol. Oceanogr. J. 61, 171–184. retrieved from: https://espace.curtin.edu.au/bitstream/handle/20.500.11937/23560/169513_169513.pdf?sequence=2. Data accessed: 3 March, 2019.

Forootan, E., Khandu, Awange, J., Schumacher, M., Anyah, R., van Dijk, A., Kusche, J., 2016. Quantifying the impacts of ENSO and IOD on rain gauge and remotely sensed precipitation products over Australia. Remote Sens. Environ. 172, 50–66. https://doi.org/10.1016/j.rse.2015.10.027.

Han, D., Currell, M., Cao, G., Hall, B., 2017. Alterations to groundwater recharge due to anthropogenic landscape change. J. Hydrol. 554, 545–557. https://doi.org/10.1016/j.jhydrol.2017.09.018.

Heberger, M., 2011. Australia's Millennium Drought: Impacts and Responses. Island Press/Center for Resource Economics, Washington, DC., pp. 97–125. https://doi.org/10.5822/978-1-59726-228-6_5.

Hill, M., Donald, G., Hyder, M., Smith, R., 2004. Estimation of pasture growth rate in the south west of Western Australia from AVHRR NDVI and climate data. Remote Sens. Environ. 93 (4), 528–545. https://doi.org/10.1016/j.res.2004.08.006.

Holbrook, N., Davidson, J., Feng, M., Hobday, A., Lough, J., McGregor, S., Risbey, J., 2009. El Niño-Southern Oscillation. A Marine Climate Chnage Impacts and Adaptation Report Card for Australia 2009. NCCARF., publication 05/09, ISBN 978-1-921609-03-09.

Hu, K., Awange, J., Khandu, Forootan, E., Goncalves, R., Fleming, K., 2017. Hydrogeological characterisation of groundwater over Brazil using remotely sensed and model products. Sci. Total Environ. 599-600, 372–386. https://doi.org/10.1016/j.scitotenv.2017.04.188.

Hughes, J., Petrone, K., Silberstein, R., 2012. Drought, groundwater storage and stream flow decline in southwestern Australia. Geophys. Res. Lett. 39 (3), L03408. https://doi.org/10.1029/2011GL050797.

Jenks, G., 1967. The data model concept in statistical mapping. International Yearbook of Cartography. 7. pp. 186–190.

Kinal, J., Stoneman, G., 2012. Disconnection of groundwater from surface water causes a fundamental change in hydrology in a forested catchment in south-western Australia. J. Hydrol. 472-473, 14–24. https://doi.org/10.1016/j.jhydrol.2012.09.013.

Knapp, C., Carter, G., 1976. The generalized correlation method for estimation of time delay. IEEE Trans. Acoust. Speech Signal Process. 24 (4), 320–327. https://doi.org/10.1109/TASSP.1976.1162830.

Leblance, M., Tregoning, P., Ramillien, G., Tweed, S., Fakes, A., 2009. Basin-scale, integrated observations of the early 21st century multiyear drought in southeast Australia. Water Resour. Res. 45 (4), W04408. https://doi.org/10.1029/2008WR007333.

Li, J., Xie, S., Cook, E., Morales, M., Christie, D., Johnson, N., Chen, F., Arrigo, R., Fowler, A., Gou, X., Fang, K., 2013. El Niño modulations over the past seven centuries. Nat. Clim. Chang. 3, 822–826. https://doi.org/10.1038/nclimate1936.

Mann, H.B., 1945. Noparametric tests against trend. Econometrica 13, 163–171.

Massey, F., 1951. The Kolmogorov-Smirnov test for goodness of fit. J. Am. Stat. Assoc. 46 (253).

Nicholls, N., Drosdowsky, W., Lavery, B., 1997. Australian rainfall variability and change. Weather 52, 66–72. https://doi.org/10.1002/j.1477-8696.1997.tb06274.x.

Niedzielski, T., 2014. Chapter two - El Niño/Southern oscillation and selected environmental consequences. Adv. Geophys. 55, 77–122. https://doi.org/10.1016/bs.agph.2014.08.002.

Nikroo, L., Zare, M., Sepaskhah, A., Shamsi, S., 2008. Groundwater depth and elevation interpolation by kriging methods in Mohr Basin of Fars province in Iran. Environ. Monit. Assess. 166, 387–407. https://doi.org/10.1007/s10661-009-1010-x.

Oliver, M.A., 1990. Kriging: a method of interpolation for geographical information systems. Int. J. Geogr. Inf. Syst. 4, 313–332.

Philip, G.M., Watson, D.F., 1982. A precise method for determining contoured surfaces. Aust. Pet. Explor. Assoc. J. 22, 205–212.

Population Australia, 2018. Population of Western Australia 2019. Population report. Australia Bureau of Statistics, Australian Government and Tourism Western Australia., retrieved from http://www.population.net.au/population-of-western-australia/. Data accessed: 3 March, 2019.

Rieser, D., Kuhn, M., Pail, R., Anjasmara, I., Awange, J., 2010. Relation between GRACE-derived surface mass variations and precipitation over Australia. Aust. J. Earth Sci. 57 (7), 887–900. https://doi.org/10.1080/08120099.2010.512645.

Robinson, T., Metternicht, G., 2006. Testing the performance of spatial interpolation techniques for mapping soil properties. Comput. Electron. Agric. 50, 97–108. https://doi.org/10.1016/j.compag.2005.07.003.

Saji, N., Yamagata, T., 2003. Possible impacts of Indian Ocean Dipole mode events on global climate. Clim. Res. 25 (2), 151–169. Retrieved from: https://www.int-res.com/abstracts/cr/v25/n2/p151-169/. Data accessed: 6 March, 2019.

Saleem, A., Awange, J.L., 2019. Coastline shift analysis in data deficient regions: exploiting the high spatiotemporal resolution Sentinel-2 products. Catena 179, 6–19. https://doi.org/10.1016/j.catena.2019.03.023.

Skurray, J., Roberts, E., Pannell, D., 2012. Hydrological challenges to groundwater trading: lessons from south-west Western Australia. J. Hydrol. (412-413), 256–268. https://doi.org/10.1016/j.jhydrol.2011.05.034.

Strassberg, G., Scanlon, B., Chambers, D., 2009. Evaluation of groundwater storage monitoring with the GRACE satellite: case study of the High Plains aquifer, central United States. Water Resour. Res. 45 (5), W05410. https://doi.org/10.1029/2008WR006892.

Suh, J., Brown, P., Birch, G., 2003. Hydrogeochemical characteristics and importance of natural and anthropogenic influences on soil and groundwater in reclaimed land adjacent to Port Jackson, Sydney, Australia. Mar. Freshw. Res. 54 (6), 767–779. https://doi.org/10.1071/MF02075.

Sun, Y., Kang, S., Li, F., Zhang, L., 2009. Comparison of interpolation methods for depth to groundwater and its temporal and spatial variations in the Minqin oasis of northwest China. Environ. Model. Softw. 24, 1163–1170. https://doi.org/10.1016/j.envsoft.2009.03.009.

Taylor, R., Scanlon, B., Döll, P., Rodell, M., van Beek, R., Wada, Y., Longuevergne, L., Leblanc, M., Famiglietti, J., Edmunds, M., Konikow, L., Green, T., Chen, J., Taniguchi, M., Bierkens, M., MacDonald, A., Fan, Y., Maxwell, R., Yechieli, Y., Gurdak, J., Allen, D., Shamsudduha, M., Hiscock, K., Yeh, P., Holman, I., Treidel, H., 2013. Groundwater and climate change. Nat. Clim. Chang. 3, 322–329. retrieved from: https://www.nature.com/articles/nclimate1744. Data accessed: 6 March, 2019.

Tregoning, P., McClusky, S., van Dijk, A., Crosbie, R., Peña-Arancibia, J., 2012. Assessment of GRACE satellites for groundwater estimation in Australia. Waterlines report. National Water Commission, Canberra.retrieved from: https://www.researchgate.net/publication/233757174. Data accessed: 3 March, 2019.

Tudhope, A., Chilcott, C., McCulloch, M., Cook, E., Chappell, J., Ellam, R., Lea, D., Lough, J., Shimmield, G., 2001. Variability in the EI Niño-Southern oscillation through a glacial-interglacial cycle. Science 291 (5508), 1511–1517. https://doi.org/10.1126/science.1057969.

Tweed, S., Leblanc, M., Webb, J., Lubczynski, M., 2007. Remote sensing and GIS for mapping groundwater recharge and discharge areas in salinity prone catchments, southeastern Australia. Hydrogeol. J. 15 (1), 75–96. https://doi.org/10.1007/s10040-006-0129-x.

Wolter, K., Timlin, M., 1998. Measuring the strength of ENSO - how does 1997/98 rank? Weather 53, 315–324. https://doi.org/10.1002/j.1477-8696.1998.tb06408.x.

Chapter 3
Understanding the balance between groundwater use and agricultural expansion in the Northern Territory

This chapter is covered by the following publication (*Hu et al.* 2022c):

1. **Hu, K.X.**, Awange, J.L., Kuhn, M. and Zerihun, A., (2022). Irrigated agriculture potential of Australia's northern territory inferred from spatial assessment of groundwater availability and crop evapotranspiration. Agricultural Water Management, 264, 107466, doi: 10.1016/j.agwat.2022.107466.

This paper estimates the irrigated agricultural potential in the Northern Territory in order to provide useful information for agricultural expansion. Two scenarios, i.e. average condition (2010-2019) and dry condition (2019; the lowest rainfall since 1961), are selected to present the influence of dry climate extremes on irrigated agricultural potential. Three types of crops, i.e. melon, maize and citrus, which represent short, medium, and high water use crops, are selected as examples for illustrating the irrigated agricultural potential. The groundwater availability is estimated based on the '80-20 rules' water policy (*MacFarlane and Fairfield*, 2017), while the crop water demands are calculated using the Pennman-Monteith equation (*Allen et al.*, 1998). The spatial maps of balance between groundwater availability and crop water demands are then provided to fill the knowledge gaps mentioned in Section 1.4.2 and to cover objective (ii) in Section 1.5. Overall, the results show that the irrigated agricultural potential generally decreases from north to south in the Northern Territory and a large-scale or an intensive irrigated agricultural expansion is generally unwise. For instance, under the average condition (2010-2019) scenario, and after excluding the non-agricultural areas such as national parks, available groundwater within every 60,000 hectares can only be used to irrigate an average of 9,430/2,780/400 (15.7%/9.1%/5.8%) hectares of melons (a low water demand crop) in northern/central/southern parts of the Northern Territory. Under the dry scenario condition (2019), this estimate can be reduced even further, by 1/3, suggesting that drought risk management remains a serious concern. Note, all calculated numbers of irrigated agricultural potential above are only a guide and may not be that accurate. This is due to the fact that the groundwater data, i.e., Global Land Data Assimilation System (GLDAS) Catchment Land Surface Model (CLSM) with data assimilated from the Gravity Recovery and Climate Experiment (GRACE; hereafter called GLDAS-DA) mostly represents the storage variation for shallow aquifers (confined or unconfined aquifers are not distinguished). Particularly, for regions

such as central Australia around Alice Springs, where the agricultural irrigation relies on groundwater at 200 m depth, the estimated irrigated agricultural potential is less representative.

Agricultural Water Management 264 (2022) 107466

Contents lists available at ScienceDirect

Agricultural Water Management

journal homepage: www.elsevier.com/locate/agwat

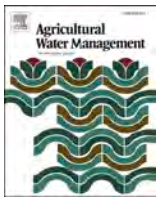

Irrigated agriculture potential of Australia's northern territory inferred from spatial assessment of groundwater availability and crop evapotranspiration

K.X. Hu [a,*], J.L. Awange [a,b], M. Kuhn [a], A. Zerihun [c]

[a] School of Earth and Planetary Sciences, Spatial Science Discipline, Curtin University, Perth, Australia
[b] Geodetic Institute, Karlsruhe Institute of Technology, Engler-Strasse 7, D-76131 Karlsruhe, Germany
[c] School of Molecular and Life Sciences, Centre for Crop Disease Management, Curtin University, Perth, Australia

ARTICLE INFO

Handling Editor - Xiying Zhang

Keywords:
Agriculture
Australia
Balance
Crop water demand
GLDAS-DA Groundwater

ABSTRACT

Agricultural expansion has been a hot topic in the Northern Territory (NT) of Australia in recent years. However, insufficient information on available water resources and crop evapotranspiration is a bottleneck to this expansion. Towards closing this gap, this study employs the newest Global Land Data Assimilation System (GLDAS; version 2.2) catchment products assimilated from the Gravity Recovery and Climate Experiment (GRACE; hereafter called GLDAS-DA) and the Food and Agriculture Organization (FAO) Penman-Monteith equation to spatially evaluate the *Balance* between water availability (i.e., groundwater and effective rainfall) and melons, maize and citrus crop evapotranspiration (water demand) of three representative (short-, medium-season and perennial) crop types over the NT for the 2010–2019 period. Specifically, this *Balance* is the estimated ratio of water availability and crop evapotranspiration, representing the crop area that can be planted in each GLDAS-DA grid cell. The larger the *Balance*, the greater the irrigated agriculture potential. Under the average 2010–2019 conditions, our results show that the northern part of the NT has the highest irrigated agriculture potentials with the average *Balance* of 9430 ha (15.7%), 5490 ha (9.1%) and 3520 ha (5.8%) for melons, maize and citrus, respectively, excluding non-agriculture areas. Irrigated agriculture in the central part of the NT shows less potential compared to the northern part of the NT, with the average *Balance* of 2780 ha (4.6%), 2000 ha (3.3%) and 970 ha (1.6%) for melons, maize and citrus, respectively (excluding non-agriculture areas). The southern part of the NT shows an average *Balance* below 1% of grid cell for all three crops, suggesting that only small-scale irrigated agriculture could be possible. In addition, the *Balance* across most of the northern and central parts of the NT decreased by 50% or more during 2019 dry period. Drought risk management should therefore be a serious consideration when exploring further expansion of irrigated agriculture in the NT.

1. Introduction

The Australian Northern Territory (NT) covers around 18% of Australia's continental area but is home to only around 1% of its population, according to the Australian Bureau of Statistics (ABS) 2020. This vast land is thought to have agricultural potential that is waiting to be developed (Ash et al., 2017). In 2015, a White Paper issued by the Australian Government specifically stressed the importance of water resources in terms of agricultural development in northern Australia (CSIRO, 2016). This renewed interest in agriculture stems from growing Asian markets (Reardon and Timmer, 2014) and increasing global demand for food (Ash et al., 2017). More importantly, seeking development of irrigated agriculture in the NT is treated as a way to reverse its long-term population decline (CSIRO, 2016). Therefore, relevant studies that address federal and state/territory governments' interests in evaluating and identifying the opportunities for irrigated agriculture may also facilitate regional economic development of the NT.

However, one major concern raised by the NT Government for expanding irrigated agriculture is the issue of sustainability since the available water for irrigation may not be able to meet the crop water demand (Thomas et al., 2018), i.e., evapotranspiration. In the NT, groundwater is the major source of water supply, e.g., for mining, irrigation and domestic use, contributing about 90% of the total water

* Corresponding author.
E-mail address: kexiang.hu@postgrad.curtin.edu.au (K.X. Hu).

https://doi.org/10.1016/j.agwat.2022.107466
Received 22 August 2021; Received in revised form 24 December 2021; Accepted 4 January 2022
Available online 24 January 2022

usage (Kinsela et al., 2012). Nevertheless, information on groundwater such as its spatio-temporal availability for irrigated agriculture is limited for the NT region. As for crop water demand, the estimation is rather complicated due to many factors involved, e.g., crop type, sowing time, stage of growth, local environmental conditions, etc. As a result, there has been relatively little research directed towards irrigated agriculture in the NT (Ash et al., 2017).

In recent years, considerable efforts have been made to assess the potential for irrigated agricultural expansion. For example, many technical reports and water monitoring plans for potential agricultural regions have been produced on the one hand (Ti Tree Water Report, 2009; Oolloo Water Allocation Plan, 2010; Northern Territory Government, 2018; CSIRO, 2016; Ash et al., 2018). On the other hand, local experiments for crop water demand have also been done (Northern Territory Government, 2007; Bithell and Smith, 2011; MacFarlane and Fairfield, 2017). These reports, however, are still insufficient to estimate the potential of irrigated agricultural expansion over the whole NT given that they are area specific, e.g., mostly in water control districts (Fig. 1) drafted by the NT Government. Other studies on water-related information and crop irrigation mainly focus on hydrological and environmental aspects, e.g., Jacobson et al. (1988), Calf et al. (1991), Erskine et al. (2003), or concentrate on hydro-chemical aspects only, e.g., Cresswell et al. (1999), Vanderzalm et al. (2011), Barry et al. (2017). Besides, there is a lack of direct linkage between groundwater and crop irrigation research in the NT, e.g., where crop water demand is studied, groundwater availability for irrigation is not evaluated and compared. Therefore, spatio-temporal groundwater availability and crop water demand over the NT, as well as the linkage between these, are not well understood.

To address this lack of information, this study uses the Global Land Data Assimilation System (GLDAS) Catchment Land Surface Model (CLSM) that simulates groundwater storage in shallow aquifers (Li et al., 2019a) and the Food and Agriculture Organization (FAO) Penman-Monteith equation (Allen et al., 1998) to model groundwater availability and estimate crop evapotranspiration in the NT over the 2010–2019 period, respectively. The newest GLDAS-V2.2 with data

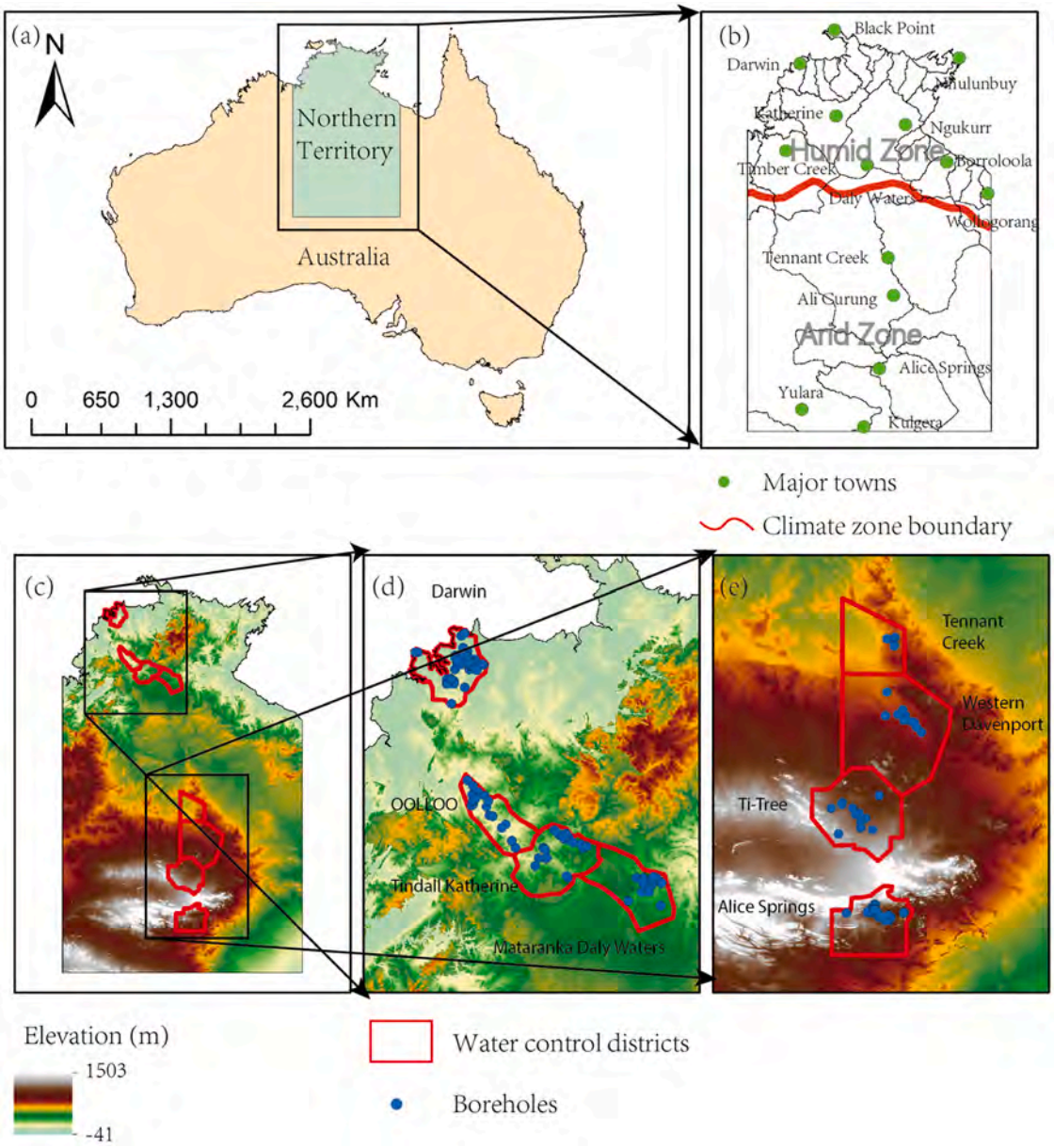

Fig. 1. Study area of the Northern Territory in Australia; (a) the Northern Territory boundary, (b) climate zones and positions of major towns, (c) elevations and the eight major water control districts drafted by the NT Government, and (d)-(e), details of names and locations of districts as well as boreholes' positions.

assimilated from the Gravity Recovery and Climate Experiment (GRACE; hereafter called GLDAS-DA) offers daily groundwater storage estimates from 2003 to present (Li et al., 2019b) at a 0.25˚ × 0.25˚ spatial resolution. The evaluation of this product shows a relatively good regional-scale correlation (0.65) with over 4000 globally distributed borehole data (Li et al., 2019b). In the NT, the GLDAS-DA is employed to make up for the scarcity of borehole data outside the water control districts (Fig. 1). The FAO Penman-Monteith equation is recommended as the sole standard method for calculating the reference crop evapotranspiration (ET_0), i.e., crop water demand (Allen et al., 1998; Pereira et al., 2015). This method is widely used in different locations and climates (Zhang et al., 2010; Yao et al., 2014; Zanotelli et al., 2019) and is not constrained by data deficiency, i.e., can be derived from remote sensing, hydrological models or re-analysis data (Zhang et al., 2010; Yao et al., 2014; Blankenau et al., 2020). In Australia, both McMahon et al. (2013) and Bithell and Smith (2011) have indicated that the FAO Penman-Monteith equation is more accurate than other methods such as pan evaporation. Ahooghlandari et al. (2016), (2017) also used the FAO Penman-Monteith equation as the reference method when evaluating crop evapotranspiration at multiple locations in Australia. However, these studies are area-specific, and the calculations are only based on point-scale (i.e., meteorological stations).

Therefore, in this study, a spatio-temporal analytical framework is used to evaluate groundwater availability, crop water demand and the resultant potential for irrigated agriculture across the NT. In particular, the study (i) evaluates the spatial variability of monthly and annual groundwater availability (at 0.25˚ × 0.25˚ resolution) based on the average condition for the 2010–2019 period and the dry condition for the year 2019, respectively; (ii) estimates the spatial variability of the monthly reference crop evapotranspiration using the Penman-Monteith equation based on two scenarios (average/dry) as mentioned in (i); (iii) calculates the *Balance*, i.e., the ratio of water availability and crop evapotranspiration for per GLDAS-DA grid cell (around 60,000 ha), as well as highlight potential areas for irrigated agricultural expansion based on the two scenarios (average/dry) as specified in (i). Subsequently, the results of *Balance* are improved by excluding those areas that are obviously not suitable for agricultural use, e.g., nature conservations, areas that do not have suitable soil and areas that have salinity issues in groundwater.

2. Data and methods

2.1. Groundwater availability estimation

Here, we assume that groundwater is the only source of irrigation in the NT since (i) surface water such as rivers are strongly seasonal and the locations of rivers are not always close to the irrigated land (Ash et al., 2017), and (ii), in the central (semi-arid) and southern (arid) parts of the NT (see Fig. 1), groundwater is the only reliable water resource that can be used for irrigation (Mossad et al., 2013).

2.1.1. Scenarios of average (2010–2019) and dry (2019) period

Considering the groundwater availability may be very different during different climatic conditions (i.e., wet and dry), it is therefore, important to understand the range of groundwater availability under average and dry scenarios in order to enable a better groundwater risk management. In this regard, this study calculates the average groundwater availability based on the 2010–2019 period, as well as the groundwater availability in the driest years, 2019, which recorded the lowest annual rainfall since 1961.

To prove the representativeness of these two periods, we download the annual rainfall records of Northern Territory from BoM (http://www.bom.gov.au/climate/change/) for the past 120 years, i.e., 1900–2019, and compared our average condition and dry condition to other periods. Specifically, we use the percentile method to identify the years under wet (above 90th percentile), average (10th to 90th percentile) and dry (below 10th percentile) climate condition. A ten-year running average (± 5 years) is also calculated to present the long-term variation of rainfall. Meanwhile, the Kolmogorov-Smirnov (K-S) test (Marsaglia et al., 2003; Awange et al., 2019) is employed to test whether the distribution of rainfall between 2010 and 2019 and 1900–2019 is the same.

According to Fig. 2, the average rainfall for the 2010–2019 period is 601 mm, while the 10-year running average is stable above 600 mm since 1996. The K-S test shows that the distribution of rainfall between 2010 and 2019 and 1900–2019 is the same at 95% confidence level with a score of 0.33 (the smaller value is the more similar distribution). Therefore, it can be safely said that our results are more or less representative at least for the last 25 years. As for year the 2019, it is the driest year except 1961, and the rainfall value of 265 mm is below the 10th percentile line. Thus, using 2019 as a showcase of dry-year conditions is also representative. Besides, one can see the 10-year running average seems to have a 30-years cycle of rainfall, e.g., 1900–1930, 1930–1960, 1960–1990, 1990-present. Considering the different behaviours of previous cycles, as well as potential increasing rainfall for future scenario, e.g., there is an obvious increasing rainfall in the most two recent cycles due to the increasing intensity of tropical cyclones (Hennessy et al., 2004), it may requires a re-estimation of results in future, particularly, when government is going to develop a long-term land irrigation program.

2.1.2. The '80–20 rules'

According to Erskine et al. (2003) and MacFarlane and Fairfield (2017), the '80–20 rules' announced by the NT Government allow only 20% of the annual groundwater recharge or discharge to be extracted for irrigation (i.e., abstraction limit, see Fig. 3). Therefore, the maximum annual groundwater availability for irrigation can either be derived from groundwater recharge:

$$A_{ar} = Sum(Recharge_{monthly}) \times 20\%, \quad (1)$$

or groundwater discharge:

$$A_{ad} = Sum(Discharge_{monthly}) \times 20\%, \quad (2)$$

where the $Recharge_{monthly}$ and $Discharge_{monthly}$ are the monthly groundwater changes (positive as recharge and negative as discharge). To obtain these data, the GLDAS-DA estimated groundwater storage in shallow aquifers (up to 6–8 m depending on input geological profiles) with 0.25˚ × 0.25˚ spatial and daily temporal resolution (Li et al., 2019b) is employed for the 2010–2019 period. The monthly groundwater changes are derived from the difference between groundwater storage records of the last day in the current month and the last day in the previous month. Since the GLDAS-DA has not been directly evaluated over the NT (Li et al., 2019b), borehole records (mostly located in water control districts, see Figs 1d and 1e) downloaded from the Australian Groundwater explorer (http://www.bom.gov.au/water/groundwater/explorer/) and the WaterGAP Global Hydrology Model (WGHM; Werth and Güntner, 2010; Doll et al., 2014) that is commonly used to compare with GRACE, see, e.g., Werth et al. (2009), are also employed to examine the performance of the GLDAS-DA over the NT. The evaluation is presented in the supplementary material. Basically, both borehole and WGHM show that GLDAS-DA has a relative good performance in the northern part of the NT, but may not be representative in the southern part of the NT. Thus, the results in southern part of the NT in this study has to be carefully treated.

As the Northern Territory is largely covered by tropical climate, most of the groundwater recharge occurs from November to March, while discharge appears from April to October based on our examination (2010–2019 average condition; different years could be slightly different). Normally, the groundwater availability for the whole year can be estimated at the end of March, i.e., A_{ar}, leading to the groundwater extraction plan, which is adjusted according to the 20% of $Discharge_{monthly}$ ('80–20 rules') in the following dry period. Note that the

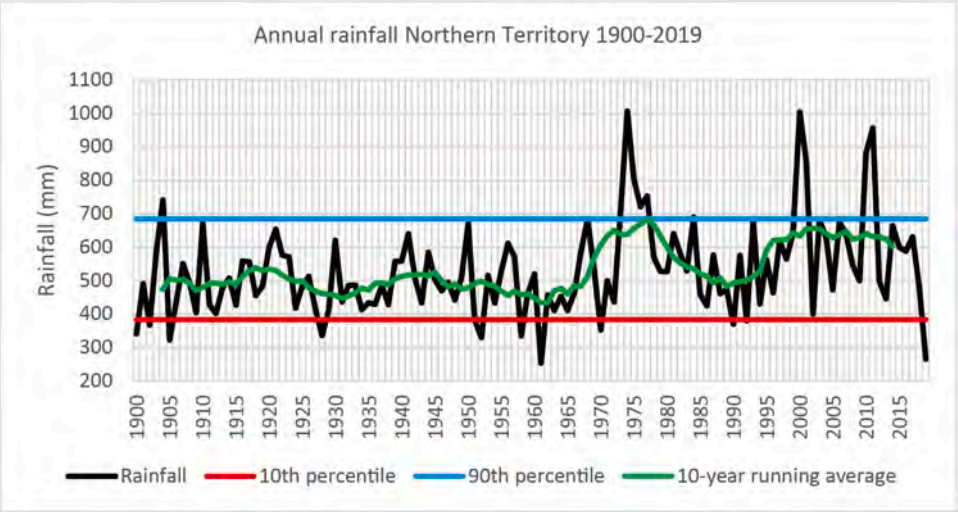

Fig. 2. The annual rainfall of Northern Territory (average over the entire area) for 1900–2019 period. The rainfall values at 10th and 90th percentile are 383 mm and 684 mm, respectively.

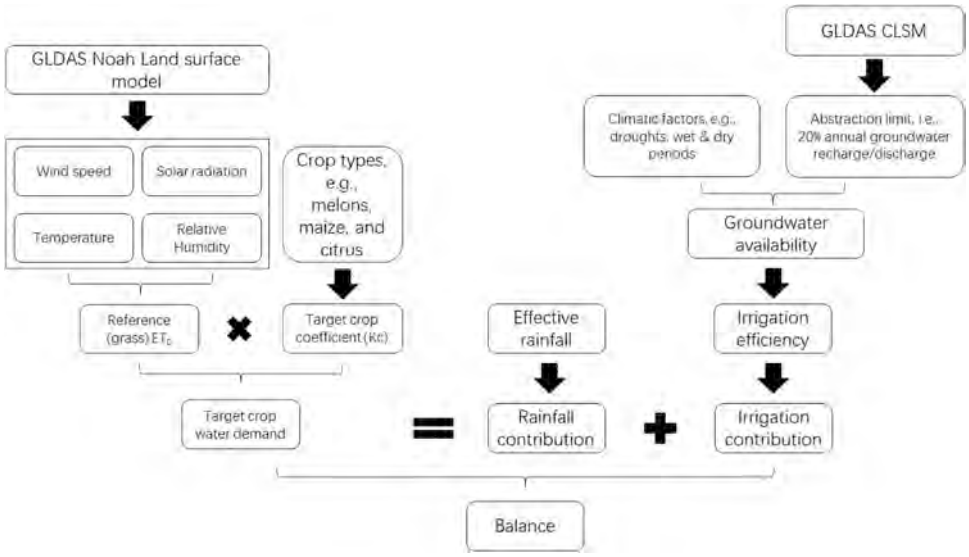

Fig. 3. The processing flowchart of calculating the balance between groundwater availability, effective rainfall and crop water demand. ET_0 represents evapotranspiration of reference crop.

20% of the monthly groundwater discharge is set as the monthly groundwater availability (not mandatory), because pumping a large amount of groundwater in a month may lead to unsustainable water use and environmental degradation in other months. However, this is only suitable for crops grown in the dry period. For some crops, e.g., perennial crops that have high water demand, irrigation is still necessary during the wet period. Thus, the distribution of the limited groundwater availability into 12 months remains questionable.Fig. 4.

Here, we firstly present the monthly 20% of groundwater changes (Fig. 5), as well as A_{ar} and A_{ad} derived from wet (November to March) and dry (April to October) periods under the average condition of 2010–2019 (Fig. 6) in order to offer the spatio-temporal information of groundwater availability over the NT. When the groundwater availability is compared to the specific crop water demands, the dry period grown crops can use the monthly 20% of groundwater discharge for irrigation (e.g., melons and maize in Fig. 8). As for perennial crops (e.g., citrus in Fig. 8), we only compare the annual groundwater availability and crop water demand since a good distribution of annual groundwater availability in each month should be determined by the monthly weights of crop water demands.

2.2. Reference ET_0 estimation

The reference ET_0 is defined as the evapotranspiration rate (mm/day) from a reference surface with adequate water. This reference surface is assumed by the Food and Agriculture Organization (FAO) Expert Consultation on the Revision of FAO Methodologies for Crop Water Demand as: a hypothetical reference (close to grass) crop with an assumed crop height of 0.12 m, a fixed surface resistance of 70 s/m and an albedo of 0.23 (Allen et al., 1998). In this study, the methodology of calculating reference ET_0 strictly follows the 'Crop evapotranspiration - Guidelines for computing crop water requirements - FAO Irrigation and drainage paper 56' (Allen et al., 1998). The major equation is shown below, and the parameter derivations are listed in the supplementary material.

The FAO Penman-Monteith equation is expressed as:

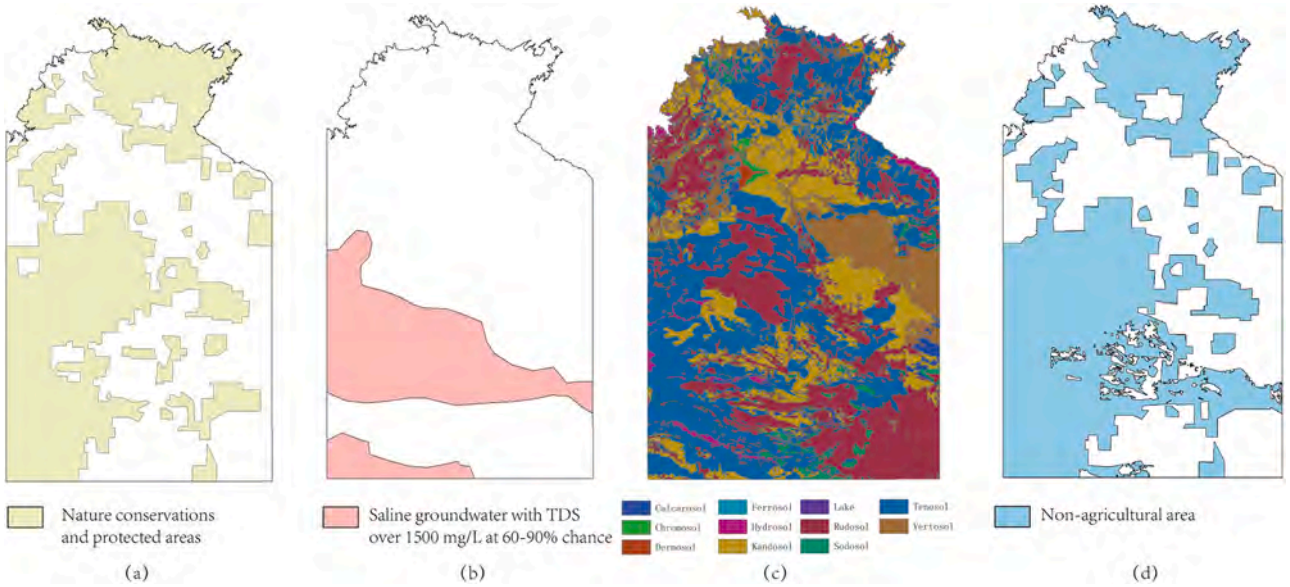

Fig. 4. Maps of (a) nature conservations and protected areas, digitalised from ABARES (2015)), (b) saline groundwater with TDS over 1500 mg/L at 60–90% chance, digitalised from Harrington and Cook (2014)), (c), distribution of major soil types in the NT (Ashton and McKenzie, 2016), and (d), non-agricultural area for exclusion derived from (a), (b) and (c).

$$ET_0 = \frac{0.408\Delta(R_n - G) + \gamma \frac{900}{T+273} u_2 (e_s - e_a)}{\Delta + \gamma(1 + 0.34u_2)}, \quad (3)$$

where R_n is the net radiation at the crop surface (MJ/m^2/day), G the soil heat flux (MJ/m^2/day), T the mean daily air temperature at 2 m height (°C), u_2 the wind speed at 2 m height (m/s), e_s the saturation vapour pressure (kPa), e_a the actual vapour pressure (kPa), Δ the slope vapour pressure curve (kPa/°C) and γ the psychrometric constant (kPa/°C). To obtain above data, the GLDAS Noah land surface model with a 0.25° × 0.25° spatial and monthly temporal resolution is employed as such other studies did, see, e.g., Park and Choi (2015) and Blankenau et al. (2020).

2.3. Balance estimation

The estimation of balance between target crop water demand and water availability is considered a key factor that determines crop demand and supply sides (Fig. 3). Crop water demand is estimated by applying target crop coefficients to reference ET_0 (see discussion below). On the supply side, water availability is estimated as the sum of effective rainfall and groundwater availability after applying irrigation efficiency (see Fig. 3). The balance, therefore, denotes the parity/disparity between the crop water demand and the water supply (effective rainfall plus irrigation).

2.3.1. Crop water demand

Crop water demand can be either obtained from previous studies, e.g., Brouwer and Heibloem (1986) and MacFarlane and Fairfield (2017), or calculated from the crop coefficient and ET_0. As an example of a former study in MacFarlane and Fairfield (2017), Table 1 illustrates some general crop water usages and growing periods in the NT. However, the crop water demand estimated from the crop coefficient and ET_0 is more useful since it provides monthly estimates based on different local environmental conditions. In this approach, crop water demand, e.g., on a monthly basis, is expressed as:

$$D_m = \frac{ET_0 \times Days \times K_c - Rain_e}{IE}, \quad (4)$$

where D_m is the monthly crop water demand for irrigation, ET_0 the reference crop evapotranspiration per day, $Days$ the number of days in that calculated month, $Rain_e$ the monthly effective rainfall and IE the irrigation efficiency, which usually takes 0.75 or 0.85 depending on irrigation methods used (Ash et al., 2018; Bithell and Smith, 2011). As for K_c, it is the crop coefficient, which can be regarded as an empirical scale factor that converts ET_0 into evapotranspiration of a specific crop. Normally, K_c varies depending on crop growth stages and crop types. For illustration, this study selects melons, maize and citrus as representative of low (short season), medium (medium season) and high (perennial) water use crops to show the adapted monthly K_c at different growth stages in Table 2 since each of these crops represents a different level of water demand.

2.3.2. Effective rainfall estimation

The effective rainfall is the rainfall that can be directly or indirectly be used for crop production. The method proposed by Dastane (1978) is employed here, which is given as:

$$Rain_e = Rain(125 - 0.2Rain)/125, \quad for \quad \text{Rain} \leq 250 \quad \text{mm}, \quad (5)$$

or

$$Rain_e = 125 + 0.1Rain, \quad for \quad Rain > 250 \quad mm, \quad (6)$$

where $Rain_e$ and $Rain$ are the effective rainfall and total monthly rainfall, respectively. This method has been employed by many studies, see e.g., Loukas et al. (2007) and Singh et al. (2020). To obtain the monthly rainfall, the Bureau of Meteorology (BoM) rainfall product with a 0.05° × 0.05° spatial and monthly temporal resolution is employed (downloaded from http://www.bom.gov.au/climate/maps/rainfall/). Before used, the data are re-scaled to 0.25° × 0.25° in order to match it with the spatial resolution of GLDAS models.

2.3.3. Parity/disparity between water supply and crop water demand

Considering the 0.25° × 0.25° spatial resolution of groundwater outputs in this study, i.e., approximately 60,000 ha per grid cell at the latitude of −20° (center of the NT), the balance between groundwater supply and total crop water demand (D, i.e., sum of D_m) for a specific crop can be expressed as an area index:

$$Balance = \frac{A_{ad} \quad or \quad A_{ar} \times 60,000}{D}, \quad (7)$$

where $A_{ad} or A_{ar} \times 60,000$ represents the total amount of useable

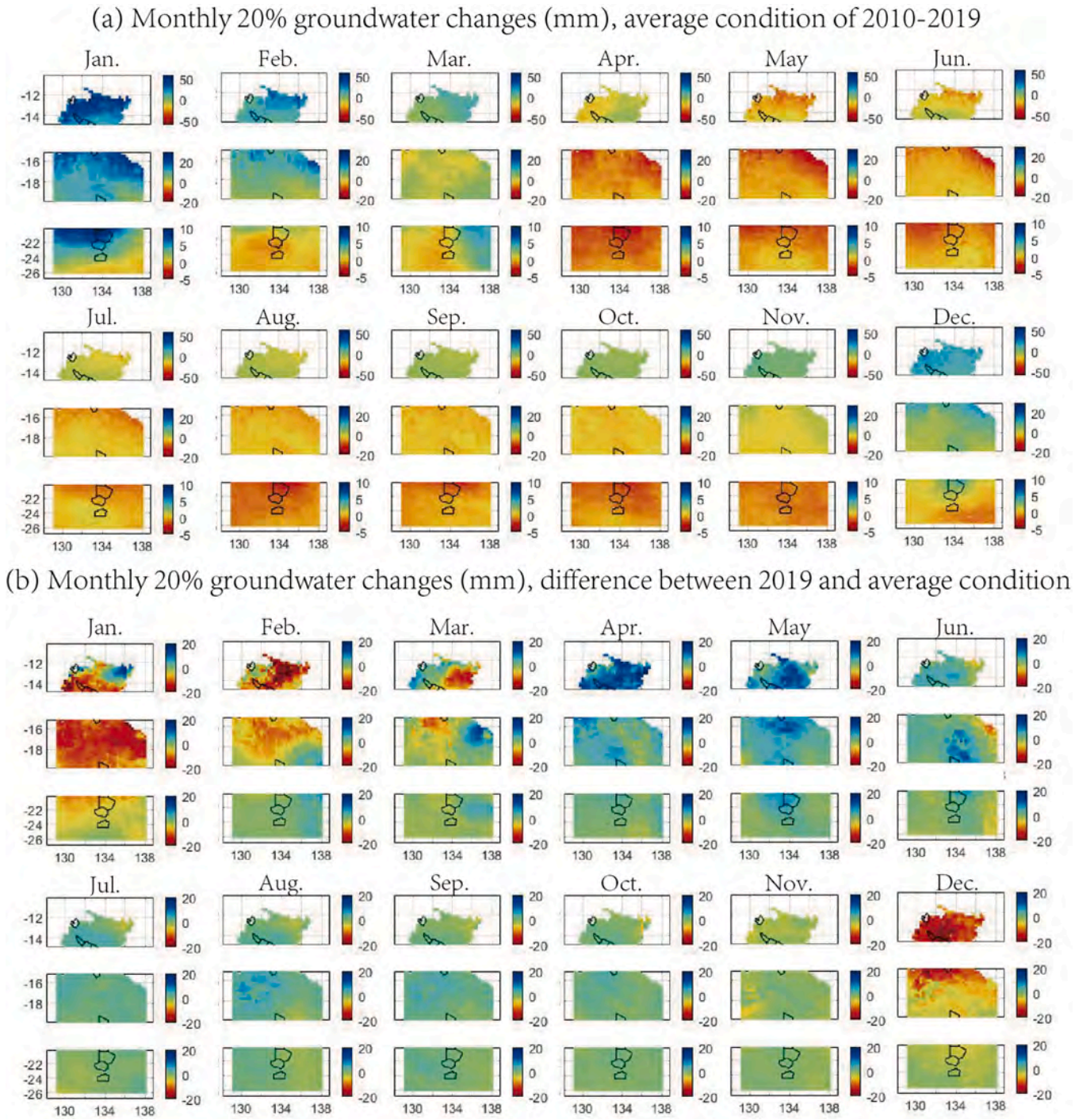

Fig. 5. Monthly 20% of groundwater changes (mm) based on the average condition 2010–2019 (a), as well as its comparison to the dry condition for the year of 2019 (b). The small polygons in the figure represent the water control districts shown in Fig. 1c.

groundwater for a grid cell under the '80–20 rules', the *Balance* theoretically indicates the number of hectares that crops can be potentially supplied by such amount of groundwater. The larger the *Balance* is, the greater the crop areas that can be irrigated, and, as such, the higher the potential for irrigated agriculture is.

2.4. Exclusion of non-agriculture areas

Besides the water availability, land use, water salinity and soil types are also important consideration for agricultural activities. For land use in the NT, there are many areas that belong to nature conservations, thus, agricultural expansion in these regions is not permitted. Fig. 4a illustrates those areas under environmental protection based on the land use map from ABARES (2015). Groundwater salinity is an indicator of water quality that sums all dissolved constituents in the water (usually called Total Dissolved Solids; TDS, unit: mg/L). Different plants and crops have different tolerance to saline water. According to the general salinity classification table from the Department of Agriculture and Food in Western Australia (https://www.agric.wa.gov.au/water-management/water-salinity-and-plant-irrigation), salinity below 1425 mg/L is considered as moderately salty and is suitable for irrigation to a major range of crops. Fig. 4b provides a general map of groundwater salinity

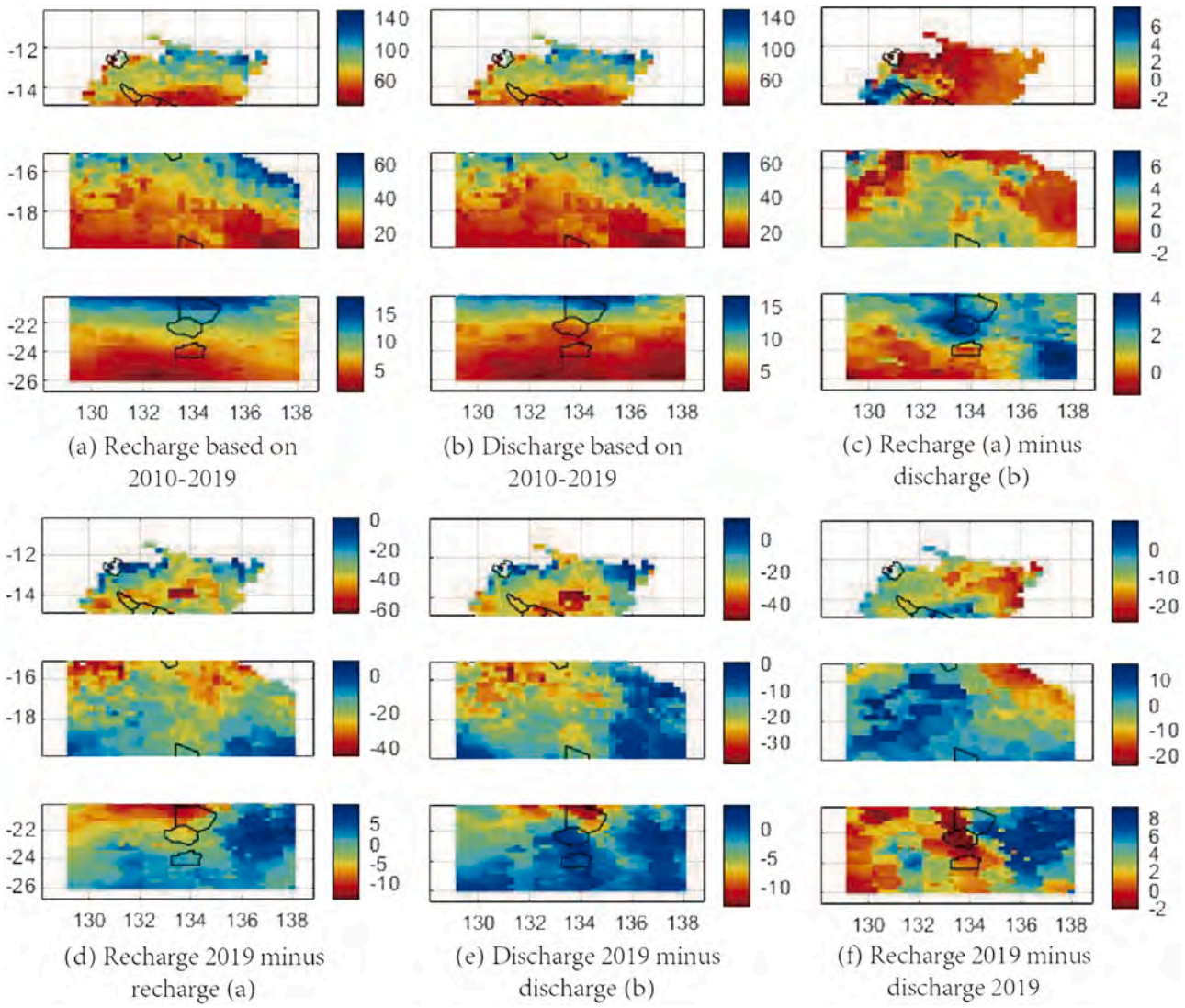

Fig. 6. Annual groundwater availability (mm) derived from recharge (November to March) and discharge (April to October) periods; (a) recharge, and (b), discharge based on 2010–2019; (c) difference between average recharge and discharge based on 2010–2019, (d) recharge of 2019, (e) discharge of 2019 minus recharge and discharge based on 2010–2019, respectively, and (f), difference between 2019 recharge and discharge. The small polygons in the figures represent the water control districts in Fig. 1c.

Table 1
Illustration of crop water usage (statistics from measurement of water consumption, water licence conversations and literature; one harvest a year considered only) and their growing periods in the Northern Territory (MacFarlane and Fairfield, 2017).

Crops	Growing periods	Water usage (mm/ha)	Crops	Growing periods	Water usage (mm/ha)
Avocado	Perennial	960	Banana	Perennial	1960
Forage	May sown	1070	Forage	April sown	1050
Lucerne	Dry season	1030	Citrus	Perennial (5 years +)	900
Maize	Apr.-Aug.	580	Mangoes	Perennial (7 years +)	860
Melons	Mar.-May	290	Melons	Apr.-Jun.	290
Melons	May-Jul.	300	Melons	Jun.-Aug.	340
Melons	Jul.-Sep.	380	Melons	Aug.-Oct.	450
Onions	Apr.-Aug.	540	Onions	May-Sep.	590
Peanuts	Mar.-Aug.	720	Peanuts	Apr.-Sep.	750
Rhodes grass	Dry season	1230	Soybeans	May-Sep.	670

(60–90% chance to have salinity over 1500 mg/L) over the NT (Harrington and Cook, 2014). Soil types and properties have direct impacts on vegetation (Jyrkama and Sykes, 2007; Fisher et al., 2016; Teng et al., 2018). For the NT, there are many types of soil, including Vertosols, Rudosols, Kandosols, Tenosols, Hydrosols, etc (Soils of the Northern Territory, 2016; Teng et al., 2018). In general, Rudosols and Tenosols (Fig. 4c) are potentially not suitable for agriculture development due to their weak soil moisture holding ability (Nikles et al., 2008; Soils of the Northern Territory, 2016).

Considering the fact that agricultural activities are absolutely not permitted in the areas of nature conservation, such are excluded from our analysis. The problem of soil and saline groundwater can be overcome to some extent, e.g., better irrigation plan for specific soil type, and by employing saline groundwater desalination techniques. Thus, an area with either soil or groundwater salinity is here considered suitable for agriculture, and, as such not excluded. However, if both soil and groundwater salinity are not suitable for agriculture for a given area, it is determined to be a non-agricultural area (Fig. 4d).

Table 2
Illustrations of monthly K_c for melons, maize and citrus at different growth stages. Melons are sown in March or April since they require the least water during this period according to MacFarlane and Fairfield (2017).

Crops' *Kc*	Jan.	Feb.	Mar.	Apr.	May	Jun.	Jul.	Aug.	Sep.	Oct.	Nov.	Dec.
Melons	–	–	–	0.6	0.9	0.5	–	–	–	–	–	–
Maize	–	–	–	0.3	0.75	1.05	1.2	0.47	–	–	–	–
Citrus (5 years +)	0.8	0.8	0.8	0.8	0.8	0.8	0.8	0.8	0.8	0.8	0.8	0.8

The table is adapted from Allen et al. (1998)

3. Results and discussion

3.1. Groundwater availability estimate

In order to capture spatio-temporal details on groundwater availability, the entire area of the NT is divided into three parts: the northern (latitude 10°S to 15°S), central (latitude 15°S to 20°S) and southern (latitude below 20°S) parts as shown in Figs 5 and 6 (hereafter simply northern, central and southern NT). Fig. 5 presents the average 20% of monthly groundwater changes for the 2010–2019 period (Fig. 5a), as well as the difference between a dry year (2019) and the average condition (Fig. 5b). In general, one can see from Fig. 5a that the NT's groundwater changes clearly follow the seasonal and regional variations of rainfall (see rainfall maps from Australia Bureau of Meteorology at: http://www.bom.gov.au/jsp/ncc/climate_averages/rainfall/) with recharge mostly occurring between November and March (Bach, 2002; Rieser et al., 2010; Kanniah et al., 2011; Awange et al., 2011, 2019; Forootan et al., 2011).

In the northern NT, groundwater is variable with the monthly 20% change ('80–20 rules') ranging from −35 to 66 mm in May and January, respectively, which is mostly due to the high sensitivity of groundwater recharge to the seasonal rainfall (McCallum et al., 2010). For example, 95% of annual rainfall (over 1000 mm) falls from November to April in Darwin (see region in Fig. 1d), and the groundwater level change during this period can reach 6–7 m (Knapton et al., 2019). In the central and southern NT, the ranges of the 20% change ('80–20 rules') are considerably narrower than those of the northern NT, ranging from −17 to 26 mm, and −2.5 to 10 mm, respectively, due to low rainfall in these regions (Harlock, 2003; Tickell, 2008). For example, Crosbie et al. (2010) indicate that groundwater recharge in the southern NT is episodic, mostly occurring only after intense rainfall.

The high sensitivity of groundwater to rainfall is further evident in dry years. For example, during the 2019 dry period (Fig. 5b), groundwater monthly change of 20% declined by around 5–20 mm during January and March, as well as December, over most of the northern NT compared to the 2010–2019 average. By contrast, in the same year, a substantial recharge (maximum 17 mm) occurred in the northeastern corner of the northern NT in January, which was associated with regional above-average rainfall (see, e.g., http://www.bom.gov.au/climate/current/annual/nt/archive/2019.summary.shtml). Similarly, the groundwater in the central NT was impacted from reduced rainfall during January and March, as well as December, having around 5–20 mm less recharge. In the southern NT, groundwater barely changed with the variation mostly between −5 and 5 mm (except in January with a maximum change of −10 mm in the northern parts of the southern NT).

Annual groundwater availabilities derived from the recharge ('wet period'; November to March) and the discharge ('dry period'; April to October) are presented in Fig. 6. The annual groundwater availabilities (between 2010 and 2019) derived from the recharge and the discharge seasons have very similar spatial patterns over the NT (Figs 6a and b), indicating that the annual groundwater change was nearly balanced or had a relatively small increasing/decreasing trend during the 2010–2019 period. This is illustrated by Fig. 6c, where the differences between Figs 6a and b are mostly within ± 2 mm over the NT. During the 2019 dry period, both annual groundwater availabilities derived from the recharge and discharge seasons showed significant drops (Figs 6d and e; i.e., a drop of about 50% for most areas), e.g., in the northern NT, there was a drop from 80 mm to 40 mm, and in the central NT from 40 mm to 20 mm, indicating a high sensitivity of groundwater change to drought (McCallum et al., 2010). The northern parts of the southern NT also had a decline from above 10 mm to less than 5 mm, while the remaining parts of southern NT were nearly unaffected. The groundwater recharge and discharge balance for the dry year of 2019 (Fig. 6f) showed qualitatively different patterns compared to the average condition of 2010–2019 (Fig. 6c). In the eastern parts of the northern NT and northeastern shoreline of the central NT, there was a 15–20 mm groundwater decline. In the remaining part of the central NT and eastern parts of the southern NT, the groundwater increased around 5–10 mm.

3.2. Reference ET_0 estimate

The reference crop evapotranspiration ET_0 derived by the FAO Penman-Monteith equation provides the spatio-temporal distribution of crop water demand as shown in Fig. 7. Under the averaged condition of 2010–2019 (Fig. 7a), the ET_0 in the northern NT is low with maximum and minimum values of 220 mm and 111 mm in July and November, respectively. For the central NT, ET_0 gradually increases following the north-south trend most of the time except for June and July, where the ET_0 is generally uniform with a minimum of 136 mm, except for a narrow wavy band of region running approximately in the NW-SE direction that has an elevated level (around 165 mm) of ET_0. After July, the ET_0 gradually increases to a maximum of 219 mm in November. The ET_0 in the southern NT is slightly different, with a minimum ET_0 in June of around 79 mm in the southern part of the southern NT and a maximum ET_0 of 306 mm in the eastern parts of the southern NT.

By simply following the principle of the lower the ET_0, the more the suitability for irrigated agriculture, the northern NT with an average ET_0 of 156 mm/month ranks top for irrigated agriculture potential based on the 2010–2019 condition, whereas the central and southern NT follow in that order with nearly the same average ET_0 of 202 mm/month and 209 mm/month, respectively. While the above regional generalisations are apparent, there are also subregional variations. In particular, in most parts of the northern NT, ET_0 is low (around 150 mm/month) throughout the year. In the southern parts of the northern NT, e.g., Katherine (Fig. 1d), ET_0 can reach above 200 mm/month from September to December. Besides, the average monthly rainfall in the northern NT is usually over 200 mm/month between January and March (see rainfall maps from Australia Bureau of Meteorology at: http://www.bom.gov.au/jsp/ncc/climate_averages/rainfall/). Considering that high intensity of rainfall can pose a serious challenge when managing intense storms and soil erosion (Smith, 2008), the sowing time would be better set to April (confirmed by Vegetable Sowing Calendar for Darwin & Katherine Regions; available on https://industry.nt.gov.au/). Therefore, the optimum windows to avoid high ET_0 and high rainfall periods is between April and August for annual crops, particularly, the northeastern corner of the northern NT has quite low ET_0 around 110 mm/month to 120 mm/month between April and July. For the central NT, the best time for irrigated agriculture could be between January and August, since the ET_0 generally goes over 230 mm/month for the southern parts of the central NT from September to December. In terms of the southern NT, the suitable time for irrigated agriculture

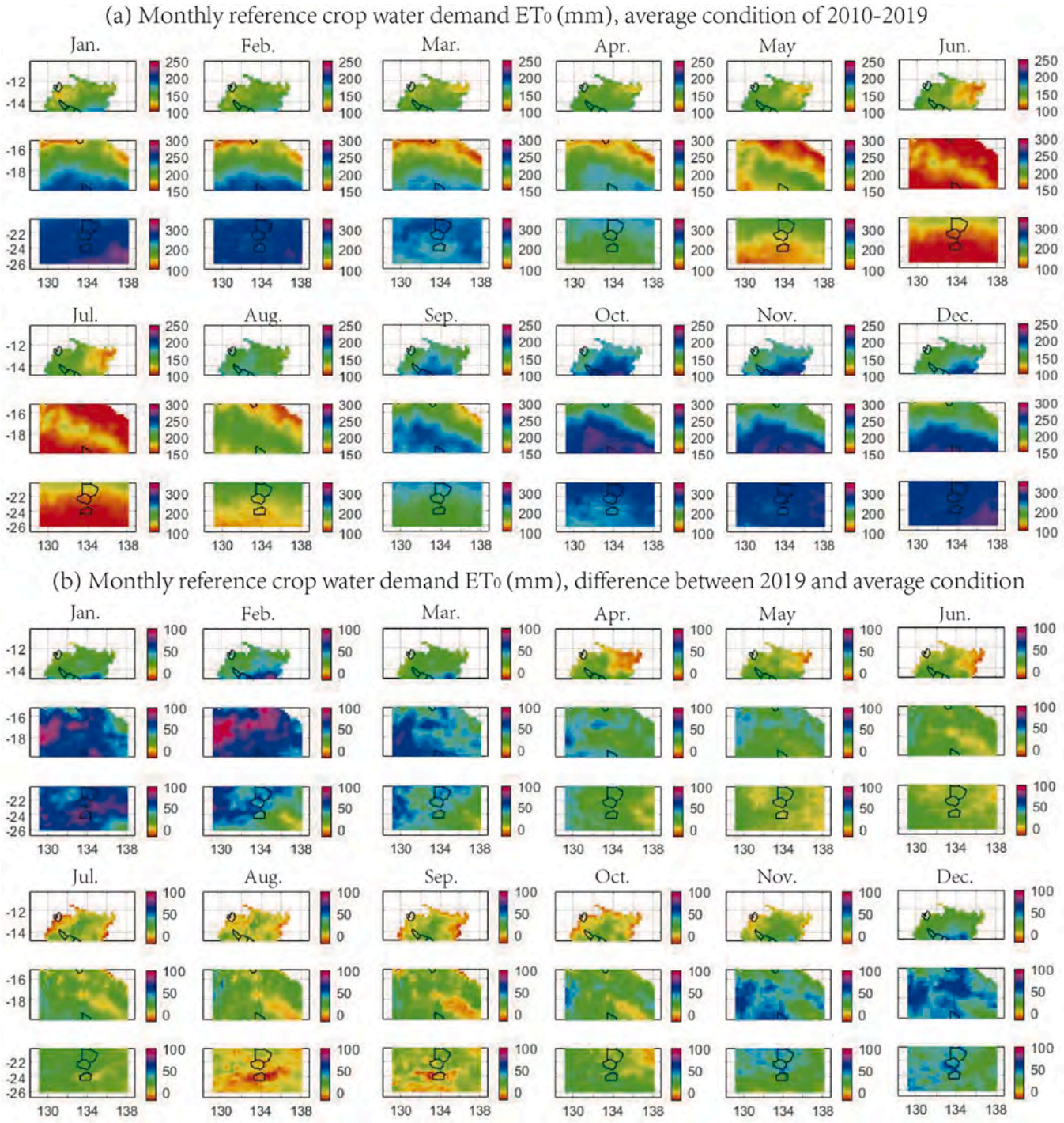

Fig. 7. Reference crop evapotranspiration (mm/month) based on the average condition for 2010–2019 (a), as well as its comparison to a dry condition for the year of 2019 (b). The small polygons in the figures represent the water control districts in Fig. 1c.

would be between April and September, where ET_0 is below 220 mm/month in most areas. In June and July, the ET_0 in the southern NT is even lower than that of the northern NT. However, one issue that should be considered is the low temperature in the southern NT (mostly desert), which may not be suitable for some crops. For example, CSIRO (2018)) indicated that Alice Springs has an average of 34 ($\pm$ 17) frosts days and near 30% chill time annually, which is better suited to high chill fruit crops.

During the 2019 dry period (Fig. 7b), ET_0 increased all over the NT. For example, the ET_0 in the northern, central, and southern NT on average increased by 13 mm/month, 32 mm/month and 22 mm/month, respectively, indicating the possibility of irrigated agriculture being more vulnerable to drought in the central NT. Possibly, this is one of the reasons why most water control districts drafted by the NT Government are outside of the central NT. In particular, the major increase in ET_0 in the central NT occurred from November to March, with an average increase of 49 mm/month. Such an increase in ET_0 was mainly associated with increased wind speed, as well as reduced relative humidity, see Fig. S3 in the supplementary material.

3.3. Balance estimate

Here melons, maize and citrus are used to illustrate the *Balance* estimates, i.e., an area index representing the agriculture potential per the GLDAS-DA pixel since these crops represent different levels of crop water demand, i.e., a total water demand of 290 mm for melons (i.e., sown in April and takes 80–90 days to mature), 580 mm for maize (sown in April and takes 140–150 days to mature) and 900 mm for citrus (perennial, > 5 years, 50% canopy with active ground cover) are required for irrigation during their entire growing period according to MacFarlane and Fairfield (2017). The irrigation efficiency is set as 0.85 throughout the NT as mentioned in section 2.3.1. With the above specifications, Fig. 8 provides the spatio-temporal distribution of the total irrigated water demand for each of the three crops above considering only one harvest a year and the *Balance* estimates under the averaged condition of 2010–2019, as well as the dry year of 2019. The

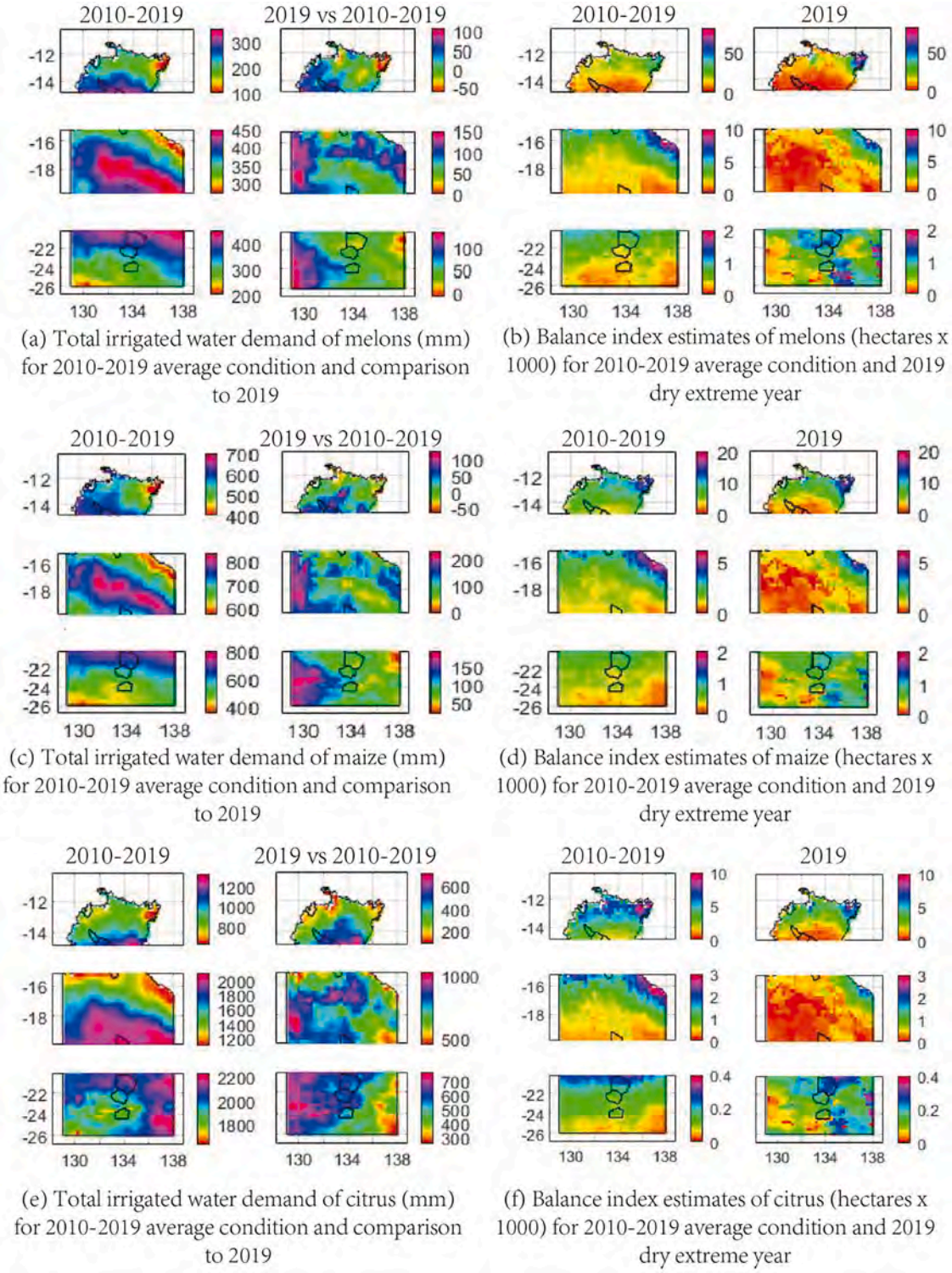

Fig. 8. The total irrigated water demand (mm) and balance estimates (hectares × 10^3) for melons (a-b), maize (c-d), and citrus (e-f) based on the averaged condition of 2010–2019 and the dry year of 2019. The small polygons in the figures represent the water control districts in Fig. 1c.

monthly irrigated water demand and *Balance* estimates can be found in the supplementary Figs. S4–S6. The monthly *Balance* of citrus is not provided since the distribution of annual groundwater availability in each month is determined by the monthly weights of crop water demands as mentioned in section 2.1.2. In other words, the *Balance* of citrus will be all the same from January to December as the annual *Balance*, if the annual groundwater availability is well distributed for each month.

Our results show that the average total irrigated water demand (under the 2010–2019 average condition) as 231 mm, 555 mm and 926 mm (northern NT), 387 mm, 722 mm and 1663 mm (central NT), and 333 mm, 552 mm and 1993 mm (southern NT) for melons, maize and citrus, respectively. These results, however, differ from the estimates of MacFarlane and Fairfield (2017), particularly, in the central and southern NT. Although MacFarlane and Fairfield (2017) claimed that the statistics in Table 1 are not precise to a specific location, these statistics collected from the measurement of water consumption and water licence still have spatial preference. For example, the current cropping and horticulture areas (where those statistics were measured) in the NT are very few and mostly located in the northern NT such as Darwin and Katherine, as well as the southern NT such as Ti-Tree and Alice Springs (see cropping areas in the NT; https://www.agriculture.gov.au/abares/research-topics/aboutmyregion/nt#regional-overview). Therefore, if we simply restrict our comparison of water demand estimates to these cropping and horticulture areas, e.g., regions from Darwin to Katherine, the average total irrigated water demand (under the average condition) is 273 mm for melons, for example, which is then very close to the estimates from MacFarlane and Fairfield (2017).

For melons, the upper half of the northern NT has more irrigated potentials than the lower half according to Figs 8a and b. For example, the upper half of the northern NT generally has total irrigated water demand below 200 mm, and the *Balance* indicates that most areas here have a sufficient amount of groundwater to support growth area of melons for more than 15,000 ha. Particularly, the region in the northeastern corner has a minimum total irrigated water demand of 97 mm and a maximum *Balance* of 41,000 ha. In the central NT, the northeastern shoreline seems to be the best regions to grow melons with a minimum total irrigated water demand of 270 mm and a maximum *Balance* of 9800 ha. As for the southern NT, although its lower parts have the lowest total irrigated water demand of 219 mm, the groundwater availability determines the maximum *Balance* in its upper parts, i.e., 1000 ha.

During the 2019 dry period, most areas of the NT had increased irrigated water demand and reduced *Balance* due to reduced rainfall and groundwater availability. In particular, the northern NT was the most vulnerable to drought since most of its lower half had reduced *Balance* by 50%, e.g., from 10,000 ha to 5000 ha. This is interesting and inconsistent with the conclusion arrived at in section 3.2 that the central NT was the most vulnerable to drought with the largest increased ET_0. The most likely explanation is that the reduced groundwater availability had more significant effects on *Balance* than increased ET_0 in the northern NT. Besides, another interesting phenomenon is that the northeastern corner of the northern NT had increased *Balance* from around 40,000–60,000 ha during the drought, probably due to the regional above-average rainfall in April and May mentioned in section 3.1. For most areas of the central NT, the *Balance* was reduced by 1000–3000 ha, e.g., northeastern shoreline from around 8000 ha to 6000 ha, and the middle parts from around 2000–500 ha below. As for the southern NT, the *Balance* was less affected, generally falling between ± 100–500 ha.

Compared to melons, maize has a relatively long growing period, i.e., from April to August. In April, during the initial growth stage, maize can fully rely on rain-fed irrigation in most of the northern NT (see supplementary Fig. S5 since crop coefficient K_c at this growth stage is only 0.3). Similar to the spatial patterns of irrigated water demand and the *Balance* for melons (Figs 8c and d), the northeastern parts of the northern NT (400–500 mm total irrigated water demand and 8000–15,000 ha *Balance*), the northeastern shoreline of the central NT (580–610 mm total irrigated water demand and 4000–5,000 ha *Balance*) and the northern parts of the southern NT (500–800 ha *Balance*) could be the most suitable areas for growing maize in each region. Under the very dry year of 2019, the northeastern corner of the northern NT maintained largely the same *Balance* (13,000–15000 ha) as in the average conditions of 2010–2019, whilst in other regions the *Balance* generally declined by 2000–4000 ha. In the central NT, the drought effects were widely seen albeit small in magnitude, e.g., an average reduction in total *Balance* of 1000 ha. As for the southern NT, still, the total *Balance* was relatively unaffected by the dry condition and generally changing by between 50 ha and 200 ha only.

Citrus as a perennial crop requires irrigation every month except in December to March in the northern NT (see Fig. S6 in supplementary material). Thus, the total irrigated water demand of citrus is much higher than annual crops and could be very different in different regions, as well as under drought conditions. For example, the northeastern corner of the northern NT has a minimum total irrigated water demand of 620 mm under 2010–2019 average conditions (Fig. 8e), while the maximum total irrigated water demand reached 2868 mm in the southern parts of the central NT in the 2019 dry period. Such a large difference in water demand could generate economical considerations, i.e., whether it is worthwhile or cost-effective to grow citrus in the central NT with water consumption 3–4 times higher than in the northern NT. Therefore, the total irrigated water demand should also be taken into consideration when choosing suitable areas for growing citrus. Based on Figs 8e and f, the northern NT and the northeastern shoreline of the central NT seem to have good potentials for citrus with total irrigated water demand ranging from 620 mm to 1300 mm and *Balance* from 3000 ha to 10,000 ha. With the dry conditions of 2019, the *Balance* significantly reduced by near 50% for the lower half of the northern NT, and the total irrigated water demand increased by around 200–500 mm. Considering that citrus is a kind of crop that is vulnerable to drought, and its production is significantly affected by irrigation (Melgar, 2014), the economical balance among groundwater use, production and risk management to drought have to be considered.

3.4. Exclusion of non-agriculture areas

Based on the principle of suitability mentioned in section 2.4, approximately 54% of non-agriculture areas constrained by physical conditions are excluded over the NT. The excluded total irrigated water demand (mm) and balance estimates are now shown in Fig. 9. Comparing Figs 9 and 8, one can see those previous large agriculture potential areas, e.g., the northeastern corner of the northern NT, are excluded. The *Balance* index is largely reduced, e.g., from maximum 40,000 ha down to 15,000 ha for melon, 20,000 ha down to 8000 ha for maize and 10,000 ha down to 6000 ha for citrus in the northern NT under the average 2010–2019 condition.

Therefore, the average *Balance* under the average 2010–2019 condition for melon/maize/citrus are around 9430/5490/3520 ha (15.7%/9.1%/5.8% area per GLDAS-DA pixel) in the northern NT, 2780/2000/970 ha (4.6%/3.3%/1.6%) in the central NT, and 400/390/110 ha (0.6%/0.6%/0.1%) in the southern NT. The most suitable crop regions in the northern NT/in the central NT/in the southern NT are near the Darwin district/the northeastern shoreline/the eastern parts.

During dry period of 2019, *Balance* is affected near the Darwin districts, e.g., reduced by about 1/3, from 15,000 ha to 10,000 ha for melons, 9000 ha to 6000 ha for maize and 6000 ha to 4000 ha for citrus. For other regions in the northern and central NT, the drought effects on *Balance* are more obvious, with a reduction of about 50% or more. In the southern NT, the drought effects in 2019 are not obvious, the *Balance* for some regions in southeastern parts are even increased. Finally, to clearly see the overall changes of *Balance* for the northern, central and southern parts of NT during average and dry period, as well as before and after

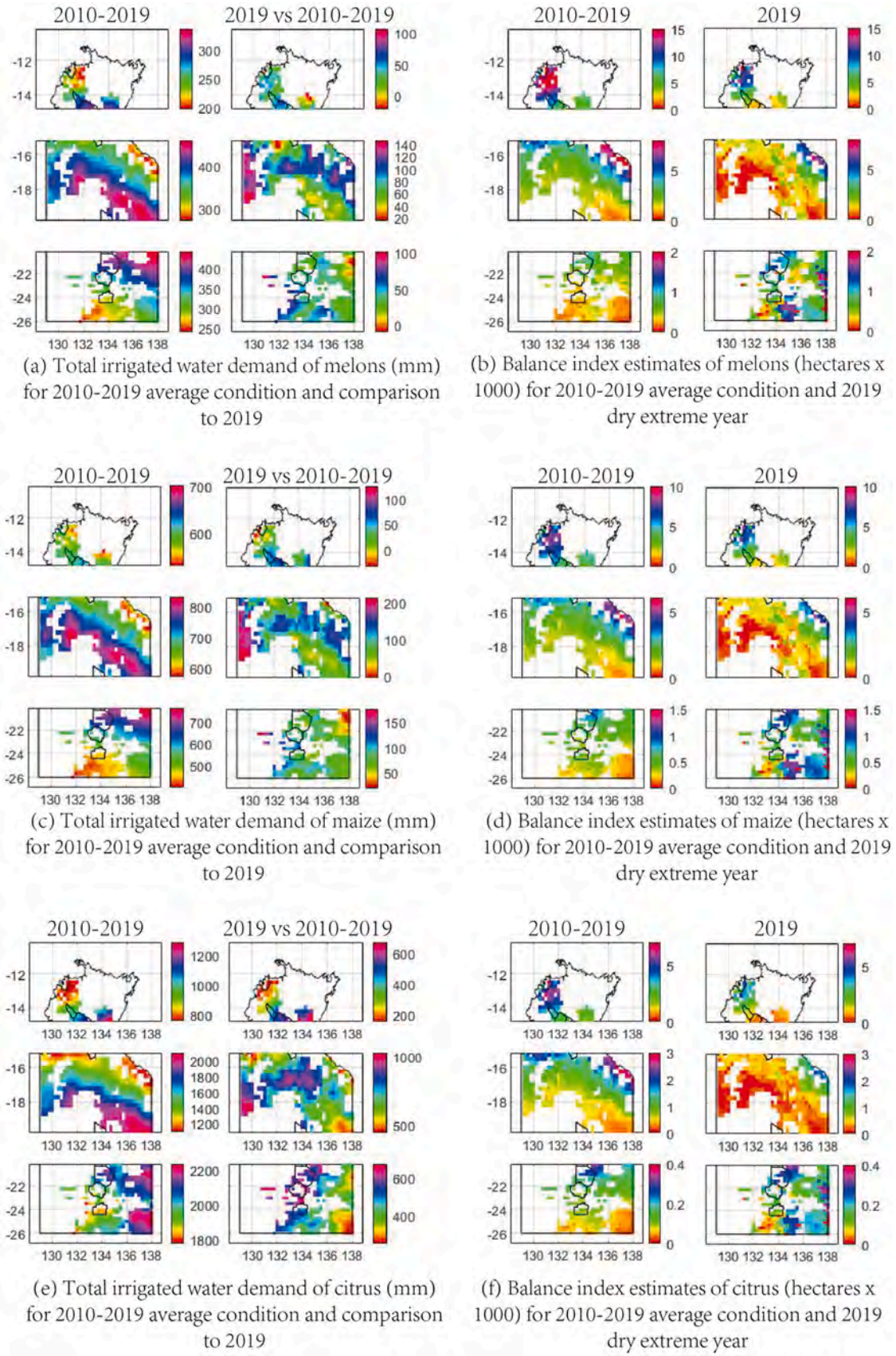

Fig. 9. The total irrigated water demand (mm) and balance estimates (hectares $\times 10^3$) for melons (a-b), maize (c-d), and citrus (e-f) based on the averaged condition of 2010–2019 and the dry year of 2019, with non-agriculture areas excluded. The small polygons in the figures represent the water control districts in Fig. 1c.

exclusion of non-agriculture areas, Table 3 summarises the average *Balance* below.

3.5. Limitations and suggestions

Despite the fact that this study infers irrigated agricultural potential through an areal balance index, the results are established based on the data of simulated models, i.e., groundwater from the GLDAS-DA and crop evapotranspiration from the GLDAS Noah. Especially, the GLDAS-DA only simulates groundwater in shallow aquifers (the depth of groundwater extraction can reach hundreds of meters in the Alice Springs). In other words, the accuracy of the results can vary spatially and temporally based on the uncertainties of the parameters simulated by these models, and the areal balance index may not be that accurate as represented in Figs 8 and 9. Most importantly, for groundwater estimates in the central and southern NT, our evaluations (see supplementary material) for the GLDAS-DA using borehole and WGHM products show that the GLDAS-DA cannot accurately reflect the seasonality change in groundwater. Unfortunately, we cannot overcome this problem since there are no better datasets that have such good spatio-temporal coverage for the whole NT. However, considering that the groundwater storage changes in the central and southern NT are small (Fig. S1; groundwater availabilities are even smaller when '80–20 rules' are applied), our results inferring a small potential of irrigated agriculture in these semi-arid and arid regions could still be reliable. Another limitation of this study is the coarse spatial resolution of the datasets, i.e., 0.25° × 0.25°, which is approximately 60,000 ha per grid cell. Nevertheless, such a size is still too large for farms (from tens of hectares to thousands of hectares) that mainly focus on irrigated agriculture. For example, in Alice Springs, the groundwater extraction from the Mereenie Aquifer for agriculture is only used for areas of 48 ha (Northern Territory Government, 2016). Also in 2016–2017, the Department of Environment and Environment and Natural Resources took an assessment for irrigated agriculture in the Ti-Tree basin, the total survey area is only 13,563 ha (https://depws.nt.gov.au/land-resource-management/development-opportunities/projects/ti-tree). Thus, our results can only be a guide to infer the irrigated agricultural potential over the NT. Extra local works, e.g., field investigations for the selection of farm sites, are still required in order to obtain more accurate estimates based on local environment conditions. Finally, as the section 2.1.1 pointed out, the results of this study are only more or less representative after 1995. Considering the increasing trend of rainfall in the Northern Territory, it may require a re-estimation when calculating the *Balance* for future scenario.

4. Conclusion

The Australian Northern Territory has a vast area with substantial potential for irrigated agriculture. However, the lack of wide-scale water-related information and irrigated agricultural studies contribute to limited agricultural expansion in the Northern Territory. Exemplified by melons, maize and citrus crops, this study therefore, employed the newest Global Land Data Assimilation System Version 2.2 with data assimilated from the Gravity Recovery and Climate Experiment and the FAO Penman-Monteith equation to evaluate the balance between groundwater availability and crop water demand over the Northern Territory. Based on the average 2010–2019 condition, the results found that:

(i) The Northern NT (areas with latitude above S15°), in comparison to other parts of the territory, had the highest potential for irrigated agriculture since it had the highest annual groundwater availability 40–140 mm under the '80–20 rules' and the lowest average total irrigated water demands of 231 mm, 555 mm and 926 mm (partly due to effective rainfall) for melons, maize and citrus, respectively. Also, the region had the highest average *Balance* (irrigable area index) of 9500 ha, 2700 ha and 400 ha for melons, maize and citrus, respectively, after excluding non-agriculture areas. Besides, another advantage of the northern NT is that it is the only region that can rely on rain-fed agriculture (effective rainfall for, e.g., perennial crop) during December and March across the NT. The most suitable crop regions in the northern NT are near the Darwin district, where the intensively irrigated agriculture may be considered.

(ii) In the central NT (areas between latitude of S15° and −20°), the annual average groundwater availability was around 20–60 mm under the '80–20 rules'. The average total irrigated water demands for melons (387 mm), maize (722 mm) and citrus (1633 mm) were much higher than the respective figures for the northern NT. The *Balance* after excluding non-agriculture areas were also low in general except for the northeastern shoreline, where they reached a maximum of 7000 ha, 5000 ha 3000 ha for melons, maize and citrus, respectively. Therefore, the northeastern shoreline could be considered the best region for irrigated agriculture in the central NT. However, due to the fact that such a region is very close to the sea, problems such as groundwater salinity and soil erosion should be seriously considered. Overall, the intensively irrigated agriculture is not seen to be viable over the central NT.

(iii) The southern NT (areas with latitude below S20°) shows only a small area of irrigated agricultural potential due to the low annual groundwater availability around 5–15 mm under the '80–20 rules'. The low reference crop evapotranspiration between April and September indicates an opportunity for small-scale irrigated agriculture during this time of the year. However, low temperature during this period may limit the crop types that can be grown.

(iv) Irrigated agriculture in the NT is highly sensitive to dry climate, e.g., with groundwater availability reduced by more than 50% in most of the northern and central NT in the dry year of 2019 (the driest year in past 58 years). This is important since we found that the decline of groundwater availability had more significant effects on *Balance* estimates than the increased irrigated water demand.

(v) Due to the coarse spatial resolution and uncertainty of the modelled products, the areal *Balance* index may not be that accurate as indicated, and the results are suggested as a guide for inferring areas of irrigated agricultural potential across the NT. Meanwhile, the *Balance* results of this study are only representative for agricultural potential after 1995. For other periods or future scenario, it may require a re-estimation.

Table 3
Summary of average *Balance* statistics (unit: ha × 1000).

Average *Balance* (2010–2019 average)	Northern NT	Central NT	Southern NT
Melon (before exclusion)	13.25	2.61	0.47
Maize (before exclusion)	7.12	1.89	0.45
Citrus (before exclusion)	4.37	0.89	0.12
Melon (after exclusion)	9.43	2.78	0.40
Maize (after exclusion)	5.49	2.00	0.39
Citrus (after exclusion)	3.52	0.97	0.11
Average *Balance* (2019)	Northern NT	Central NT	Southern NT
Melon (before exclusion)	10.55	1.29	0.71
Maize (before exclusion)	5.18	0.95	0.60
Citrus (before exclusion)	2.4	0.34	0.15
Melon (after exclusion)	5.40	1.37	0.83
Maize (after exclusion)	3.30	0.99	0.70
Citrus (after exclusion)	1.71	0.37	0.17

Declaration of Competing Interest

The authors declare that they have no known competing financial

interests or personal relationships that could have appeared to influence the work reported in this paper.

Acknowledgment

Kexiang Hu is grateful for the CIPRS and Research Stipend Scholarship provided by Curtin University and the Australian Government Research Training Program (RTP) Stipend Scholarship that are supporting his Ph.D. studies. J.L. Awange would like to thank the financial support of the Alexander von Humboldt Foundation that supported his stay at the Karlsruhe Institute of Technology. He is grateful to the good working atmosphere provided by his hosts Prof. Hansjörg Kutterer and Prof. Bernhard Heck. The authors would like to thank the following organizations for providing the data used in this study: the Australia Bureau of Meteorology, and the National Aeronautics and Space Administration (NASA) Earth Data Centre. The authors would also like to thank Prof. Charlie Fairfield from Charles Darwin University, Australia, for offering their data as a reference in our study.

Appendix A. Supporting information

Supplementary data associated with this article can be found in the online version at doi:10.1016/j.agwat.2022.107466.

References

ABARES, 2021. Addendum to the Guidelines for land use mapping in Australia: principles, procedures and definition, 4th Edition Add., Aust. Bur. Agric. Resour. Econ. Sci., Canberra, retrieve 2015.File accessed: 18 Feb ⟨https://data.gov.au/data/dataset/bb37e83f-c99d-4350-97b3-958a39316cd1⟩.

Ahooghlandari, M., Khiadani, M., Jahromi, M., 2016. Developing equations for estimating reference evapotranspiration in Australia. Water Resour. Manag. 30, 3815–3828. https://doi.org/10.1007/s11269-016-1386-7.

Ahooghlandari, M., Khiadani, M., Jahromi, M., 2017. Calibration of Valiantzas' reference evapotranspiration equations for the Pilbara region, Western Australia. Theor. Appl. Climatol. 128, 845–856. https://doi.org/10.1007/s00704-016-1744-7.

Allen, R., Pereira, L., Raes, D., Smith, M., (1998), Crop Evapotranspiration, Guidelines for computing crop water requirements, available online: ⟨http://www.fao.org/3/X0490E/x0490e00.htm#Contents⟩.

Ash, A., Gleeson, T., Hall, M., Higgins, A., Hopwood, G., MacLeod, N., Paini, D., Poultion, P., Prestwidge, D., Webster, T., Wilson, P., 2017. Irrigated agricultural development in northern Australia: Value-chain challenges and opportunities. Agric. Syst. 155, 116–125. https://doi.org/10.1016/j.agsy.2017.04.010.

Ash, A., Bristow, M., Laing, A., MacLeod, N., Nisciolo, A., Paini, D., Palmer, J., Poulton, P., Prestwidge, D., Stokes,, C., Watson, I., Webster T., Yeates, S., 2018. Agricultural viability: Darwin catchments, A technical report to the Australian Government from the CSIRO Northern Australia Water Resource Assessment, part of the National Water Infrastructure Development Fund: Water Resource Assessments, Technique report, CSIRO, Australia, retrieve from ⟨https://www.researchgate.net/publication/331518397_Agricultural_viability_Darwin_catchments_A_technical_report_to_the_Australian_Government_from_the_CSIRO_Northern_Australia_Water_Resource_Assessment_part_of_the_National_Water_Infrastructure_Developme⟩.File accessed: 18 Feb 2021.

Ashton, L., McKenzie, N., 2016. Conversion of the Atlas of Australian Soils to the Australian Soil Classification CSIRO Land Water (Unpubl.) 2016.

Awange, J., Fleming, K., Featherstone, W., Heck, B., Anjasmara, I., 2011. On the suitability of the 4° × 4° GRACE mascon solutions for remote sensing Australian hydrology. Remote Sens. Environ. 115 (3), 864–875. https://doi.org/10.1016/j.rse.2010.11.014.

Awange, J., Hu, K., Khaki, M., 2019. The newly merged satellite remotely sensed, gauge and reanalysis-based multi-source weighted-ensemble precipitation: evaluation over Australia and Africa (1981-2016). Sci. Total Environ. 670, 448–465. https://doi.org/10.1016/j.scitotenv.2019.03.148.

Bach, C., 2002. Phenological patterns in monsoon rainforests in the Northern Territory, Australia. Austral Ecol. 27 (5) https://doi.org/10.1046/j.1442-9993.2002.01209.x.

Barry, K.E., Vanderzalm, J.L., Miotlinski, K., Dillon, P.J., 2017. Assessing the impact of recycled water quality and clogging on infiltration rates at a pioneering soil aquifer treatment (SAT) site in alice springs, Northern Territory (NT), Australia. J. Hydrol. 9 (3), 179. https://doi.org/10.3390/w9030179.

Bithell, S., Smith, S., 2011. The method for estimating crop irrigation volumes for the tindall limestone aquifer, katherine, water allocation plan, Technical bulletin no. 337, Northern Territory Government, Australia, retrieve from ⟨https://catalogue.nla.gov.au/Record/5754886⟩.File accessed: 18 Feb 2021.

Blankenau, P., Kilic, A., Allen, R., 2020. An evaluation of gridded weather data sets for the purpose of estimating reference evapotranspiration in the United States, 106,376 Agric. Water Manag. 242. https://doi.org/10.1016/j.agwat.2020.106376.

Brouwer, C., Heibloem, M., 1986. Irrigation Water Management: Irrigation water Needs, Irrigation water management trainning manual no.3, available online: ⟨http://www.fao.org/3/s2022e/s2022e00.htm#Contents⟩.

Calf, G.E., McDonald, P.S., Jacobson, G., 1991. Recharge mechanism and groundwater age in the Ti-Tree Basin, Northern Territory. Aust. J. Earth Sci. 38 (3), 299–306. https://doi.org/10.1080/08120099108727974.

Cresswell, R., Wischusen, J., Jacobson, G., Fifield, K., 1999. Assessment of recharge to groundwater systems in the arid southwestern part of Northern Territory, Australia using chlorine-36. Hydrogeol. J. 7 (4), 393–404. https://doi.org/10.1007/s100400050211.

Crosbie, R., Jolly, I., Leaney, F., Petheram, C., Wohling, D., 2010. Review of Australian groundwater recharge studies, Review, CSIRO: Water for a Healthy Country National Research Flagship, retrieve from ⟨https://publications.CSIRO.au/rpr/download?pid=CSIRO:EP101470&dsid=DS2⟩.File accessed: 18 Feb 2021.

CSIRO (2016), Proposed methods report for the Darwin catchments. A report from the csiro Northern Australia Water Resources Assessment to the Government of Australia., Technique report, csiro, retrieve from publications.csiro.au/rpr/pub?pid=csiro:EP164615. File accessed: 18 Oct 2020.

CSIRO (2018), Investing in the horticultural growth of central Australia, Technique report, CSIRO, retrieve from ⟨https://dpir.nt.gov.au/_data/assets/pdf_file/0007/426994/Invest-in-the-NT-June-2018-web-002.pdf⟩.File accessed: 25 Nov 2020.

Dastane, N., 1978. Effective rainfall in irrigated agriculture Fao Irrig. Drain. Pap., Available Online 1978.⟨http://www.Fao.org/3/x5560e/x5560e00.htm⟩.

Döll, P., Schmied, H., Schuh, C., Portmann, F., Eicker, A., 2014. Global-scale assessment of groundwater depletion and related groundwater abstractions: combining hydrological modeling with information from well observations and GRACE satellites. Water Resour. Res. 50 (7), 5698–5720. https://doi.org/10.1002/2014WR015595.

Erskine, W., Begg, G., Jolly, P., Georges, A., O'Grady, A., Eamus, D., Rea, N., Dostine, P., Townsend, S., Padovan, A., 2003. Recommended enviromental water requirements for the Daly River, Northern Terrritory, based on ecological, hydrological and biological principles, Supervising scientist report 175, National River Health Program, Environmental Flows Initiative, Technical Report 4, Supervising Scientist, Darwin NT. Retrieve from ⟨https://www.environment.gov.au/science/supervising-scientist/publications/ssr/recommended-environmental-water-requirements-daly-river⟩.File accessed: 18 Feb 2021.

Fisher, J., Estop-Aragonés, C., Thierry, A., Charman, D., Wolfe, S., Hartley, L., Murton, J., Williams, M., Phoenix, G., 2016. The influence of vegetation and soil characterisitcs on active layer thickness of permafrost soils in boreal forest. Glob. Change Biol. 22 (9), 3127–3140. https://doi.org/10.1111/gcb.13248.

Forootan, E., Khandu, Awange, J., Schumacher, M., Anyah, R., Dijk, A. van, Kusche, J., 2011. Quantifying the impacts of ENSO and IOD on rain gauge and remotely sensed precipitation products over Australia. Remote Sens. Environ. 172, 50–66. https://doi.org/10.1016/j.rse.2015.10.027.

Harlock, J., 2003. NT Waterwatch Education Kit. Part 7 Groundwater in the Northern Territory Educ. Rep., Dep. Infrastruct., Plan. Environ., Darwin, retrieve denr. nt. Gov. au/Land-Resour. -Manag. /Water/Water-Publ. /Educ. -Resour. /Water -kit 2003.Data accessed: 8 May 2019.

Harrington, N., Cook, P., 2014. Groundwater in Australia, Technique report, National Centre for Groundwater Research and Training, Australia, accessed 2021–5-21 at ⟨http://www.groundwater.com.au/media/W1siZiIsIjIwMTQvMDMvMjUvMDFfNTFfMTNfMTMzX0dyb3VuZHdhdGVyX2luX0F1c3RyYWxpYV9GSU5BTF9mb3Jfd2ViLnBkZiJdXQ/Groundwater%20in%20Australia_FINAL%20for%20web.pdf⟩.

Hennessy, K., Bathols, C., McInnes, K., Pittock, B., Suppiah, R., Walsh, K., 2004. Climate change in the northern territory, consultancy report. Department of Infrastructure, Planning and Enviroment. CSIRO, Northern Territory. Data accessed: 29 April 2019. ⟨http://citeseerx.ist.psu.edu/viewdoc/download?doi=10.1.1.461.1243&rep=rep1&type=pdf⟩.

Jacobson, G., Arakel, A.V., Chen, Y.J., 1988. The central Australian groundwater discharge zone: Evolution of associated calcrete and gypcrete deposits. Aust. J. Earth Sci. 35 (4), 549–565. https://doi.org/10.1080/08120098808729469.

Jyrkama, M., Sykes, J., 2007. The impact of climate change on spatially varying groundwater recharge in the grand river watershed (Ontario). J. Hydrol. 338 (3–4), 237–250. https://doi.org/10.1016/j.jhydrol.2007.02.036.

Kanniah, K., Beringer, J., Hutley, L., 2011. Environmental controls on the spatial variability of savanna productivity in the Northern Territory, Australia. Agric. For. Meteorol. 151 (11), 1429–1439. https://doi.org/10.1016/j.agrformet.2011.06.009.

Kinsela, A., Jones, A., Collins, R., Waite, T., 2012. The impacts of low-cost treatment options upon scale formation potential in remote communities reliant on hard groundwaters. A case study: Northern Territory, Australia. Sci. Total Environ. 416, 22–31. https://doi.org/10.1016/j.scitotenv.2011.12.005.

Knapton, A., Page, D., Vanderzalm, J., Gonzalez, D., Barry, K., Taylor, A., Horner, N., Chilcott, C., Petheram, C., 2019. Managed aquifer recharge as a strategic storage and urban water management tool in Darwin, Northern Territory, Australia. Water 11 (9), 1869. https://doi.org/10.3390/w11091869.

Li, B., Rodell, M., Sheffield, J., Wood, E., Sutanudjaja, E., 2019a. Long-term, non-anthropogenic groundwater storage changes simulated by three global-scale hydrological models. Sci. Rep. 9 (10746) https://doi.org/10.1038/s41598-019-47219-z.

Li, B., Rodell, M., Kumar, S., Beaudoing, H., Getirana, A., Zaitchik, B., et al., 2019b. Global GRACE data assimilation for groundwater and drought monitoring: advances and challenges. Water Resour. Res. 55, 7564–7586. https://doi.org/10.1029/2018WR024618.

Loukas, A., Mylopoulos, N., Vasiliades, L., 2007. A modeling system for the evaluation of water resources management strategies in Thessaly, Greece. Water Resour. Manag. 21, 1673–1702. https://doi.org/10.1007/s10668-020-00619-y.

MacFarlane, S., Fairfield, C., 2017. Groundwater abstraction in the roper region - Northern Terriotry. Water: J. Aust. Water Assoc. 2 (3), 1–26. https://doi.org/10.21139/wej.2017.026.

Marsaglia, G., Tsang, W., Wang, J., 2003. Evaluating kolmogorov's distribution. J. Stat. Softw. 8 (18) retrieve from: https://www.researchgate.net/publication/5142829_Evaluating_Kolmogorov's_Distribution.

McCallum, J., Crosbie, R., Walker, G., Dawes, W., 2010. Impacts of climate change on groundwater in Australia: a sensitivity analysis of recharge. Hydrogeol. J. 18, 1625–1638. https://doi.org/10.1007/s10040-010-0624-y.

McMahon, T., Peel, M., Lowe, L., Srikanthan, R., McVicar, T., 2013. Estimating actual, potential, reference crop and pan evaporation using standard meteorological data: a pragmatic synthesis. Hydrol. Earth Syst. Sci. 17, 1331–1363. https://doi.org/10.5194/hess-17-1331-2013.

Melgar, J. (2014), Issues in citrus fruit production, Stewart Postharvest Review, 10(2), 1–4, accessd from ⟨https://access.portico.org/stable?au=phx64r3rfcr⟩ at 9th March, 2021.

Mossad, M., Zhang, W., Zou, L., 2013. Using capacitive deionisation for inland brackish groundwater desalination in a remote location. Desalination 308, 154–160. https://doi.org/10.1016/j.desal.2012.05.021.

Nikles, D., Bevege, D., Dickinson, G., Griffiths, M., Reilly, D., Lee, D., 2008. Developing African mahogany (Khaya senegalensis) germplasm and its management for a sustainable forest plantation industry in northern Australia: progress and needs. Aust. For. 71 (1), 33–47. https://doi.org/10.1080/00049158.2008.10676269.

Northern Territory Government (2007), Irrigated Maize Production in the Top End of the Northern Territory, Production Guidelines and Research Results, Technical bulletin no. 326, Northern Territory Government, Crops, Forestry and Horticulture Division, retrieve from ⟨https://industry.nt.gov.au/_data/assets/pdf_file/0016/233413/tb326.pdf⟩.File accessed: 18 Feb 2021.

Northern Territory Government (2016), Alice Springs Water Allocation Plan 2016–2026, Report, Northern Territory Government, Department of Land Resource Management, retrieve from ⟨https://haveyoursay.nt.gov.au/63186/widgets/317420/documents/187135⟩.Data accessed: 29 April 2019.

Northern Territory Government (2018), Western Davenport Water Allocation Plan 2018–2021, Technique report, Department of Environment and Natural Resources: Northern Territory, Australia, retrieve from ⟨https://depws.nt.gov.au/_data/assets/pdf_file/0011/624863/Western-Davenport-WAP-04012019.pdf⟩.File accessed: 18 Feb 2021.

Oolloo Water Allocation Plan (2010), Information Report for the Oolloo Dolostone Aquifer Water Allocation Plan, Technique report, Northern Territory Government, Departement of Natural Resources, Environment, The Arts and Sport, PO Box 496, Palmerston NT, 0831, Australia, retrieve from denr.nt.gov.au/_data/assets/pdf_file/0007/254545/info_report_oolloo.pdf. File accessed: 24 Oct 2020.

Park, J., Choi, M., 2015. Estimation of evapotranspiration from ground-based meteorological data and global land data assimilation system (GLDAS). Stoch. Environ. Res. Risk Assess. 29, 1963–1992. https://doi.org/10.1007/s00477-014-1004-2.

Pereira, L., Allen, R., Smith, M., Raes, D., 2015. Crop evapotranspiration estimation with FAO56: past and future. Agric. Water Manag. 147, 4–20. https://doi.org/10.1016/j.agwat.2014.07.031.

Reardon, R., Timmer, C., 2014. Five inter-linked transformations in the Asian agrifood economy: food security implications. Glob. Food Secur. 3, 108–117. https://doi.org/10.1016/j.gfs.2014.02.001.

Rieser, D., Kuhn, M., Pail, R., Anjasmara, I., Awange, J., 2010. Relation between GRACE-derived surface mass variations and precipitation over Australia. Aust. J. Earth Sci. 57 (7), 887–900. https://doi.org/10.1080/08120099.2010.512645.

Singh, L., Jha, M., Chowdary, V., 2020. Evaluation of water demand and supply under varying meteorological conditions in Eastern India and mitigation strategies for sustainable agricultural production, Environment. Dev. Sustain. https://doi.org/10.1007/s10668-020-00619-y.

Smith, S. (2008), The Environment Impact of Plant Industries on Inland Water in the Northern Territory, Technical Bulletin 330, Northern Territory Govement, Australia, retrieve from dpir.nt.gov.au/_data/assets/pdf_file/0015/233403/tb330.pdf. Data accessed: 8 May 2019.

Soils of the Northern Territory (2016), Soils of the Northern Territory, Factsheet, Northern Territory Governemtn, Department of Land Resource Management, retrieve from denr.nt.gov.au/_data/assets/pdf_file/0016/261061/soils-of-the-nt-factsheet.pdf. Data accessed: 29 April 2019.

Teng, H., Rossel, R., Shi, Z., Behrens, T., 2018. Updating a national soil classification with spectroscopic predictions and digital soil mapping. Catena 164, 125–134. https://doi.org/10.1016/j.catena.2018.01.015.

Thomas, M., D. Brough, E. Bui, B. Harms, J. Hill, K. Holmes, D. Morrison, S. Philip, R. Searle, H. Smolinski, S. Tuomi, D. Van Gool, I. Watson, P. Wilson, and P. Wilson (2018), Digital soil mapping of the Fitzroy, Darwin and Mitchell catchments, Tech. rep., CSIRO, Australia, a technical report from the CSIRO Northern Australia Water Resource Assessment, part of the National Water infrastructure Development Fund: Water Resource Assessments. Retrieve from ⟨https://publications.csiro.au/rpr/pub?pid=csiro:EP178822⟩.

Ti Tree Water Report (2009), Ti Tree Basin Water Resource Report, Technique report, Northern Territory Government, Departement of Natural Resources, Environment, The Arts and Sport, PO Box 496, Palmerston NT, 0831, Australia, retrieve from denr.nt.gov.au/_data/assets/pdf_file/0019/254602/basin_water_resource_report_09.pdf. File accessed: 24 Oct 2020.

Tickell, S. (2008), Explanatory notes to the Groundwater Map of the Northern Territory, Technical report, Northern Territory Government Department of Natural Resources the Environment The Arts and Sport, retrieve from territorystories.nt.gov.au/handle/10070/228493. Data accessed: 24 April 2019.

Vanderzalm, J.L., Jeuken, B.M., Wischusen, J.D.H., Pavelic, P., Salle, C.L., Knaption, A., Dillon, P.J., 2011. Recharge sources and hydrogeochemical evolution of groundwater in alluvial basins in arid central Australia. J. Hydrol. 397 (1–2), 71–82. https://doi.org/10.1016/j.jhydrol.2010.11.035.

Werth, S., Güntner, A., 2010. Calibration analysis for water storage variability of the global hydrological model WGHM. Hydrol. Earth Syst. Sci. 14 (1), 59–78. https://doi.org/10.5194/hess-14-59-2010.

Werth, S., Güntner, A., Petrovic, S., Schmidt, R., 2009. Integration of GRACE mass variations into a global hydrological model. Earth Planet. Sci. Lett. 277 (1–2), 166–173. https://doi.org/10.1016/j.epsl.2008.10.021.

Yao, Y., Zhao, S., Zhang, Y., Jia, K., Liu, M., 2014. Spatial and decadal variations in potential evapotranspiration of china based on reanalysis datasets during 1982-2010. Atmosphere 5 (4), 737–754. https://doi.org/10.3390/atmos5040737.

Zanotelli, D., Montagnani, L., Andreotti, C., Tagliavini, M., 2019. Evapotranspiration and crop coefficient patterns of an apple orchard in a sub-humid environment, 105,756 Agric. Water Manag. 226. https://doi.org/10.1016/j.agwat.2019.105756.

Zhang, Y., Yang, S., Ouyang, W., Zeng, H., Cai, M., 2010. Applying multi-source remote sensing data on estimating ecological water requirement of grassland in ungauged region. Procedia Environ. Sci. 2, 953–963. https://doi.org/10.1016/j.proenv.2010.10.107.

Chapter 4
Development and testing of a new approach by which to infer groundwater spatio-temporal distribution in data deficient areas

This chapter is covered by the following publications (*Hu et al.* 2021, 2022a):

1. **Hu, K.X.**, Awange, J.L., Kuhn, M. and Nanteza, J., (2021). Inference of the spatio-temporal variability and storage potential of groundwater in data-deficient regions through groundwater models and inversion of impact factors on groundwater, as exemplified by the Lake Victoria Basin. Science of The Total Environment, 800, 149355, doi: 10.1016/j.scitotenv.2021.149355.

2. **Hu, K.X.**, Awange, J.L. and Kuhn, M., (2022). Testing a knowledge-based approach for inferring spatio-temporal characteristics of groundwater in the Australian State of Victoria. Science of The Total Environment, 821, 153113, doi: 10.1016/j.scitotenv.2022.153113.

Considering the lack of reliable groundwater information in Australia and many regions around the globe, this chapter contributes a knowledge-based approach for inferring groundwater spatio-temporal behaviours without actual monitoring data. Such an approach takes advantage of both a hydrological model and inversion analysis of hydrogeological conditions. The former is able to provide spatio-temporal information globally, and the latter allows the localised interpretation of groundwater behaviours by using high resolution of climatic, topographical and hydrogeological data. Thus, even without in-situ observation as validation, the uncertainty from the hydrological model can still be largely reduced by the inversion analysis of hydrogeological conditions. Specifically, the approach can be divided into three steps: step (i) evaluates the groundwater storage potential and recharge timing by exploring the annual groundwater change amplitude and the monthly recharge frequency in a different season, step (ii) still evaluates the groundwater storage potential and recharge timing, but through exploring the topographical, hydrogeological and climatic data, and in step (iii), the linkages or mismatches between steps (i) and (ii) are searched in order to reduce or confirm the uncertainty of the hydrological model. The strength of this approach is that it can flexibly select different hydrological models in step (i), climatic, topographical, and geological data in step (ii), according to different sizes of study areas, and thereby is almost universal. Considering that this approach has been successfully applied in the Lake Victoria Basin (Africa) and the Australian State of Victoria

through the two publications shown above, the issues outlined in Section 1.4.3 and objective (iii) listed in Section 1.5 are addressed.

To avoid potential misunderstandings, few clarifications have been made on the two publications presented in this Chapter:

(i) Considering the large size of Lake Victoria and that part of the shoreline consists of unconsolidated rock (see Fig.8 in publication 1), it is therefore, assumed that the groundwater level very close to the shoreline is almost equal to the lake level, since groundwater and lake are very likely to be connected to these coastal aquifers composed of unconsolidated rock (*Owor et al.*, 2010).

(ii) The long, dry climate mentioned in Section 2.2 publication 1, refers to a climate that has low level of rainfall both in amount and frequency within a year.

(iii) In Section 2.2.1 publication 1, Global Land Data Assimilation System (GLDAS) Catchment Land Surface Model (CLSM) simulates the groundwater storage volume (not the variation of groundwater storage) only for 5-8 m aquifers. Thus, for those deeper aquifers with groundwater level depth of more than 8-10 m, GLDAS CLSM's simulation is not representative.

(iv) For the two publications in this Chapter, the water balance equation has been used to calculate groundwater recharge frequency. To avoid uncertainty from the input data source, the data selection principle is to give preference to data that is local or whose data quality has already been demonstrated in previous publications. For example, the Climate Hazards Group InfraRed Precipitation with Station data (CHIRPS) is selected due to its lower uncertainty over Africa proven by previous studies (see reference in Section 2.1.1, publication 1). For parameters that do not guarantee data quality, e.g., evaporation, their uncertainties are also examined (see Fig.3 in publication 1). Besides, the reason for using recharge frequency instead of residual of groundwater storage change, is also to avoid uncertainties and misguidance, as even the same source of data will generate uncertainty, and such uncertainty cannot be clarified.

(v) In Section 3.2 publication 2, the difficulty of groundwater extraction in steep terrain refers to the expensive costs of transportation, equipment, and the difficulty of drill process in mountainous regions.

(vi) In Section 3.3, (i), publication 2, the results infer that the eastern and southwestern parts of Victoria are suitable regions for groundwater extraction, which is consistent with the current government-planned groundwater management areas. These results, however, ignore deep or confined aquifers that may have large storage potential, since GLDAS-DA is not representative of deep or confined aquifers on the one hand. On the

other hand, this ignorance is also due to the consideration of sustainable groundwater development. For example, deep or confined aquifers normally have low recharge rates and are less renewable compared to unconfined shallow aquifers.

Science of the Total Environment 800 (2021) 149355

Contents lists available at ScienceDirect

Science of the Total Environment

journal homepage: www.elsevier.com/locate/scitotenv

Inference of the spatio-temporal variability and storage potential of groundwater in data-deficient regions through groundwater models and inversion of impact factors on groundwater, as exemplified by the Lake Victoria Basin

K.X. Hu [a,*], J.L. Awange [a,b], M. Kuhn [a], J. Nanteza [c]

[a] School of Earth and Planetary Sciences, Spatial Science Discipline, Curtin University, Perth, Australia
[b] Geodetic Institute, Karlsruhe Institute of Technology, Engler-Strasse 7, D-76131 Karlsruhe, Germany
[c] Department of Geography, Geo-Informatics and Climatic Sciences, Makerere University, Uganda

HIGHLIGHTS

- A knowledge-based approach is proposed for inferring groundwater behaviours.
- The feasibility of such method is proven and exemplified by the Lake Victoria Basin.
- The core of method is the analysis and inversion of impact factors on groundwater.
- Groundwater model, topographical and geological data is important to such method.

GRAPHICAL ABSTRACT

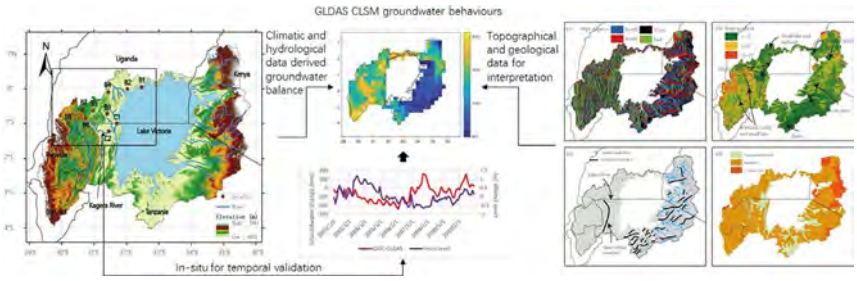

ARTICLE INFO

Article history:
Received 14 December 2020
Received in revised form 24 June 2021
Accepted 26 July 2021
Available online 30 July 2021

Editor: Christian Herrera

Keywords:
Geology
Groundwater
Hydrology
Lake Victoria
Topograph

ABSTRACT

Groundwater is an important resource for supporting domestic water use for people's livelihoods and for maintaining ecosystems. Borehole observations provide the first-hand data that characterise the fluctuation, depth, and aquifer conditions of the groundwater. Unfortunately, such observations are not available or are insufficient for scientific use in many regions. Taking the Lake Victoria Basin (LVB) as an example of data-deficient regions, this study proposes a simple knowledge-based approach that uses the Global Land Data Assimilation System (GLDAS) Catchment Land Surface Model (CLSM) for the main data, with rainfall, hydrological, topographical and geological datasets as supports, by which to infer the spatio-temporal variability and storage potential of groundwater. The method is based on analysis and inversion of impact factors on groundwater, and the feasibility of such a method is proven by showing that the groundwater results from GLDAS CLSM can correctly indicate the seasonality, as well as the link to topographical and geological features. For example, both results from the water balance equation (WBE) and GLDAS CLSM indicate that there are two groundwater recharge seasons in the basin, e.g., March to May and September to November. Compared to the eastern side of the LVB, the western side has mountains blocking surface runoff, and thus, reasonably, has larger storage potential estimates in GLDAS CLSM. Due to the low degree of weathering of the basement rocks, it is expected that there is only small storage potential and variation of groundwater in the southeastern parts of the LVB. GLDAS CLSM also correctly reflects this behaviour. Additionally, the largest groundwater storage potential over the LVB is found in regions near the Kagera River and the western shoreline, since it associates with unconsolidated rocks and behaviours of large groundwater recharge from GLDAS CSLM during the wet year of 2006. The major limitation of this knowledge-based

* Corresponding author.
E-mail address: kexiang.hu@postgrad.curtin.edu.au (K.X. Hu).

https://doi.org/10.1016/j.scitotenv.2021.149355

method is that the uncertainty in terms of magnitude on GLDAS CLSM groundwater changes cannot be assessed, in addition to the fact that the reliability of the results cannot be quantified in terms of specific numbers. Therefore, the results and interpretation of groundwater behaviours using such methods can only be a guide for 'where' and 'when' to find groundwater.

1. Introduction

Groundwater is stored in the pore spaces and fractures inside rocks underground, taking around 0.61% of the earth's water (Mananp et al., 2013; Hu et al., 2017). Because groundwater is one of the important water resources for human livelihood and ecosystems (Gleeson et al., 2016), monitoring of its spatio-temporal variability and areas for storage potential is essential for exploitation and management purposes (Pandey et al., 2013; Kumar et al., 2014). However, the conventional method for monitoring groundwater, i.e., drilling boreholes, is expensive and time consuming (Mananp et al., 2013). In many developing regions, e.g., in Africa and Asia, studying groundwater is difficult, due to the fact that sufficient spatial density and temporal coverage of borehole data are required to obtain reliable results. Therefore, seeking alternative approaches for studying groundwater spatio-temporal variability and areas of storage potential is important, especially for those countries suffering from water scarcity (MacDonald et al., 2012; Masih et al., 2014; Mekonnen and Hoekstra, 2016).

One such alternative approach is provided by the Gravity Recovery and Climate Experiment (GRACE) remote sensing product, which has become popular in estimating groundwater spatio-temporal variability and storage potential (see, e.g., Syed et al. (2008), Werth and Güntner (2009), Döll et al. (2014), Hu et al. (2017), Li et al. (2019)). However, such a technique that has been widely used globally to study spatio-temporal groundwater changes (e.g., Döll et al. (2014), Castellazzi et al. (2016)), and used regionally (e.g., Nanteza et al. (2016), Hu et al. (2017), Agutu et al. (2019), Awange (2021b)), lacks adequate spatial resolution (e.g., it has 300–400 km of resolution) from which to support localised interpretations. As for modelled products that simulate groundwater behaviours, they have finer spatial resolutions (28–56 km), but are mainly forced by climatic parameters, and have uncertainties that have not been validated in many regions (e.g., *Li* et al. (Li et al., 2019)). Some other techniques (see, e.g., Adiat et al. (2012), Mananp et al. (2013), Nouayti et al. (2019)) have used remote sensing and geographic information system (GIS) tools for high spatial resolution of groundwater potential mapping. The accuracy of these approaches, however, depends on the number and weight of the input parameters (e.g., the settings of the topographical, geological and rainfall conditions) and on the design of the local knowledge/experience-driven model (Adiat et al., 2012; Mananp et al., 2013; Kumar et al., 2014), and thus varies from one region to another. More importantly, although this approach identifies the areas of groundwater storage potential based on the exploration of multiple datasets and criteria, the result does not offer groundwater spatio-temporal variability.

Using the Lake Victoria Basin (LVB, Fig. 1, 2°N–4°S; 29°E–36°E) as an example of a data-deficient region, where the GRACE product can only offer two pixels' groundwater spatio-temporal information due to the small size of the basin, localised interpretation is impossible. For groundwater models, e.g., the Global Land Data Assimilation System (GLDAS) Catchment Land Surface Model (CLSM), the uncertainty has not been validated by any in-situ data in the LVB (Li et al., 2019), since such data are very limited and generally inaccessible. Even when accessible, the data are sparsely distributed, making it hard to be used for validation. As a result, previous LVB groundwater studies are mostly area-specific and focus on

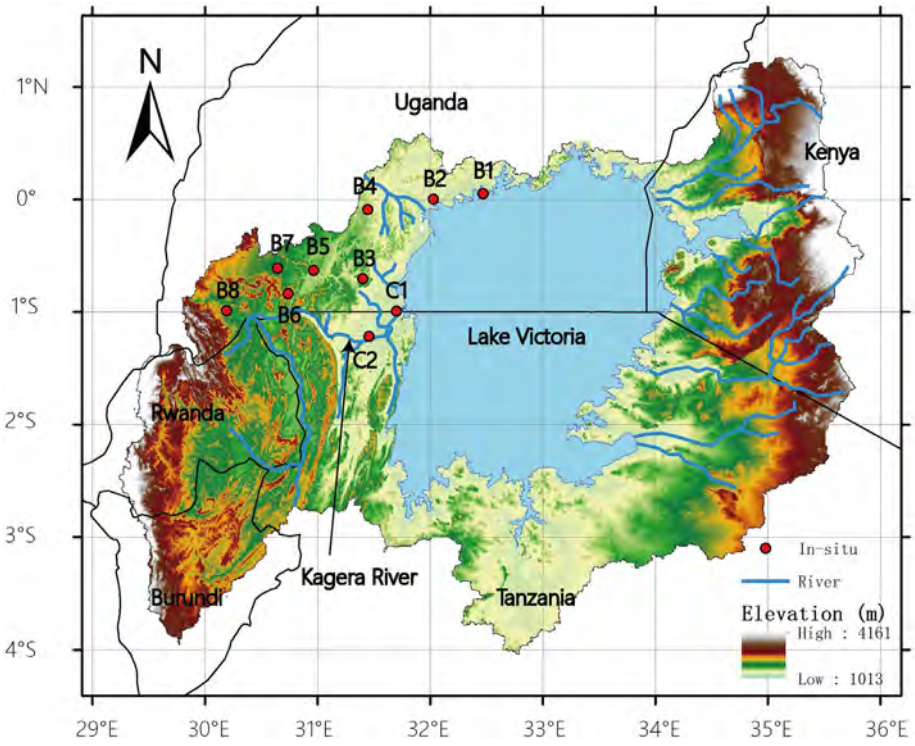

Fig. 1. Locations of the LVB's in-situ (boreholes(B)/catchments(C)) used in this study. In this study, borehole records are taken from well monitoring, and catchment records from the level of rivers/streams.

hydro-chemical aspects (see, e.g., Nyilitya et al. (2020), Kashaigili (2010), Owor et al. (2011)). The information of groundwater spatio-temporal variability and areas for storage potential is only sporadically mentioned in a few studies in their respective countries, e.g., Kashaigili (2010), Aheebwa and Akampurira (2019), and Owuor (2019).

Considering the advantage of groundwater models, i.e., complete spatio-temporal coverage, they are difficult to be replaced. This study still employs GLDAS CLSM, since it directly offers estimates of groundwater spatio-temporal variability and storage distribution. On the other hand, the uncertainty of GLDAS CLSM is reduced through a number of types of extra data, i.e., rainfall, hydrological, topographical and geological datasets, based on the analysis and inversion of impact factors on groundwater. This knowledge-based method allows a better localised groundwater interpretation, and, as such, improves the understanding of groundwater in those data-deficient regions. To prove the feasibility of such a method, this study takes LVB as the case, and infers the basin's groundwater spatio-temporal variability and storage potential distribution. Subsequently, the advantages and limitations of using such a method are discussed.

2. Data and methods

2.1. Data

2.1.1. Rainfall product

The Climate Hazards Group InfraRed Precipitation with Station data (CHIRPS) is a multiple source rainfall product that includes, e.g., the National Oceanic and Atmospheric Administration's (NOAA's) Rainfall Estimate (Love et al., 2004), African Rainfall Climatology (Novella and Thiaw, 2013), the CHPclim dataset (Funk et al., 2015b) and gauge products (Funk et al., 2015a). It has a $0.05^{\circ} \times 0.05^{\circ}$ spatial and monthly temporal resolution and is validated for the region, e.g., by Funk et al. (2015a), Awange et al. (2015) and Awange et al. (2019) who showed it as the least biased rainfall product over Africa.

2.1.2. Hydrological products

(a) GLDAS Noah land surface model

The Global Land Data Assimilation System (GLDAS), developed by the National Aeronautics and Space Administration (NASA) Goddard Space Flight Center (GSFC) and the National Oceanic and Atmospheric Administration (NOAA) National Centers, is a ground- and space-based assimilated product. It provides various land surface parameters used in this study, i.e., evaporation, canopy, and snow estimations (Rodell et al., 2004). The selected Noah land surface model in this study has a monthly temporal and $0.25^{\circ} \times 0.25^{\circ}$ spatial resolution and is commonly used in the water balance equation (WBE; see, e.g., Syed et al. (2008), Li et al. (2018), Birylo et al. (2018), Awange et al. (2019), Awange (2021a, 2022, 2021b)).

(b) GLDAS CLSM

GLDAS CLSM (Catchment Land Surface Model) uses the same static and forcing input data as Noah to simulate not only soil moisture in daily temporal resolution, but also to provide global groundwater storage estimates (absolute water equivalent heights in mm) that have above 0.5 correlation with GRACE-derived groundwater and in-situ datasets in most regions (Li et al., 2019). In this study, the data of the same $0.25^{\circ} \times 0.25^{\circ}$ spatial resolution as GLDAS Noah are employed in order to obtain soil moisture (root zone) and groundwater storage estimates.

(c) WGHM

The WaterGAP Global Hydrology Model (WGHM) offers simulations for most core hydrological processes of the continental water cycle (Werth and Güntner, 2009; Döll et al., 2014). With the $0.5^{\circ} \times 0.5^{\circ}$ spatial and monthly temporal resolution available from 2002 to 2014, the datasets are used to evaluate river storage changes over the LVB when deriving the WBE.

2.1.3. MODIS product

Version 16A2 of the Moderate Resolution Imaging Spectroradiometer (MODIS) remotely sensed data product offers evapotranspiration estimation with 500 m and 8 days spatio-temporal resolution at global scale (Mu et al., 2011). This product has been validated over the African continent, e.g., by Trambauer et al. (2014), mostly showing approximately negative 5–20% relative annual mean bias (underestimated), but good correlation with other evapotranspiration products such as GLEAM (Global Land Evaporation: the Amsterdam Methodology) in the LVB. In this study, MODIS datasets from 2001 to 2014 are used to examine the evapotranspiration of GLDAS Noah.

2.1.4. Topographical product

In order to assess the impacts of topography (e.g., slope and aspect) on the LVB's groundwater, a 30 arc-second digital elevation model (DEM) of Africa for the LVB (Fig. 1), created by the U.S. Geological Survey's Center for Earth Resources Observation and Science (EROS), is employed. The data is available at https://www.arcgis.com/home/item.html?id=c891f64c13be4a2c96491e386bfed8c5.

2.1.5. Geological product

The geological classifications have many types and are complex, e.g., based on age or rock categories. Also, since geological investigations in mountainous regions are hard to process, most geological maps in the LVB are plotted empirically (e.g., based on experience and/or interpolation), based on different records, thus, even for the same type of geological maps, different versions provide different information (see the differences in Owor (2010), Kashaigili (2010), Aheebwa and Akampurira (2019), and Owuor (2019)). Considering this, this study mainly takes reference from the Africa Groundwater Atlas (2019), providing hydrogeological maps with a special focus on groundwater resource information. Other studies from the literature, such as Owor (2010), Kashaigili (2010) Aheebwa and Akampurira (2019) and Owuor (2019) are also employed to enhance the detailed analysis of the geological impact on groundwater in each country within the LVB.

2.1.6. Borehole product

Monthly records of boreholes data collected from Nanteza et al. (2016) and two River Kagera catchment data (daily instant river levels from Hydroweb; http://hydroweb.theia-land.fr/?lang=en&) are employed as independent data for groundwater validation over the Ugandan part of the basin (see spatial distribution in Fig. 1). The levels of Lake Victoria (water level height) from satellite altimetry (Crétaux et al., 2011) are also included, since they represent groundwater levels near the shoreline. Finally, all data used in this study are summarised in Table 1, below.

2.2. Methods

Since GLDAS CLSM has offered the spatio-temporal variability and storage potential of groundwater, the main focus of this study is to reduce the uncertainty of GLDAS CLSM through the analysis and inversion of potential impact factors on groundwater. Therefore, understanding the principle of groundwater change and its potential relationship to impact factors is important (see land water cycle running process in Fig. 2). Firstly, temporal groundwater change is a dynamic difference between groundwater recharge and discharge. For recharge, it comes from the penetration of part of the rainwater into soil and rocks, as well as groundwater flowing in from other areas (Fig. 2). For discharge, groundwater flowing out is the main reason for groundwater level decline (Fig. 2). As for groundwater evaporation, it is usually neglected,

Table 1
Summary of products used in this study. For a consistent data analysis, all gridded datasets (except DEM) are converted to 0.25° and monthly spatio-temporal resolution by interpolation.

Products	Spatial resolution	Temporal resolution	Parameter used	Period used or covered
CHIRPS	0.05°	Monthly	Rainfall	2000–2014
GLDAS Noah	0.25°	Monthly	Evaporation, snow, canopy	2000–2014
GLDAS CLSM	0.25°	Daily	Soil moisture, groundwater	2000–2014
WGHM	0.5°	Monthly	River water storage	2002–2014
MODIS16A2	500 m	8-Days	Evaporation	2001–2014
DEM	30 Arc-second	None	Elevation	None
Geology Map	Digitized	None	Rock types	None
In-situ	Point	Monthly, daily	Groundwater/river level	Unequal from 2000 to 2014

unless the study areas have features of sparse vegetation, abundance of bare soil, shallow groundwater table and long, dry climate (Balugani et al., 2017). Secondly, the spatial variability of groundwater is mainly related to the topographical and geological conditions that affect the conversion of rainfall to groundwater. For example, steep terrain will cause the rapid loss of surface water converted from rainfall (surface flow out, in Fig. 2), resulting in a decrease in the amount of groundwater that can be converted (Tate et al., 2004). Meanwhile, the permeability of soil and rock determines the water penetration speed (Fig. 2), and the porosity of rock determines the capacity of groundwater storage (Hu et al., 2017). Theoretically, the more data collected on groundwater-related impact factors, the better the localised interpretation that can be made through analysis and inversion.

As for the method processing steps, (i) the performance of GLDAS CLSM in terms of areas of storage potential is examined by considering that it is the 'background' data for the study. Also, the spatio-temporal variability is prepared for evaluation in the next step. (ii) The results of groundwater spatio-temporal variability are evaluated through available means, e.g., WBE, in terms of annual and monthly scale. (iii) Meanwhile, topographical and geological analyses for surface water flows and rock types are carried out in order to infer the possible regions that have good conditions for water gathering and penetration. Finally (iv), the abnormal (i.e., uncertainties) and featured groundwater behaviours in (i) and (ii) seek possible interpretation from (iii). The detailed methodologies (exemplified mostly by the LVB) inside each step are described below.

2.2.1. Groundwater storage potential and spatio-temporal variability from GLDAS CLSM

GLDAS CLSM directly provides groundwater storage estimates in terms of water equivalent heights (mm), thus, monthly averages over the 2000–2014 study period are calculated to infer the areas of storage potential. However, it is noted that GLDAS CLSM simulates groundwater storage only for non-anthropogenic, shallow aquifers with a depth around 5–8 m, thus, the deeper aquifer, such as over 10 m, and human impacts are not considered in the results of groundwater storage distribution (Li et al., 2019). In short, groundwater storage estimated by GLDAS CLSM is not equal to the real groundwater storage, and it can only be used to refer to the relative storage potential (i.e., large or small) rather than to accurate numbers. In this case, when evaluating the spatio-temporal variability of GLDAS CLSM, the groundwater storage change (i.e., ΔGW) should be used instead of storage itself. Considering that the temporal resolution of GLDAS CLSM is in daily format (24 h average), ΔGW is calculated as:

$$\Delta GW = GW_{cl} - GW_{pl}; \quad (1)$$

where GW_{cl} represents the records of the last day in the current year or month (depending on which scale is used) for groundwater, and GW_{pl} represents the records of the last day in the previous year or month. The soil moisture change ΔSM used in Eq. (4) is also derived from GLDAS CLSM using Eq. (1).

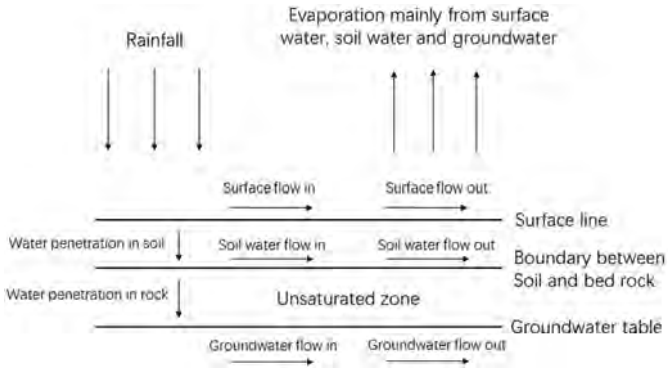

Fig. 2. A simple illustration of the running process for the land–water cycle.

2.2.2. Groundwater spatio-temporal evaluation of GLADS CLSM

(a) Annual groundwater variability over the LVB

In this study, we use the common layout of the WBE (see, e.g., Nanteza et al. (2016), Vanderkelen et al. (2018)):

$$\Delta TWS = P - ET - \frac{Q_{out} - Q_{in}}{A_{land}}, \quad (2)$$

where ΔTWS represents the total water storage change (water equivalent heights) within a specific time (e.g., annual). During this time, P (rainfall) and Q_{in} (inflow from other regions) are the incoming water sources, while ET (evaporation) and Q_{out} (runoff) are the outgoing water sources. A_{land} is the land area of LVB. The division of Q_{in} and Q_{out} (given as volume, e.g., total amount of water) by A_{land} ensures that the respective water volumes are expressed as water equivalent heights. Also, P and ET are derived over the land area only.

In this study, the CHIRPS and GLDAS Noah products provide estimates for P and ET, respectively. Since the ET from the GLDAS Noah model has uncertainty, which is not discussed in the LVB, the MODIS16A2 product that has already been validated by Trambauer et al. (2014) is used to examine the behaviour of trend and magnitude. Fig. 3 presents the annual total ET, average monthly spatial mean relative bias (derived from GLDAS minus the mean of GLDAS and MODIS), and the correlation from 2001 to 2014 between MODIS16A2 and GLDAS Noah. In Fig. 3a, one can see that MODIS16A2 ET has smaller magnitudes than GLDAS Noah annually, with differences of maximum −255.39 mm (27% relative mean bias) and minimum −36.23 mm (4% relative mean bias), which are close to Trambauer et al. (2014)'s estimations in the LVB when comparing MODIS16A2 to other evapotranspiration products (underestimated with 5–20% relative annual mean bias). Spatially (Fig. 3b, c and d), the monthly mean relative bias is smaller in the western than in the eastern LVB. The southern LVB has the highest correlations of above 0.7 (all correlations are provided to 95% confidence level), while the main part of the basin generally has between 0.4 and 0.5 correlation. Therefore, by comparing our results with Trambauer et al. (2014)'s estimations, GLDAS Noah ET is found to have a good consistency and reasonable relative annual mean bias when

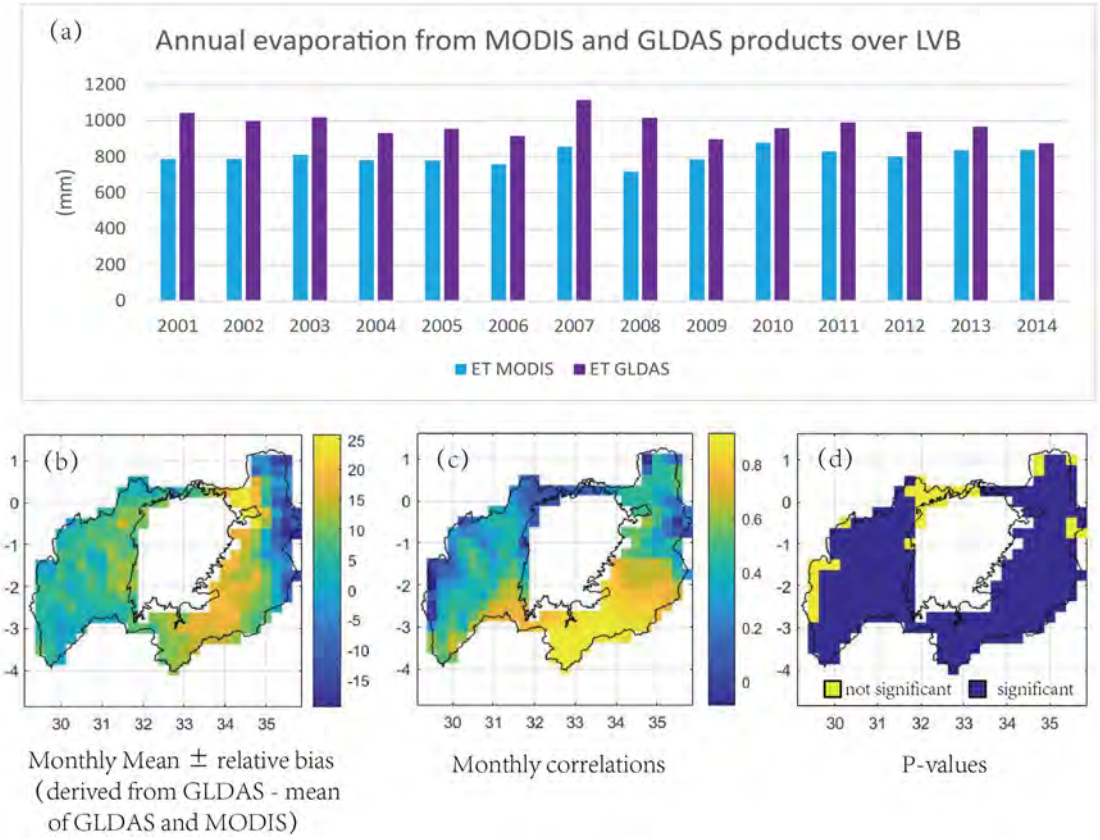

Fig. 3. Evaporation comparison between MODIS16A2 and GLDAS Noah. (a) Annual evaporation over the LVB, (b) average spatial monthly mean relative bias (mm, derived from GLDAS minus the mean of GLDAS and MODIS), (c) spatial correlation at 95% confidence level, and (d), *P*-values (significant and not significant).

compared to other *ET* products over the LVB, and, as such, is employed in this study.

In the WBE, by regarding the whole basin as a system for ΔTWS calculation (i.e., the spatial average of all pixels to one value), Q_{in} is set to zero because of the following reasons: (i) the boundary of the LVB is the watershed where no surface water or rainfall enters from the outside region; (ii) the Great Rift Valley (faults) surrounds the eastern and western parts of the LVB, and normally does not allow groundwater to flow in or out; (iii) there is no large aquifer system in the LVB (MacDonald et al., 2012), particularly in the mountainous regions covered by basement (see, Fig. 8d). Thus, though there exists groundwater change near the LVB boundary, it is negligible compared to the groundwater change of the whole basin, and (iv), the groundwater interaction between land and Lake Victoria is weak, as proven by Vanderkelen et al. (2018), who simulated Lake Victoria's level without considering groundwater. As Q_{out} is not directly given, here we use the findings from Vanderkelen et al. (2018) who found that the runoff into Lake Victoria accounts for about 24% of the total annual input into the lake, while direct rainfall over the lake (e.g., P_{lake}) accounts for about 76% (Awange, 2021a, Awange and Ongángá, 2006 put the values at 20% and 80%, respectively). Based on this information, and obtaining P_{lake} from the rainfall product, the total runoff (Q_{out}) can be indirectly obtained by:

$$Q_{out} = \frac{P_{lake}}{76\%} \times 24\% \times A_{lake}. \quad (3)$$

Note the scaling of Eq. (3) with A_{lake}, e.g., the area ensures that Q_{out} is given as a volume to be used in Eq. (2). After obtaining ΔTWS from Eq. (2), the annual ΔGW (groundwater change expressed as water equivalent heights) is then derived according to (see, e.g., Agutu et al. (2019)):

$$\Delta GW = \Delta TWS - \Delta SM - \Delta SW - \Delta CW - \Delta SN, \quad (4)$$

where ΔSM is the soil moisture (calculated from GLDAS CLSM), ΔSW the surface water (mainly rivers), ΔCW is the canopy water and ΔSN is snow. Among these components, ΔSW, ΔCW and ΔSN are neglected, since they contribute only around 0 to 0.5 mm annually in Eq. (4), under our test against the GLDAS Noah land surface model and the WaterGAP Global Hydrology Model (WGHM) (Werth and Güntner, 2009; Döll et al., 2014).

(b) Monthly spatial variability over the basin

Due to the lack of Q_{in} data for each pixel inside the basin, the WBE, Eqs. (3) and (4) become incomplete and may not be accurate when deriving at pixel scale, particularly in those steep terrains that generate large and quick runoff. Based on this feature, we can compare the groundwater performance of GLDAS CLSM and WBE (without considering runoff) in steep and flat terrains. The expected outcomes would be that there are small differences between GLDAS CLSM and WBE in flat terrain, due to not much runoff, while there are obvious differences in the steep terrain. Here, we choose to employ a statistical calculation of the recharge frequency to evaluate the difference between GLDAS CLSM and WBE, which is still established based on the WBE:

$$RF = \frac{counts(P-E-\Delta SM) > 0}{T} \times 100\%, \quad (5)$$

where *RF* is the recharge frequency that represents the number of months ($counts(P - E - \Delta SM)>0$) that have sufficient rainfall with

which to recharge groundwater during the *T* period. *T* is the number of months over the whole time period, e.g., 2001–2014 (168 months) for average conditions, or a total number of each months (e.g., January, 14 months) for monthly average conditions.

Since we also collected some borehole data (Fig. 1, B1–B8), they are directly employed to validate GLDAS CLSM performance over the Ugandan part of the basin. The assumption is made that, if GLDAS CLSM is representative over the Ugandan part of the basin, then it could be representative, to some extent, over the remaining areas of the basin as well. Due to unequal temporal coverage for each borehole, the common period 2002–2010 is selected (C1 and C2 are outside of this period) and the monthly changes are calculated using differences between consecutive months. Finally, the averaged time series from all boreholes and from all pixels over the Ugandan part of the basin from GLDAS in terms of the 2002–2010 period are plotted.

2.2.3. Topographic and geological analyses

(a) Topographical analysis

Topography determines the flow of surface water and affects the recharge of groundwater. For example, a flat area is more conducive to retaining surface water than is a steeply sloped terrain, thus providing more water and time for infiltration. Accordingly, the slope and aspect are calculated from the Digital Elevation Model (DEM) heights (Section 2.1.4) in ArcGIS using 'Slope' and 'Aspect' tools. Based on both results of the slope gradient and the slope face direction (e.g., North represents 315° to 45° in a compass direction, South from 135° to 225°, etc.), the flat area and obstacles (e.g., mountains) that slow down or block surface water flow are marked as potential recharge areas.

(b) Geological analysis

In referencing to the (Africa Groundwater Atlas, 2019), the rock environment of the whole basin is divided into three parts: unconsolidated, basement, and volcanic rocks. Among them, the unconsolidated rock has a large groundwater storage potential, while basement and volcanic rocks basically have small storage potentials. The spatial distribution of each rock type helps to identify the groundwater storage potential in different areas of the LVB. During the interpretation, this storage potential that relates to rock types can also be reflected by groundwater behaviours during wet/dry events. For example, areas with large variation during wet/dry events commonly indicate high porosity or fractures that are well developed, thus allowing groundwater flow in and out quickly, and vice versa (Hu et al., 2017). Therefore, here annual rainfall is firstly used to identify the wet/dry years. Secondly, the spatial cumulative groundwater storage changes (i.e., the sum of groundwater storage changes) of these years are calculated in order to observe the groundwater behaviours during wet/dry events.

3. Results exemplified by the Lake Victoria Basin

3.1. Groundwater storage potential from GLDAS CLSM

The groundwater storage distribution results provide the most important information that is used to track groundwater locations within the LVB. Fig. 4 illustrates the average groundwater storage estimation over all monthly estimates for the 2000–2014 period from GLDAS CLSM. In general, the results indicate that the western side of the basin has about two to three times the groundwater storage potential compared to the eastern side of the basin. On the western side, regions around River Kagera show the largest groundwater storage in the shallow aquifer, i.e., around 1800–2000 mm, while the southeastern part of the basin indicates the lowest groundwater storage potential, of only around 500 mm.

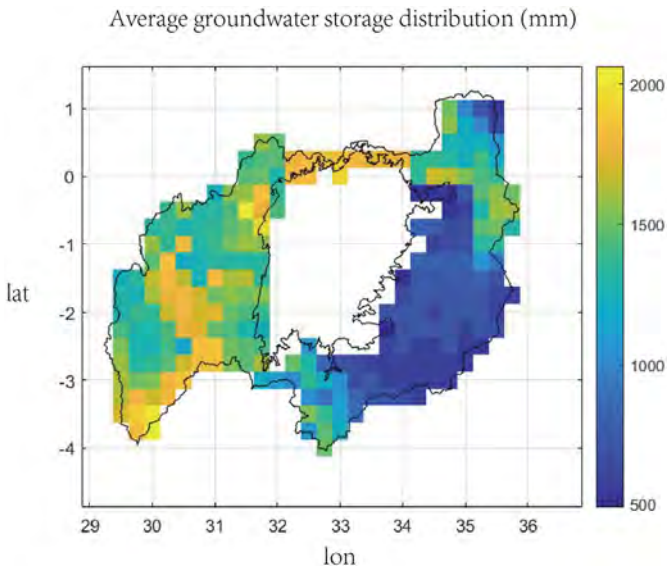

Fig. 4. Average groundwater storage distribution for the period 2000–2014, derived from GLDAS CLSM. The western side of the basin shows more groundwater storage potential than does the eastern side. It is noted that GLDAS CLSM simulates groundwater storage only for non-anthropogenic shallow aquifers around 5–8 m, thus the deeper aquifer, such as over 10 m, is not counted in the results of groundwater storage distribution.

3.2. Groundwater spatio-temporal evaluation of GLADS CLSM

3.2.1. Annual groundwater variability over the LVB

Considering the basin as a whole, Fig. 5a shows that annual groundwater changes (GWC) obtained from the WBE have similar variations to the results of GLDAS CLSM, i.e., a correlation of around 0.60. However, the amplitudes of GWC from WBE are larger than are those of GLDAS CLSM. Particularly, the mismatches appear obviously after 2006, which results in different cumulative annual groundwater changes, as shown in Fig. 5b. For instance, since 2001, the GWC from GLDAS kept relatively stable at a similar level, between −70 mm to 120 mm, while GWC from WBE showed a falling trend before 2008–2009, and a rising trend thereafter. Therefore, the basin-scale annual groundwater variability after 2006 has uncertainty, which requires further possible interpretation. In addition, the cumulative GWC from WBE shows somewhat similar behaviour to the variation of the lake water level height (Fig. 4b). However, the rising trend of the lake level starts 3–4 years earlier (around 2005) than does that of GWC from WBE (2008–2009), thus making it hard to see any linkages between groundwater and lake level.

3.2.2. Monthly groundwater spatial variability over the LVB

The results of recharge frequency (RF) derived from WBE (without considering surface runoff) and GLDAS CLSM are presented in Fig. 6. One can see that RFs are similar in the western side of the basin (around 45–60%) for both WBE and GLDAS CLSM under average conditions (2001–2014, Fig. 6a), while the spatial patterns of RFs on the eastern side of the basin are obviously different, with differences (WBE minus GLDAS, Fig. 6b) from −10% to 40%.

From the perspective of monthly RFs, both WBE and GLDAS CLSM results indicate that there are two rainy seasons influencing groundwater recharge in LVB. The first is the long rainy season of March to May, and the second is the short rainy season of September to November (Anyah et al., 2006; Awange and Ongáng'á, 2006; Kizza et al., 2009; Awange, 2021a; Awange, 2021b) with groundwater recharge in most of the LVB. In detail, the northeastern portion of the basin over Kenya has a relatively long groundwater recharge period that lasts from March to November, which is associated with the two rainy seasons mentioned

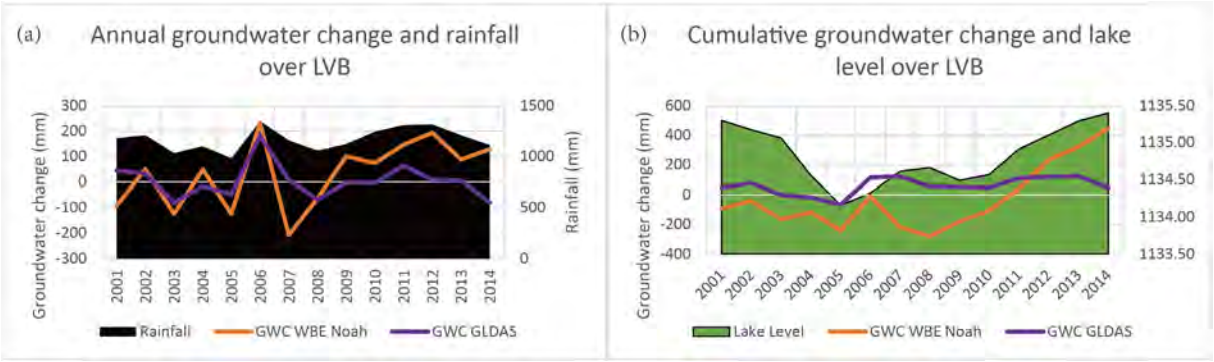

Fig. 5. Plots of temporal time series, (a) annual groundwater change (GWC) calculated from the water balance equation (WBE) and GLDAS CLSM for the 2001–2014 period, and (b) cumulative annual groundwater change and lake level for the 2001–2014 period.

above (see also Owuor (2019)). Although the southeastern portion of the basin in Tanzania also has the same two rainy seasons as does the Kenyan part (Kashaigili, 2010), the groundwater recharge only occurs with high probability (e.g., over 80%) in November to January and April. The major reason for obvious differences appearing in the eastern side of the basin between WBE and GLDAS CLSM (2001–2014 average condition) is due to the fact that (i) WBE has lower estimates of RFs than does GLDAS CLSM in the southeastern parts of the basin between January to March, and (ii) GLDAS CLSM has higher estimates of RFs than does WBE in the northeastern parts of the basin between March and October.

As for monthly GLDAS CLSM groundwater changes and borehole level over the Ugandan part of the basin, shown in Fig. 7a, the two time series do not match well with each other, with a low correlation of only 0.35 (insignificant) over the whole period. Only for the period 2004–2006 is the correlation relatively higher (0.64). In terms of cumulative monthly groundwater changes, in Fig. 7b, GLDAS CLSM basically shows a close trend with borehole data except for a sharp rise mismatch during 2007. Considering that the annual rainfall for 2007 is only around 1106 mm (based on our calculations) in Uganda, which is lower than that of 2010 (1181 mm), which has the same sharp rise (Fig. 7b), the GLDAS CLSM data of 2007 used in the spatio-temporal analysis should therefore be treated with caution.

3.3. Topographical and geological analyses

3.3.1. Topographical analysis

The LVB is a highland basin with complex terrain within the Great Rift Valley, i.e., containing many hills and mountains (see Fig. 1). According to the slope aspect analysis in Fig. 8a, the terrain of the western part of the basin is significantly different from that of the eastern side. In the western part, the mountains are aligned in a north-south direction (see, e.g., north-south green strips; East slopes) that generally block the surface water flow (i.e., in an eastward direction towards the lake). The River Kagera is an example that is forced to flow northwards into Tanzania by a significantly steep north-south orientated mountain (see Figs. 1 and 8c). In the eastern basin, the North (blue), South (red) and West (black) slopes (Fig. 8a) account for major parts, whereas only a few East slopes (green) exist. Considering that the general surface water flow direction follows the elevation gradient, going mainly westwards, no large north-south mountains (i.e., East slopes) block the rivers and streamflow in the eastern part of the basin, except one at the northeastern corner of the basin, in Kenya (see the surface water flow analysis in Fig. 8c).

3.3.2. Geological analysis

The whole LVB is divided into unconsolidated, basement, and volcanic rocks (Fig. 8d). According to Owor (2010), the basement is the major geological rock type in the basin that consists of Precambrian crystalline rocks. Volcanic rock is a kind of fractured rock that is strongly controlled by geometry and the weathering of former lava flows (Africa Groundwater Atlas, 2019). The groundwater storage capacity, productivity, and inter-flow mainly depend on the degree of weathering/fracturing of these two types of rocks. Although the degree of weathering/fracturing for these two types of rocks is spatially variable over the LVB, it is generally low, according to many studies, e.g., Owor (2010), Kashaigili (2010), Aheebwa and Akampurira (2019), Owuor (2019), and Africa Groundwater Atlas (2019). The basement transmissivity is generally below 10 m^2/day in Kenya (Owuor, 2019), and its average is around 14 m^2/day in Uganda (Aheebwa and Akampurira, 2019). Lower transmissivity represents fewer pores or fractures in the rocks, and thus has lower groundwater storage potential. Only a part of volcanic rocks in Kenya over the northeastern part of the basin has high transmissivity, ranging from 30 to 200 m^2/day (Owuor, 2019). The unconsolidated rocks have better groundwater storage potentials and they are mostly distributed around the coastal alluvial plains, flat regions or near large rivers and small lakes (see Fig. 8d). The groundwater in these regions is mainly stored in inter-granular rocks, such as sands, sandstone or gravels, as well as a few weathered fractural rocks. The transmissivity in these fluvial sands can be around 30 to 80 m^2/day in Uganda, Kenya and Tanzania (e.g., Kashaigili (2010), Aheebwa and Akampurira (2019), Owuor (2019)).

4. Discussion

4.1. Interpretation of results exemplified by the Lake Victoria Basin

4.1.1. Groundwater spatio-temporal variability

Based on results in Section 3.2, abnormal and featured groundwater behaviours are summarised in four parts: (i) the amplitudes of annual groundwater storage changes are obviously different between WBE and GLDAS CLSM, particularly after 2006; (ii) WBE cumulative groundwater storage changes show somewhat similar behaviour to the variation of the lake water level height, while GLDAS CLSM does not; (iii) the spatial patterns of RF between WBE (without considering surface runoff) and GLDAS CLSM are significantly different in the eastern side of the basin; (iv) there is a poor correlation between borehole in-situ data and GLDAS CLSM.

For part (i), it is normal to see such a difference, since the ways of deriving WBE and GLDAS CLSM, and the parameters used for WBE and GLDAS CLSM, are different. Also, both WBE and GLDAS CLSM may not be able to accurately reflect the storage change, since all kinds of modelling results can have a great deal of uncertainty, due to various reasons (Diodato and Ceccarelli, 2006). Based on our observations, the parameter of evaporation (ET) used in WBE could be the major reason causing such a difference after 2006 (Fig. 5). For example, the average ET between 2001 and 2014 is 972 mm, while the ET during 2007–2008 and 2009–2014 is significantly higher (1066 mm) and lower (937 mm)

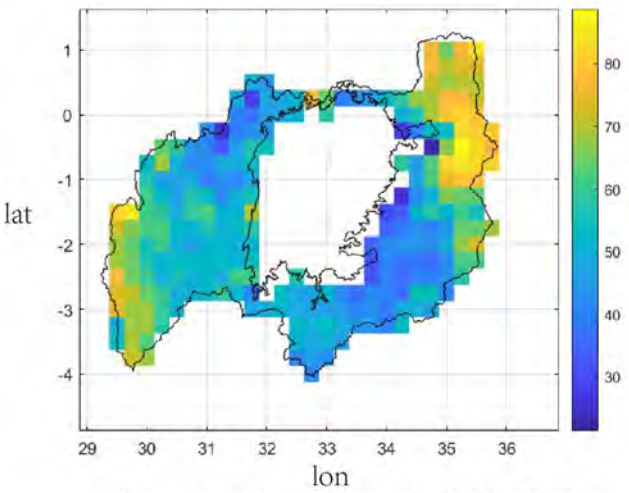

(a) Recharge frequency derived from WBE for the 2001-2014 period

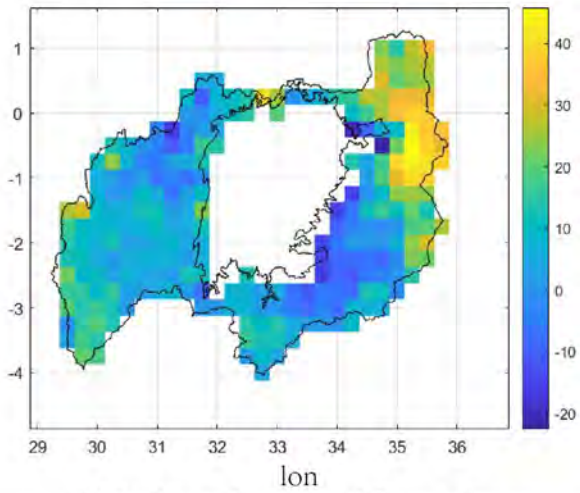

(b) Recharge frequency difference between WBE and GLDAS CLSM, 2001-2014 period

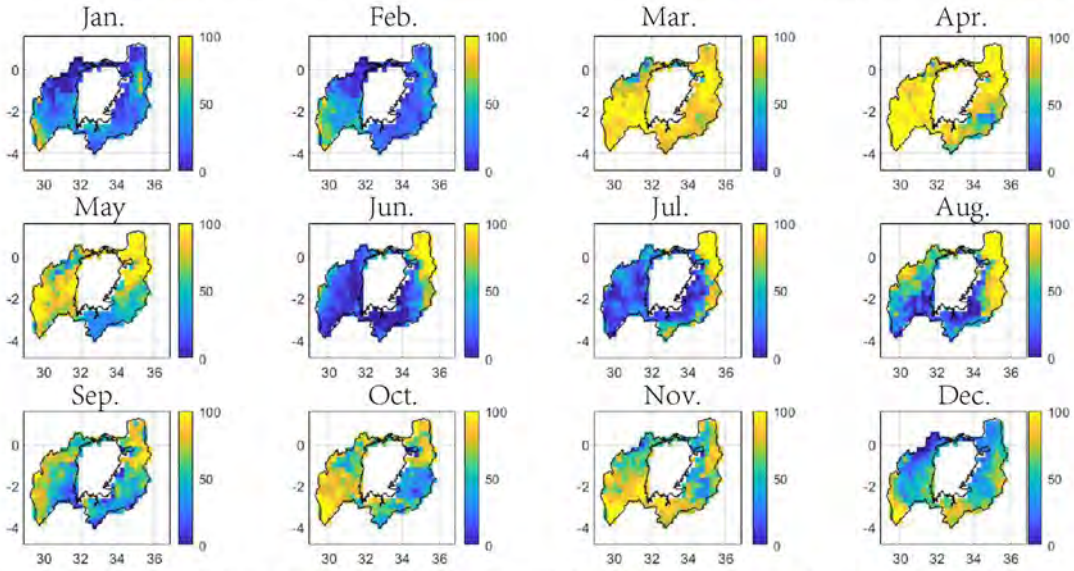

(c) Monthly recharge frequency derived from WBE for the 2001-2014 period

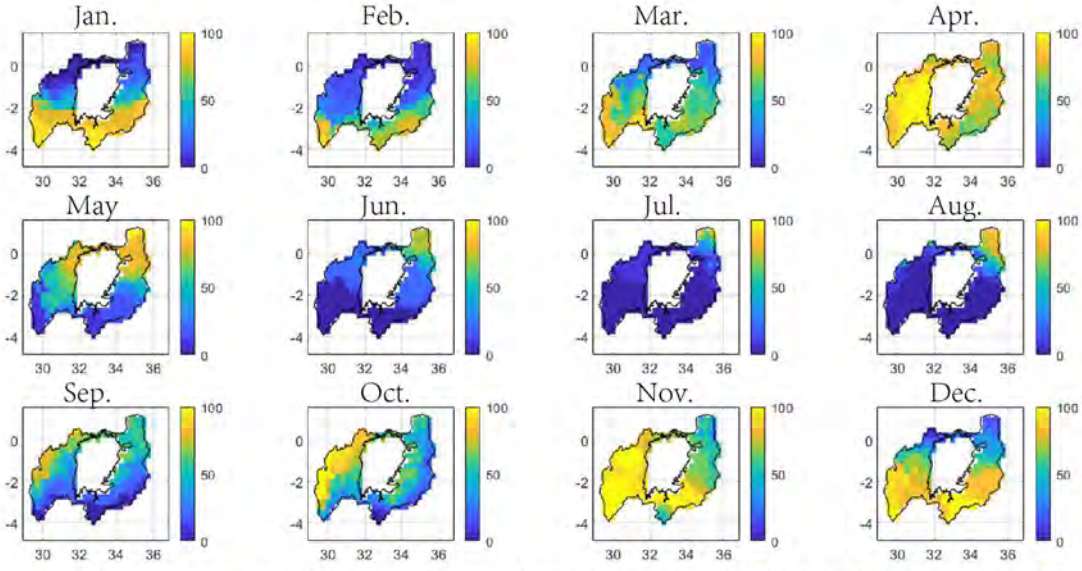

(d) Monthly recharge frequency derived from GLDAS CLSM for the 2001-2014 period

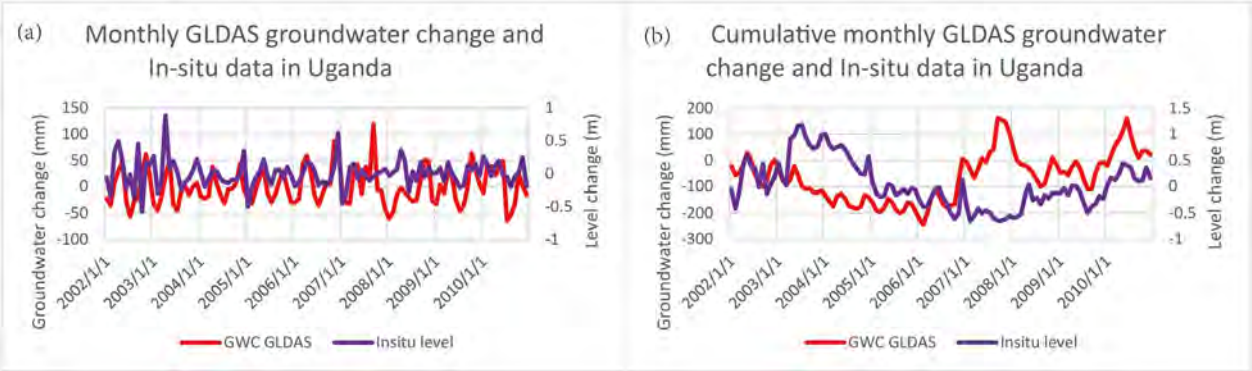

Fig. 7. Comparison between GLDAS CLSM and borehole level in Uganda regions in terms of the 2002–2010 period, (a) monthly groundwater change, and (b) cumulative monthly groundwater change.

than average, respectively. Compared to the mismatches of amplitudes, the good correlation (0.6) between WBE and GLDAS CLSM is the information of real importance since it indicates that there is a good agreement on temporal groundwater behaviours, which can more or less correctly reflect wet/dry years.

For part (ii), it is hard to see any correlations between groundwater and lake level over the basin, since the lake level starts to rise 3–4 years earlier (see Fig. 5b). The consideration of the interactions between lake and groundwater near the shoreline still exist. This is because the aquifers consisting of unconsolidated rock layers near the coastal regions (see Fig. 8d) theoretically will be affected by the lake level. To investigate this further, Table 2 presents the cross-correlation between borehole level in Uganda and lake level for their common period. The results are arranged based on the borehole's distance from the lake.

According to Table 2, the results indicate that catchments/boreholes that are close to the lake, e.g., within the range of 40 km, have higher correlations with the lake level, i.e., 0.34–0.75, with no obvious lag. The groundwater in regions far away from the lake, e.g., at a distance over 40 km, generally does not correlate with the lake level and is spatially variable. In more detail, basement rock is the aquifer environment for all boreholes except B3. The groundwater storage and connection in the basement rock depend on the development of fractures, which is low, according to Owor (2010) and Aheebwa and Akampurira (2019). That is also one of the most important reasons concluded by (MacDonald et al., 2012), that there is no large aquifer in the LVB. Therefore, aquifers far away from the lake, e.g., over 40 km, are mostly independent and small, lacking connections to other aquifers and to the lake (B4–B8, no obvious correlation). Although B1 and B2 are very close to the lake and shallow, the linkages between groundwater and lake still depend on the number of fractures and channels from boreholes to the lake, which, sometimes, can behave very differently. As for B3 in unconsolidated rock, in the coastal region where groundwater has a direct and good link to the lake, the correlation is high (i.e., 0.60), even though the distance to the lake is relatively far. As a result, only very limited aquifers close to the lake or belonging to coastal unconsolidated rock can discharge groundwater into the lake. This explains such a small contribution (1% or even less) from groundwater to the total input of the lake, according to Vanderkelen et al. (2018).

In Section 2.2.2, we mentioned that, due to the fact that the RFs from WBE have not considered the surface runoff, it is expected that the RFs from WBE will have obvious differences from GLDAS CSLM in those sharp terrains. Unexpectedly, the western parts of the basin that have a large slope gradient (see Fig. 8b) have close RFs between WBE and GLDAS CLSM, while the eastern parts of the basin have different RFs, as mentioned in part (iii). This can be interpreted by Section 3.3.1, where, in the western parts of the basin, the surface runoff is reduced due to topographical influence, i.e., north-south directional mountains block the eastwards surface runoff, thereby forming many wetlands and small lakes (Owor, 2010). For the eastern side of the basin, although it is less sharp than the western side, there are nearly no buffers that can slow down surface runoff (see Fig. 8c), particularly, in the Kenya parts (Tate et al., 2004). Thus, the WBE that has not removed surface runoff appears as a significant difference in RFs in the eastern side of the basin (see Fig. 6b). In addition, regions near the lake, such as the mouth of the Kagera River and the eastern shoreline, generally have the negative difference in Fig. 6b, e.g., −10% to −20%. This is due to the considerable surface runoff that comes from the mountainous region and that has not been added in the WBE (i.e., Q_{in}). Meanwhile, these regions near the lake are mostly alluvial plains, where the surface runoff is slow (i.e., Q_{out} is small). Therefore, from the performance of RF, GLDAS CLSM can correctly reflect the topographical influence on groundwater behaviours.

Finally for part (iv), the poor correlation between borehole in-situ data and GLDAS CLSM is acceptable, since the comparison is between point-scale groundwater data (with insufficient numbers and sparse distribution) and regional model products. Also, as mentioned in part (ii), boreholes from B1–B8 have very different groundwater behaviours, due to differences in geology. Therefore, the averaged time series in Fig. 7 may not be representative for Ugandan regions.

4.1.2. Groundwater storage potential

Based on results in Section 3.1 (see Fig. 4), the featured groundwater behaviours can be summarised as the western parts of the basin having larger groundwater storage potential than does the eastern side of the basin. Specifically, in the western parts of the basin, regions around the River Kagera have larger groundwater storage potential than do the rest of regions, while, in the eastern parts of the basin, the Kenyan parts (northeast) have relatively larger groundwater storage potential than do the parts in Tanzania (southeast).

Firstly, the fact that the western parts of the basin have larger groundwater storage potential than does the eastern side of the basin is mostly due to the topographic difference between the western and eastern sides of the basin. As mentioned in Section 3.3.1, the western side of the basin has north-south mountains to retain the surface runoff (Owor, 2010). The surface runoff is easy to lose on the eastern side of the basin without mountains as buffers, and thus can hardly recharge

Fig. 6. Recharge frequency plots for the 2001–2014 period in %, (a) derived from WBE, (b) derived from the difference, e.g., WBE minus GLDAS CLSM, (c) monthly values derived from WBE, and (d) monthly values derived from GLDAS CLSM.

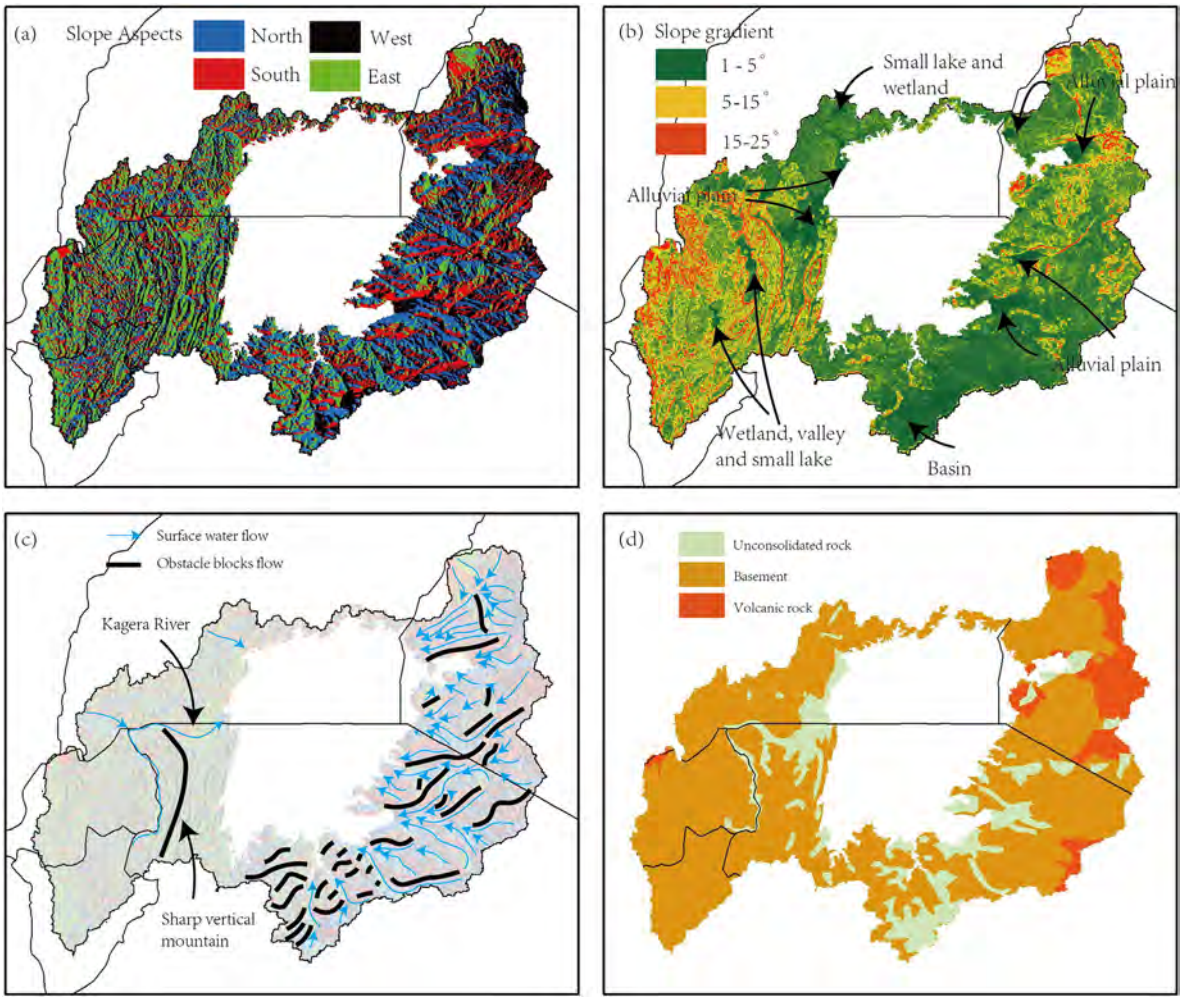

Fig. 8. Surface water flow analysis based on DEM data (a)-(c), and simplified geological conditions within LVB (d); (a) slope aspects, (b) slope gradient, (c) surface water flow analysis based on (a), and (d), geological characteristics over LVB. Since the terrain on the western side of the lake is too complex to analyse, the surface water flow analysis in (c) presents more detail on the eastern and southern sides of the lake, while generalising on the western side of the lake. Map (d) is modified from the Africa Groundwater Atlas (2019). Large groundwater storage potential is mainly related to the unconsolidated rock.

groundwater (Tate et al., 2004). Secondly, the geological conditions with unconsolidated rocks near the River Kagera and the lake shoreline on the western side (see Fig. 8d) provide a suitable environment for storing groundwater (Kashaigili, 2010; Aheebwa and Akampurira, 2019; Owuor, 2019). The northeastern corner of the basin in Kenya has relatively larger groundwater storage potential, mostly because a mountain blocks the surface flow (see Fig. 8c) and it has a weathered volcanic rock with high transmissivity that ranges from 30 to 200 m^2/day (Owuor, 2019). Additionally, the southeastern side of the basin has the smallest storage potential in the LVB, mostly due to inadequate topographical and geological conditions (mostly covered by basement), as well as to low groundwater recharge frequency. Finally, groundwater behaviours during wet/dry periods are shown in Fig. 9. The large groundwater variation areas, e.g., the northeastern and western parts of the basin, are correctly linked to large storage potential areas, as expected. The southeastern parts of the basin that have less groundwater variation are linked to small storage potential, i.e., there is not much water for variation. Therefore, the results of GLDAS groundwater

Table 2
Cross-correlation between borehole in-situ groundwater levels and nearest lake level for their common periods. The borehole-related results are calculated by ignored missing data in each in-situ time series. The distance is calculated as the closest straight distance from borehole/catchment to the boundary of the lake.

In-situ	Distance (km)	Correlation with lake level	Lags (months)	Average groundwater table depth	Significance ($p < 0.05$)	Common period
B1	0.36	0.43	1	5.7	Significant	2000–2010
B2	4.20	0.75	0	2.7	Significant	2000–2010
C1	7.60	0.34	0	–	Significant	2011–2014
B3	34.60	0.60	0	28.8	Significant	2000–2010
C2	39.50	0.42	0	–	Significant	2011–2014
B4	53.26	−0.05	0	62.6	Not significant	2007–2010
B5	83.90	0.31	0	13.5	Significant	2002–2011
B6	106.67	0.05	0	28.8	Not significant	2007–2010
B7	119.24	−0.29	0	3.7	Significant	2000–2010
B8	168.64	−0.02	0	20.5	Not significant	2007–2009

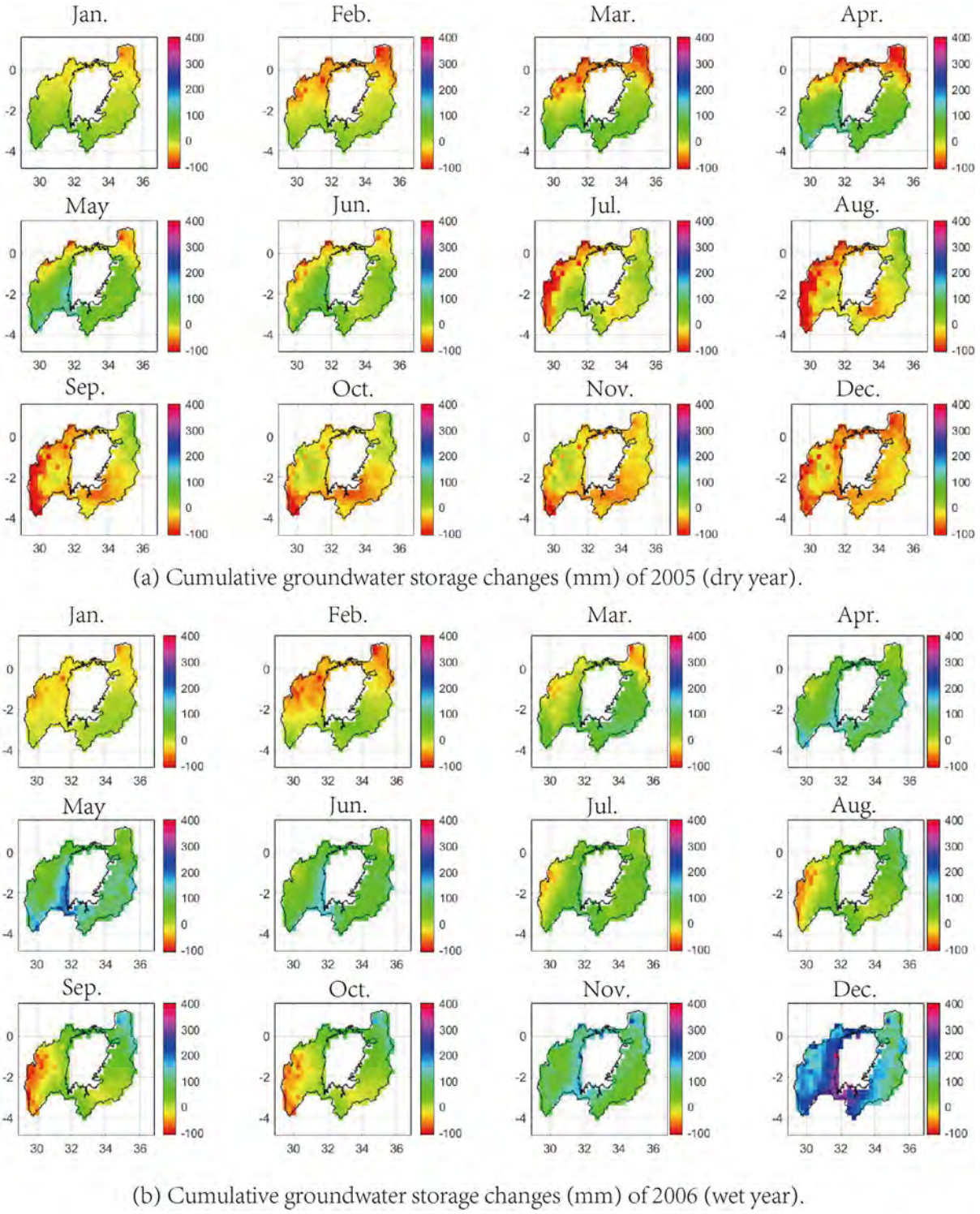

Fig. 9. Spatial cumulative groundwater storage changes (i.e., sum of groundwater storage changes) of each month during the dry year of 2005 (a), and during the wet year of 2006 (b), respectively.

storage distribution in Section 3.1 are reasonable, since they can correctly reflect the topographic and geological influence on groundwater behaviours.

4.2. Advantages and limitations

For groundwater study in data-deficient regions, the most important goal is to answer 'where' and 'when' to find groundwater, and to ensure that the answer is reliable. By using the GLDAS CLSM groundwater model for the main data, with rainfall, hydrological, topographical and geological datasets as supports, this study fulfils the goals mentioned above through a knowledge-based method that can also be applied in most other global regions. Such a knowledge-based method is based on the analysis and inversion of potential impact factors on groundwater. More importantly, it allows a localised interpretation in terms of groundwater behaviours without using actual groundwater monitoring data.

It can be seen from the example of the LVB basin that the whole processing method contains three simple steps. Firstly, a

groundwater model is needed that simulates groundwater storage as 'background' data, since the advantage of complete spatio-temporal coverage is not easily replaced by other data, such as boreholes. GLDAS CLSM, used in this study (Li et al., 2019), is a global product, and thus, can also be applied in other regions besides the LVB. For some specific study regions or countries, some localised models even have a higher spatial resolution, e.g., $0.05^{\circ} \times 0.05^{\circ}$ for the Australian Water Resources Assessment Landscape (AWAR-L) model (Frost and Wright, 2018). Secondly, to reduce the uncertainty of groundwater models and to enhance the understanding of groundwater behaviours within selected study regions, some extra data (any data having a potential relationship with groundwater) is needed for inversion, most of which will not be hard to obtain, e.g., rainfall, evaporation and digital elevation models. The more data that can be used for inversion, the more uncertainties from the model that can be reduced. Among such data, the digital elevation model and geological data (e.g., aquifer distribution, or hydro-geological settings) are extremely important, since they have a considerable impact on groundwater recharge and storage. Although we used borehole data in the LVB example, it is optional and usually unavailable in data-deficient regions. Finally, we try to find any possible linkages between the groundwater model and extra data, in order to interpret the groundwater behaviours, and thus, obtain a reliable answer of 'where' and 'when' to find groundwater.

The major limitation of this knowledge-based method is that the uncertainty in terms of magnitude cannot be assessed. This may generate large errors, particularly for long-term cumulative estimates; see Fig. 5b, for example. Meanwhile, the reliability of the results cannot be quantified, since it is inferred, as based upon groundwater knowledge. Therefore, the results and interpretations of groundwater can only be a guide. For real applications, e.g., seeking the specific location of the groundwater extraction well, experimentation, such as drilling and pumping tests in local areas, are still required.

5. Conclusion

Groundwater monitoring is essential for purposes of exploitation and management. However, the conventional method, such as drilling boreholes, involves high cost and long time, and thus, requires other alternative ways of monitoring groundwater spatio-temporal variability and areas for storage potential. In order to overcome issues of data deficiency, the present study used the LVB as a case study region, and proposed a simple knowledge-based approach that uses groundwater models and inversion of impact factors on groundwater to infer 'where' and 'when' to find groundwater. This method allows a localised interpretation of how groundwater is linked to topographical and geological factors. From the LVB case study, the results have proven that groundwater seasonality and storage from GLDAS CLSM can correctly link to features of topography and geology, and, as such, has proven the feasibility of our method for inferring groundwater spatio-temporal variability and areas for storage potential in data-deficient regions.

CRediT authorship contribution statement

K.X, Hu: Conceptualization, Methodology, Software, Writing - original draft, Visualization. **J.L, Awange:** Writing - review & editing, Supervision. **Kuhn, M:** Writing - review & editing, Results Validation. **J, Nanteza:** Writing - review & editing, Data support.

Declaration of competing interest

The authors declare that they have no known competing financial interests or personal relationships that could have appeared to influence the work reported in this paper.

Acknowledgment

Kexiang Hu is grateful for the CIPRS and Research Stipend Scholarship provided by Curtin University and Australian Government Research Training Program Stipend Scholarship that are supporting his PhD studies. The authors would like to thank the following organizations for providing the data used in this study; Earthwise^{TM} British Geological Survey (BGS), and National Aeronautics and Space Administration (NASA) Earth Data Centre.

References

Adiat, K., Nawawi, M., Abdullah, K., 2012. Assessing the accuracy of GIS-based elementary multi criteria decision analysis as a spatial prediction tool – a case of predicting potential zones of sustainable groundwater resources. J. Hydrol. 400–441, 75–89. https://doi.org/10.1016/j.jhydrol.2012.03.028.

Africa Groundwater Atlas, 2019. Africa Groundwater Atlas Country Hydrogeology Maps, Tech. Rep. accessed from. British Geological Survey at 2020, 6 Jan. http://earthwise.bgs.ac.uk/index.php/Africa_Groundwater_Atlas_Hydrogeology_Maps.

Agutu, N., Awange, J., Ndehedehe, C., Kirimi, F., Kuhn, M., 2019. GRACE-derived groundwater changes over greater horn afirca: temporal variability and potential for irrigated agriculture. Sci. Total Environ. 693 (133), 467. https://doi.org/10.1016/j.scitotenv.2019.07.273.

Aheebwa, J., Akampurira, S., 2019. Regional Training on Integrated Groundwater Resources Management Within River Basins, Country Report on Groundwater Situation-uganda. retrieve from. Republic of Uganda, Ministry of Water and Environment at 2019, 16 December. http://www.unesco.org/new/fileadmin/MULTIMEDIA/FIELD/Nairobi/uganda.pdf.

Anyah, R., Semazzi, F., Xie, L., 2006. Simulated physical mechanisms associated with climate variability over Lake Victoria Basin in East Africa. Mon. Weather Rev. 134 (12), 3588–3609. https://doi.org/10.1175/MWR3266.1.

Awange, J., 2021. Lake Victoria Monitored From Space. 1st edition. Springer International Publishing https://doi.org/10.1007/978-3-030-60551-3.

Awange, J., 2021. The Nile Waters, Weighed From Space. 1st edition. Springer International Publishing https://doi.org/10.1007/978-3-030-64756-8.

Awange, J., 2022. Greater Horn of Africa's Hydroclimate - Potential for Agriculture Amidst Extreme Drought. 1st edition. Springer International Publishing.

Awange, J., Ongángá, O., 2006. Lake Victoria. Springer, Berlin, Heidelberg https://doi.org/10.1007/3-540-32575-1.

Awange, J., Ferreira, V., Forootan, E., Khandu, S., Andam-Akorful, N.Agutu, He, X., 2015. Uncertainties in remotely sensed precipitation data over Africa. Int. J. Climatol. 36 (1). https://doi.org/10.1002/joc.4346.

Awange, J., Hu, K., Khaki, M., 2019. The newly merged satellite remotely sensed, gauge and reanalysis-based multi-source weighted-ensemble precipitation: evaluation over Australia and Africa (1981–2016). Sci. Total Environ. 670, 448–465. https://doi.org/10.1016/j.scitotenv.2019.03.148.

Balugani, E., Lubczynski, M., Reyes-Acosta, L., van der Tol, C., Francés, A., Metselaar, K., 2017. Groundwater and unsaturated zone evaporation and transpiration in a semi-arid open woodland. J. Hydrol. 547, 54–66. https://doi.org/10.1016/j.jhydrol.2017.01.042.

Birylo, M., Rzepecka, Z., Nastula, J., 2018. Assessment of the water budget from GLDAS model. BGC Geomatics https://doi.org/10.1109/BGC-Geomatics.2018.00022.

Castellazzi, P., Martel, R., Galloway, D.L., Longuevergne, L., Rivera, A., 2016. Assessing groundwater depletion and dynamics using GRACE and inSAR: potential and limitations. Groundwater 54 (6).

Crétaux, J., Jelinski, W., Calmant, S., Kouraev, A., Vuglinski, V., Bergé-Nguyen, M., Gennero, M., Nino, F., del Rio, R., Cazenave, A., Maisongrande, P., 2011. SOLS: a lake database to monitor in the near real time water level and storage variations from remote sensing data. Bull. Am. Meteorol. Soc. 47 (9), 1497–1507. https://doi.org/10.1016/j.asr.2011.01.004.

Diodato, N., Ceccarelli, M., 2006. Computational uncertainty analysis of groundwater recharge in catchment. Ecol. Inform. 1, 377–389. https://doi.org/10.1016/j.ecoinf.2006.02.003.

Döll, P., Schmied, M.C., Schuh, C., Portmann, F.T., Eicker, A., 2014. Global-scale assessment of groundwater depletion and related groundwater abstractions: combining hydrological modeling with information from well observations and GRACE satellites. Water Resour. Res. 50 (7), 5698–5720. https://doi.org/10.1002/2014WR015595.

Frost, A., Wright, D., 2018. Evaluation of the Australian Landscape Water Balance Model (AWRA-L v6): Comparison of AWRA-L v6 Against Observed Hydrological Data and Peer Models, Technical Report. Bureau of Meteorology.

Funk, Chris, Peterson, P., Landsfeld, M., Pedreros, D., Verdin, J., Shukla, S., Husak, G., Rowland, J., Harrison, L., Hoell, A., Michaelsen, A., 2015. The climate hazards infrared precipitation with stations—a new environmental record for monitoring extremes. Sci. Data 2 (150066), 2015. https://doi.org/10.1038/sdata.2015.66.

Funk, C., Verdin, A., Michaelsen, J., Peterson, P., Pedreros, D., Husak, G., 2015. A global satellite assisted precipitation climatology. Earth Syst. Sci. Data Discuss. 7, 1–13. https://doi.org/10.5194/essd-7-275-2015.

Gleeson, T., Befus, K., Jasechko, S., Luijendijk, E., Cardenas, M., 2016. The global volume and distribution of modern groundwater. Nat. Geosci. 9, 161–167. https://doi.org/10.1038/ngeo2590.

Hu, K.X., Awange, J.L., Khandu, Forootan, E., Goncalves, R.M., Fleming, K., 2017. Hydrogeological characterisation of groundwater over Brazil using remotely sensed and model products. Sci. Total Environ. 599-600, 372–386. https://doi.org/10.1016/j.scitotenv.2017.04.188.

Kashaigili, J., 2010. Assessment of Groundwater Availability and its Current and Potential Use and Impacts in Tanzania, Tech. Rep. retrieve from. International Water Management Institute at 2019, 16 December. http://41.73.194.142:8080/xmlui/bitstream/handle/123456789/1484/Kashaigili21.pdf?sequence=1&isAllowed=y.

Kizza, M., Rodeh, A., Xu, C., Ntale, H., Halldin, S., 2009. Temporal rainfall variability in the Lake Victoria Basin in East Africa during the twentieth century. Theor. Appl. Climatol. 98, 119–135. https://doi.org/10.1007/s00704-008-0093-6.

Kumar, T., Gautam, A., Kumar, T., 2014. Appraising the accuracy of GIS-based multicriteria decision making technique for delineation of groundwater potential zones. Water Resour. Manag. 28, 4449–4466. https://doi.org/10.1007/s11269-014-0663-6.

Li, B., Rodell, M., Sheffield, J., Wood, E., Sutanudjaja, E., 2019. Long-term, non-anthropogenic groundwater storage changes simulated by three global-scale hydrological models. Sci. Rep. 9 (10746). https://doi.org/10.1038/s41598-019-47219-z.

Li, Q., Luo, Z., Zhong, B., Zhou, H., 2018. An improved approach for evapotranspiration estimation using water balance equation: case study of Yangtze River basin. Water 10 (6).

Love, T.B., Kumar, V., Xie, P., Thiaw, W., 2004. A 20-year daily Africa precipitation climatology using satellite and gauge data. retrieve from: Proceedings of the 84th AMS Annual Meeting, vol. Conference on Applied Climatology, Seattle at 2019, 10 Oct. http://www.cpc.ncep.noaa.gov/products/fews/AFR_CLIM/SAVED_20070403/appl_clim.pdf.

MacDonald, A., Bonsor, H., Dochartaigh, B., Taylor, R., 2012. Quantitative maps of groundwater resources in Africa. Environ. Res. Lett. 7 (024), 009. https://doi.org/10.1088/1748-9326/7/2/024009.

Mananp, M., Sulaiman, W., Ramli, M., Pradhan, B., Surip, N., 2013. A knowledge-driven GIS modeling technique for groundwater potential mapping at the Upper Langat Basin, Malaysia. Arab. J. Geosci. 6, 1621–1637. https://doi.org/10.1007/s12517-011-0469-2.

Masih, I., Maskey, S., Mussá, F., Trambauer, P., 2014. A review of droughts on the African continent: a geospatial and long-term perspective. Hydrol. Earth Syst. Sci. 18, 3635–3649. https://doi.org/10.5194/hess-18-3635-2014.

Mekonnen, M., Hoekstra, A., 2016. Four billion people facing severe water scarcity. Sci. Adv. 2 (2).

Mu, Q., Zhao, M., Running, S., 2011. Improvements to a MODIS global terrestrial evapotranspiration algorithm. Remote Sens. Environ. 115 (8).

Nanteza, J., de Linage, C., Thomas, B., Famiglietti, J., 2016. Monitoring groundwater storage changes in complex basement aquifers: an evaluation of the GRACE satellites over East Africa. Water Resour. Res. 52, 9542–9564. https://doi.org/10.1002/2016WR018846.

Nouayti, A., Khattach, D., Hilali, M., Nouayti, N., 2019. Mapping potential areas for groundwater storage in the high Guir Basin (Morocco): contribution of remote sensing and geographic information system. J. Groundw. Sci. Eng. 7 (4).

Novella, N., Thiaw, W., 2013. African rainfall climatology version 2 for famine early warning systems. J. Appl. Meteorol. Climatol. 52, 588–606. https://doi.org/10.1175/JAMC-D-11-0238.1.

Nyilitya, B., Mureithi, S., Boeckx, P., 2020. Tracking sources and fate of groundwater nitrate in Kisumu City and Kano Plains, Kenya. J. Spat. Sci. 12, 401. https://doi.org/10.3390/w12020401.

Owor, M., 2010. Groundwater - Surface Water Interactions on Deeply Weathered Surfaces of Low Relief in the Upper Nile Basin of Uganda. retrieve from: University College London at 2019, 31 Oct. https://discovery.ucl.ac.uk/id/eprint/19757/1/19757.pdf.

Owor, M., Taylor, R., Mukwaya, C., Tindimugaya, C., 2011. Groundwater/surface-water interactions on deeply weathered surfaces of low relief: evidence from Lakes Victoria and Kyoga, Uganda. Hydrogeol. J. 19, 1403–1420. https://doi.org/10.1007/s10040-011-0779-1.

Owuor, S., 2019. Groundwater Occurrence in Kenya, Tech. rep. retrieve from. Ministry of Water and Sanitation at 2019, 16 December. http://www.unesco.org/new/fileadmin/MULTIMEDIA/FIELD/Nairobi/kenya.pdf.

Pandey, V., Shrestha, S., Kazama, F., 2013. A GIS-based methodology to delineate potential areas for groundwater development: a case study from Kathmandu Valley, Nepal. Appl Water Sci 3, 453–465. https://doi.org/10.1007/s13201-013-0094-1.

Rodell, M., Houser, P.R., Jambor, U., Gottschalck, J., et al., 2004. The global land data assimilation system. Bull. Am. Meteorol. Soc. 85, 381–394. https://doi.org/10.1175/BAMS-85-3-381.

Syed, T., Famiglietti, J., Rodell, M., Chen, J., Wilson, C., 2008. Analysis of terrestrial water storage changes from GRACE and GLDAS. Water Resour. Res. 44 (2).

Tate, E., Sutcliffe, J., Conway, D., Farquharson, F., 2004. Water balance of Lake Victoria: update to 2000 and climate change modelling to 2100. Hydrol. Sci. J. 49, 563–574. https://doi.org/10.1623/hysj.49.4.563.54422.

Trambauer, P., Dutra, E., Maskey, S., Werner, M., Pappenberger, F., van Beek, P., Uhlenbrook, S., 2014. Comparison of different evaporation estimates over the african continent. Hydrol. Earth Syst. Sci. 18, 193–212. https://doi.org/10.5194/hess-18-193-2014.

Vanderkelen, I., van Lipzig, N., Thiery, W., 2018. Modelling the water balance of Lake Victoria (East Africa)-Part1: observational analysis. Hydrol. Earth Syst. Sci. 22, 5509–5525. https://doi.org/10.5194/hess-22-5509-2018.

Werth, S., Güntner, A., 2009. Calibration analysis for water storage variability of the global hydrological model WGHM. Hydrol. Earth Syst. Sci. 6, 4813–4861.

Science of the Total Environment 821 (2022) 153113

Contents lists available at ScienceDirect

Science of the Total Environment

journal homepage: www.elsevier.com/locate/scitotenv

Testing a knowledge-based approach for inferring spatio-temporal characteristics of groundwater in the Australian State of Victoria

K.X. Hu *, J.L. Awange, M. Kuhn

School of Earth and Planetary Sciences, Spatial Science Discipline, Curtin University, Perth, Australia

HIGHLIGHTS

- Confirms reliability of knowledge-based approach in data rich test area.
- Suitable groundwater extracted areas are related to groundwater renewability.
- Inversion analysis improves understanding of groundwater behaviour.
- Borehole data show high correlations with GLDAS-DA in data-rich test area.

GRAPHICAL ABSTRACT

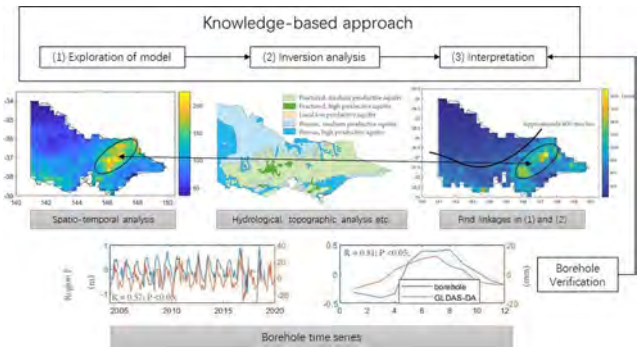

ARTICLE INFO

Article history:
Received 17 November 2021
Received in revised form 7 January 2022
Accepted 10 January 2022
Available online 19 January 2022

Editor: Christian Herrera

Keywords:
Groundwater
Hydrogeology
Rainfall
Topograph
State of Victoria

ABSTRACT

Groundwater spatio-temporal characteristics are important information for groundwater development and management. However, such information is usually insufficient or even unavailable in many regions around the world due to insufficient or even lack of in-situ data such as from boreholes. Recently, a knowledge-based approach was proposed to infer 'where' and 'when' to find groundwater using Lake Victoria Basin (LVB) as an example for data-deficient regions. In this knowledge-based approach, groundwater model and inversion analysis of groundwater impact factors are used to infer groundwater storage potential and recharge timing. In the LVB's case, only 10 borehole data were used to test the spatio-temporal behaviours of groundwater, which are insufficient. In this contribution, therefore, using the Australian State of Victoria as an example, with over 15,000 boreholes data, the performance of the same knowledge-based approach is further tested in a well-controlled area. The results indicate that the knowledge-based approach is able to correctly infer regions with large groundwater storage potential suitable for extraction. The recharge timing of groundwater is also correctly indicated as the results show consistency with the borehole data. This provides further evidence of the reliability of the knowledge-based approach for inferring spatio-temporal characteristics of groundwater.

1. Introduction

Under the scenarios of global warming, population increase, and agricultural expansion, mankind's demand for groundwater resources has become stronger (Earman and Dettinger, 2011; Famiglietti, 2014). According to the statistics from Siebert et al. (2010); Elshall et al. (2020), 50% of drinking water and 43% of irrigation water in the world are extracted from aquifers. Groundwater, therefore, is the largest storage and most widely distributed freshwater resource on the inhabited continents (Elshall et al., 2020). Therefore, knowledge about its spatio-temporal characteristics is of great significance to water development and management. However, the direct monitoring approach, e.g., using boreholes, usually has insufficient density/coverage over many regions around the globe on the one hand. On the other hand, the combination of Gravity Recovery and Climate Experiment (GRACE) and hydrological models does not

* Corresponding author.
E-mail address: kexiang.hu@postgrad.curtin.edu.au (K.X. Hu).

http://dx.doi.org/10.1016/j.scitotenv.2022.153113

Table 1
Summary of products used in this study. For a consistent data analysis, all gridded datasets (except DEM) are converted to 0.25° and monthly spatio-temporal resolution by interpolation.

Products	Spatial resolution	Temporal resolution	Parameter used	Period used
AWARL	0.05°	Monthly	Rainfall and evaporation	2004–2019
GLDAS-DA	0.25°	Daily	Groundwater and soil moisture	2004–2019
DEM	3 Arc-second	None	Elevation	N/A
Hydrogeology Map	Digitized	None	Rock types	N/A
In-situ	Point	Daily	Groundwater level	2004–19 (non-continuous)

provide satisfactory spatial resolution to support localised interpretations (Khaki et al., 2017; Hu et al., 2021). To address the above issues, some physical models based on the water balance equation (WBE) combined with the simulation of the groundwater recharge process have been proposed, see, e.g., Scibek et al. (2007); de Graaf et al. (2015). Nevertheless, Von Freyberg et al. (2015) indicated that different models will perform inconsistently in space and time due to the uncertainty of each parameter used in the model. Eventually, the spatio-temporal performance of the groundwater model still requires verification from borehole data (Yin et al., 2021).

Recently, as an alternative approach, Hu et al. (2021) proposed a knowledge-based approach to infer 'where' and 'when' to find groundwater in data-deficient regions exemplified by Lake Victoria Basin (LVB). This approach seeks featured linkages or mismatches between the groundwater model and the inversion of groundwater impact factors (e.g., rainfall, topography and hydrogeology) to allow a more localised understanding of groundwater behaviours without actual monitoring data. In other words, the inversion of groundwater impact factors plays the role of borehole data in this approach, which helps to verify the performance of the groundwater model.

To assess the inferred results of LVB, Hu et al. (2021) employed only 10 borehole data to test the spatio-temporal behaviours of groundwater in the Ugandan region. While the assessment of other regions in LVB relied on literature. Thus, more controlled studies clearly need to be undertaken to further test the performance of the approach in other regions around the globe since LVB (i), could be a special case for this approach, and (ii), did not possess enough borehole data (only 10) to undertake a comprehensive spatio-temporal verification. Using the Australian State of Victoria as an example (a large area that contains multiple basins), this contribution extends the work of Hu et al. (2021) by testing the same knowledge-based approach in a data-rich environment with over 15,000 boreholes available in the study area. If the inferred results are consistent with the known knowledge, the reliability of this approach, then, can be proved.

2. Data and methods

2.1. Data

The knowledge-based approach requires a groundwater model combined with the use of rainfall, evaporation, soil moisture, topography, and hydrogeology, see Hu et al. (2021). Borehole data is optional once the reliability of the knowledge-based approach is proved. In this study, borehole data is important since it is used to verify results from the knowledge-based approach. Here, the Global Land Data Assimilation System (GLDAS) Catchment Land Surface Model (CLSM; version 2.2) with data assimilated from GRACE, hereafter called GLDAS-DA, is selected as the groundwater model since it is one of the most advanced groundwater models that integrates a huge quantity of observation-based data (Zhao and Li, 2015) and has global coverage with free access (Li et al., 2019). Besides, GLDAS-DA also provides root zone soil moisture estimates. The Australian Water Resources Assessment Landscape (AWRA-L) model (version 6.0; Frost et al., 2018; Frost and Wright, 2018) is employed for rainfall and evaporation since the local model is usually more representative than those of global models. As for topography and hydrogeology, the 3 arc-second Digital Elevation Model (DEM) and the Hydrogeology Map of Australia (Lau and Jacobson, 1987) are used. Finally, the borehole data used to verify the groundwater spatio-temporal characteristics is retrieved from The Australian Groundwater Explorer (Bureau of Meteorology, 2015) for the Australian State of Victoria. Table 1 summarises the characteristics of all data used in this study.

2.2. Methods

The knowledge-based approach proposed in Hu et al. (2021) has four steps as shown in Fig. 1; (i) exploration of groundwater model, (ii) inversion analysis of groundwater impact factors, (iii) interpretation of linkages or mismatches between (i) and (ii), and (iv), verification using borehole

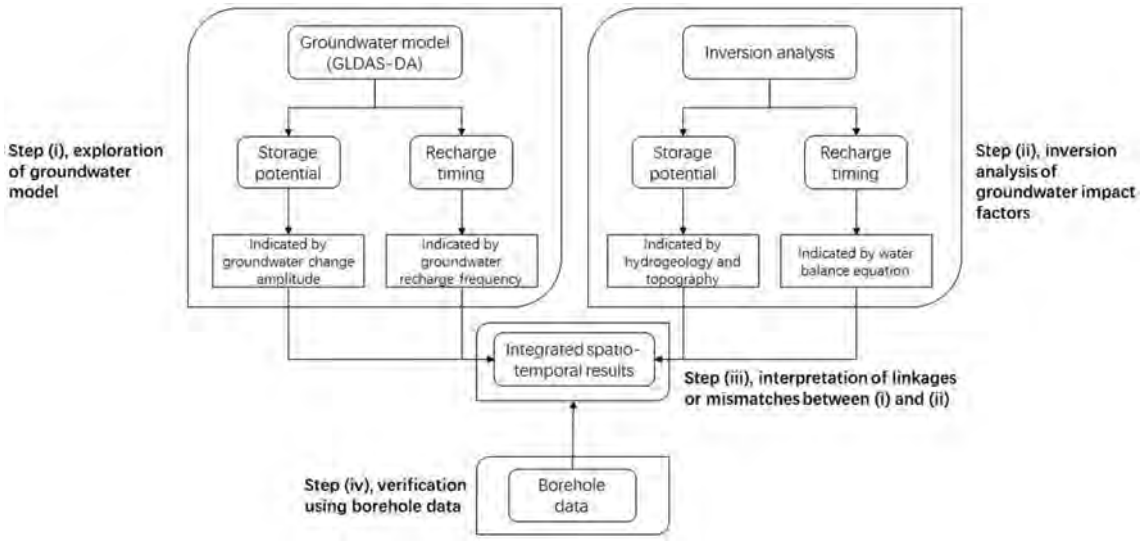

Fig. 1. Processing flowchart of the knowledge-based approach. For the detail methodologies used in each step, please refer to Hu et al. (2021).

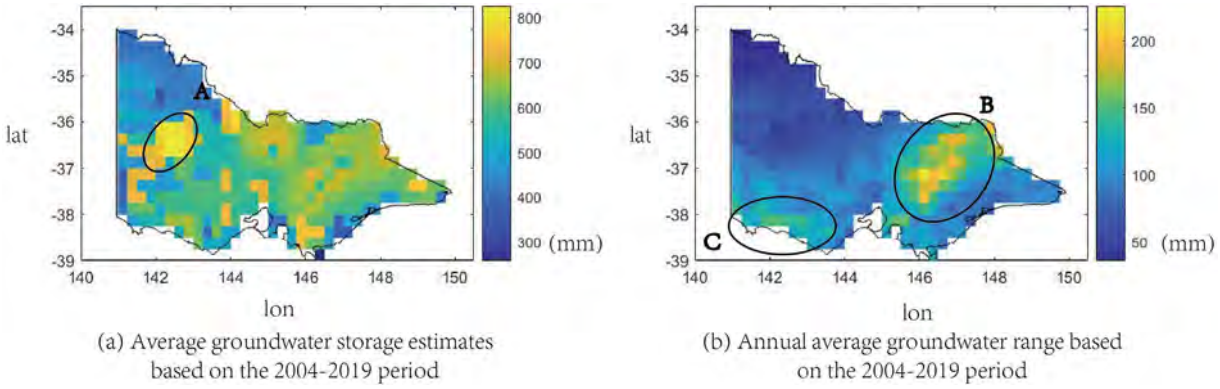

Fig. 2. Groundwater storage potential characteristics, (a) average groundwater storage estimates (relative values for shallow aquifers), and (b), annual average groundwater range (average differences between maximum and minimum storage for each year) based on the 2004–2019 period. Circled areas of in (a) and (b) are possible regions with large groundwater storage and high groundwater renewability, respectively.

data. Note the borehole data is optional if unavailable. In this study, however, borehole data is necessary for the verification of the knowledge-based approach.

Note that the methods of this contribution are slightly different from Hu et al. (2021), including:

1. Step (i) not only uses groundwater storage estimates from GLDAS-DA, but also calculates annual average groundwater range (e.g., average differences between maximum and minimum storage for each year) to identify regions with high groundwater renewability. This is important since a region with large groundwater storage does not necessarily represent a suitable region for groundwater extraction. Especially now that environmental protection and sustainable development are emphasized, for example, the Australian Northern Territory sets 20% of annual groundwater recharge or discharge as the groundwater extraction limit (MacFarlane and Fairfield, 2017).
2. This contribution only focuses on 'where' and 'when' to find groundwater. Other aspects such as groundwater behaviours under climatic extremes as covered in Hu et al. (2021), are not considered here.
3. Since there are over 15,000 boreholes in the Australian State of Victoria and the downloaded borehole data are daily, instant, discontinuous records, it is necessary to convert these data to monthly groundwater level changes according to the method of Hu et al. (2019). Subsequently, these monthly records are spatially averaged based on a 0.25° × 0.25° grid in order to compare with GLDAS-DA groundwater estimates (see a similar process in Chen et al., 2016 or Yin et al., 2021). However, it is worth mentioning that this process may produce biased results since each grid covers a different number of boreholes in different periods, and sometimes the results are only derived from one or two borehole records. To avoid this circumstance to a certain extent, at least 10 borehole records are required to process the spatial averaging.

3. Results

3.1. Exploration of GLDAS-DA

Since GLDAS-DA directly provides groundwater storage estimates, Fig. 2a presents the average groundwater storage distribution over the Australian State of Victoria for the 2004–2019 period. It can be seen that except for the northwestern parts of Victoria (300–400 mm), groundwater storage is generally above 600 mm (other study periods may result slightly different). Particularly in region A (see the circle in Fig. 2a), 800 mm maximum groundwater storage is indicated by GLDAS-DA. It is worth mentioning that the above number of estimates does not represent the absolute

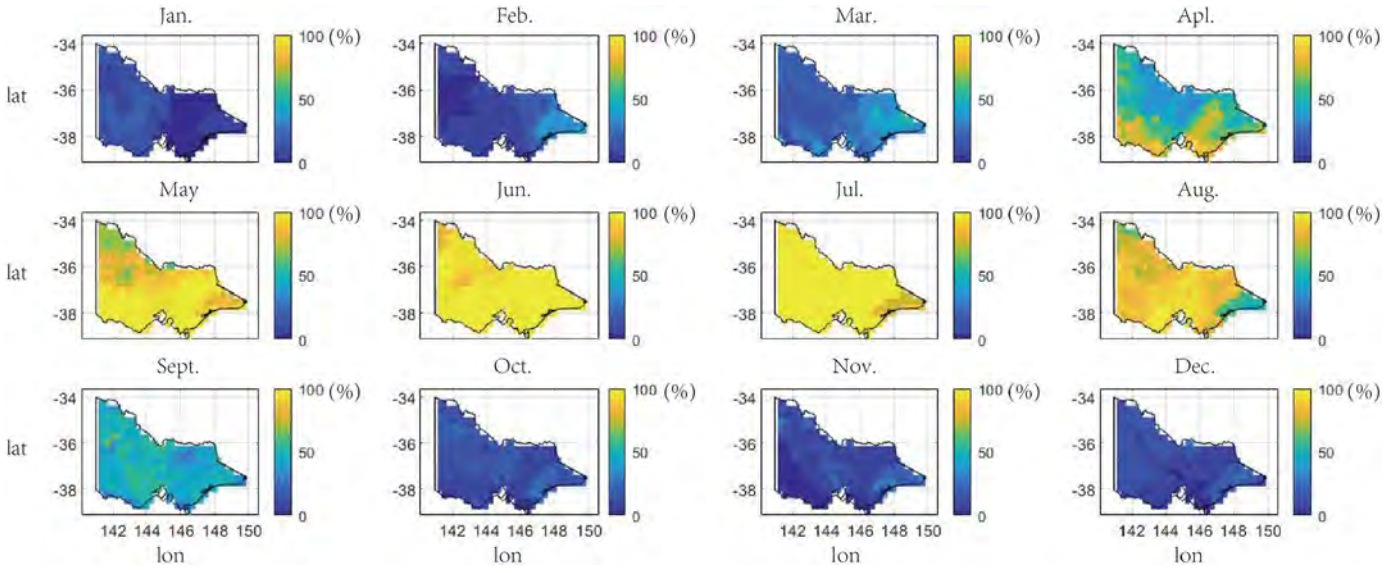

Fig. 3. Monthly average groundwater recharge frequency (from January to December) derived from GLDAS-DA for the period 2004–2019.

groundwater storage estimates but rather relative storage potential (i.e., large or small compared to the average of study area). Also, GLDAS-DA is only a simulated product and more importantly, it only simulates groundwater storage for shallow aquifers with a depth of 5–8 m (Li et al., 2019; Hu et al., 2021). To present the groundwater renewability, Fig. 2b shows the annual average groundwater range based on the 2004–2019 period. One can see that groundwater has higher renewability in the eastern (150–200 mm; region B) and southwestern parts (100–150 mm; region C) than the northwestern parts (around or below 50 mm) of Victoria.

The monthly average groundwater recharge frequency shown in Fig. 3 evaluates the probability of groundwater recharge over the 2004–2019 period for each month from GLDAS-DA. According to Fig. 3, groundwater recharge has a clear seasonal pattern in Victoria with May to August identified as recharge season (recharge frequency mostly above 75%), October to March as discharge season (recharge frequency mostly below 10–30%), and April and September as transition season (recharge frequency mostly around 50%). Therefore, groundwater levels in most parts of Victoria reach their maximum level in August or September, which would be a suitable time to start extracting.

3.2. Inversion analysis of groundwater impact factor

Rocks with high porosity or well-developed fractures have more spaces and channels to store groundwater, and as such, can be associated with large groundwater storage potential. Fig. 4a shows that the Australian State of Victoria has a good hydrogeological environment for storing groundwater, with medium to high productive porous (northwestern parts and southern coastal regions) and fractured (mostly southern parts) aquifers covered nearly in all areas. Besides the hydrogeological environment, the amount of recharge resources (i.e., rainfall and runoff) owned

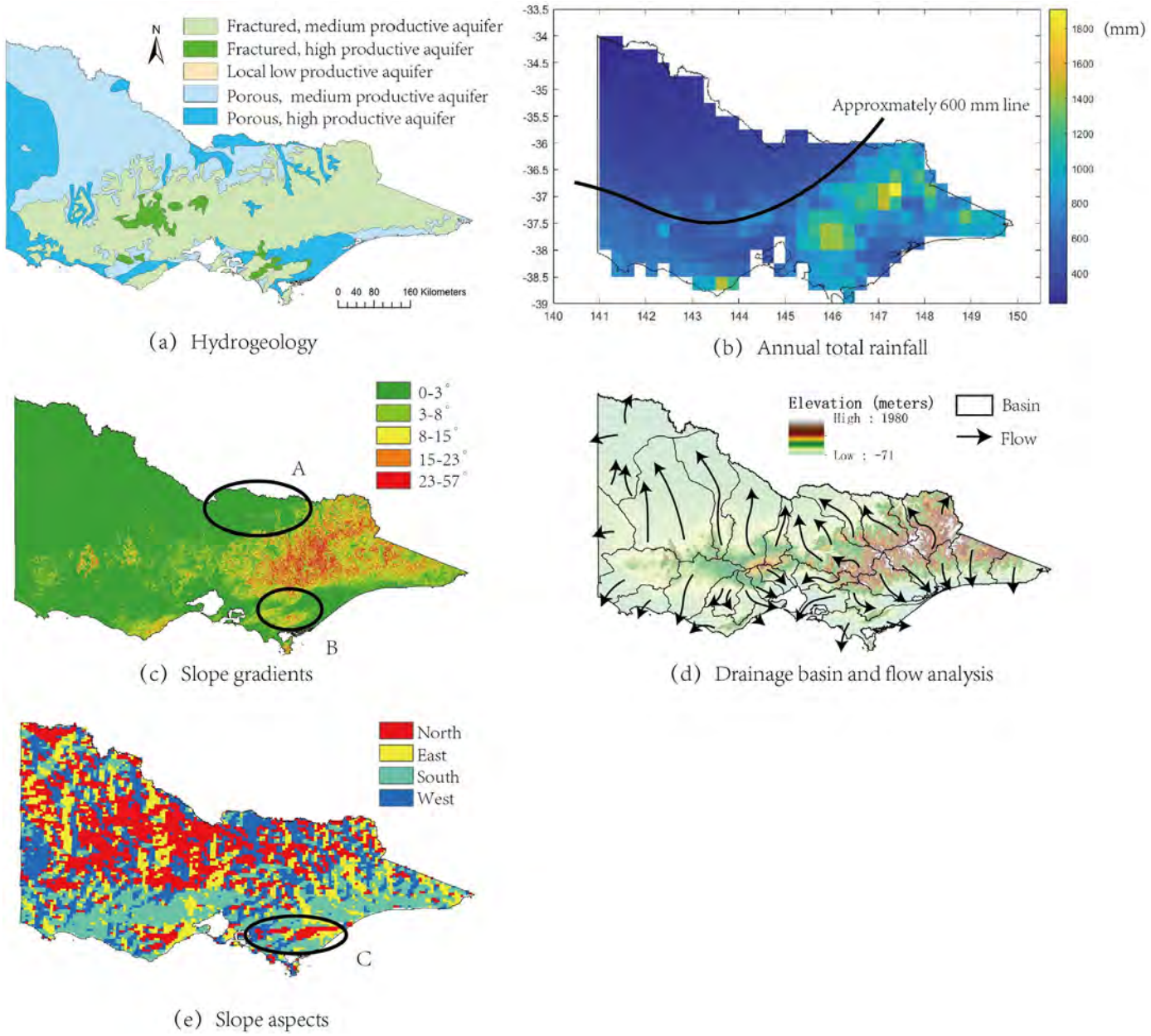

Fig. 4. Inversion analysis of the Australian Victoria State; (a) hydrogeological map (Lau and Jacobson, 1987), (b) average annual total rainfall with a line of 600 mm dividing humid and arid regions, (c)–(e) surface flow analysis based on slope gradient, drainage basin and aspects. The circled regions A and B in (c) are the areas receiving large amounts of runoff from the mountains. The circled region C in (e) indicates an obvious obstacle (north face slope; red) preventing runoff to reach the ocean.

by each region also determines its groundwater storage potential. Fig. 4b presents annual total rainfall and an approximate rainfall line of 600 mm (normally as the threshold of dividing humid and arid regions in Australia). According to this line, one can simply infer that the eastern and southwestern parts of the line have more groundwater storage potential that can be extracted than the northwestern parts. It is worth noting, however, that high rainfall, e.g., 1000–1800 mm in Fig. 4b mainly falls in the eastern mountainous region (see colour red in Fig. 4c, also see Fig. 4d). This generates a large amount of runoff to the northern and southern sides of the mountains, as shown in the flow directions in Fig. 4d. Meanwhile, considering the difficulty of groundwater extraction in steep terrain, the ideal answer for 'where' to find groundwater would be these flat areas near the foot of the mountain (regions A and B in Fig. 4c). Particularly, region B, covered by porous, high productive aquifers (Fig. 4a), has high rainfall of 600–1200 mm, and has an obvious north-face (see red in circle C; Fig. 4e) mountain that blocks runoff flowing from north to south. Similar phenomenons of mountains or hills blocking runoff may not be very obvious in other regions since Fig. 4c indicates that the slope gradients are generally flat, ranging from 0 to 3°. Also, coastal regions may quickly lose groundwater after recharging since the porous aquifers directly link to the sea. For the rest of the regions, the northwestern parts of Victoria have a good hydrogeological setting for storing groundwater, however, low annual rainfall in this region may lead to low renewability of groundwater. The southwestern parts have annual rainfall above 600 mm, with medium to high productive aquifer covered, and thus, could have relative large groundwater storage potential (smaller than regions A and B due to lower rainfall and less runoff coming from other regions).

Based on the water balance equation, Fig. 5 presents the monthly average groundwater recharge frequency to infer groundwater recharge timing. One can see a clear groundwater recharge season during May and August in the southern parts of Victoria with recharge frequencies generally above 75%. For the northwestern parts (see region A in Fig. 5, July), the groundwater recharge is unstable since the maximum recharge frequency is only around 60% during May and August.

3.3. Interpretation of linkages and mismatches

For 'where' and 'when' to find groundwater, Sections 3.1 and 3.2 have given the results independently. The linkages and mismatches between Sections 3.1 and 3.2 are summarised in Fig. 6 and discussed below:

(i) Both GLDAS-DA and inversion analysis of impact factors on groundwater indicate that the eastern and southwestern parts of Victoria (regions B and C in Fig. 2b) have large groundwater storage potential that can be extracted. This is confirmed by the Fig. 6 (regions A to C), a map of current groundwater management areas modified from Victoria State Government (2021), indicating that most of the current groundwater management areas are within the eastern and southwestern parts of Victoria.

(ii) Differently, in the eastern parts of Victoria, GLDAS-DA locates large groundwater storage potential that can be extracted in mountainous regions (region B in Fig. 2b), which is not realistic due to difficulties in drilling boreholes. The inversion analysis infers large groundwater storage potential that can be extracted in the flat areas near the foot of the mountain (regions A and B in Fig. 4c), covered with porous, high productive aquifers, and high rainfall or a large amount of runoff as recharge source. This matches with results in Fig. 6, see, e.g., regions A and B, indicating that there are no groundwater management areas in mountainous regions.

(iii) GLDAS-DA indicates that region A in Fig. 2a has the largest groundwater storage potential (shallow aquifers) in Victoria. However, Fig. 4a shows that region A is only a porous, medium productive aquifer, with rainfall below 600 mm. Meanwhile, Fig. 6 also shows no groundwater management area in there. Thus, this is a mismatch between GLDAS-DA and the inversion analysis, and thus, the annual average groundwater range is better suited for inferring groundwater storage potential that can be extracted.

(iv) For groundwater recharge timing, both GLDAS-DA and the inversion analysis show that the period of May to August is the main recharge season for the southern parts of Victoria (Figs. 3 and 5), which aligns with the results of Chen et al. (2016) and Yin et al. (2021).

(v) A mismatch for groundwater recharge timing can be identified in the northwestern parts of Victoria (region A; Fig. 5), where GLDAS-DA shows a high recharge frequency (above 70-80%) during May and August, while WBE shows that there is only about 50% chance to recharge groundwater. From previous experience in Hu et al. (2021), this difference could be due to the missing count of runoff received from other regions, since WBE is just a simple 'vertical' model. However, considering the flat terrain and low annual rainfall in the northwestern parts of Victoria, it is unlikely to have a large amount of runoff. Thus, the GLDAS-DA inferred groundwater recharge timing in such a region also has uncertainty and needs verification.

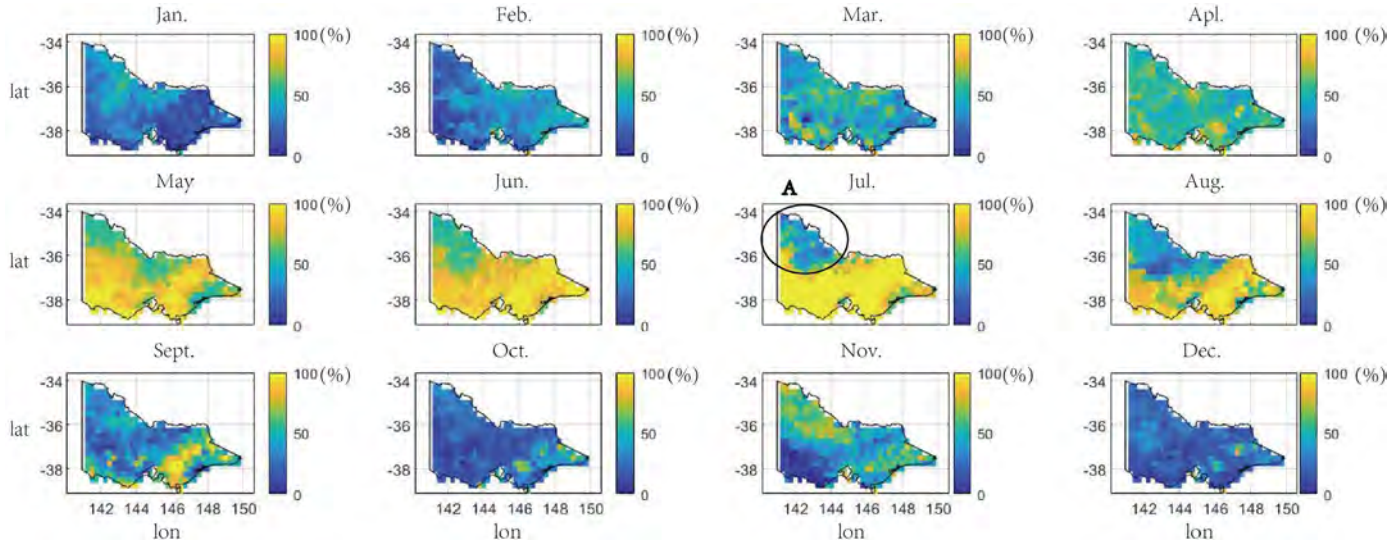

Fig. 5. Monthly average groundwater recharge frequency (from January to December) derived from WBE for the period 2004–2019. Region A circled in July shows a low (around 50%) groundwater recharge frequency during groundwater recharge season.

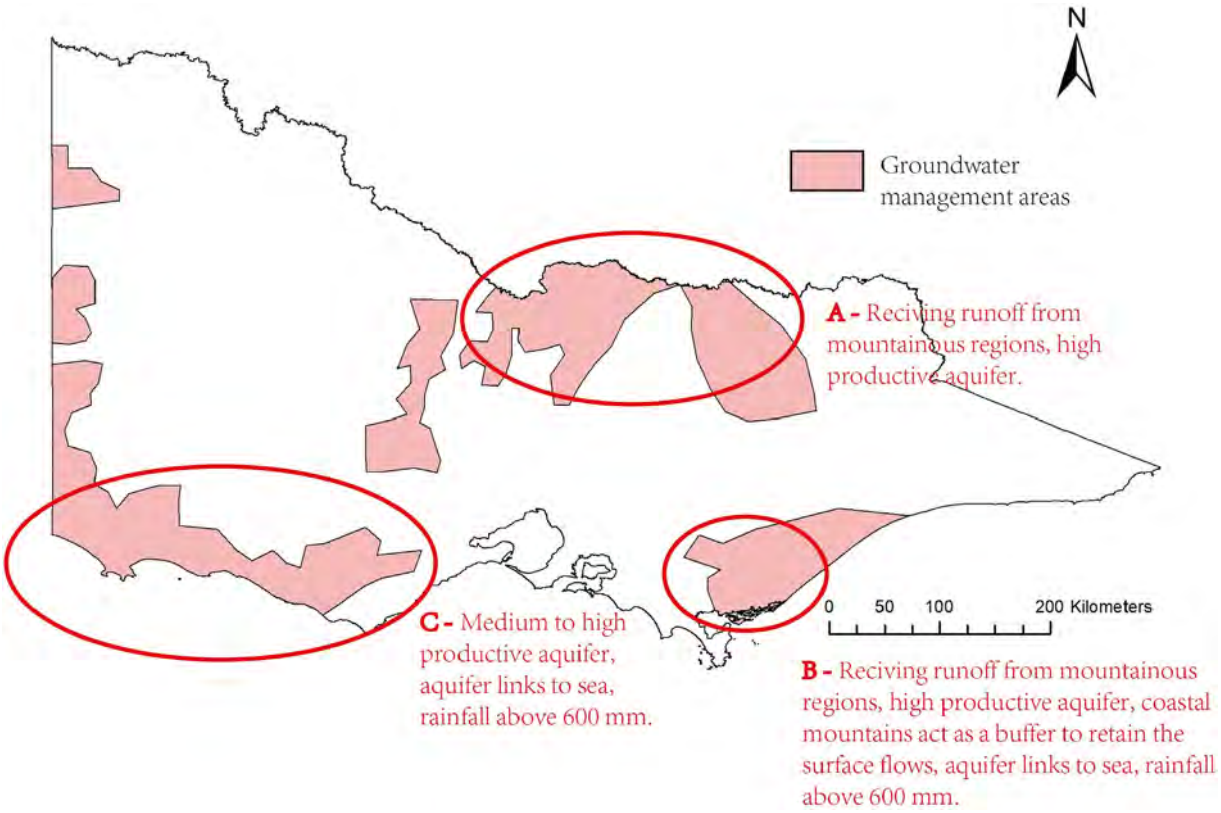

Fig. 6. Map of groundwater management areas in Australian State of Victoria, modified from Victoria State Government (2021). The red circles (A to C) are the suitable areas to find groundwater during August or September (reaching maximum groundwater level), inferred from the knowledge based approach.

3.4. Verification using borehole data

Since borehole measures groundwater as standing water level and GLDAS-DA measures groundwater in equivalent water height (e.g., amount of groundwater), the magnitudes of these two data cannot be compared unless the porosity is known for each pixel. Therefore, the verification mainly focuses on the characteristics of groundwater spatio-temporal variation, since Section 3.3 indicated that there are no obvious mismatches for inference of 'where' to find groundwater.

From Fig. 7a, it can be seen that many boreholes (around 15,000) have groundwater records in the Australian State of Victoria. However, the monthly temporal coverage is not ideal for many pixels, e.g., many pixels with coverage rate below 50% as shown in Fig. 7b. Therefore, six scattered regions (polygons A to E in Fig. 7b) that contains a high coverage rate (above 75%) are selected for verification. Fig. 8 presents the monthly groundwater storage change timeseries and average monthly groundwater storage change for both borehole and GLDAS-DA for the regions A to E. Overall, borehole and GLDAS-DA data show a relatively good agreement (most correlations significant with *P*-value smaller than 0.05) in all six regions. Although region E seems to obtain a poor correlation for both monthly groundwater storage timeseries and average monthly groundwater storage change, the borehole data between 2010 and 2015 show an abnormal behaviour and the obtained correlations could be biased. More importantly, all six regions, particularly, region F in the northwestern

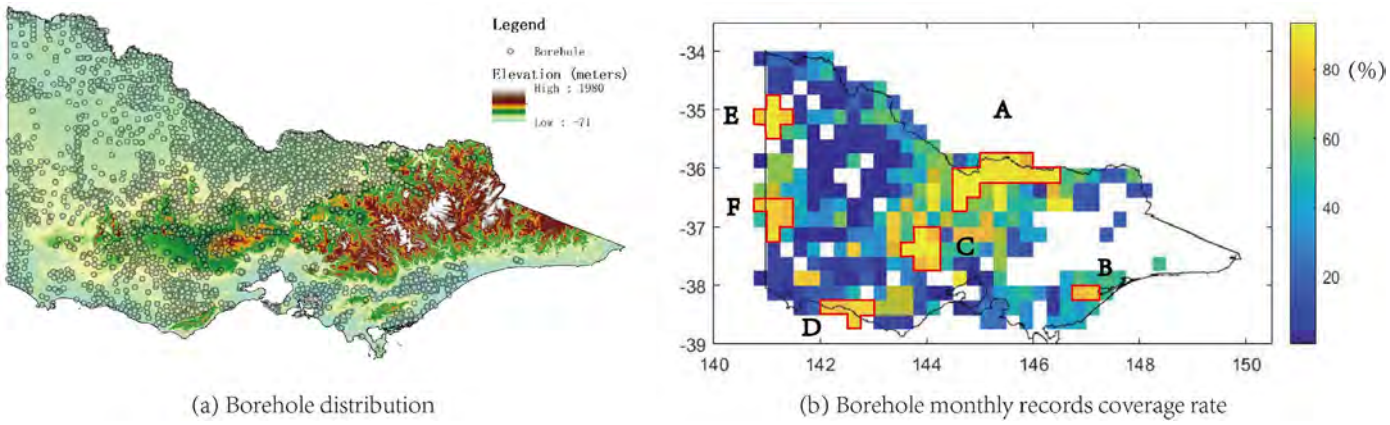

Fig. 7. Borehole availability; (a) spatial distribution, and (b), monthly temporal coverage rate based on 2004–2019 period. The polygons A to E in (b) delineate the pixels selected for verification.

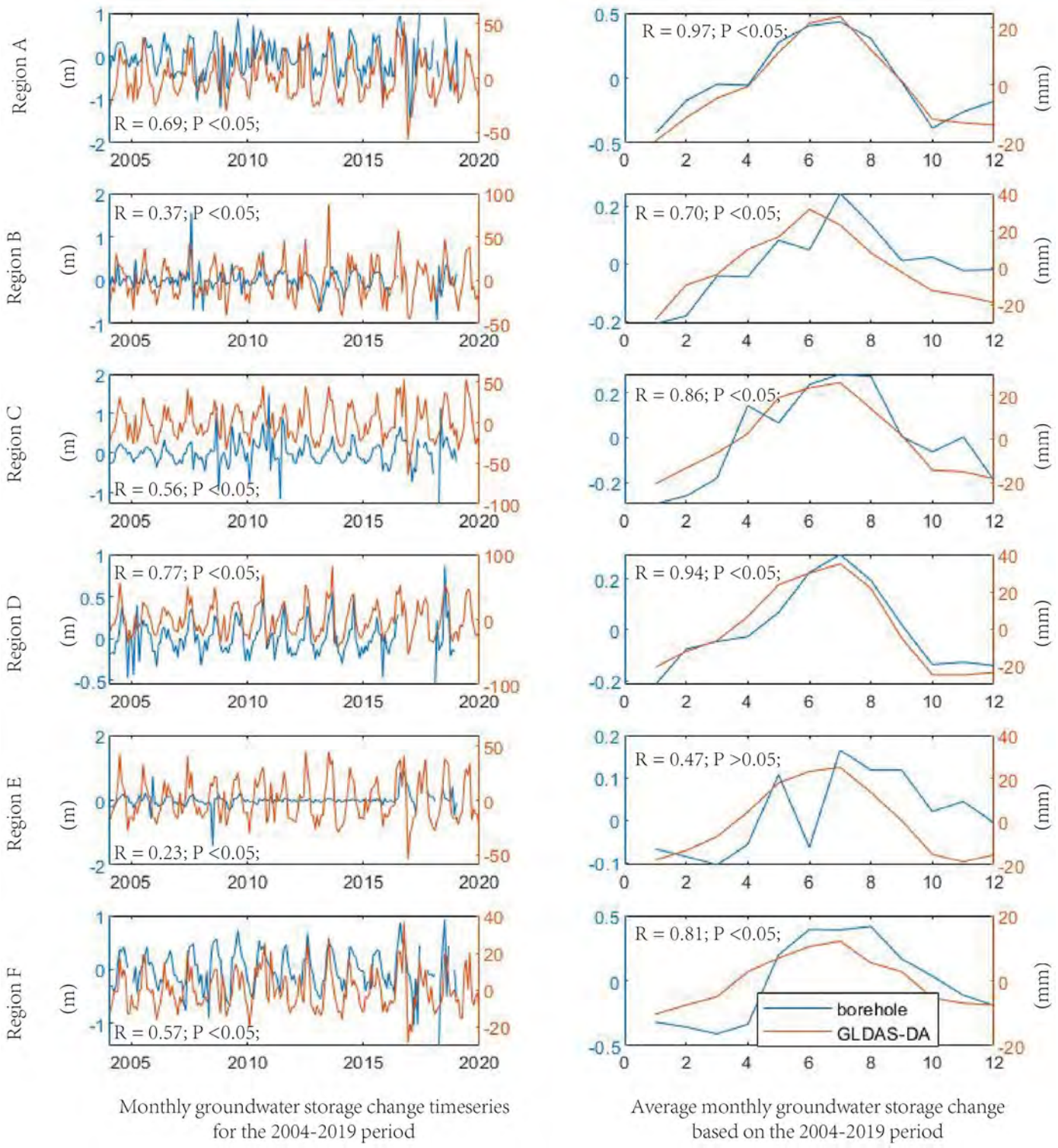

Fig. 8. The comparisons of monthly groundwater storage change timeseries (left) and average monthly groundwater storage change (right) between borehole (unit: m) and GLDAS-DA (unit: mm) based on the 2004–2019 period, for regions A to E presented in Fig. 7. R and P are the correlation and P-value, respectively.

parts of Victoria shows a clear groundwater recharge season during May and September. This excludes the uncertainty of GLDAS-DA and indicates that the recharge frequency results of WBE in the northwestern parts of Victoria are incorrect, possibly due to the uncertainty of parameters in WBE equation or missing considerations such as groundwater internal flow. In other words, GLDAS-DA seems to be more likely reliable compared to WBE when mismatches appear (if there is no borehole data for verification).

4. Discussion

Table 2 summarise the major results of Hu et al. (2021) and this contribution as a comparison. Overall, it can be seen that the knowledge-based approach for inferring spatio-temporal characteristics of groundwater works well in both LVB and Australian Victoria.

Specifically, both studies show that the GLDAS groundwater models (GLDAS CLSM in Hu et al. (2021) and GLDAS-DA in this contribution) are

Table 2
Comparison of results in Hu et al. (2021) and this contribution.

Steps	Lake Victoria Basin	Australian State of Victoria
(i) Model exploration	The eastern parts have large groundwater storage potential; recharge season is March to May and October to December	The eastern and southwestern parts have large groundwater storage potential; recharge season is May to August
(ii) Inversion analysis	Hydrological and topographic environment also indicate that the eastern parts of LVB have large groundwater storage potential; WBE indicates March to May and September to November as groundwater recharge season	Hydrological, topographic and rainfall identify large groundwater storage potential regions in the flat areas near the foot of the eastern mountainous regions, and southwestern coastal regions; WBE also identifies May to August as recharge season
(iii) Interpretation of linkages or mismatches	Steps (i) and (ii) basically align with each other	Steps (i) and (ii) basically align with each other, mismatch of recharge timing in the northwestern parts is found
(iv) Verification using borehole data	Only Ugandan regions have few boreholes (only 10), verification may not be representative	Over 15,000 boreholes are used, 6 different parts of Victoria State are verified, results show good correlation with GLDAS-DA

able to correctly reflect the spatio-temporal behaviours of groundwater since the results basically algin with the inversion analysis of groundwater impact factors. The only problem in LVB was that the poor correlation between borehole and GLDAS CLSM in the Ugandan regions (may not be representative due to insufficient numbers of boreholes; see Hu et al., 2021) made us unable to prove the reliability of the knowledge-based approach. Now with a data-rich region like the Australian State of Victoria; the borehole data show a high agreement with GLDAS-DA and the inferred large groundwater storage potential regions mostly belong to current groundwater management areas (Victoria State Government, 2021). The reliability of the knowledge-based approach, therefore, has clearly been confirmed.

5. Conclusion

After testing the knowledge-based approach using the Australian State of Victoria as another example, it has been further confirmed that such an approach is simple and reliable for inferring spatio-temporal characteristics of groundwater. The feature of this approach combines the advantages of the groundwater model and inversion analysis, i.e., the groundwater model is able to offer specific numerical estimates, while inversion analysis supports more advanced groundwater understanding in localised regions. Therefore, even without actual borehole monitoring data, it is projected that the knowledge-based approach is able to correctly infer 'where' and 'when' to find groundwater over many regions around the globe. This is important, particularly for those countries and regions with data deficient issues.

CRediT authorship contribution statement

K.X, Hu: Conceptualization, Methodology, Software, Writing - Original Draft, Data Visualization. **J.L, Awange**: Writing - Review & Editing, Supervision. **Kuhn, M**: Writing - Review & Editing, Supervision.

Declaration of competing interest

The authors declare that they have no known competing financial interests or personal relationships that could have appeared to influence the work reported in this paper.

Acknowledgment

Kexiang Hu is grateful for the CIPRS and Research Stipend Scholarship provided by Curtin University and the Australian Government Research Training Program (RTP) Stipend Scholarship that are supporting his PhD studies. The authors would like to thank the following organizations for providing the data used in this study: the Australia Bureau of Meteorology, and the National Aeronautics and Space Administration (NASA) Earth Data Centre.

References

Bureau of Meteorology, 2015. Australian groundwater explorer, datasets, Australian government. Available at http://www.bom.gov.au/water/groundwater/explorer/map.shtml.

Chen, J., Wilson, C., Tapley, B., Scanlon, B., Güntner, A., 2016. Long-term groundwater storage change in Victoria, Australia from satellite gravity and in situ observations. Glob. Planet. Chang. 139, 56–65. https://doi.org/10.1016/j.gloplacha.2016.01.002.

de Graaf, I., Sutanudjaja, E., van Beek, L., Bierkens, M., 2015. A high-resolution global-scale groundwater model. Hydrol. Earth Syst. Sci. 19, 823–837. https://doi.org/10.1016/j.jhydrol.2006.08.005.

Earman, S., Dettinger, M., 2011. Potential impacts of climate change on groundwater resources - a global review. J. Water Clim. Chang. 2 (4), 213–229. https://doi.org/10.2166/wcc.2011.034.

Elshall, A., Arik, A., EI-Kadi, A., Pierce, S., Ye, M., Burnett, K., Wada, C., Bremer, L., Chun, G., 2020. Groundwater sustainability: a review of the interactions between science and policy. Environ. Res. Lett. 15 (9). https://doi.org/10.1088/1748-9326/ab8e8c.

Famiglietti, J., 2014. The global groundwater crisis. Nat. Clim. Chang. 4, 945–948. https://doi.org/10.1038/nclimate2425.

Frost, A., Wright, D., 2018. Evaluation of the Australian Landscape Water Balance model (AWRA-L v6): Comparison of AWRA-L v6 against Observed Hydrological Data and Peer Models, Technical report. Bureau of Meteorology.

Frost, A., Ramchum, A., Smth, A., 2018. The Australian Landscape Water Balance model (AWRA-L v6). Technical Description of the Australian Water Resources Assessment Landscape model version 6, Technical report. Bureau of Meteorology.

Hu, K., Awange, J., Kuhn, M., Saleem, A., 2019. Spatio-temporal groundwater variations associated with climatic and anthropogenic impacts in South-West Western Australia. Sci. Total Environ. 696 (133), 599. https://doi.org/10.1016/j.scitotenv.2019.133599.

Hu, K., Awange, J., Kuhn, M., Nanteza, J., 2021. Inference of the spatio-temporal variability and storage potential of groundwater in data-deficient regions through groundwater models and inversion of impact factors on groundwater, as exemplified by the Lake Victoria Basin. Sci. Total Environ. 800 (149), 355. https://doi.org/10.1016/j.scitotenv.2021.149355.

Khaki, M., Schumacher, M., Forootan, E., Kuhn, M., Awange, J., van Dijk, A., 2017. Accounting for spatial correlation errors in the assimilation of GRACE into hydrological models through localization. Adv. Water Resour. 108, 99–112. https://doi.org/10.1016/j.advwatres.2017.07.024.

Lau, J., Jacobson, G., 1987. Hydrogeology Map of Australia, Research data, Geoscience Australia. Retrieve from researchdata.ands.org.au/hydrogeology-map-australia-hydrogeology-map/688413?source=suggested_datasets. (Accessed 5 March 2019).

Li, B., Rodell, M., Kumar, S., Beaudoing, H., Getirana, A., Zaitchik, B., et al., 2019. Global GRACE data assimilation for groundwater and drought monitoring: advances and challenges. Water Resour. Res. 55, 7564–7586. https://doi.org/10.1029/2018WR024618.

MacFarlane, S., Fairfield, C., 2017. Groundwater abstraction in the roper region - northern territory. Water 2 (3), 1–26. https://doi.org/10.21139/wej.2017.026.

Scibek, J., Allen, D., Cannon, A., Whitfield, P., 2007. Groundwater-surface water interaction under scenarios of climate change using a high-resolution transient groundwater model. J. Hydrol. 333, 165–181. https://doi.org/10.1016/j.jhydrol.2006.08.005.

Siebert, S., Burke, J., Faures, M., Frenken, K., Hoogeveen, J., Döll, P., Portmann, F., 2010. Groundwater use for irrigation – a global inventory. Hydrol. Earth Syst. Sci. 14 (10), 1863–1880. https://doi.org/10.5194/hess-14-1863-2010.

Victoria State Government, 2021. Groundwater licensing and trading - Fact sheet no. 2, Tech. rep., Victoria State Government, Earth Resources. https://earthresources.vic.gov.au/legislation-and-regulations/guidelines-and-codes-of-practice/groundwater-licensing-and-trading.

Von Freyberg, J., Moeck, C., Schirmer, M., 2015. Estimation of groundwater recharge and drought severity with varying model complexity. J. Hydrol. 527, 844–857. https://doi.org/10.1016/j.jhydrol.2015.05.025.

Yin, W., Fan, Z., Tangdamrongsub, N., Hu, L., Zhang, M., 2021. Comparison of physical and data-driven models to forecast groundwater level changes with the inclusion of GRACE – a case study over the state of Victoria, Australia. J. Hydrol. 602 (126), 735. https://doi.org/10.1016/j.jhydrol.2021.126735.

Zhao, W., Li, A., 2015. A review on land surface processes modelling over complex terrain. Adv. Meteorol. https://doi.org/10.1155/2015/607181.

Chapter 5
Understanding of groundwater recharge threshold conditions across the Australian continent

This chapter is covered by the following publication (*Hu et al.* 2022b):

1. **Hu, K.X.**, Awange, J.L. and Kuhn, M., (2022). Large-scale quantification of groundwater recharge threshold conditions using machine learning classifications: An attempt over the Australian continent. Groundwater for Sustainable Development, submitted.

This chapter presents the first large-scale quantification of groundwater recharge threshold conditions across the Australian continent, which addresses the issues discussed in Section 1.4.4 and objective (iv) listed in Section 1.5. Given the complexity of handling multiple conditions, i.e. rainfall, evaporation, soil moisture, runoff and vegetation, the machine learning classification techniques are applied. This is because quantifying a value of a threshold condition can be regarded as a classification task, i.e. finding a certain value as an indication of groundwater recharge and discharge. Compared to the traditional statistical methods, machine learning techniques are powerful for dealing with a large quantity of data and handling multiple factor issues; nevertheless, the results still remain uncertain due to the fact that the performance of training models could be different among different machine learning techniques. Also, the input data from different products for training is the source of uncertainty. Therefore, this study compares the performance of three machine learning methods (classification and regression tree, *Breiman et al.* 1984, random forest, *Breiman* 2001, and logistical regression, *Pregibon* 1981) derived from different input datasets. The results suggest that all three techniques offer similar high groundwater recharge/discharge prediction accuracy (all above 75%) at a continental scale with similar types of threshold conditions identified spatially. For instance, rainfall is identified as the primary condition that controls groundwater recharge in most of the Australian continent. However, when using different input datasets for training, the identification of primary threshold conditions such as soil moisture, evaporation and runoff could become different, indicating that data selection has a strong impact on the classification results. This should be of particular concern since different primary threshold conditions identified will infer different groundwater recharge mechanisms. Finally, although the classification and regression tree method has slightly lower prediction accuracy than random forest and logistical regression, this method is able to provide specific values for each threshold condition, while the other two can only act as groundwater recharge/discharge prediction tools.

Large-scale quantification of groundwater recharge threshold conditions using machine learning classifications: An attempt over the Australian continent

K.X, Hu[a], J.L, Awange[a], M, Kuhn[a]

[a]*School of Earth and Planetary Sciences, Spatial Science Discipline, Curtin University, Perth, Australia*

Abstract

Understanding groundwater recharge threshold conditions is key to predicting whether groundwater will be recharged and revealing its recharge mechanism. However, the quantification of the groundwater recharge threshold condition is difficult since the recharge mechanism can be rather complex affected by multiple factors that differ from one region to another. To avoid this complexity, previous studies either focused on a local to regional scale or were limited to a single factor such as rainfall. Thus, the large-scale quantification (e.g., basin to continental scales) of groundwater recharge threshold conditions has never been done before, yet such information is important for managers to carry out a good plan over a large area. Considering that finding a threshold to instantly determine whether the groundwater is in the state of recharge or discharge is a classification task, this study explores three machine learning classification techniques; Classification and Regression Tree (CART), Random Forest (RF), and Logistical Regression (LR), to quantify the specific threshold values for each condition (including rainfall, evaporation, soil moisture, runoff and vegetation) and ensure their reliability. Using the Australian continent as an example, CART is the fastest method and provides an average classification accuracy (76%) at almost the same levels compared to RF (77-78%) and LR (79-80%). Meanwhile, CART is the only method that is able to provide specific threshold values for each condition. When inferring the groundwater recharge mechanism through threshold conditions, the CART method suggests that a primary (the most important) threshold condition is sufficient for most parts of the Australian continent, e.g., rainfall as primary threshold condition in northern Australia indicate a direct recharge mechanism. Only the coastal areas of southeastern and southwestern Australia are dominated by multiple threshold conditions, showing the complex groundwater recharge mechanism.

Keywords: Classification Tree, Groundwater, Logistical Regression, Random Forest,

Threshold.

1. Introduction

Groundwater recharge is a complex hydrological process affected by many conditions such as rainfall, evaporation, soil, vegetation, topography, geology (*Fu et al.*, 2019; *Moeck et al.*, 2020; *Hu et al.*, 2021). Groundwater recharge threshold conditions, defined as the necessary conditions required and the specific values that these conditions must reach to trigger the groundwater level rise (*Baker et al.*, 2020; *Moeck et al.*, 2020). For example, *Hu et al.* (2019) indicate that groundwater will not recharge in the coastal areas of Perth (Australia) unless rainfall exceeds 60-70 mm/month (normally April to September). In this example, rainfall of 60-70 mm/month is considered as the groundwater recharge threshold condition, and such information is important for predicting groundwater recharge timing needed for agricultural activity and adjusting an annual water allocation plan (*Carroll et al.*, 2019).

Previous studies have tried to quantify groundwater recharge threshold conditions using various methods such as isotope, cave drip and borehole monitoring network (*Jones and Banner*, 2003; *Kotchoni et al.*, 2019; *Baker et al.*, 2020). However, these methods are only suitable at local or regional scales (usually coupled with geological investigations), requiring specialised knowledge to place or operate equipment, expensive and time-consuming. More importantly, these methods have certain constraints when discussing groundwater recharge, such as studying only 'rainfall threshold condition', or discussing threshold conditions in terms of specific aquifers or climates. This is possibly due to the complexity of handling multiple threshold conditions over a large area or at high spatial resolution. For example, each condition has a different weight of influence on groundwater recharge that varies spatially since the recharge mechanisms are different in various hydrogeological regions (*Barron et al.*, 2012; *Hu et al.*, 2017; *Motiee and McBean*, 2017; *Hu et al.*, 2021).

Large-scale quantification of groundwater recharge threshold conditions is very difficult. *Small* (2005) tried to quantify the groundwater recharge threshold over the southwestern United States using precipitation and potential evapotranspiration. However, the conclusion reached was that using these two conditions was insufficient to predict groundwater recharge occurrence, suggesting that other conditions have significant impacts on groundwater recharge, which were not considered. For example, *Moeck et al.* (2020) indicate that except for climatic conditions

(e.g., rainfall and evaporation), non-climatic conditions such as vegetation and runoff also have obvious impacts on groundwater recharge over some regions around the world. *Fu et al.* (2019) also make similar deductions based on a case study over the southeast corner of South Australia. However, both studies do not provide the threshold values of each condition, nor do they rank the importance of each condition. To the best of the authors' knowledge, no study has ever provided the information of groundwater recharge threshold in terms of large areas (e.g., basin to continental scales) and multiple conditions. Yet such information is important for groundwater prediction, understanding of recharge mechanisms, and enabling managers to adjust water use plans for other applications. Besides, for groundwater models that simulate the hydrological process, such information can enhance the understanding of recharge processes, thus, improving model performance (*Von Freyberg et al.*, 2015).

From a statistical point of view, quantifying groundwater recharge threshold conditions can be regarded as a classification task that requires the determination and quantification of the threshold conditions that instantly distinguish between net groundwater recharge (class one: level rises) and discharge (class two: level drops). Machine learning classifications, thus, are likely to be the solution to this task since they normally do not require the understanding of the complex hydrological process of groundwater recharge (*Yin et al.*, 2021). Also, they can be applied on nonparametric data distribution (*Maxwell et al.*, 2018). Most importantly, they are powerful enough to deal with large datasets and multi-condition problems as considered in this study. Although, we have not found any previous studies using machine learning classification techniques to quantify groundwater recharge threshold conditions, there have been many similar studies on threshold conditions in other fields, see, e.g., *Miao et al.* (2011); *Belgiu and Drăgut* (2016); *Wu et al.* (2018); *Yang et al.* (2019). Among many machine learning classification methods, Classification And Regression Tree (CART; *Breiman et al.* 1984) is probably the most suitable method for addressing this task since it is the only method that can directly quantify the specific threshold value for each condition. The only concern is that the classification accuracy could be lower than for other more advanced machine learning classifications. For example, previous studies, e.g., *Long et al.* (1993); *Ali et al.* (2012); *Deschamps et al.* (2012); *Belgiu and Drăgut* (2016) showed that Random Forest (RF; *Breiman* 2001) and Logistical Regression (LR; *Pregibon* 1981) perform better than CART. Thus, a comparison between CART and other machine learning classifications is necessary to confirm whether CART quantifies the groundwater recharge threshold conditions with satisfactory classification accuracy.

This study, therefore, tries to quantify large-scale groundwater recharge threshold conditions through an exploration of the CART, RF and LR methods as exemplified by the Australian continent. Specifically, (i) the classification accuracies and computation time of these three machine learning methods are compared, (ii) the importance ranking of threshold conditions of these three methods are compared, (iii) the specific threshold values (monthly based) of each condition from CART are presented spatially since it is the only method that provides threshold values, (iv) the potential groundwater recharge mechanisms inferred by different threshold conditions are discussed, and (v), the strength, limitation and future direction of this study are discussed.

2. Method and material

2.1. Data preparation

Since we are going to use machine learning techniques, the training data that includes the condition variable and the response variable must be prepared for the training process.

2.1.1. Response variable

In the training process, the response variables, which in our case are groundwater recharge (class one) and discharge (class two), are used to classify the condition variables. Here, the Global Land Data Assimilation System (GLDAS) Catchment Land Surface Model (CLSM; version 2.2) with data assimilated from the Gravity Recovery and Climate Experiment and Follow On products (GRACE/GRACE-FO; hereafter referred to as GLDAS-DA) is employed to offer groundwater storage estimates at a $0.25^\circ \times 0.25^\circ$ spatial and daily temporal resolution (*Li et al.*, 2019). GLDAS-DA has been chosen here due to its high spatial resolution, long temporal span, data with global coverage and is freely available. As for the quality of the data, *Li et al.* (2019) evaluated the GRACE-DA using over 4,000 in-situ data around the world and obtained an average 4.3 cm groundwater variation root mean square errors, and a correlation of 0.65 at regional scale. Note that the GRACE product is not used due to its coarse spatial resolution on the one hand, and on the other hand, GLDAS model is still required to derive groundwater storage changes from GRACE total water storage. To prepare the monthly resolution datasets, the monthly groundwater change is calculated using the groundwater storage estimates from GLDAS-DA for the last day of the current month minus the last day of the previous month. When groundwater change is above/below zero, the groundwater for the current month is classified as 'recharge'/'discharge'.

2.1.2. Condition variable

The condition variable is used to predict the response variable after training. In our case, we selected five condition variables, rainfall, evaporation, runoff, soil moisture and vegetation greenness, since previous studies have reported these as the major threshold conditions that determine whether groundwater recharges (see, e.g., *Small* 2005; *Diodato and Ceccarelli* 2006; *Fu et al.* 2019; *Moeck et al.* 2020). To evaluate the uncertainty of the machine learning classifications derived from different input training data, the Australian local products, i.e., Australian

Bureau of Meteorology rainfall products and Australian Water Resources Assessment Landscape (AWRA-L) model (version 6; *Frost et al.* 2018; *Frost and Wright* 2018), and the global products, i.e., GLDAS Noah land surface model (version 2.1; *Rodell et al.* 2004; *Beaudoing et al.* 2020), are employed for the condition variables of rainfall, evaporation, soil moisture and runoff since it uses the same forcing input data as GLDAS-DA (GLDAS-DA does not provide some of these parameters in daily format due to policy issues). As for the vegetation greenness, the enhanced vegetation index (EVI) of Moderate Resolution Imaging Spectroradiometer (MOD13C2; *Didan* 2015) products are used for the same month.

Note that for groundwater and vegetation, there are no Australian local products, and as such, only two types of products are prepared for the condition variables of rainfall, evaporation, soil moisture and runoff. Also, the common water balance equation; "rainfall minus evaporation" iis not used as a condition variable due to the fact that the output will lose the ability to distinguish which one is the primary condition. Finally, Table 1 summarises The products that offer data as condition variables and response variables. To unify the spatial resolution among different datasets, all data with $0.05° \times 0.05°$ spatial resolution are resized into $0.25° \times 0.25°$ before being used for the 2004-2019 period.

Table 1: Summary of the products used for the methods' comparison over the Australian continent.

Products	Spatial Resolution	Temporal Resolution	Parameter Used
BoM	0.05°	Monthly	Rainfall
GLDAS CLSM	0.25°	Daily	Groundwater
GLDAS Noah	0.25°	Monthly	Rainfall, evaporation, soil moisture, surface runoff
AWRA-L	0.05°	Monthly	Evaporation, soil moisture, surface runoff
MOD13C2	0.05°	Monthly	Vegetation

2.2. Machine learning classifications

Note all the classification methods in this study are done through MATLAB software. For specific codes of each method, we recommend referring to the following web pages: `https://www.mathworks.com/help/stats/choose-a-classifier.html`.

2.2.1. *Classification And Regression Tree (CART)*

The Classification And Regression Tree (CART) method proposed by *Breiman et al.* (1984) is a widely used decision tree (see, e.g., *Gray and Fan* 2008; *Zheng et al.* 2009; *Elliott and Owens* 2015; *Xu et al.* 2021). The core part of the CART method is to grow a binary decision tree by using recursive splitting rules (see tree example in Fig 1). For 'classification tree', the rules normally used are entropy or Gini's Diversity Index (GDI). Both of them can get similar results, however, GDI is computationally faster than entropy, thus, is used in our study. For GDI, it measures the impurity of a node, which is expressed as (*Breiman et al.*, 1984):

$$G = 1 - \sum_i p_i^2, \tag{1}$$

where p_i is the proportion of categories with the category i that reach the node. Since there are only two categories in the response variables in our case, i.e., recharge (p_1) and discharge (p_2), GDI can be rewritten as:

$$G = 1 - (p_1^2 + p_2^2). \tag{2}$$

If a node has just one category, e.g., all the response variables are marked as recharge (perfectly being classified), then G is equal to 0, otherwise, G is positive. Therefore, the rule of node division in CART is to choose the smallest G. Taking our case as an example, suppose we are trying to quantify the rainfall threshold for groundwater recharge for a specific region, and the total number of samples is $|D|$. Based on a test threshold value of rainfall, such as M mm/month, all samples are divided into two parts, D_a (rainfall above M mm/month) and D_b (rainfall below M mm/month). Then the GDI of this M threshold ($G(rainfall, M)$) for creating two nodes (D_a and D_b) can be calculated as:

$$G(rainfall, M) = \frac{|D_a|}{|D|} \times G(D_a) + \frac{|D_b|}{|D|} \times G(D_b). \tag{3}$$

The calculation of Equation 3 runs continuously for different test values of M, until M covers all the range of rainfall values. After that, the M value corresponding to the minimum G, is selected as the rainfall threshold for groundwater recharge. After this process, one node is split into two nodes. Correspondingly, the training data is split into two parts by M (i.e.,

above/below M). In terms of multi-condition variables, we simply line up all the samples of variables and loop the steps above. Each loop will quantify a threshold condition based on GDI and split a node into two. The loop will continue until the impurity of the new node is 0, or it reaches the stopping criterion. The decision tree is then complete.

Normally, if we do not set a stopping criterion, the resulting tree could be very complicated and over-fitting. In other words, its classification accuracy in the training data is very high, but it is low in actual application. Thus, post-pruning is usually required after the tree is complete (*Song and Lu*, 2015). However, post-pruning needs to apply cross-validation (or similar approaches) for all possible subtrees (tree stops to grow at some nodes) of the full tree (tree grows without limitation), and it takes significant time to compute. Given that our aim is to quantify the groundwater recharge threshold conditions at a large scale (e.g., Australia has around 11,000 pixels and each pixel needs to train a tree), the pre-pruning approach (*Song and Lu*, 2015) by setting global stopping criterion, such as maximum split, is more suitable for our study since it saves massive time. In general, the more maximum split allowed, the more accurate the decision tree, but the greater the potential risk of over-fitting. In our case, the maximum split number is set as the number of condition variables so that each variable has a chance to play a role in the groundwater recharge threshold condition at each split (see a similar process in *Ghosh et al.* 2014).

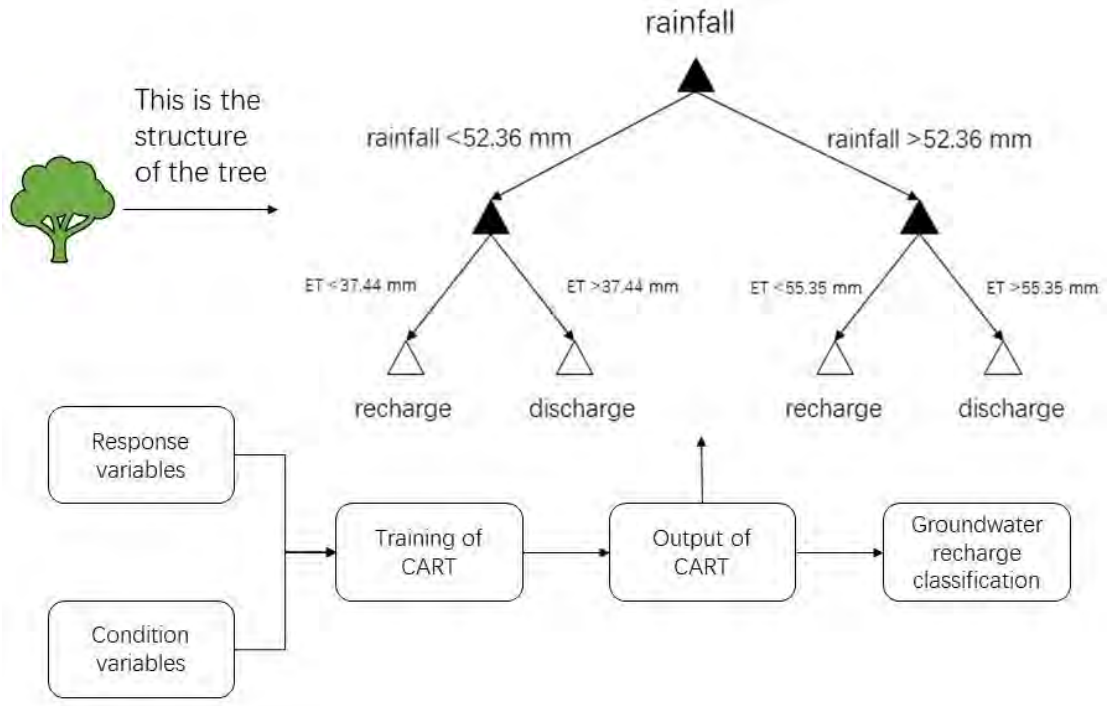

Figure 1: Example of processing flowchart of the CART method. The response variables include groundwater recharge (class one) and discharge (class two), while condition variables contain rainfall, evaporation, soil moisture, runoff and vegetation greenness.

2.2.2. Random Forest (RF)

Random forest (RF), introduced by *Breiman* (2001), is an ensemble classification method using the CART algorithm to grow many trees. As shown in Fig 2, every tree in the forest is grown independently by randomly selecting a subset of the training sample through replacement, the so-called bootstrap sampling or bagging (*Belgiu and Drăgut*, 2016). Specifically, in the process of random sampling, RF not only randomly selects the number of samples, but also randomly selects condition variables. For example, some trees may be grown by using just rainfall and evaporation rather than all the condition variables. This operation increases the randomness of the tree and prevents over-fitting since the final classification results are generated by voting (see Fig 2) from every tree in the forest. Thus, RF is said to have low variance, robust model and better classification accuracy than CART, see, e.g., *Ali et al.* (2012); *Deschamps et al.* (2012); *Awange et al.* (2020). However, compared to the CART method, the random forest loses its interpretability and cannot provide the specific values of groundwater recharge threshold conditions (*Maxwell et al.*, 2018).

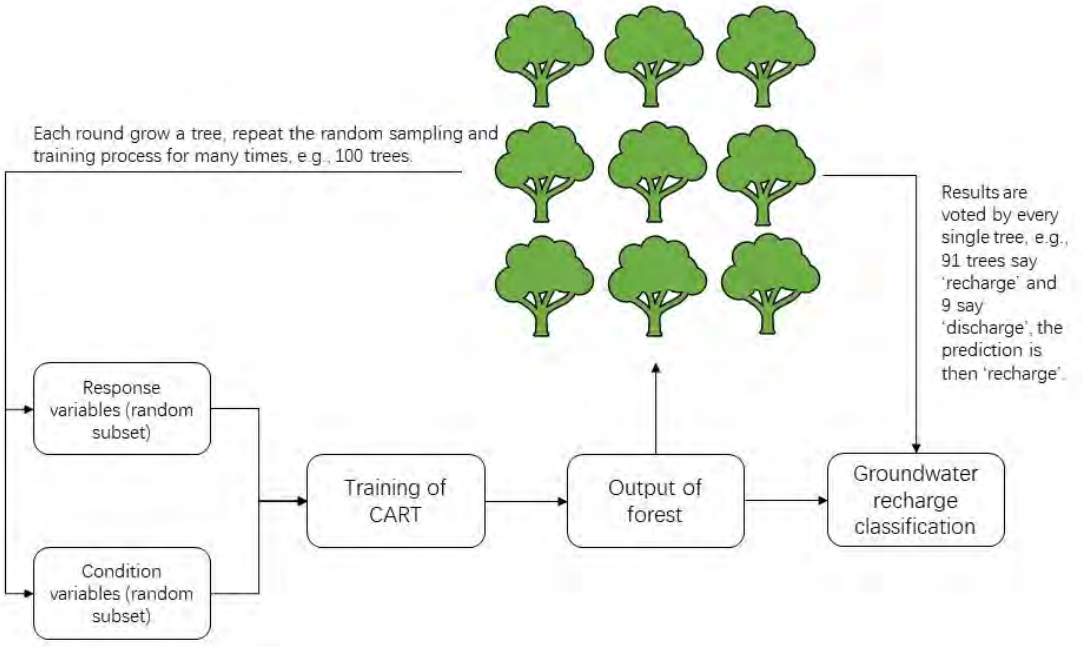

Figure 2: The processing flowchart of the RF method.

For the RF training, the number of trees to be generated is a parameter that needs to be pre-set (*Belgiu and Drăgut*, 2016). Although, some studies have reported that this parameter has no obvious influence on the classification results (at least three trees are required for voting otherwise meaningless), see, e.g., *Du et al.* (2015), different number of trees will still be tested in our case. Besides, the pre-pruning process mentioned in Section 2.2.1 is also necessary for RF to reduce the computation time (*Belgiu and Drăgut*, 2016). Since the RF will be compared to CART in this study, the same maximum split as CART is applied to RF.

2.2.3. Logistical Regression (LR)

Logistical Regression (LR) is a widely used generalized linear regression model with features of simple and fast, especially for binary classification, see, e.g., *Dixon* (2009); *Yang et al.* (2019); *Adiat et al.* (2020). In our case, LR simply calculates the probability (P, from 0 to 1) of groundwater recharge through a sigmoid function of the linear combination of condition variables (X_n), which is expressed as (*Yang et al.*, 2019):

$$ln(\frac{P}{1-P}) = a_0 + a_1X_1 + a_2X_2 + ... + a_nX_n, \tag{4}$$

where $a_i|i = 0...n$ are the regression coefficients corresponding to $X_i|i = 1...n$. The final classification results depend on P. When P is above/below 0.5, then groundwater is classified as 'recharge'/'discharge'. Thus, similar to RF, LR also cannot directly provide the specific values of groundwater recharge threshold conditions. During the training process, the $a_i|i = 0...n$ will be adjusted for numerous iterations until the classification accuracy stops improving, or iteration times reaches the pre-set limit. For more details of the LR approach, we refer the reader to *Awange et al.* 2020, pp. 99-109.

2.3. Classification accuracy evaluation using K-fold cross-validation

K-fold cross-validation (*Fushiki*, 2009; *Rodriguez et al.*, 2010) is commonly used for predictive models generated by machine learning in terms of accuracy evaluation. The main theory of this method is to randomly divide all samples into k folds (many previous studies used a default value of 10 folds; *Mahmood and Khan* 2009; *Ramezan et al.* 2019), use the $k-1$ folds for training, and leave one out of the fold for validation. This process of training and validation gives a percentage of prediction error and is regarded as one iteration. The process is repeated for k iterations and each iteration uses a different leaving one out of the fold for validation. Finally, after k iterations, the average prediction error of k times is the overall prediction error, and the classification accuracy is equal to 1 minus the overall prediction error.

2.4. Ranking of the importance of threshold conditions

Since groundwater recharge is determined by multiple conditions, ranking the importance of each condition is important to improve the understanding of the groundwater recharge mechanism. For the CART and RF methods, the importance of threshold conditions are calculated using Mean Decrease in Gini (MDG) and Mean Decrease in Accuracy (MDA), respectively, see, e.g., *Breiman* (2001); *Belgiu and Drăgut* (2016). The MDG ranks the importance of conditions by measuring how much Gini's Diversity Index can be reduced by a condition. Generally speaking, the further the condition is from the top of the tree (Fig 1), the lower the importance (*Sandri and Zuccolotto*, 2008) is. The MDA estimates the importance of conditions by measuring the influence of a condition on the classification accuracy, i.e., the larger the influence, the higher the importance. As for LR, it is a generalized linear regression model, the importance of conditions cannot be determined directly, since the regression coefficient and its corresponding

p-value only indicate the influence of each condition on the probability of groundwater recharge, rather than the importance of being a threshold condition.

2.5. Uncertainty from input datasets

Machine learning techniques are pure statistical tools for data mining (e.g., *Awange et al.* 2020), and thus, the performance of output depends on the accuracy of the input training data (*Yin et al.*, 2021). In our case, some condition variables such as rainfall can be represented by multiple products (e.g., in-situ based, satellite-based and re-analysis). Therefore, the uncertainty generated by different input training data for the CART, RF and LR methods needs to be compared and discussed. Previous studies, e.g., *Von Freyberg et al.* (2015) also strongly recommends using at least two methods, while applying different input data to show the uncertainty of the groundwater models.

2.6. Lag issue

Despite many previous studies such as *Yu and Lin* (2015); *Hu et al.* (2017); *Kotchoni et al.* (2019) have indicated that there are lags between rainfall and groundwater recharge. This study, however, does not consider the lag issue due to the following reasons:

(i) The lag indicated by previous studies is associated with groundwater level changes, which are real observations. GLDAS-DA is mainly a simulation product based on water balance calculation (see, e.g., *Rui and Beaudoing* 2019), theoretically, it is unable to reflect the lag between rainfall and groundwater recharge.

(ii) According to *Hu et al.* (2019), many previous studies take the statistical lags (e.g., calculated using cross-correlation) between rainfall and groundwater variation as the real lags. This is a misunderstanding since rainfall has to reach a certain threshold to recharge groundwater, otherwise, the rainfall may evaporate or be absorbed by vegetation before it becomes groundwater.

(iii) The real lag between rainfall and groundwater mainly depends on the depth of aquifers, as well as the surface terrain and the geological structure of the subsurface, which is very complex and beyond the scope of this study.

2.7. Computation time

Since our target is to quantify groundwater threshold conditions on a large scale, the computation time of each machine learning classification would be one of concern. In our case, the CART, RF and LR classification methods are all processed using Matlab 2018b software on a PC whose settings are Intel(R) Core(TM) i7-9750H CPU (2.60GHz), and 16GB RAM. Note that the computation time can also vary greatly if other techniques such as cloud computing and parallel computing are applied. The computation time shown in the results is only a reference for the efficiency of each machine learning classification method.

3. Results

3.1. Classification accuracy

3.1.1. CART method

For the CART method, the maximum split of five is set as the stopping criterion during the training process as mentioned in Section 2.2.1. However, during the results inspection phase, we found that many pixels only needed one maximum split to achieve almost the same high classification accuracy (usually above 75%) as the five maximum splits. This potentially means that in most parts of the Australian continent, a single threshold condition is sufficient to classify whether groundwater will be recharged or not (this observation might, however, be different for other areas around the world).

To confirm this conjecture, Figs 3a and b show the classification accuracy of CART (using k-fold cross-validation; k is set as a default value of 10; see details in *Mahmood and Khan* 2009; *Ramezan et al.* 2019) at the five maximum splits using inputs of Australian local and GLDAS global products, respectively; while Figs 3c and d present the difference in the classification accuracy between five and one maximum split. Considering the influence of random sampling on the k-fold cross-validation, a maximum 5% ($\pm$ 2.5%) accuracy error is assumed to be allowed (based on our test); thus, values below 5% are not shown in Figs 3c and d. From Figs 3a and b, one can see that the CART method (using five maximum splits) using local and global products achieve high classification accuracies (above 80%) in the northern, southeastern and southwestern parts of Australia. The middle inland areas and southern parts of Australia have relative low classification accuracy (around 60%). Compared to the one maximum split CART (Figs 3c and d), five maximum splits CART have significant accuracy advantages of 5-15% in the southwestern (A) and southeastern (B) parts of Australia. For the rest of the areas, the five maximum splits CART have no accuracy advantage and are even worse than the one maximum split CART (over-fitting). This confirms our conjecture that a single (primary) threshold condition is sufficient to classify groundwater recharge/discharge in most parts of the Australian continent. Groundwater recharge determined by multi-threshold conditions only exists in the southwestern (A) and southeastern (B) parts of Australia.

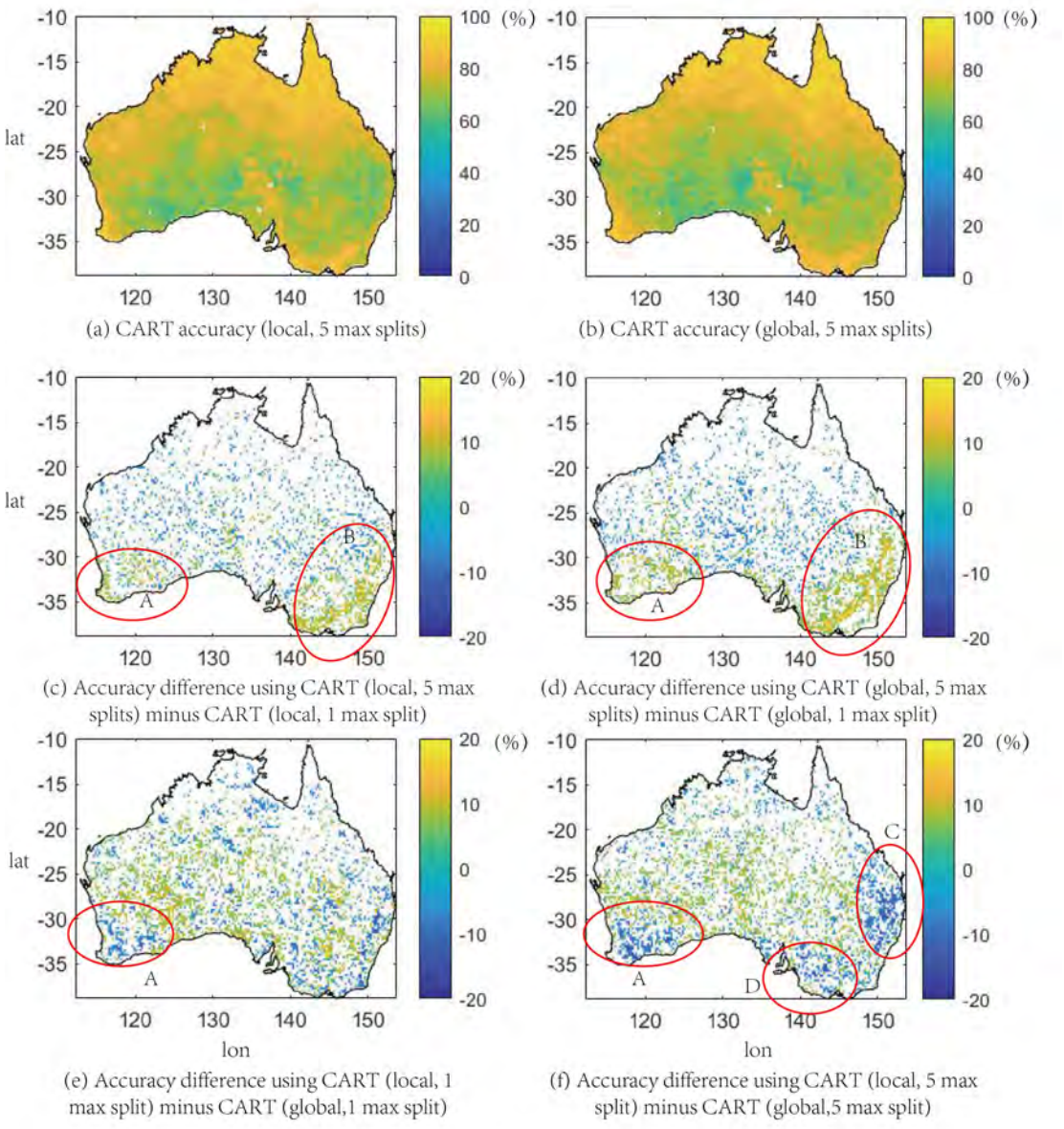

Figure 3: Comparison between the different settings (maximum split and input data) of CARTs in terms of 10-fold cross-validation accuracy (%). 'Local' represents the use of Australian products of BoM and AWRA-L, and 'global' represents the use of GLDAS Noah as the condition variable inputs. The red circles in (b), (c), (e) and (f) indicate areas with obvious differences clustered (i.e., A, B, C and D). Moreover, values smaller than 5% in (b), (c), (e) and (f) are removed.

To evaluate the uncertainty caused by the different inputs (Australian local and GLDAS global products), Figs 3e and f present a comparison of the local and global CART at one and five maximum splits, respectively. Generally, the CART trained by Australian local products

(BoM and AWRA-L) has better classification accuracy (5-11%) in the middle inland areas. However, in the southwestern (A) and southeastern (C and D) parts of Australia, the CART trained by global products (GLDAS Noah) has better classification accuracy (5-18%).

3.1.2. CART compared to RF

As mentioned in Section 2.2.2, RF requires a pre-set number of trees to be generated before training (*Belgiu and Drăgut*, 2016). Considering there are about 11,000 pixels over the entire Australian continent to be processed by the RF method, blindly increasing the number of trees to be generated in each pixel will lead to a drastic increase in computation time. For example, we tried to generate 50 trees in each pixel, and it took about 10 hours to complete. More importantly, it was found that the classification accuracy of the RF method with 50 trees did not significantly improve in comparison to that of the CART method (see the Table 1 in Supplementary Material). This is consistent with previous studies, e.g., *Du et al.* (2015), reported similar situation and concluded that the classification accuracy is not very sensitive to the number of tree to be generated in RF (*Belgiu and Drăgut*, 2016; *Awange et al.*, 2020). Therefore, we reduced the number of trees from 50 to 10, and computed the classification accuracy of 4 RF models (about 2 hours each) under different settings (maximum split and input data). The classification accuracy of the 4 RF models is subsequently compared to CART, as shown in Figs 4a-d. From Figs 4a-d, there are many scattered pixels showing that the classification accuracy of RF is improved 6% on average compared to CART. However, in these scattered pixels from RF, the five maximum splits for example (Figs 4c-d), only account for 10% and 16% of the areas of Australia. This confirms that the CART and RF methods have almost the same classification accuracy over most parts of the Australian continent. However, when compared to the computation time of the CART method (10 minutes), RF took hours to calculate the results depending on the number of trees generated, e.g., for 10 trees, RF required 2 hours' computation time for the entire Australian continent, while for 50 trees, it took approximately 10 hours. For 500 trees commonly seen in previous studies (*Belgiu and Drăgut*, 2016), RF needs more than 100 hours to train if no other acceleration technique such parallel computing is invoiced.

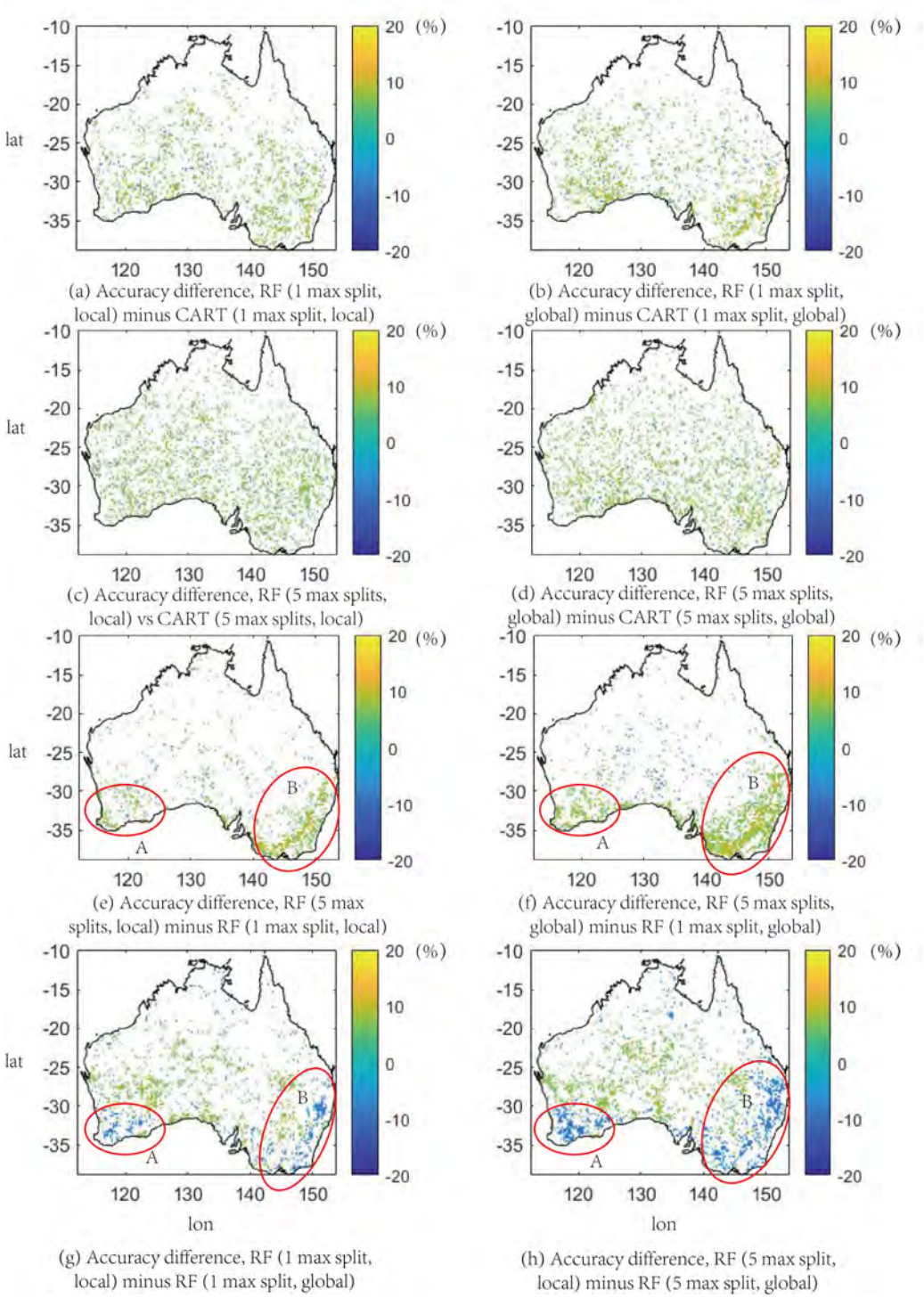

(a) Accuracy difference, RF (1 max split, local) minus CART (1 max split, local)

(b) Accuracy difference, RF (1 max split, global) minus CART (1 max split, global)

(c) Accuracy difference, RF (5 max splits, local) vs CART (5 max splits, local)

(d) Accuracy difference, RF (5 max splits, global) minus CART (5 max splits, global)

(e) Accuracy difference, RF (5 max splits, local) minus RF (1 max split, local)

(f) Accuracy difference, RF (5 max splits, global) minus RF (1 max split, global)

(g) Accuracy difference, RF (1 max split, local) minus RF (1 max split, global)

(h) Accuracy difference, RF (5 max split, local) minus RF (5 max split, global)

Figure 4: Comparison between RF and CART under different settings (maximum split and input data) in terms of 10-fold cross-validation accuracy (%). The red circles in (e), (f), (g) and (h) indicate areas with obvious differences clustered (i.e., A and B). Values smaller than 5% are removed in all sub figs since 5% is considered a reasonable error caused by cross-validation random sampling.

To examine the uncertainty of RF caused by different maximum splits and the inputs between Australian local and GLDAS global products, Figs 4e-h compare the local and global RF at one and five maximum splits, respectively. One can see that the uncertainty results are similar to CART (see Figs 3c-f); for example, RF with five maximum splits have obvious advantages in terms of classification accuracy (5-14%) in the southwestern (A) and southeastern (B) parts of Australia (see red circles). Furthermore, RF trained by local products have 5-11% higher classification accuracy in the middle inland areas, while trained by global products lead to 5-12% higher classification accuracy in the southwestern (A) and southeastern (B) parts of Australia (see red circles).

3.1.3. CART compared to LR

As for the LR, Figs 5a-d show the comparison of classification accuracy difference between LR and CART (one and five maximum splits). One can see that the LR has advantages on classification accuracy for some pixels (averagely improved 7-9% in terms of local and global LR; RF has 6% improvement on average). These pixels with classification accuracy improved cover around 33-35% areas of the Australian continent (RF only covers 10-16%). For the uncertainty evaluation between the Australian local and GLDAS global LR (see Fig 5e), still, local LR has higher classification accuracy in the middle inland areas, while global LR has higher classification accuracy in the southwestern and southeastern parts of Australia.

Overall, the classification accuracy rankings of the three methods (local and global input training data) are; LR (average 79-80%), RF (average 77-78%) and CART (on average 76%). Although the CART method presents a lower percentage, the difference of average classification accuracy (maximum 4%) on a continent-wide scale is not very obvious.

3.2. Ranking of the importance of threshold conditions

As discussed in Section 2.2.1, the CART method indicated that a single (primary) condition was sufficient to classify whether groundwater will be recharged or not in most parts of the Australian continent except the southwestern and southeastern parts (see red circles A and B in Figs 3c or d). Thus, for a single threshold condition, it is important to identify the type of condition that mainly controls groundwater recharge in order to understand its recharge mechanism. For the multiple threshold conditions in the southwestern and southeastern parts of

Australia, the importance ranking will be presented in Section 3.3 together with the illustration of threshold values.

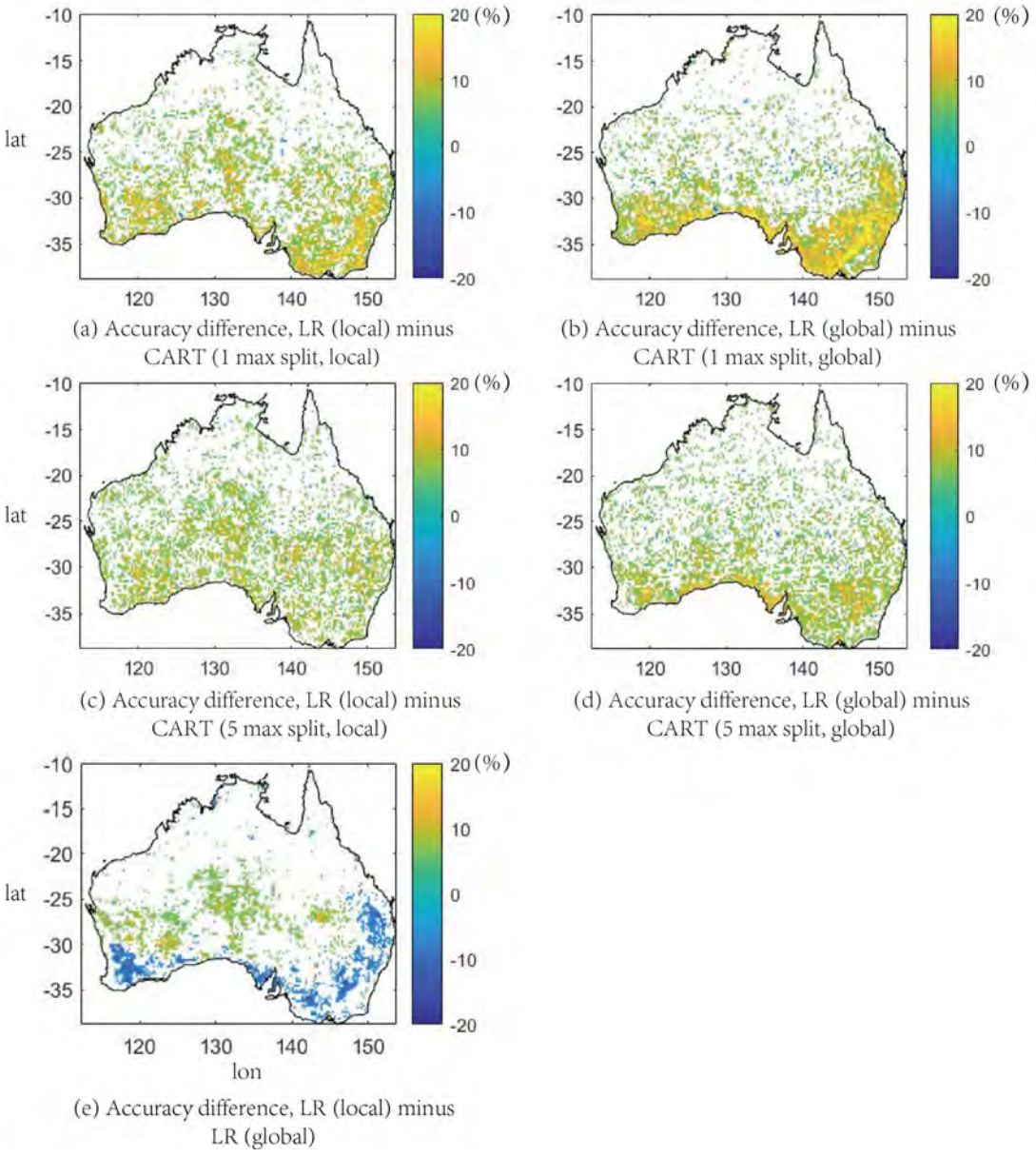

(a) Accuracy difference, LR (local) minus CART (1 max split, local)

(b) Accuracy difference, LR (global) minus CART (1 max split, global)

(c) Accuracy difference, LR (local) minus CART (5 max split, local)

(d) Accuracy difference, LR (global) minus CART (5 max split, global)

(e) Accuracy difference, LR (local) minus LR (global)

Figure 5: Comparison between LR and CART under different settings (maximum split and input data) in terms of 10-fold cross-validation accuracy (%). Values smaller than 5% are removed in all sub figs since 5% is considered a reasonable error caused by cross-validation random sampling.

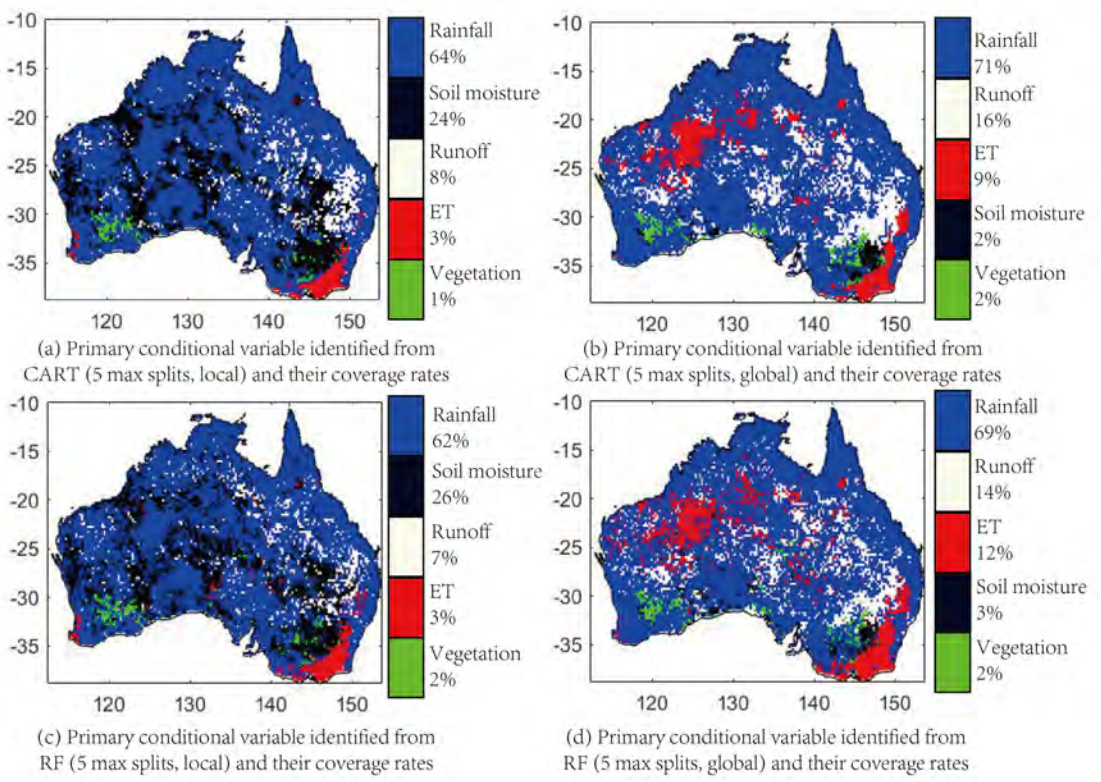

Figure 6: Primary threshold conditions identified from CART (a-local;b-global) and RF (c-local;d-global) and their coverage rates.

Since LR is unable to rank the condition's importance, Fig 6 presents the identified primary threshold conditions from CART and RF using inputs of local and global products. Note that CART at one maximum split can be regarded as the results of CART at five maximum splits after post-pruning. Thus, for identifying the primary threshold condition, there is no difference between CART at one maximum split and five maximum splits. As seen in Fig 6, CART and RF have a similar spatial pattern of primary threshold conditions if they are derived from the same training data (local or global; see Figs 6a, c and b, d, respectively). This confirms the reliability of CART for ranking the importance of threshold conditions. Specifically, for the local product derived results (Figs 6a, c), rainfall (62-64%; blue) and soil moisture (24-26%; black) are the primary threshold conditions for the Australian continent. While for the global product derived results (Figs 6b, d), rainfall (69-71%; blue), runoff (14-16%; white), and evaporation (9-12%; red) are identified as the primary threshold conditions. Vegetation (1-2%; green) plays the role of the groundwater threshold condition only in a few pixels over southwestern and southeastern

Australia.

3.3. The specific threshold values of each condition from CART

3.3.1. Single threshold condition

Considering that CART is the only method that can provide the specific values of the threshold conditions, Fig 7 presents the values of each primary threshold condition derived from it. As seen from Fig 7, the monthly rainfall recharge groundwater threshold ranged from 10-150 mm (Figs 7a and b), with the threshold in the northern parts of Australia being above 70 mm, while the threshold in the middle inland areas being below 50 mm. For monthly evaporation in the northwestern parts of Australia, the global CART (Fig 7d) shows some additional coverage in comparison to the local CART (Fig 7c), with thresholds ranging from 10-50 mm. The remaining parts have thresholds of generally above 40 mm. In terms of soil moisture, Figs 7e and f cannot be compared due to the differences in the unit and spatial coverage between the local and global CART. The spatial patterns and values of vegetation recharge threshold (0.15-0.30 EVI) are similar in Figs 7g and h. Finally, despite some differences in spatial coverage in the western parts of Australia, the runoff shown in Figs 7i and j have similar ranges of threshold around 0.1-1.0 mm.

3.3.2. Multiple threshold conditions

When groundwater is controlled by multiple threshold conditions, a visual examination of the tree in a specific pixel is required to assess the structure of the tree and the specific values of each threshold condition for the CART. Figure 8 uses the local CART as an example, and randomly selects one pixel (A) in the southwestern part of Australia and one pixel (B) in the southeastern part of Australia to show the thresholds of the multiple conditions.

As seen in Fig 8a, the structure of the tree shows that the recharge of groundwater in pixel (A) is determined by two threshold conditions: rainfall and evaporation. As the primary condition, the threshold value of rainfall is 52.36 mm. By only using this threshold, the classification accuracy is about 76% (results generated by one maximum split). By adding evaporation as the second threshold (i.e., 37.44 mm and 55.35 mm in Fig 8a), the classification accuracy improves to 89% (results generated by five maximum splits). RF also identifies the rainfall and evaporation as the major threshold conditions for this pixel according to MDA. However, this results

are not stable since RF sometimes judges that evaporation is more important than rainfall, and this is most likely due to the influence of random sampling or these two conditions have similar importance of being threshold conditions.

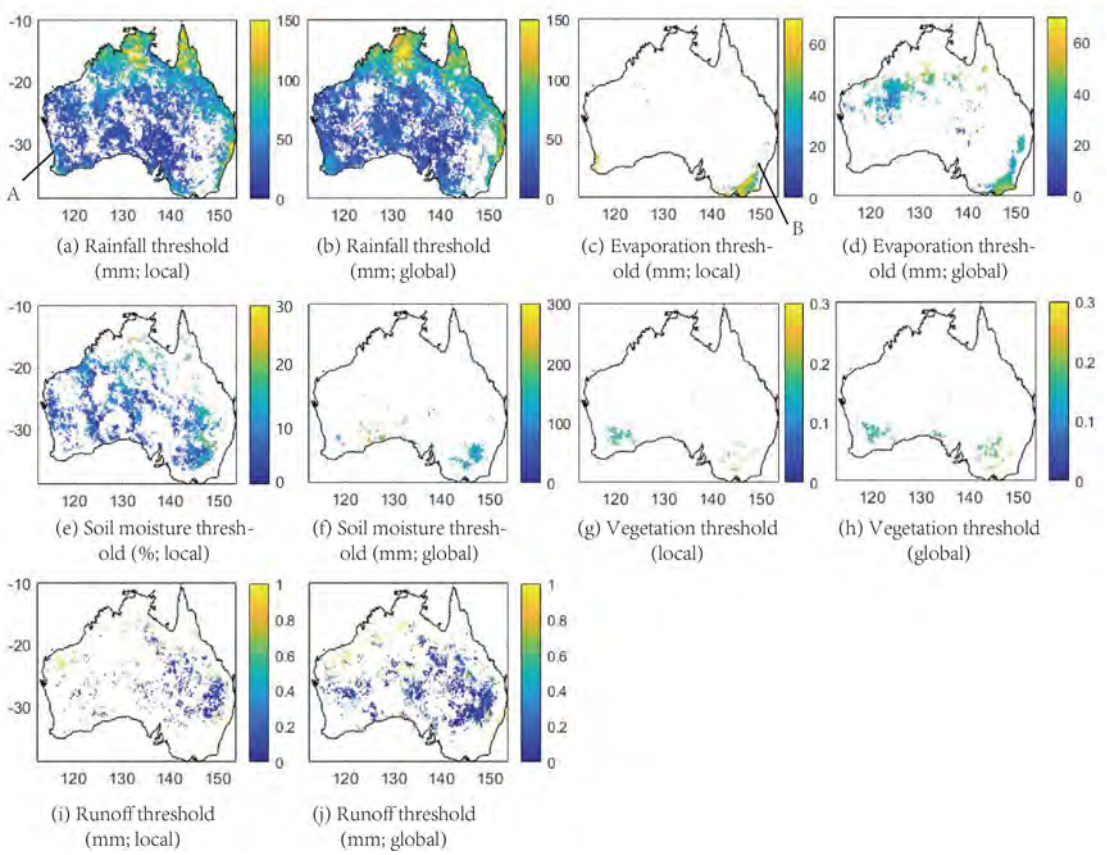

Figure 7: The specific threshold values (monthly based) of each primary condition in the CART model. Note that when a new value above the rainfall (a-b), soil moisture (e-f), vegetation (g-h) and runoff (i-j) thresholds or below the evaporation (c-d) threshold is input into the CART model, the model will classify the groundwater as recharge, vice versa. A and B in (a) and (c) are selected pixels for showing the structure of trees in Fig **??**.

The pixel illustrated in the southeastern part of Australia (Fig 8b) is much more complex than the pixel in the southwestern part of Australia, which involves four threshold conditions: evaporation, rainfall, runoff, and soil moisture. Evaporation in this pixel is the primary threshold condition that determines whether groundwater recharges or not. At this stage, only using evaporation, the classification accuracy is around 65%. However, if the complete tree that also includes the rainfall (31.65 mm and 83.65 mm), runoff (3.57 mm) and soil moisture (9.4%) thresholds is used, the classification accuracy improves to 83%. For this pixel, RF has the same

ranking results as CART in terms of evaporation and rainfall for most of tests according to MDA, however, the ranking results of soil moisture and runoff is unstable. This is also likely due to the influence of random sampling, where such influence seems more obvious on those threshold conditions that are less important. Therefore, non-primary threshold conditions and their corresponding values may not be reliable.

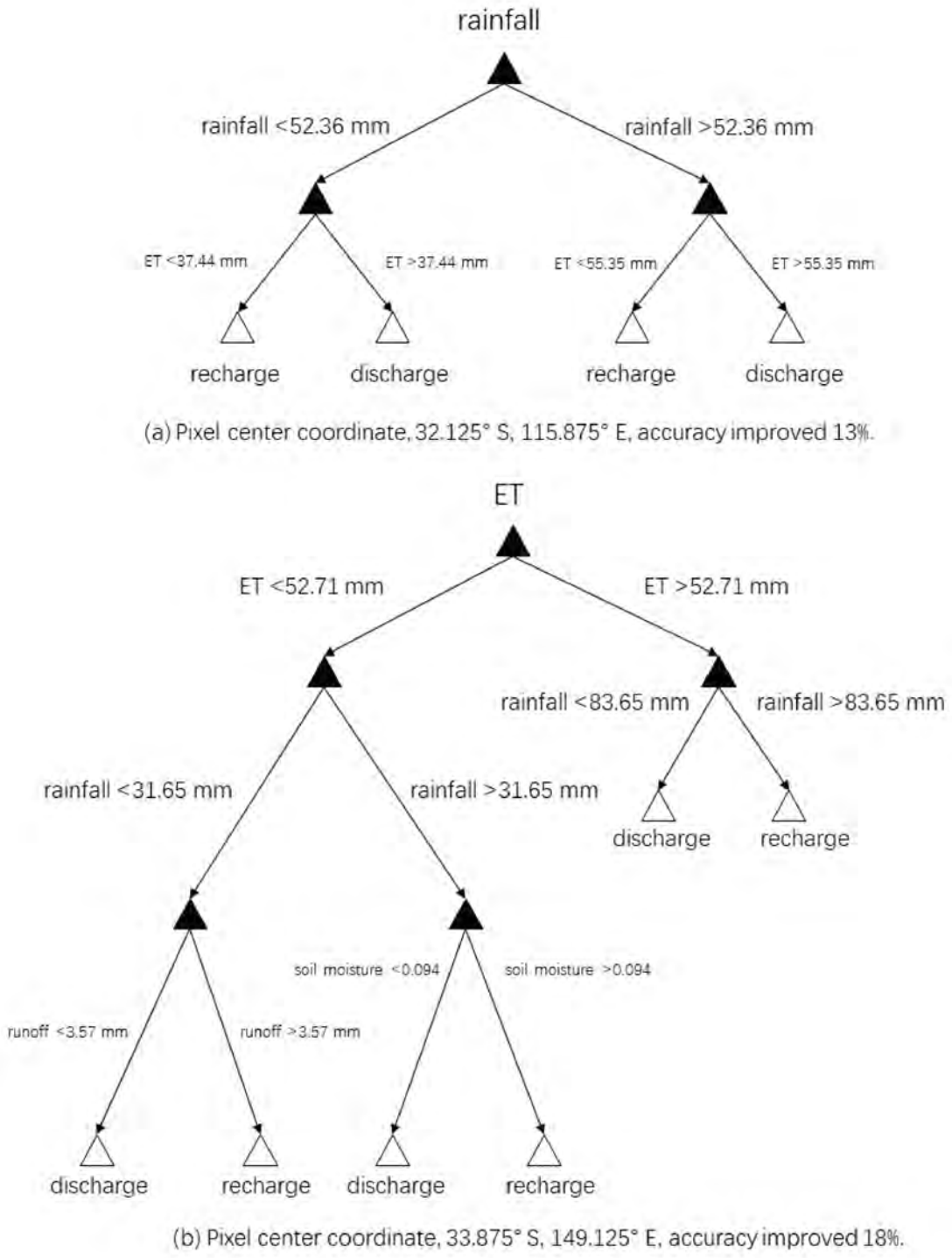

Figure 8: Illustration of the tree structures for two random pixels (local CART) in the southwestern (a) and southeastern (b) parts of Australia (see positions A and B in Figs 7a and c, respectively). 'ET' represents the evaporation. The significantly increased accuracy of the CART's one to five maximum splits indicates that the groundwater recharges in these two pixels are controlled by multiple condition variables.

4. Discussion

4.1. Inferring groundwater recharge mechanism (shallow aquifer) through threshold conditions

Section 3.3 has shown the results of groundwater threshold conditions and their importance ranking (mostly for primary threshold conditions). By analysing this result and combining it with some simple hydrogeological knowledge as shown in Fig 9, the groundwater recharge mechanism can be inferred.

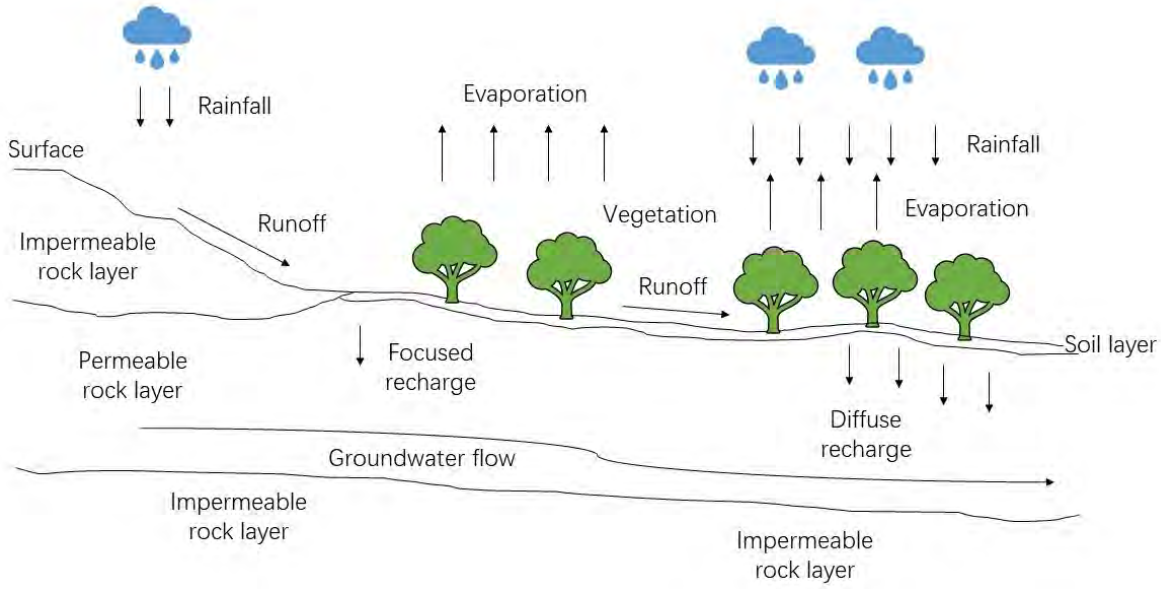

Figure 9: A simple illustration of land hydrological cycle.

Figure 9 is a simple illustration of the land hydrological cycle. One can see that rainfall as the major input of the land water cycle is very important to groundwater recharge. Some studies, e.g., *Jones and Banner* (2003) directly define the groundwater recharge threshold as the amount of rainfall required to recharge an aquifer. It can be said that without rainfall, there is no groundwater recharge. Although *Moeck et al.* (2020) and *Barron et al.* (2012) indicates that most studies have not been able to confidently confirm that rainfall is the major determinant of groundwater recharge on a large scale due to the lack of data, our results in Fig 6 and Fig 7, i.e., rainfall as the primary threshold condition covers 64-71% of the Australian continent, supports the validity of this idea. When rainfall is identified as the primary threshold condition, it could represent a direct recharge mechanism for the shallow aquifers within the pixel as well as an indication of variable rainfall or a clear seasonal pattern of rainfall. The greater

rainfall threshold may refer to a faster loss of groundwater due to evaporation or groundwater drainage, and to a larger amplitude of seasonal groundwater variations. The northern part of the Australian continent is a good example that has a tropical climate (clear seasonal rainfall during November-April; *Hu et al.* 2022b), high evaporation, and is almost fully covered by rainfall threshold conditions. According to *Knapton et al.* (2019), the groundwater level in Darwin (capital city of Northern Territory) changes rapidly during the recharge/discharge period and the variation could be over 10 meters for some boreholes.

According to *Moeck et al.* (2020) and Fig 9, evaporation, as the major output of the land water cycle, is another threshold condition that significantly affects groundwater recharge globally. However, in the case of the Australian continent (see Figs 6 and Fig 7), only a few regions show that evaporation is the primary threshold condition in terms of groundwater recharge. This is due to the fact that most parts of Australia are very dry and with sparse vegetation cover, so there is not much water for evaporation. Evaporation only occurs when rainfall arrives, thus, usually act as the second threshold condition after rainfall, as shown in Fig 8a. When evaporation is identified as the primary threshold condition, it potentially infers a relative constant monthly rainfall that generates a relatively constant groundwater input, and thus, groundwater recharge depends largely on the variation of evaporation (output). According to *Johnson* (1992) and *Hu et al.* (2022a), the southeastern part of the Australian continent indicated by both local and global results in Figs 6c and d, has uniform monthly rainfall. The evaporation there is low during winter, e.g., average below 30 mm in July, and high in summer, e.g., average 90-100 mm in January (see official statistics: `http://www.bom.gov.au/jsp/ncc/climate_averages/evapotranspiration`).

Soil moisture and runoff are related conditions of rainfall; thus, they are usually discussed together (*Alvarez-Garreton et al.*, 2014; *Wasko and Nathan*, 2019). From Fig 9, one can see that rainfall need to penetrate the soil and then, can become groundwater. Thus, soil moisture as the primary condition indicates the diffuse recharge, and represents a threshold of hydraulic power (*Zhang et al.*, 1999). In other words, the soil moisture must reach a certain capacity to allow the water in the soil to pass down and become groundwater. This process relates to soil structure, thickness, and soil properties, which is complex and hardly represented by a percentage or storage volume. Thus, it is difficult to judge which is more representative in the local or global result since they are very different (see Figs 7e and f). Unlike soil moisture, rainfall and

evaporation, runoff are usually less discussed in relation to groundwater, because runoff is not obvious in some flat regions, e.g., arid or semi-arid areas, while runoff in mountainous regions is complex (*Chiew et al.*, 2009; *Petheram et al.*, 2012; *Silberstein et al.*, 2012). When runoff is identified as the primary threshold condition, it indicates that groundwater recharges when runoff appears and thus, may refer to focused recharge mechanism.

Vegetation can have both positive and negative relationships with groundwater recharge on a global scale (*Koirala et al.*, 2017). This indicates that vegetation can help recharge groundwater on the one hand and prevent its recharge on the other hand. The main role of vegetation in helping groundwater recharge is to retain surface water and soil water. Spreading branches and leaves can also reduce evaporation (see Fig 9). However, the roots of vegetation need to absorb groundwater to grow or sustain life, and as such, to some extent, they also consume groundwater. In our case, Figs 7g and h both indicate that some southwestern (Kalgoorlie) and southeastern (Mungo) parts of the Australian continent are covered by vegetation threshold condition. All the classifications above the vegetation threshold are groundwater recharge. This indicates that vegetation shows the function of helping groundwater recharge in these regions. Although the detail mechanism is not clear, we found that these two parts of regions both have many scattered lakes and are surrounded by massive vegetation, this possibly indicates that vegetation is important in maintaining groundwater level in wetlands.

For inference of multiple threshold conditions in southeastern and southwestern parts of the Australian continent (see, e.g., A and B in Fig 3d), it requires the inspection of the tree due to the fact that each pixel has a different structure of the tree as shown in Fig 8. Here, Fig 8b is used as an example for inferring the groundwater recharge mechanism. First, evaporation as the primary and rainfall as the secondary threshold conditions is because of the little seasonality of rainfall and strong seasonality of evaporation in southeastern Australia (see pixel location in Fig 7b). If the evaporation is high (above 52.71 mm; usually occurs in summer), then the groundwater recharge depends on rainfall amount. If the monthly rainfall is above 83.65 mm, then, groundwater will recharge, vice versa. Under this scenario, the groundwater recharge in this pixel only depends on the balance of rainfall and evaporation, showing a direct recharge mechanism. When the evaporation (below 52.71 mm; usually occurs in winter) and rainfall (below 31.65 mm) are both low, the groundwater recharge depends on the runoff flowing from other regions (recharge when runoff above 3.57 mm). When evaporation is low (below 52.71 mm)

but there are some rainfall (above 31.65 mm) in this pixel, the groundwater recharge depends on if soil moisture has enough hydrological power to penetrate the soil, which associates with rainfall intensity and soil structure.

Finally, note that for the same machine learning classification using different data, the results are still going to be different, see, e.g., Figs 6 and 7, and as such, the inference of groundwater recharge mechanism will be different. The possible reason is likely to be the different ways of building models. At this moment, the reliability of results depends on the classification accuracy of models. For example, our results (Figs 3, 4 and 5) show that the classifications using Australian local products have better accuracy in the middle inland areas, while global products have better accuracy in the southeastern and southwestern parts of the Australian continent. Thus, for the middle inland areas and the southeastern and southwestern parts of the Australian continent, we should use the models trained from Australian local and GLDAS global products to infer groundwater recharge mechanism, respectively.

4.2. Strength, limitations and future direction

4.2.1. Strength

This study offers a possible solution to quantify groundwater recharge threshold conditions at a large scale using machine learning classification. To the best of the authors' efforts, no previous study has ever done this topic, and our study is the first attempt. By using and comparing three different machine learning classification methods (CART as core, RF and LR as supplements), the results offer the specific threshold values for multiple conditions spatially with an average accuracy of 76% at least. Meanwhile, the results also provide a ranking of importance for multiple threshold conditions so that the groundwater recharge mechanisms in different areas are able to be inferred. More importantly, in section 4.1, we show that the inferred groundwater recharge mechanism matches with the physical reality to some extent. This proves the potential of using machine learning techniques to interpret groundwater recharge mechanism, i.e., cheap, fast, and do not require geological investigation and isotopic knowledge compared to traditional physical measurement.

4.2.2. Limitations and future works

This is the first attempt to quantify groundwater threshold condition at a large scale using machine learning techniques. Although, the possibility using machine learning classification for such task is well explored, substantial work is required to address the current limitations presented in this manuscript.

(i) The reliability of the results as the study is attempting to reproduce model-simulated recharge, rather than 'real' recharge. Despite the fact that the results showing some consistency with physical reality as shown in Section 4.1, the reliability of the results still lacks confidence due to the fact that most of the training data are simulated (e.g., groundwater) rather than real observation (e.g., vegetation). For example, according to *Li et al.* (2019) and *Hu et al.* (2022b), GLDAS-DA products for groundwater may not be reliable in central Australia since it has not been validated there. To address this issue, as many real observational products from the field should be collected as possible. However, this is very difficult, considering the expensive cost and time of building borehole networks in a large scale. Picking some regional areas that have sufficient data for validation could be a possible solution.

(ii) Lag issue. As mentioned in Section 2.6, this study does not consider lags between rainfall, groundwater and soil moisture. In future studies, we will try to replace models with real observation data, as well as taking lag into consideration when building the machine learning model so that the results will be closer to 'reality'. Lags between groundwater and other parameters such as vegetation will also be tested in future studies.

(iii) Different threshold values may have different recharge mechanisms. In this manuscript, we only quantify the threshold conditions and their corresponding values to distinguish net groundwater recharge/discharge. However, considering the seepage in the unsaturated zone and the drainage of groundwater are nonlinear, the threshold conditions for groundwater recharge (level rise) over e.g., 10 mm, 20 mm and 30 mm may become different, and thus, requires multiple tests.

(iv) CART method. This study takes the CART as the core classification method, the RF and LR are employed to examine the classification accuracy and threshold condition importance ranking. As Table 2 shown below, CART as the only method that is able to

provide specific values of threshold conditions is believed as the most suitable path to quantify groundwater recharge threshold conditions on a large scale. The problem of CART, however, is the lower classification accuracy compared to other advanced classification techniques. Although, from the results of the Australian continent, the difference in average classification accuracy between CART, RF and LR (maximum 4% compared to LR; Table 2) is not obvious. For some specific pixels, the differences are over 10-20% (see Figs 4 and 5). Thus, some improvements are required for CART method, e.g., *Wijaya and Bisri* (2016) presented an approach that uses LR to reduce the data noise and improves the classification accuracy of CART.

Table 2: Summary of features for the CART, RF, and LR methods.

Features/Methods	CART	RF	LR
Classification Accuracy (Australian continent)	76%	77-78%	79-80%
Computation time	10-12 Minutes	2 Hours (10 trees)	50-55 Minutes
Ranking importance of threshold conditions	✓	✓	×
Specific threshold values	✓	×	×
Recharge mechanism interpretability	Easy	Hard	Hard

5. Conclusion

By exploring different machine learning classification techniques; CART, RF and LR, using the Australian continent as a case study area, the results prove that it is possible to quantify groundwater recharge threshold conditions in a large scale, as well as infer groundwater recharge mechanism, though, significant work is still required to improve the reliability of the results as such including real observation data, lag consideration etc. For the current result, it indicates that:

(i) The CART method classifies groundwater recharge/discharge with an average classification accuracy of 76%. This accuracy is consistent with other advanced machine learning methods: RF (77-78%) and LR (79-80%). More importantly, the CART indicates that a single (primary) condition is sufficient to classify groundwater recharge/discharge. Only the southeastern and southwestern parts of the Australian continent is dominated by multiple threshold conditions.

(ii) The CART method seems to correctly rank the importance of the primary threshold condition since it shows similar results to the RF method. The less important threshold conditions identified by CART may not be reliable since RF shows that these threshold conditions are easily affected by the influence of random sampling. This should be careful when inferring groundwater recharge mechanism for multiple threshold conditions.

(iii) The CART method is able to provide the spatial distribution of the monthly groundwater recharge threshold conditions (primary) and the specific values of each condition. Rainfall is the most primacy common threshold condition.

(iv) The groundwater recharge mechanism can be largely inferred through the primary threshold conditions and their corresponding values. For multiple threshold condition, the less/more splits may indicate simpler/more complex mechanisms. However, using different training data generates uncertainty of classification results. The inference of groundwater recharge mechanism, therefore, should rely on results with better classification accuracy or be treated cautiously.

Acknowledgment

Kexiang Hu is grateful for the CIPRS and Research Stipend Scholarship provided by Curtin University and the Australian Government Research Training Program (RTP) Stipend Scholarship that are supporting his PhD studies. The authors would like to thank the following organizations for providing the data used in this study: the Australia Bureau of Meteorology, and the National Aeronautics and Space Administration (NASA) Earth Data Centre.

Supplementary Material

Table 1: The prediction accuracy influence test for random forest; the effects from the number of trees and random sampling. The accuracy is tested separately on 10, 50 and 500 trees. For 500 trees, we tested the accuracy three more times to show the influence of random sampling. No obvious improvements of prediction accuracy are observed with the increasing number of trees.

Pixel No.	Pixel latitude	Pixel longitude	10 trees	50 trees	500 trees	500 trees	500 trees	500 trees
1	31.875°S	150.875°E	72.2%	71.9%	75.1%	74.0%	75.0%	71.9%
2	12.125°S	134.625°E	84.7%	85.8%	85.9%	85.9%	85.4%	84.4%
3	32.375°S	116.125°E	91.1%	91.1%	89.0%	89.1%	89.4%	88.5%
4	29.625°S	132.125°E	68.3%	65.5%	65.6%	67.8%	67.7%	68.2%
5	26.375°S	152.625°E	77.6%	77.6%	79.7%	79.2%	79.7%	79.2%
6	22.875°S	132.375°E	75.0%	78.6%	77.1%	79.2%	77.6%	75.5%
7	24.875°S	149.875°E	74.5%	74.0%	74.0%	73.4%	74.0%	72.9%
8	15.875°S	136.625°E	87.5%	85.4%	87.0%	87.5%	86.5%	87.5%
9	37.375°S	140.125°E	88.5%	89.1%	89.1%	89.1%	90.1%	89.1%
10	26.625°S	133.125°E	69.8%	68.2%	68.8%	68.2%	68.2%	70.3%

References

Adiat, K., B. Akeredolu, and G. Olayanju (2020), Application of logistic regression analysis in prediction of groundwater vulnerability in gold mining environment: a case of Ilesa gold mining area, southwestern, Nigeria, *Environmental Monitoring and Assessment*, *192*, 577, doi:10.1007/s10661-020-08532-7.

Ali, J., R. Khan, N. Ahmad, and I. Maqsood (2012), Random Forests and Decision Trees, *International Journal of Computer Science Issues*, *9*(3), 272–278, available on: https://citeseerx.ist.psu.edu/viewdoc/download?doi=10.1.1.402.3863&rep=rep1&type=pdf.

Alvarez-Garreton, C., D. Ryu, A. Western, W. Crow, and D. Robertson (2014), The impacts of assimilating satellite soil moisture into a rainfall–runoff model in a semi-arid catchment, *Journal of Hydrology*, *519*, 2763–2774, doi:10.1016/j.jhydrol.2014.07.041.

Awange, J., B. Palancz, and L. Völgyesi (2020), *Hybrid Imaging and Visualization, Employing Machine Learning with Mathematica - Python*, 1 ed., Springer International Publishing, doi:10.1007/978-3-030-26153-5.

Baker, A., R. Berthelin, M. Cuthbert, P. Treble, A. Hartmann, and the KSS Cave Studies Team (2020), Rainfall recharge thresholds in a subtropical climate determined using a regional cave drip water monitoring network, *Journal of Hydrology*, *587*, 125,001, doi:10.1016/j.jhydrol.2020.125001.

Barron, O., R. Crosbie, W. Dawes, S. Charles, T. Pickett, and M. Donn (2012), Climatic controls on diffuse groundwater recharge across Australia, *Hydrological Earth System Science*, *16*, 4557–4570, doi:10.5194/hess-16-4557-2012.

Beaudoing, H., M. Rodell, and NASA/GSFC/HSL (2020), GLDAS Noah Land Surface Model L4 3 hourly 0.25 x 0.25 degree V2.1, *Data*, Goddard Earth Sciences Data and Information Services Center (GES DISC), Greenbelt, Maryland, USA, accessed: 2021 July 3.

Belgiu, M., and L. Drăgut (2016), Random forest in remote sensing: A review of applications and future directions, *ISPRS Journal of Photogrammetry and Remote Sensing*, *114*, 24–31, doi:10.1016/j.isprsjprs.2016.01.011.

Breiman, L. (2001), Random Forests, *Machine Learning*, *45*, 5–32.

636 Breiman, L., J. Friedman, R. Olshen, and C. Stone (1984), Classification and Regression Trees,
637 *Boca Raton, FL: CRC Press*.

638 Carroll, R., J. Deems, R. Niswonger, R. Schumer, and K. Williams (2019), The Importance of
639 Interflow to Groundwater Recharge in a Snowmelt-Dominated Headwater Basin, *Geophysical*
640 *Research Letters*, *46*, 5899–5908, doi:10.1029/2019GL082447.

641 Chiew, F., J. Teng, J. Vaze, D. Post, J. Perraud, D. Kirnon, and N. Viney (2009), Es-
642 timating climate change impact on runoff across southeast Australia: Method, results,
643 and implications of the modeling method, *Water Resources Research*, *45*(10), W10,414,
644 doi:10.1029/2008WR007338.

645 Deschamps, B., H. McNairn, J. Shang, and X. Jiao (2012), Towards operational radar-only crop
646 type classification: comparison of a traditional decision tree with a random forest classifier,
647 *Canadian Journal of Remote Sensing*, *38*, 60–68, doi:10.5589/m12-012.

648 Didan, K. (2015), MOD13C2 MODIS/Terra Vegetation Indices Monthly L3 Global 0.05Deg
649 CMG V006, *Data set*, NASA EOSDIS Land Processes DAAC, accessed 2021-04-15 from
650 https://doi.org/10.5067/MODIS/MOD13C2.006.

651 Diodato, N., and M. Ceccarelli (2006), Computational uncertainty analysis of groundwater
652 recharge in catchment, *Ecological Informatics*, *1*, 377–389, doi:10.1016/j.ecoinf.2006.02.003.

653 Dixon, B. (2009), A case study using support vector machines, neural networks and logistic
654 regression in a GIS to identify wells contaminated with nitrate-N, *Hydrogeology Journal*, *17*,
655 1507–1520, doi:10.1007/s10040-009-0451-1.

656 Du, P., A. Samat, B. Waske, S. Liu, and Z. Li (2015), Random Forest and Rotation Forest for
657 fully polarized SAR image classification using polarimetric and spatial features, *ISPRS Jour-*
658 *nal of Photogrammetry and Remote Sensing*, *105*, 38–53, doi:10.1016/j.isprsjprs.2015.03.002.

659 Elliott, L., and L. Owens (2015), CART analysis of environmental factors, biomarkers and gill-
660 associated virus to predict production outcomes for farmed Penaeus monodon, *Aquaculture*,
661 *448*, 298–305, doi:10.1016/j.aquaculture.2015.05.006.

662 Frost, A., and D. Wright (2018), Evaluation of the Australian Landscape Water Balance model
663 (AWRA-L v6): Comparison of AWRA-L v6 against Observed Hydrological Data and Peer
664 Models, *Technical report*, Bureau of Meteorology.

Frost, A., A. Ramchum, and A. Smth (2018), The Australian Landscape Water Balance model (AWRA-L v6). Technical Description of the Australian Water Resources Assessment Landscape model version 6, *Technical report*, Bureau of Meteorology.

Fu, G., R. Crosbie, O. Barron, S. Charles, W. Dawes, X. Shi, T. Niel, and C. Li (2019), Attributing variations of temporal and spatial groundwater recharge: A statistical analysis of climatic and non-climatic factors, *Journal of Hydrology*, *568*, 816–834, doi:10.1016/j.jhydrol.2018.11.022.

Fushiki, T. (2009), Estimation of prediction error by using K-fold cross-validation, *Statistics and Computing*, *21*, 137–146, doi:10.1007/s11222-009-9153-8.

Ghosh, A., F. Fassnacht, P. Joshi, and B. Koch (2014), A framework for mapping tree species combining hyperspectral and LiDAR data: Role of selected classifiers and sensor across three spatial scales, *International Journal of Applied Earth Observation and Geoinformation*, *26*, 49–63, doi:10.1016/j.jag.2013.05.017.

Gray, J., and G. Fan (2008), Classification tree analysis using TARGET, *Computational Statistics and Data Analysis*, *52*(3), 1362–1372, doi:10.1016/j.csda.2007.03.014.

Hu, K., J. Awange, Khandu, E. Forootan, R. Goncalves, and K. Fleming (2017), Hydrogeological characterisation of groundwater over Brazil using remotely sensed and model products, *Science of The Total Environment*, *599-600*, 372–386, doi:10.1016/j.scitotenv.2017.04.188.

Hu, K., J. Awange, M. Kuhn, and A. Saleem (2019), Spatio-temporal groundwater variations associated with climatic and anthropogenic impacts in South-West Western Australia, *Science of The Total Environment*, *696*, 133,599, doi:10.1016/j.scitotenv.2019.133599.

Hu, K., J. Awange, M. Kuhn, and J. Nanteza (2021), Inference of the spatio-temporal variability and storage potential of groundwater in data-deficient regions through groundwater models and inversion of impact factors on groundwater, as exemplified by the Lake Victoria Basin, *Science of The Total Environment*, *800*, 149,355, doi:10.1016/j.scitotenv.2021.149355.

Hu, K., J. Awange, and M. Kuhn (2022a), Testing a knowledge-based approach for inferring spatio-temporal characteristics of groundwater in the Australian State of Victoria, *Science of The Total Environment*, p. 153113, doi:10.1016/j.scitotenv.2022.153113, in press.

693 Hu, K., J. Awange, M. Kuhn, and A. Zerihun (2022b), Irrigated agriculture poten-
694 tial of Australia's northern territory inferred from spatial assessment of groundwater
695 availability and crop evapotranspiration, *Agricultural Water Management*, *264*, 107,466,
696 doi:10.1016/j.agwat.2022.107466.

697 Johnson, K. (1992), The AUSMAP Atlas of Australia, *Map*, Cambridge University Press &
698 Australian Surveying and Land Information Group (AUSLIG), Cambridge, UK/Melbourne,
699 Australia.

700 Jones, I., and J. Banner (2003), Estimating recharge thresholds in tropical karst island aquifers:
701 Barbados, Puerto Rico and Guam, *Journal of Hydrology*, *278*, 131–143, doi:10.1016/S0022-
702 1694(03)00138-0.

703 Knapton, A., D. Page, J. Vanderzalm, D. Gonzalez, K. Barry, A. Taylor, N. Horner, C. Chilcott,
704 and C. Petheram (2019), Managed Aquifer Recharge as a Strategic Storage and Ur-
705 ban Water Management Tool in Darwin, Northern Territory, Australia, *Water*, *11*, 1869,
706 doi:10.3390/w11091869.

707 Koirala, S., M. Jung, M. Reichstein, I. de Graaf, G. Campus-Valls, K. Ichii, D. Papale,
708 B. Ráduly, C. Schwalm, G. Tramontana, and N. Carvalhais (2017), Global distribution of
709 groundwater-vegetation spatial covariation, *Geophysical Research Letters*, *44*(9), 4134–4142,
710 doi:10.1002/2017GL072885.

711 Kotchoni, D., J. Vouillamoz, F. Lawson, P. Adjomayi, M. Boukari, and R. Taylor (2019), Rela-
712 tionships between rainfall and groundwater recharge in seasonally humid Benin: a compara-
713 tive analysis of long-term hydrographs in sedimentary and crystalline aquifers, *Hydrogeology*
714 *Journal*, *27*, 447–457, doi:10.1007/s10040-018-1806-2.

715 Li, B., M. Rodell, S. Kumar, H. Beaudoing, A. Getirana, B. Zaitchik, and et al. (2019), Global
716 GRACE Data Assimilation for groundwater and Drought Monitoring: Advances and Chal-
717 lenges, *Water Resources Research*, *55*, 7564–7586, doi:10.1029/2018WR024618.

718 Long, W., J. Griffith, H. Selker, and R. D'Agostino (1993), A Comparison of Logistic Regression
719 to Decision-Tree Induction in a Medical Domain, *Computers and Biomedical Research*, *26*,
720 74–97, doi:10.1006/cbmr.1993.1005.

721 Mahmood, Z., and S. Khan (2009), On the Use of K-Fold Cross-Validation to Choose Cut-
722 off Values and Assess the Performance of Predictive Models in Stepwise Regression, *The*
723 *International Journal of Biostatistics*, *5*, doi:10.2202/1557-4679.1105, article 25.

724 Maxwell, A., T. Warner, and F. Fang (2018), Implementation of machine-learning classification
725 in remote sensing: an applied review, *International Journal of Remote Sensing*, *39*, 2784–
726 2817, doi:10.1080/01431161.2018.1433343.

727 Miao, X., J. Heaton, S. Zheng, D. Charlet, and Liu (2011), Applying tree-based en-
728 semble algorithms to the classification of ecological zones using multi-temporal multi-
729 source remote-sensing data, *International Journal of Remote Sensing*, *33*(6), 1823–1849,
730 doi:10.1080/01431161.2011.602651.

731 Moeck, C., N. Grech-Cumbo, J. Podgorski, A. Bretzler, J. Gurdak, M. Berg, and M. Schirmer
732 (2020), A global-scale dataset of direct natural groundwater recharge rates: A review of
733 variables, processes and relationships, *Science of the Total Environment*, *717*, 137,042,
734 doi:10.1016/j.scitotenv.2020.137042.

735 Motiee, H., and E. McBean (2017), Assessment of Climate Change Impacts on Groundwater
736 Recharge for Different Soil Types-Guelph Region in Grand River Basin, Canada, *Ecopersia*,
737 *5*(2), 1731–1744, doi:10.18869/MODARES.ECOPERSIA.5.2.1731.

738 Petheram, C., P. Rustomji, F. Chiew, and J. Vleeshouwer (2012), Rainfall–runoff modelling
739 in northern Australia: A guide to modelling strategies in the tropics, *Journal of Hydrology*,
740 *462-463*, 28–41, doi:10.1016/j.jhydrol.2011.12.046.

741 Pregibon, D. (1981), Logistic Regression Diagnostics, *The Annals of Statistics*, *9*, 705–724,
742 doi:10.1214/aos/1176345513.

743 Ramezan, C., T. Warner, and A. Maxwell (2019), Evaluation of Sampling and Cross-Validation
744 Tuning Strategies for Regional-Scale Machine Learning Classification, *Remote Sensing*, *11*,
745 185, doi:10.3390/rs11020185.

746 Rodell, M., P. R. Houser, U. Jambor, J. Gottschalck, and et al. (2004), The global land
747 data assimilation system, *Bulletin of the American Meteorological Society*, *85*, 381–394,
748 doi:10.1175/BAMS-85-3-381.

749 Rodriguez, J., A. Perez, and J. Lozano (2010), Sensitivity Analysis of k-Fold Cross Valida-
750 tion in Prediction Error Estimation, *IEEE Transactions on Pattern Analysis and Machine*
751 *Intelligence*, *32*(3), 569–575, doi:10.1109/TPAMI.2009.187.

752 Rui, H., and H. Beaudoing (2019), README Document for NASA GLDAS Version 2 Data
753 Products, *Report*, National Aeronautics and Space Administration Goddard Earth Science
754 Data Information and Services Center.

755 Sandri, M., and P. Zuccolotto (2008), A Bias Correction Algorithm for the Gini Variable Im-
756 portance Measure in Classification Trees, *Journal of Computational and Graphical Statistics*,
757 *17*(3), 611–628, doi:10.1198/106186008X344522.

758 Silberstein, R., S. Aryal, J. Durrant, M. Pearcey, M. Braccia, S. Charles, L. Boniecka, G. Hodg-
759 son, M. Bari, N. Viney, and D. McFarlane (2012), Climate change and runoff in south-western
760 Australia, *Journal of Hydrology*, *475*, 441–455, doi:10.1016/j.jhydrol.2012.02.009.

761 Small, E. (2005), Climatic controls on diffuse groundwater recharge in semiarid envi-
762 ronments of the southwestern United States, *Water Resources Research*, *41*, W04,012,
763 doi:10.1029/2004WR003193.

764 Song, Y., and Y. Lu (2015), Decision tree methods: applications for classification and prediction,
765 *Shanghai Arch Psychiatry*, *27*(2), 130–135, doi:10.11919/j.issn.1002-0829.215044.

766 Von Freyberg, J., C. Moeck, and M. Schirmer (2015), Estimation of groundwater recharge
767 and drought severity with varying model complexity, *Journal of Hydrology*, *527*, 844–857,
768 doi:10.1016/j.jhydrol.2015.05.025.

769 Wasko, C., and R. Nathan (2019), Influence of changes in rainfall and soil moisture on trends
770 in flooding, *Journal of Hydrology*, *575*, 432–441, doi:10.1016/j.jhydrol.2019.05.054.

771 Wijaya, A., and A. Bisri (2016), Hybrid Decision Tree and Logistic Regression Classifier for
772 Email Spam Detection, in *2016 8th International Conference on Information Technology and*
773 *Electrical Engineering (ICITEE)*, pp. 1–4, doi:10.1109/ICITEED.2016.7863267.

774 Wu, W., A. Li, X. He, R. Ma, H. Liu, and J. Lv (2018), A comparison of support
775 vector machines, artificial neural network and classification tree for identifying soil tex-
776 ture classes in southwest China, *Computers and Electronics in Agriculture*, *144*, 86–93,
777 doi:10.1016/j.compag.2017.11.037.

778 Xu, L., H. Du, and X. Zhang (2021), A classification approach for urban metabolism us-
779 ing the CART model and its application in China, *Ecological Indiicators*, *123*, 107,345,
780 doi:10.1016/j.ecolind.2021.107345.

781 Yang, H., F. Wei, Z. Ma, H. Guo, P. Su, and S. Zhang (2019), Rainfall threshold for landslide
782 activity in Dazhou, southwest China, *Landslides*, *17*, 61–77, doi:10.1007/s10346-019-01270-z.

783 Yin, W., Z. Fan, N. Tangdamrongsub, L. Hu, and M. Zhang (2021), Comparison of physical
784 and data-driven models to forecast groundwater level changes with the inclusion of GRACE
785 – A case study over the state of Victoria, Australia, *Journal of Hydrology*, *602*, 126,735,
786 doi:10.1016/j.jhydrol.2021.126735.

787 Yu, H., and Y. Lin (2015), Analysis of space–time non-stationary patterns of rain-
788 fall–groundwater interactions by integrating empirical orthogonal function and cross wavelet
789 transform methods, *Journal of Hydrology*, *525*, 585–597, doi:10.1016/j.jhydrol.2015.03.057.

790 Zhang, L., W. Dawes, T. Hatton, P. Reece, G. Beale, and I. Packer (1999), Estimation of
791 soil moisture and groundwater recharge using the TOPOG_IRM model, *Water Resources*
792 *Research*, *35*(1), 149–161, doi:10.1029/98WR01616.

793 Zheng, H., L. Chen, X. Han, X. Zhao, and Y. Ma (2009), Classification and regression tree
794 (CART) for analysis of soybean yield variability among fields in Northeast China: The im-
795 portance of phosphorus application rates under drought conditions, *Agriculture, Ecosystems*
796 *and Environment*, *132*(1-2), 98–105, doi:10.1175/BAMS-85-3-381.

Chapter 6
Conclusion and future outlook

6.1 Conclusion

This thesis considers different groundwater issues in Australia through understanding of the groundwater spatio-temporal variability in relation to hydroclimate and hydrogeology. Special focuses were put on the groundwater decline issue in Western Australia, the irrigated agriculture issue in the Northern Territory, the lack of a way to provide reliable groundwater spatio-temporal information, and the missing information of groundwater recharge threshold conditions across the Australian continent. The following summarises the main outcomes of the thesis, which, to the best of the author's knowledge, are important and novel academic contributions.

- The decline of groundwater levels in south-west Western Australia poses a serious threat to society and the environment. To this end, the spatio-temporal groundwater behaviours, e.g. long-term annual and seasonal variation, and monthly spatial patterns, are organised from 2,997 boreholes in order to investigate the climate change and anthropogenic impacts on groundwater. The decline of groundwater levels is found to be obvious after 2000, occurring in the northern and southern parts around Perth, where groundwater extraction frequently happens. Compared to the continued decline in groundwater, rainfall after 2000 has kept a steady annual trend, suggesting that human exploitation has a greater impact on the dropping groundwater level than does climate change. Although other studies indicate that the decline of rainfall after 1975 is one of the causes leading to groundwater decline, the results, however, show a relatively stable groundwater level for the 1980-2000 period. From the perspective of spatial patterns, groundwater has a quick response to rainfall, recharging mainly between May to August/September. Some regions show a clear lag between rainfall and groundwater, e.g. 2 months in the northern parts of Perth, and some regions reflect the fact that rainfall needs to exceed a certain threshold to recharge groundwater, e.g. 60 mm/month in the southern parts of Perth. Additionally, the groundwater behaviours in the coastal plain are different from those in mountainous regions, most likely due to topographical and geological impacts. Overall, anthropogenic impact is the primary reason for groundwater decline, while climate change mainly controls the timing of groundwater variation with less influence on groundwater decline.

- Agricultural water use in the Northern Territory almost entirely relies on groundwater. The government is concerned that the available groundwater resource is unable to meet the requirement of irrigated agricultural

expansion due to the fact that the information on irrigated agricultural potential is insufficient. To address this issue, the groundwater availability and crop water demand are estimated under two scenarios, i.e. average condition (2010-2019) and dry condition (2019; the lowest annual rainfall since 1961). Melon, maize and citrus crops are selected as representatives of short, medium and high water use crops. The balance between groundwater availability and crop water demand is estimated for every 60,000 hectares (the spatial resolution). The results under average 2010-2019 conditions show that the northern parts of the Northern Territory have the most irrigated agricultural potential for expansion, with groundwater availability capable of supporting 15.7%/9.1%/5.8% per 60,000 hectares for the growths of melons, maize and citrus, respectively. For the central and southern parts, these values are only about 4.6%/3.3%/1.6% and 0.6%/0.6%/0.1%, respectively. Under 2019 dry condition, the above numbers basically reduced by 1/3, indicating the sensitivity of agricultural potential to climate extremes. Therefore, large-scale intensive agricultural expansion is not suggested, and regional-scale intensive agricultural expansion should be carefully considered due to the risk of climatic extremes.

- Many parts of Australia are currently facing a lack of groundwater spatio-temporal information, which hinders the development and management of groundwater resources. Considering the cost of building a borehole network, the coarse spatial resolution of GRACE, and the uncertainty from hydrological models, a knowledge-based approach is proposed for quickly and reliably obtaining groundwater spatio-temporal information without actual groundwater monitoring data. The main principle of this approach is to use the inversion analysis of groundwater impact factors, such as climate, topography and geology, to validate the performance of hydrological models. In other words, the inversion analysis replaces the function of borehole observations. With this approach proposed in a data-deficient region, e.g. Lake Victoria Basin (Africa), and tested in a data-rich region, e.g. the Australian State of Victoria, its reliability is proven since both results in the two studies indicate that such an approach is able to correctly reflect the groundwater spatial storage potential and temporal changes. More importantly, this approach can be applied to a variety of different regions around the world by adjusting the model, climate, topographic and geological data used.

- Groundwater recharge threshold conditions provide useful information for groundwater plan adaption; nevertheless, the topic has seldom been discussed in Australia, possibly due to the difficulty of handling big data and multiple relationships between factors and groundwater. Machine learning, for its power in handling big data and multiple relationships, is therefore employed to quantify the groundwater threshold conditions across the Australian continent. Among all the machine learning techniques, classification and regression tree is an ideal method by which to

quantify the groundwater recharge threshold since it is easy to interpret. However, models trained with this approach are often criticised for not being as accurate in their predictions as are other advanced methods, e.g. random forest and logistical regression. Therefore, the results of the three machine learning techniques, i.e. classification and regression tree, random forest, and logistical regression, for groundwater recharge threshold quantification are compared. Overall, the three methods obtained similar average prediction accuracies, with 76% for classification and regression tree, 77-78% for the random forest, and 79-80% for logistical regression. Apart from the prediction accuracy, the classification and regression tree method has the advantages of fast training and is the only method providing specific threshold values for every condition. Based on this, the spatial distribution of the primary threshold condition, and its corresponding maps of values are provided using the classification and regression tree method. It is worth noting that the performance of the model can vary greatly, depending on the choice of data, e.g. the primary threshold condition and threshold values could change if different datasets such as rainfall are selected for training. Therefore, when using the classification and regression tree method to quantify groundwater recharge thresholds, we recommend using multiple datasets to train different models and to compare their performance in order to assess the uncertainty of the results.

6.2 Future outlook

Despite the significant efforts of this thesis, understanding groundwater in Australia is a complex topic that requires further work. From the author's point of view, the outlook for the future should be in the following aspects:

- Improve the observational data. Currently, a major problem in this thesis is that the groundwater data are heavily model-dependent, and thus, have uncertainties and cannot be verified in many regions without in-situ data. Considering the expensive cost of building the in-situ networks, GRACE seems to be the only observational data that can be used on a large scale. However, the coarse spatial resolution of GRACE makes it difficult to capture small hydrological signals and interpret them with local hydrogeological features. Hence, possible ways such as the improved K(a)-band ranging (KBR) and laser ranging instrument (LRI) data processing, spatial downscaling using hydrogeological data, machine learning or artificial intelligence techniques, are helpful for describing more detailed spatio-temporal groundwater characteristics in the future.

- More focuses on median and deep aquifers. Currently, shallow aquifers with rainfall direct recharge are frequently discussed. However, in some arid or semi-arid regions, median and deep aquifers may be the only reliable water resource, e.g., Alice Springs in central Australia, thus,

requiring more attention. Investigating the recharge source, rate, and timing for these aquifers will be of great significance to groundwater sustainable development. This will require a detailed local hydrogeological investigation.

- Understanding the impact of geology on groundwater. Rocks as groundwater containers have a considerable impact on groundwater behaviour, nevertheless, few studies have carefully linked groundwater spatio-temporal behaviours to geology such as rock types, granule size, fracture development, confined or unconfined aquifers, water transmission between different rock layers, etc. Collecting borehole data, figuring out the geological layer and structure would be the key to this direction.

- Lag issues. Groundwater can be regarded as an infiltration process from rainfall to groundwater. During this process, lag issues are usually ignored in model establishment, e.g., water balance equation, or misunderstood, e.g., taking groundwater recharge threshold as the lag. Although, this thesis is aware of the above problems, it does not propose a suitable method to correctly quantify this lag. Using the combination of classification tree, linear regression, and correlation analysis could be a way to address this.

- Water contamination. Although the hydrochemical aspect is not within the scope of this thesis, its spatio-temporal information, such as how groundwater distribution and contamination changes spatially and temporally, is also important to inform groundwater quality management. To address this, field investigations such as water salinity testing and isotope tracking are required.

Bibliography

Adiat, K., M. Nawawi, and K. Abdullah (2012), Assessing the accuracy of GIS-based elementary multi criteria decision analysis as a spatial prediction tool – A case of predicting potential zones of sustainable groundwater resources, *Journal of Hydrology*, *400-441*, 75–89, doi:10.1016/j.jhydrol.2012.03.028.

Agutu, N., J. Awange, C. Ndehedehe, F. Kirimi, and M. Kuhn (2019), GRACE-derived groundwater changes over Greater Horn of Africa: Temporal variability and the potential for irrigated agriculture, *Science of The Total Environment*, *693*, 133,467, doi:10.1016/j.scitotenv.2019.07.273.

Ajami, H. (2021), *Encyclopedia of Geology*, vol. 6, chap. Geohydrology: Groundwater, pp. 408–415, United Kingdom: Academic Press, doi:10.1016/B978-0-12-409548-9.12388-7.

Ali, R., D. McFarlane, S. Varma, W. Dawes, I. Emelyanova, and G. Hodgson (2012), Potential climate change impacts on groundwater resources of south-western Austalia, *Journal of Hydrology*, *475*, 456–472, doi:10.1016/j.jhydrol.2012.04.043.

Allen, R., L. Pereira, D. Raes, and M. Smith (1998), Crop Evapotranspiration, *Guidelines for computing crop water requirements*, available online: http://www.fao.org/3/X0490E/x0490e00.htm#Contents.

Arye, G., J. Tarchitzky, and Y. Chen (2011), Treated wastewater effects on water repellency and soil hydraulic properties of soil aquifer treatment infiltration basins, *Journal of Hydrology*, *397*, 136–145, doi:10.1016/j.jhydrol.2010.11.046.

Ash, A., T. Gleeson, M. Hall, A. Higgins, G. Hopwood, N. MacLeod, D. Paini, P. Poultion, D. Prestwidge, T. Webster, and P. Wilson (2017), Irrigated agricultural development in northern Australia: Value-chain challenges and opportunities, *Agricultural Systems*, *155*, 116–125, doi:10.1016/j.agsy.2017.04.010.

Awange, J., M. Sharifi, O. Baur, W. Keller, W. Featherstone, and M. Kuhn (2009), GRACE hydrological monitoring of Australia: Current limitations and future prospects, *Science of The Total Environment*, *54*, 23–36, doi:10.1080/14498596.2009.9635164.

Awange, J., A. Saleem, S. Konneh, R. Goncalves, J. Kiema, and K. Hu (2018), Liberia's coastal erosion vulnerability and LULC change analysis: Post-civil war and Ebola epidemic, *Applied Geography*, *101*, 56–67, doi:10.1016/j.apgeog.2018.10.007.

Awange, J., K. Hu, and M. Khaki (2019a), The newly merged satellite remotely sensed, gauge and reanalysis-based Multi-Source Weighted-Ensemble Precipitation: Evaluation over Australia and Africa (1981–2016), *Science of The Total Environment*, *670*, 448–465, doi:10.1016/j.scitotenv.2019.03.148.

Awange, J., A. Saleem, R. Sukhadiya, Y. Ouma, and K. Hu (2019b), Physical dynamics of Lake Victoria over the past 34 years (1984-2018): Is the lake dying?, *Science of The Total Environment*, *658*, 199–218, doi:10.1016/j.scitotenv.2018.12.051.

Baker, A., R. Berthelin, M. Cuthbert, P. Treble, A. Hartmann, and the KSS Cave Studies Team (2020), Rainfall recharge thresholds in a subtropical climate determined using a regional cave drip water monitoring network, *Journal of Hydrology*, *587*, 125,001, doi:10.1016/j.jhydrol.2020.125001.

Barnett, S., N. Harringtom, P. Cook, and C. Simmons (2020), *Sustainable Groundwater Management*, chap. Groundwater in Australia: Occurrence and Management Issues, Global Issues in Water Policy, vol 24. Springer, Cham., doi:10.1007/978-3-030-32766-8_6.

Bekesi, G., M. McGuire, and D. Moiler (2009), Groundwater Allocation Using a Groundwater Level Response Management Method—Gnangara Groundwater System, Western Australia, *Water Resources Management*, *23*, 1665–1683, doi:10.1007/s11269-008-9346-5.

Belgiu, M., and L. Drăgut (2016), Random forest in remote sensing: A review of applications and future directions, *ISPRS Journal of Photogrammetry and Remote Sensing*, *114*, 24–31, doi:10.1016/j.isprsjprs.2016.01.011.

Bierkens, M., and Y. Wada (2019), Non-renewable groundwater use and groundwater depletion: a review, *Environmental Research Letters*, *14*, 063,002, doi:10.1002/app5.269.

Bithell, S., and S. Smith (2011), The method for estimating crop irrigation volumes for the tindall limestone aquifer, katherine, water allocation plan, *Technical bulletin no. 337*, Northern Territory Government, Australia, retrieve from https://catalogue.nla.gov.au/Record/5754886. File accessed: 18 Feb 2021.

Breiman, L. (2001), Random Forests, *Machine Learning*, *45*, 5–32.

Breiman, L., J. Friedman, R. Olshen, and C. Stone (1984), Classification and Regression Trees, *Boca Raton, FL: CRC Press.*

Bureau of Meteorology (2018), Water in Australia 2016-17, *Annual report*, Australain Government Bureau of Meteorology.

Bureau of Meteorology (2020a), Water in Australia 2018-19, *Annual report*, Australain Government Bureau of Meteorology.

Bureau of Meteorology (2020b), State of the Climate 2020, *Annual report*, Australain Government Bureau of Meteorology.

Bureau of Meteorology (2021), Water in Australia 2019-20, *Annual report*, Australain Government Bureau of Meteorology.

Cao, Y., Z. Nan, and G. Cheng (2015), GRACE Gravity Satellite Observations of Terrestrial Water Storage Changes for Drought Characterization in the Arid Land of Northwestern China, *Remote Sensing*, *7*(1), 1021–1047, doi: 10.3390/rs70101021.

Castellazzi, P., R. Martel, D. Galloway, L. Longuevergne, and A. Riversa (2016), Assessing Groundwater Depletion and Dynamics Using GRACE and InSAR: Potential and Limitations, *Groundwater*, *54*, 768–780, doi: 10.1111/gwat.12453.

Chen, J., J. Famigliett, B. Scanlon, and M. Rodell (2016a), *Remote Sensing and Water Resources*, chap. Groundwater Storage Changes: Present Status from GRACE Observations, Space Sciences Series of ISSI, vol 55. Springer, Cham, doi:10.1007/978-3-319-32449-4_9.

Chen, J., C. Wilson, B. Tapley, B. Scanlon, and A. Güntner (2016b), Long-term groundwater storage change in Victoria, Australia from satellite gravity and in situ observations, *Global and Planetary Change*, *139*, 56–65, doi: 10.1016/j.gloplacha.2016.01.002.

Chindarkar, N., and R. Grafton (2019), India's depleting groundwater: When science meets policy, *Asia & the Pacific Policy Studies*, *6*, 108–124, doi: 10.1002/app5.269.

Colloff, M. J., and J. Pittock (2022), Mind the Gap! Reconciling Environmental Water Requirements with Scarcity in the Murray–Darling Basin, Australia, *Water*, *14*(2), 208, doi:10.3390/w14020208.

Crosbie, R., J. McCallum, G. Walker, and F. Chiew (2010), Modelling climate-change impacts on groundwater recharge in the Murray-Darling Basin, Australia, *Hydrogeology Journal*, *18*, 1639–1656, doi:10.1007/s10040-010-0625-x.

Dalin, C., M. Taniguchi, and T. Green (2019), Unsustainable groundwater use for global food production and related international trade, *Global Sustainability*, *2*, E12, doi:10.1017/sus.2019.7.

Das, S. (2017), Delineation of groundwater potential zone in hard rock terrain in Gangajalghati block, Bankura district, India using remote sensing and GIS techniques, *Modeling Earth Systems and Environment*, *3*, 1589–1599, doi:10.1007/s40808-017-0396-7.

de Graaf, I., E. Sutanudjaja, L. van Beek, and M. Bierkens (2015), A high-resolution global-scale groundwater model, *Hydrology and Earth System Sciences*, *19*, 823–837, doi:10.5194/hess-19-823-2015.

Döll, P., H. Schmied, C. Schuh, F. Portmann, and A. Eicker (2014), Global-scale assessment of groundwater depletion and related groundwater abstractions: Combining hydrological modeling with information from well observations and GRACE satellites, *Water Resources Research*, *50*, 5698–5720, doi:10.1002/2014WR015595.

Feng, W., M. Zhong, J. Lemoine, R. Biancale, H. Hsu, and J. Xia (2013), Evaluation of groundwater depletion in North China using the Gravity Recovery and Climate Experiment (GRACE) data and ground-based measurements, *Water Resources Research*, *49*, 2110–2118, doi:10.1002/wrcr.20192.

Frappart, F., and G. Ramillien (2018), Monitoring Groundwater Storage Changes Using the Gravity Recovery and Climate Experiment (GRACE) Satellite Mission: A Review, *Remote Sensing*, *10*(6), 829, doi:10.3390/rs10060829.

Fu, G., R. Crosbie, O. Barron, S. Charles, W. Dawes, X. Shi, T. Niel, and C. Li (2019), Attributing variations of temporal and spatial groundwater recharge: A statistical analysis of climatic and non-climatic factors, *Journal of Hydrology*, *568*, 816–834, doi:10.1016/j.jhydrol.2018.11.022.

Garg, S., M. Motagh, J. Indu, and V. Karanam (2022), Tracking hidden crisis in India's capital from space: implications of unsustainable groundwater use, *Scientific Reports*, *12*, 651, doi:10.1038/s41598-021-04193-9.

Gleeson, T., J. VanderSteen, M. Sophocleous, M. Taniguchi, W. Alley, D. Allen, and Y. Zhou (2010), Groundwater sustainability strategies, *Nature Geoscience*, *3*, 378–379, doi:10.1038/ngeo881.

Gleeson, T., Y. Wada, M. Bierkens, and L. van Beek (2012), Water balance of global aquifers revealed by groundwater footprint, *Nature*, *488*, 197–200, doi:10.1038/nature11295.

Gonzalez, D., P. Dillon, D. Page, and J. Vanderzalm (2020), The Potential for Water Banking in Australia's Murray–Darling Basin to Increase Drought Resilience, *Water*, *12*(10), 2936, doi:10.3390/w12102936.

Grönwall, J., and K. Danert (2020), Regarding Groundwater and Drinking Water Access through A Human Rights Lens: Self-Supply as A Norm, *Water*, *12*(2), 419, doi:10.3390/w12020419.

Harrington, N., and P. Cook (2014), Groundwater in Australia, *Report*, National Centre for Groundwater Research and Training, Australia.

Hartfield, K., W. van Leeuwen, and J. Gillan (2020), Remotely Sensed Changes in Vegetation Cover Distribution and Groundwater along the Lower Gila River, *Land*, *9*(9), 326, doi:10.3390/land9090326.

Howard, K. (2014), Sustainable cities and the groundwater governance challenge, *Environmental Earth Sciences*, *73*, 2543–2554, doi:10.1007/s12665-014-3370-y.

Hu, A. J., K.X. and, M. Kuhn, and A. Saleem (2019), Spatio-temporal groundwater variations associated with climatic and anthropogenic impacts in South-West Western Australia, *Science of The Total Environment*, *696*(133599), doi:10.1016/j.scitotenv.2019.133599.

Hu, K., J. Awange, Khandu, E. Forootan, R. Goncalves, and K. Fleming (2017), Hydrogeological characterisation of groundwater over Brazil using remotely sensed and model products, *Science of The Total Environment*, *599-600*, 372–386, doi:10.1016/j.scitotenv.2017.04.188.

Hu, K., J. Awange, M. Kuhn, and J. Nanteza (2021), Inference of the spatio-temporal variability and storage potential of groundwater in data-deficient regions through groundwater models and inversion of impact factors on groundwater, as exemplified by the Lake Victoria Basin, *Science of The Total Environment*, *800*(149355), doi:10.1016/j.scitotenv.2021.149355.

Hu, K., J. Awange, and M. Kuhn (2022a), Testing a knowledge-based approach for inferring spatio-temporal characteristics of groundwater in the Australian State of Victoria, *Science of The Total Environment*, *821*(153113), doi:10.1016/j.scitotenv.2022.153113.

Hu, K., J. Awange, and M. Kuhn (2022b), Large-scale quantification of groundwater recharge threshold conditions using machine learning classifications: Exemplified over the Australian continent, *Science of The Total Environment*.

Hu, K., J. Awange, M. Kuhn, and A. Zerihun (2022c), Irrigated agriculture potential of Australia's northern territory inferred from spatial assessment of groundwater availability and crop evapotranspiration, *Agricultural Water Management*, *264*(107466), doi:10.1016/j.agwat.2022.107466.

Hughes, J., K. Petrone, and R. Silberstein (2012), Drought, groundwater storage and stream flow decline in southwestern Australia, *Geophysical Research Letters*, *39*, doi:10.1029/2011GL050797.

Ilstedt, U., B. Bargués Tobella, H. Bazié, and et. al. (2016), Intermediate tree cover can maximize groundwater recharge in the seasonally dry tropics, *Scientific Reports*, *6*(21930), doi:10.1038/srep21930.

Jasechko, S., and R. Taylor (2015), Intensive rainfall recharges tropical groundwaters, *Environmental Research Letters*, *10*(12), 124,015, doi:10.1088/1748-9326/10/12/124015.

Jasechko, S., S. Birks, T. Gleeson, Y. Wada, P. Fawcett, Z. Sharp, J. McDonnell, and J. Welker (2014), The pronounced seasonality of global groundwater recharge, *Water Resources Research*, *50*, 8845–8867, doi:10.1002/2014WR015809.

Keshavarzi, M., A. Baker, B. Kelly, and M. Andersen (2016), River–groundwater connectivity in a karst system, Wellington, New South Wales, Australia, *Hydrogeology Journal*, *25*, 557–574, doi:10.1007/s10040-016-1491-y.

Kinsela, A., A. Jones, R. Collins, and T. Waite (2012), The impacts of low-cost treatment options upon scale formation potential in remote communities reliant on hard groundwaters. A case study: Northern Territory, Australia, *Science of The Total Environment*, *416*, 22–31, doi:10.1016/j.scitotenv.2011.12.005.

Koirala, S., M. Jung, M. Reichstein, I. de Graaf, G. Campus-Valls, K. Ichii, D. Papale, B. Ráduly, C. Schwalm, G. Tramontana, and N. Carvalhais (2017), Global distribution of groundwater-vegetation spatial covariation, *Geophysical Research Letters*, *44*(9), 4134–4142, doi:10.1002/2017GL072885.

Konikow, L. (2013), Groundwater depletion in the United States (1900-2008), *U.S. Geological Survey Scientific Investigations Report 2013-5079*, 63 p., http://pubs.usgs.gov/sir/2013/5079. (Available only online.).

Kumar, C. (2012), Climate Change and Its Impact on Groundwater Resources, *International Journal of Engineering and Science*, *1*, 43–60.

Lall, U., L. Josset, and T. Russo (2020), A Snapshot of the World's Groundwater Challenges, *Annual Review of Environment and Resources*, *45*, 171–194, doi:10.1146/annurev-environ-102017-025800.

Li, B., M. Rodell, S. Kumar, H. Beaudoing, A. Getirana, B. Zaitchik, and et al. (2019a), Global GRACE Data Assimilation for groundwater and Drought Monitoring: Advances and Challenges, *Water Resources Research*, *55*, 7564–7586, doi:10.1029/2018WR024618.

Li, B., M. Rodell, J. Sheffield, E. Wood, and E. Sutanudjaja (2019b), Long-term, non-anthropogenic groundwater storage changes simulated by three global-scale hydrological models, *Scientific Reports*, *9*(10746), doi:10.1038/s41598-019-47219-z.

MacFarlane, S., and C. Fairfield (2017), Groundwater abstraction in the roper region - Northern Terriotry, *Water: Journal of the Australian Water Association*, *2*(3), 1–26.

Mananp, M., W. Sulaiman, M. Ramli, B. Pradhan, and N. Surip (2013), A knowledge-driven GIS modeling technique for groundwater potential mapping at the Upper Langat Basin, Malaysia, *Arabian Journal of Geosciences*, *6*, 1621–1637, doi:10.1007/s12517-011-0469-2.

Martinez, J., M. Raiber, and M. Cox (2015), Assessment of groundwater–surface water interaction using long-term hydrochemical data and isotope hydrology: Headwaters of the Condamine River, Southeast Queensland, Australia, *Science of The Total Environment*, *536*, 499–516, doi:10.1016/j.scitotenv.2015.07.031.

McFarlane, D., R. Stone, S. Martens, J. Thomas, R. Siberstein, R. Ali, and G. Hodgson (2012), Climate change impacts on water yields and demands in south-western Australia, *Journal of Hydrology*, *475*, 488–498, doi:10.1016/j.jhydrol.2012.05.038.

McFarlane, D., R. George, J. Ruprecht, and S. Charles (2020), Runoff and groundwater responses to climate change in South West Australia, *Journal of the Royal Society of Western Australia*, *103*, 9–27.

McMahon, T., M. Peel, L. Lowe, R. Srikanthan, and T. McVicar (2013), Estimating actual, potential, reference crop and pan evaporation using standard meteorological data: a pragmatic synthesis, *Hydrology and Earth System Sciences*, *17*, 1331–1363, doi:10.5194/hess-17-1331-2013.

Miao, X., J. Heaton, S. Zheng, D. Charlet, and Liu (2011), Applying tree-based ensemble algorithms to the classification of ecological zones using multi-temporal multi-source remote-sensing data, *International Journal of Remote Sensing*, *33*(6), 1823–1849, doi:10.1080/01431161.2011.602651.

Moeck, C., N. Grech-Cumbo, J. Podgorski, A. Bretzler, J. Gurdak, M. Berg, and M. Schirmer (2020), A global-scale dataset of direct natural groundwater recharge rates: A review of variables, processes and relationships, *Science of the Total Environment*, *717*, 137,042, doi:10.1016/j.scitotenv.2020.137042.

Morgan, B., J. Awange, A. Saleem, and K. Hu (2020), Understanding vegetation variability and their "hotspots" within Lake Victoria Basin (LVB: 2003–2018), *Applied Geography*, *122*, 102,238, doi:10.1016/j.apgeog.2020.102238.

Mukherjee, A., S. Bhanja, and Y. Wada (2018), Groundwater depletion causing reduction of baseflow triggering Ganges river summer drying, *Scientific Reports*, *8*, 12,049, doi:10.1038/s41598-018-30246-7.

Nanteza, J., C. de Linage, B. Thomas, and J. Famiglietti (2016), Monitoring groundwater storage changes in complex basement aquifers: an evaluation of the GRACE satellites over East Africa, *Water Resources Research*, *52*, 9542–9564, doi:10.1002/2016WR018846.

Nevill, J., P. Hancock, B. Murray, W. Ponder, W. Humphreys, M. Phillips, and P. Groom (2010), Groundwater-dependent ecosystems and the dangers of groundwater overdraft: a review and an Australian perspective, *Pacific Conservation Biology*, *16*(3), 187–208, doi:10.1071/PC100187.

Newsome, A., and L. Corbett (1975), *Rodents in Desert Environments*, chap. Outbreaks of Rodents in Semi-Arid and Arid Australia: Causes, Preventions, and Evolutionary Considerations, Monographiae Biologicae, vol 28. Springer, Dordrecht, doi:10.1007/978-94-010-1944-6_6.

Northern Territory Government (2018), Western Davenport Water Allocation Plan 2018-2021, *Technique report*, Department of Environment and Natural Resources: Northern Territory, Australia.

Nouayti, A., D. Khattach, M. Hilali, and N. Nouayti (2019), Mapping potential areas for groundwater storage in the High Guir Basin (Morocco): Contribution of remote sensing and geographic information system, *Journal of Groundwater Science and Engineering*, *7*(4).

Oliverira, P., M. Leite, T. Mattos, and et. al. (2016), Groundwater recharge decrease with increased vegetation density in the Brazilian cerrado, *Ecohydrology*, *10*, e1759, doi:10.1038/srep21930.

Oolloo Water Allocation Plan (2010), Information Report for the Oolloo Dolostone Aquifer Water Allocation Plan, *Technique report*, Northern Territory Government, Departement of Natural Resources, Environment, The Arts and Sport, PO Box 496, Palmerston NT, 0831, Australia, retrieve from denr.nt.gov.au/__data/assets/pdf_file/0007/254545/info_report_oolloo.pdf. File accessed: 24 Oct 2020.

Owor, M., R. Taylor, C. Mukwaya, and C. Tindimugaya (2010), Groundwater/surface-water interactions on deeply weathered surfaces of low relief: evidence from Lakes Victoria and Kyoga, Uganda, *Hydrogeology Journal*, *19*, 1403–1420, doi:10.1007/s10040-011-0779-1.

Panzeri, M., M. Riva, A. Guadagnini, and S. Neuman (2016), Comparison of Ensemble Kalman Filter groundwater-data assimilation methods based on stochastic moment equations and Monte Carlo simulation, *Advances in Water Resources*, *66*, 8–18, doi:10.1016/j.advwatres.2014.01.007.

Patle, G., D. Singh, A. Sarangi, A. Rai, M. Khana, and R. Sahoo (2015), Time series analysis of groundwater levels and projection of future trend, *Journal of the Geological Society of India*, *85*, 232–242, doi:10.1007/s12594-015-0209-4.

Perrone, D., and S. Jasechko (2019), Deeper well drilling an unsustainable stopgap to groundwater depletion, *Nature Sustainability*, *2*, 773–782, doi:10.1038/s41893-019-0325-z.

Preeja, K., S. Joseph, J. Thomas, and H. Vijith (2011), Identification of Groundwater Potential Zones of a Tropical River Basin (Kerala, India) Using Remote Sensing and GIS Techniques, *Journal of Hydrology*, *39*, 83–94, doi:10.1007/s12524-011-0075-5.

Pregibon, D. (1981), Logistic Regression Diagnostics, *The Annals of Statistics*, *9*, 705–724, doi:10.1214/aos/1176345513.

Qiao, L., R. Herrmann, and Z. Pan (2013), Parameter Uncertainty Reduction for SWAT Using Grace, Streamflow, and Groundwater Table Data for Lower Missouri River Basin, *JAWRA Journal of the American Water Resources Association*, *49*, 343–358, doi:10.1111/jawr.12021.

Rasmussen, J., H. Madesn, K. Jensen, and J. Refsgaard (2016), Data assimilation in integrated hydrological modelling in the presence of observation bias, *Hydrology and Earth System Sciences*, *20*, 2103–2118, doi:10.5194/hess-20-2103-2016.

Rogers, C., and J. Beringer (2017), Describing rainfall in northern Australia using multiple climate indices, *Biogeosciences*, *14*, 597–615, doi:10.5194/bg-14-597-2017.

Rojas, R., S. Kahunde, L. Peeters, O. Batelaan, L. Feyen, and A. Dassargues (2010), Application of a multimodel approach to account for conceptual model and scenario uncertainties in groundwater modelling, *Journal of Hydrology*, *394*, 416–435, doi:10.1016/j.jhydrol.2010.09.016.

Rosa, L., D. Chiarelli, C. Tu, M. Rulli, and P. D'Odorico (2019), Global unsustainable virtual water flows in agricultural trade, *Environmental Research Letters*, *14*, 114,001, doi:10.1088/1748-9326/ab4bfc/meta.

Saleem, A., J. Awange, M. Kuhn, B. John, and K. Hu (2021), Impacts of extreme climate on Australia's green cover (2003–2018): A MODIS and mascon probe, *Science of The Total Environment*, *766*, 142,567, doi:10.1016/j.scitotenv.2020.142567.

Sandoval, J. A., and C. L. Tiburan Jr. (2019), Identification of potential artificial groundwater recharge sites in Mount Makiling Forest Reserve, Philippines using GIS and Analytical Hierarchy Process, *Applied Geography*, *105*, 73–85, doi:10.1016/j.apgeog.2019.01.010.

Schmied, H., D. Cáceres, S. Eisner, and et al. (2021), The global water resources and use model WaterGAP v2.2d: model description and evaluation, *Geoscientific Model Development*, *14*, 1037–1079, doi:10.5194/gmd-14-1037-2021.

Schumacher, M., E. Forootan, A. van Dijk, H. Schmied, R. Crosbie, J. Kuche, and P. Döll (2018), Improving drought simulations within the Murray-Darling Basin by combined calibration/assimilation of GRACE data into the WaterGAP Global Hydrology Model, *Remote Sensing of Environment*, *204*, 212–228, doi:10.1016/j.rse.2017.10.029.

Schwartz, F., and M. Ibaraki (2011), Groundwater: A Resource in Decline, *Elements*, *7*(3), 175–179, doi:10.2113/gselements.7.3.175.

Skurray, J., E. Roberts, and D. Pannell (2012), Hydrological challenges to groundwater trading: Lessons from south-west Western Australia, *Journal of Hydrology*, *412-413*, 256–268, doi:10.1016/j.jhydrol.2011.05.034.

Sun, H., X. Zhang, E. Wang, S. Chen, and L. Shao (2015), Quantifying the impact of irrigation on groundwater reserve and crop production - A case study in the North China Plain, *European Journal of Agronomy*, *70*, 48–56, doi:10.1016/j.eja.2015.07.001.

Tang, Q., X. Zhang, and T. Y. (2013), Anthropogenic impacts on mass change in North China, *Geophysical Research Letters*, *40*, 3924–3928, doi:10.1002/grl.50790.

Tapley, B., S. Bettadpur, M. Wakins, and C. Reigber (2004), The gravity recovery and climate experiment: Mission overview and early results, *Geophysical Research Letters*, *31*, doi:10.1029/2004GL019920.

Taylor, R., B. Scanlon, P. Döll, and et al. (2013a), Ground water and climate change, *Nature Climate Change*, *3*, 322–329, doi:10.1038/nclimate1744.

Taylor, R., M. Todd, L. Kongola, L. Maurice, E. Nahozya, H. Sanga, and A. N. MacDonald (2013b), Evidence of the dependence of groundwater resources on extreme rainfall in East Africa, *Nature Climate Change*, *3*, 374–378, doi:10.1038/nclimate1731.

Thomas, M., D. Brough, E. Bui, B. Harms, J. Hill, K. Holmes, D. Morrison, S. Philip, R. Searle, H. Smolinski, S. Tuomi, D. Van Gool, I. Watson, P. Wilson, and P. Wilson (2018), Digital soil mapping of the Fitzroy, Darwin and Mitchell catchments, *Tech. rep.*, CSIRO, Australia, a technical report from the CSIRO Northern Australia Water Resource Assessment, part of the National Water infrastructure Development Fund: Water Resource Assessments. Retrieve from https://publications.csiro.au/rpr/pub?pid=csiro:EP178822.

Ti Tree Water Report (2009), Ti Tree Basin Water Resource Report, *Technique report*, Northern Territory Government, Departement of Natural Resources, Environment, The Arts and Sport, PO Box 496, Palmerston NT, 0831, Australia, retrieve from denr.nt.gov.au/__data/assets/pdf_file/0019/254602/basin_water_resource_report_09.pdf. File accessed: 24 Oct 2020.

Turner, S., M. Hejazi, K. Calvin, P. Kyle, and S. Kim (2019), A pathway of global food supply adaptation in a world with increasingly constrained groundwater, *Science of The Total Environment*, *673*, 165–176, doi:10.1016/j.scitotenv.2019.04.070.

van Dijk, A., H. Beck, R. Crosbie, R. de Jeu, Y. Liu, G. Podger, B. Timbal, and N. Viney (2013), The millennium drought in southeast australia

(2001–2009): Natural and human causes and implications for water resources, ecosystems, economy, and society, *Water Resources Research*, *49*, 1040–1057, doi:10.1002/wrcr.20123.

Vanderzalm, J., B. Jeuken, J. Wischusen, P. Pavelic, C. Salle, A. Knapton, and P. Dillon (2011), Recharge sources and hydrogeochemical evolution of groundwater in alluvial basins in arid central Australia, *Journal of Hydrology*, *397*, 71–82, doi:10.1016/j.jhydrol.2010.11.035.

Voisin, J., B. Cournoyer, A. Vienney, and F. Mermillod-Blondin (2018), Aquifer recharge with stormwater runoff in urban areas: Influence of vadose zone thickness on nutrient and bacterial transfers from the surface of infiltration basins to groundwater, *Science of The Total Environment*, *637-638*, 1496–1507, doi:10.1016/j.scitotenv.2018.05.094.

Von Freyberg, J., C. Moeck, and M. Schirmer (2015), Estimation of groundwater recharge and drought severity with varying model complexity, *Journal of Hydrology*, *527*, 844–857, doi:10.1016/j.jhydrol.2015.05.025.

Wang, Y., C. Zheng, and R. Ma (2018), The research of groundwater flow model in Ejina Basin, Northwestern China, *Hydrogeology Journal*, *26*, 1301–1324, doi:10.1007/s10040-018-1795-1.

Wheeler, S., A. Loch, A. Zuo, and H. Bjornlund (2014), Reviewing the adoption and impact of water markets in the Murray–Darling Basin, Australia, *Journal of Hydrology*, *518*, 28–41, doi:10.1016/j.jhydrol.2013.09.019.

Wu, W., A. Li, X. He, R. Ma, H. Liu, and J. Lv (2018), A comparison of support vector machines, artificial neural network and classification tree for identifying soil texture classes in southwest China, *Computers and Electronics in Agriculture*, *144*, 86–93, doi:10.1016/j.compag.2017.11.037.

Xi, H., Q. Feng, W. Liu, J. Si, Z. Chang, and Y. Su (2009), The research of groundwater flow model in Ejina Basin, Northwestern China, *Environmental Earth Sciences*, *60*, 953–963, doi:10.1007/s12665-009-0231-1.

Yang, H., F. Wei, Z. Ma, H. Guo, P. Su, and S. Zhang (2019), Rainfall threshold for landslide activity in Dazhou, southwest China, *Landslides*, *17*, 61–77, doi:10.1007/s10346-019-01270-z.

Yin, W., T. Li, W. Zheng, L. Hu, S. Han, N. Tangdamrongsub, M. Šprlák, and Z. Huang (2020), Improving regional groundwater storage estimates from GRACE and global hydrological models over Tasmania, Australia, *Hydrogeology Journal*, *28*, 1809–1825, doi:10.1007/s10040-020-02157-3.

Zhao, F., L. Zhang, F. Chiew, J. Vaze, and L. Cheng (2013), The effect of spatial rainfall variability on water balance modelling for southeastern Australian catchments, *Journal of Hydrology*, *493*, 16–29, doi:10.1016/j.jhydrol.2013.04.028.

Zhong, Y., M. Zhong, Y. Mao, and B. Ji (2020), Evaluation of Evapotranspiration for Exorheic Catchments of China during the GRACE Era: From a Water Balance Perspective, *Remote Sensing*, *12*(3), 511, doi: 10.3390/rs12030511.

Every reasonable effort has been made to acknowledge the owners of copyright material. I would be pleased to hear from any copyright owner who has been omitted or incorrectly acknowledged.

Kexiang Hu

Appendix A. Copyright permission statements

I certify that I collected permission from the copyright owners to use my own publications in which the copyright is held by another party (e.g. publishers, co-author). The obtained permissions for individual publishers are enclosed below.

KeXiang Hu

Spatio-temporal groundwater variations associated with climatic and anthropogenic impacts in South-West Western Australia

Author: K.X. Hu,J.L. Awange,M. Kuhn,A. Saleem

Publication: Science of The Total Environment

Publisher: Elsevier

Date: 15 December 2019

Journal Author Rights

Please note that, as the author of this Elsevier article, you retain the right to include it in a thesis or dissertation, provided it is not published commercially. Permission is not required, but please ensure that you reference the journal as the original source. For more information on this and on your other retained rights, please visit: https://www.elsevier.com/about/our-business/policies/copyright#Author-rights

BACK CLOSE WINDOW

Irrigated agriculture potential of Australia's northern territory inferred from spatial assessment of groundwater availability and crop evapotranspiration

Author: K.X. Hu,J.L. Awange,M. Kuhn,A. Zerihun

Publication: Agricultural Water Management

Publisher: Elsevier

Date: 30 April 2022

Journal Author Rights

Please note that, as the author of this Elsevier article, you retain the right to include it in a thesis or dissertation, provided it is not published commercially. Permission is not required, but please ensure that you reference the journal as the original source. For more information on this and on your other retained rights, please visit: https://www.elsevier.com/about/our-business/policies/copyright#Author-rights

BACK CLOSE WINDOW

Inference of the spatio-temporal variability and storage potential of groundwater in data-deficient regions through groundwater models and inversion of impact factors on groundwater, as exemplified by the Lake Victoria Basin

Author: K.X. Hu,J.L. Awange,M. Kuhn,J. Nanteza

Publication: Science of The Total Environment

Publisher: Elsevier

Date: 15 December 2021

Journal Author Rights

Please note that, as the author of this Elsevier article, you retain the right to include it in a thesis or dissertation, provided it is not published commercially. Permission is not required, but please ensure that you reference the journal as the original source. For more information on this and on your other retained rights, please visit: https://www.elsevier.com/about/our-business/policies/copyright#Author-rights

Testing a knowledge-based approach for inferring spatio-temporal characteristics of groundwater in the Australian State of Victoria

Author: K.X. Hu,J.L. Awange,M. Kuhn

Publication: Science of The Total Environment

Publisher: Elsevier

Date: May 15, 2022

Journal Author Rights

Please note that, as the author of this Elsevier article, you retain the right to include it in a thesis or dissertation, provided it is not published commercially. Permission is not required, but please ensure that you reference the journal as the original source. For more information on this and on your other retained rights, please visit: https://www.elsevier.com/about/our-business/policies/copyright#Author-rights

BACK CLOSE WINDOW

Appendix B. Statements of contribution by others

This thesis collects 4 published and 1 submitted paper in peer-reviewed journals. Here, the author and coauthor's contributions for all of these papers are indicated.

To Whom It May Concern,

I, KeXiang Hu, designed and built the framework of this thesis, processed the data using my own software/algorithm, interpreted the numerical results, plotted the figures, and wrote the manuscripts. Co-authors provided their technical comments to improve the manuscripts for submission. All of the above hold for the following publications listed below:

1. **Hu, K.X.**, Awange, J.L., Kuhn, M. and Saleem, A., (2019). Spatio-temporal groundwater variations associated with climatic and anthropogenic impacts in South-West Western Australia. Science of The Total Environment, 696, 133599, doi: 10.1016/j.scitotenv.2019.133599.

2. **Hu, K.X.**, Awange, J.L., Kuhn, M. and Nanteza, J., (2021). Inference of the spatio-temporal variability and storage potential of groundwater in data-deficient regions through groundwater models and inversion of impact factors on groundwater, as exemplified by the Lake Victoria Basin. Science of The Total Environment, 800, 149355, doi: 10.1016/j.scitotenv.2021.149355.

3. **Hu, K.X.**, Awange, J.L., Kuhn, M. and Zerihun, A., (2022). Irrigated agriculture potential of Australia's northern territory inferred from spatial assessment of groundwater availability and crop evapotranspiration. Agricultural Water Management, 264, 107466, doi: 10.1016/j.agwat.2022.107466.

4. **Hu, K.X.**, Awange, J.L. and Kuhn, M., (2022). Testing a knowledge-based approach for inferring spatio-temporal characteristics of groundwater in the Australian State of Victoria. Science of The Total Environment, 821, 153113, doi: 10.1016/j.scitotenv.2022.153113.

5. **Hu, K.X.**, Awange, J.L. and Kuhn, M., (2022). Large-scale quantification of groundwater recharge threshold conditions using machine learning classifications: Exemplified over the Australian continent. Science of The Total Environment, submitted.

Kexiang Hu _____

I, as a Co-Author, endorse that this level of contributions by the candidate indicated above is appropriate.

Joseph L. Awange _____

Michael Kuhn _____

Ashty Saleem _____

Nanteza Jamiat _____

Ayalsew Zerihun _____